

AD-A258 629

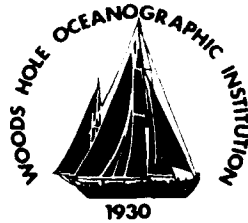
WHOI-90-31

1



Woods Hole Oceanographic Institution

S DTIC
ELECTE
DEC 18 1992 **D**
C



Abstracts of Manuscripts Submitted in 1989 for Publication

Technical Report WHOI-90-31

DISTRIBUTION STATEMENT A
Approved for public release
Distribution Unlimited

92-31915



92 12 17 039

WHOI-90-31

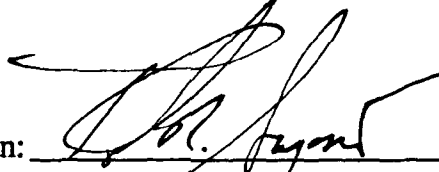
Research In Progress

**Abstracts of Manuscripts
Submitted in 1989 for Publication**

Woods Hole Oceanographic Institution
Woods Hole, Massachusetts

Editor: Alora K. Paul

Approved for Distribution:



Robert B. Gagosian
Associate Director for Research

WHOI Quality Assurance

When citing this report, it should be referenced as:

Woods Hole Oceanographic Institution
Technical Report No. WHOI-90-31

Accession For	
NTIS GR&I	<input checked="" type="checkbox"/>
DDP Tab	<input type="checkbox"/>
Unannounced	<input type="checkbox"/>
Justification	
By	
Distribution/	
Availability Codes	
Dist	Mail and/or Special
A-1	

PREFACE

This volume contains the abstracts of manuscripts submitted for publication during calendar year 1989 by the staff and students of the Woods Hole Oceanographic Institution. We identify the journal of those manuscripts which are in press or have been published. The volume is intended to be informative, but not a bibliography.

The abstracts are listed by title in the Table of Contents and are grouped into one of our five departments, marine policy, or the student category. An author index is presented in the back to facilitate locating specific papers.

ACKNOWLEDGEMENTS

Special thanks to Suzanne B. Volkmann, Research Associate; Staff Assistants Cheri Ann Perry, IPCL; Alice I. Tricca, Public Information Office; Peggy Dimmock, Biology; Molly M. Lumping, Chemistry, Pamela Foster, Geology & Geophysics; Shirley Bowman, Applied Ocean Physics and Engineering; Lisa Wolfe, Physical Oceanography; Ellen Gately, Marine Policy Center; Pamela Goulart, Education; and Maureen O'Donnell, Library Assistant.

TABLE OF CONTENTS

DEPARTMENT OF BIOLOGY

BENTHOS

- Abyssotherma pacifica* n. gen. n. sp., a Recent Remaneicid (Foraminiferida: Remaneicacea) from the East Pacific Rise
Paul Brönnimann, Cindy Lee Van Dover and John E. Whittaker B-1
- Benthic Mariculture and Research Rig Developed for Diver Operations
George R. Hampson, Donald C. Rhoads and Dan W. Clark B-1
- Adaptations for Reproduction Among Deep-Sea Molluscs: An Appraisal of Existing Evidence
Rudolf S. Scheltema B-1
- Behavior, Survival and Sediment Surface Traces of Deep-Sea Benthic Invertebrates in the Laboratory
James R. Weinberg B-1

BIOGEOGRAPHY AND SYSTEMATICS

- The Aplacophora as a Tethyan Slope Taxon: Evidence from the Pacific
Amélie H. Scheltema B-2

EVOLUTION

- Morphological Divergence of Eastern Pacific and Caribbean Isopods: Effects of a Land Barrier and the Panama Canal
J. R. Weinberg and V. R. Starczak B-2
- Premating Isolation and Chromosome Variation Between Populations of a Coastal Marine Polychaete
James R. Weinberg, Victoria R. Starczak, Cornelia Mueller, Gerald G. Pesch and Sara M. Lindsay B-3

FISHES

- Sonic Signatures of Spawning Fishes
Phillip S. Lobel B-3
- Anadromous Behavior of Brook Charr (*Salvelinus fontinalis*) in the Moisie River, Quebec
W. Linn Montgomery, Stephen D. McCormick, Robert J. Naiman, Frederick G. Whoriskey and Geoff Black B-4

GEOCHEMISTRY

- A Conceptual Framework for Interpreting Lead in Marine Planktonic Organisms and Pelagic Food Webs
Anthony F. Michaels and A. Russell Flegal B-4
- Unexpected Changes in the Oxic/Anoxic Interface in the Black Sea
J. W. Murray, H. W. Jannasch, S. Honjo, R. F. Anderson, W. S. Reeburgh, Z. Top, G. E. Friederich, L. A. Codispoti and E. Izdar B-4
- Mineralogical and Chemical Composition of Hydrothermal Deposits at Deep-Sea Vents of the East Pacific Rise and the Gulf of California
D. Rose, R. Huber and H. W. Jannasch B-5

MARINE MAMMALS

- Review of the Signature-Whistle Hypothesis for the Atlantic Bottlenose Dolphin
Melba C. Caldwell, David K. Caldwell and Peter L. Tyack B-5

Humpback Whales <i>Megaptera novaeangliae</i> Fatally Poisoned by Dinoflagellate Toxin <i>Joseph A. Geraci, Donald M. Anderson, Ralph J. Timperi, David J. St. Aubin, Gregory A. Early, John H. Prescott and Charles A. Mayo</i>	B-5
Signature Whistles of Free-Ranging Bottlenose Dolphins <i>Tursiops truncatus</i>: Stability and Mother-Offspring Comparisons <i>Laela S. Sayigh, Peter L. Tyack, Randall S. Wells and Michael D. Scott</i>	B-6
An Acoustic Model Describing How Migrating Gray Whales <i>Eschrichtius robustus</i> Avoid Industrial Noise <i>Peter L. Tyack, Charles I. Malme, Robert W. Pyle, Paul R. Miles, Christopher W. Clark and James E. Bird</i>	B-6
MARINE POLLUTION	
Polychlorinated Biphenyl Concentration and Altered Cytochrome P-450E Expression in Winter Flounder from Contaminated Environments <i>Adria A. Elskus, Lucia C. Susani, Dianne Black, Richard J. Pruell, Steven J. Ptuck and John J. Stegeman</i>	B-7
Induction of Cytochrome P450E (P450IA1) by 2,3,7,8-Tetrachlorodibenzofuran (2,3,7,8-TCDF) in the Marine Fish Scup (<i>Stenotomus chrysops</i>) <i>Mark E. Hahn, Bruce R. Woodin and John J. Stegeman</i>	B-7
The Relationship Between Lipid Composition and Seasonal Differences in the Distribution of PCBs in <i>Mytilus edulis</i> L. <i>Judith McDowell Capuzzo, John W. Farrington, Pirjo Rantamaki, C. Hovey Clifford, Bruce A. Lancaster, Dale F. Leavitt and Xiaoping Jia</i>	B-8
MICROBIOLOGY	
Denitrification, Nitrogen-Fixation and Nitrous Oxide Concentrations through the Black Sea Oxic-Anoxic Interface <i>Dennis A. Bazylinski, Brian L. Howes and Holger W. Jannasch</i>	B-8
Microbial Utilization of Naturally-Occurring Hydrocarbons at the Guaymas Basin Hydrothermal Vent Site <i>Dennis A. Bazylinski, Carl O. Wirsen and Holger W. Jannasch</i>	B-8
Stable Isotope Studies of the Carbon, Nitrogen and Sulfur Cycles in the Black Sea and the Cariaco Trench <i>Brian Fry, Holger W. Jannasch, Stephen Molyneaux, Carl O. Wirsen, Jo Ann Nicholson and Stagg King</i>	B-9
Ammonium Regeneration and Carbon Utilization by Marine Bacteria Grown on Mixed Substrates <i>J. C. Goldman and M. R. Dennett</i>	B-9
A Novel Group of Abyssal Methanogenic Archaeobacteria (<i>Methanopyrus</i>) Growing at 110°C <i>R. Huber, M. Kurr, H. W. Jannasch and K. O. Stetter</i>	B-10
Barophiles and Their Potential in Biotechnology <i>Holger W. Jannasch</i>	B-10
Chemolithotrophic Productivity at Deep-Sea Hydrothermal Vents <i>Holger W. Jannasch</i>	B-10
Massive Natural Occurrence of Unusually Large Bacteria (<i>Beggiatoa</i> sp.) at a Hydrothermal Deep-Sea Vent Site <i>H. W. Jannasch, D. C. Nelson and C. O. Wirsen</i>	B-10

Chemoautotrophic Sulfur-Oxidizing Bacteria from the Black Sea <i>H. W. Jannasch, C. O. Wirsen and S. J. Molyneux</i>	B-11
Sulfide Oxidation in the Anoxic Black Sea Chemocline <i>Bo Barker Jorgensen, Henrik Fossing, Carl O. Wirsen and Holger W. Jannasch</i>	B-11
Biom mineralization of Ferrimagnetic Greigite (Fe ₃ S ₄) and Iron Pyrite (FeS ₂) in a Magnetotactic Bacterium <i>Stephen Mann, Nicholas H. C. Sparks, Richard B. Frankel, Dennis A. Bazylinski and Holger W. Jannasch</i>	B-11
Comparison of Magnetite Particles Produced Anaerobically by Magnetotactic and Dissimilatory Iron-Producing Bacteria <i>Bruce M. Moskowitz, Richard B. Frankel, Dennis A. Bazylinski, Holger W. Jannasch and Derek R. Lovley</i>	B-12
Massive Occurrence of Large, Autotrophic <i>Beggiatoa</i> at Hydrothermal Vents of the Guaymas Basin <i>Douglas C. Nelson, Carl O. Wirsen and Holger W. Jannasch</i>	B-12
<i>Thermococcus litoralis</i> sp. nov.: A Novel Species of Extremely Thermophilic Marine Archaeobacteria <i>Annemarie Neuner, Holger W. Jannasch and Shimshon Belkin</i>	B-12
<i>Erythrosphaera marina</i> Gen. Nov., Sp. Nov.: A Diazotrophic Unicellular Cyanobacterium Cultured From the Tropical Atlantic Ocean <i>S. W. Watson, F. W. Valois, D. Distel and J. B. Waterbury</i>	B-13
PHYSIOLOGY AND BIOCHEMISTRY	
Changes in Digestive Enzyme Activities during Early Development of the American Lobster <i>Homarus americanus</i> Milne-Edwards <i>Patricia M. Biesiot and Judith McDowell Capuzzo</i>	B-13
Digestive Protease, Lipase and Amylase Activities in Stage I Larvae of the American Lobster <i>Homarus americanus</i> <i>Patricia M. Biesiot and Judith McDowell Capuzzo</i>	B-14
Uptake Kinetics of Paralytic Shellfish Toxins from the Dinoflagellate <i>Alexandrium fundyense</i> in the Mussel <i>Mytilus edulis</i> <i>V. M. Bricelj, J. H. Lee, A. D. Cembella and D. M. Anderson</i>	B-14
The Use of Biochemical Indicators in the Study of Trophic Interactions in Animal-Bacteria Symbioses: <i>Solemya velum</i> , a Case Study <i>Noellette Conway and Judith McDowell Capuzzo</i>	B-15
Changes in the Biochemical Composition of a Subtropical Bivalve, <i>Arca zebra</i> , in Response to Contaminant Gradients Near Bermuda <i>D. Leavitt, B. Lancaster, A. Lancaster and J. McDowell Capuzzo</i>	B-15
Incidence of Hematopoietic Neoplasia in <i>Mya arenaria</i> : Monthly Monitoring of Prevalence and Indices of Physiological Condition <i>Dale F. Leavitt, Judith McDowell Capuzzo, Donna Miosky, Roxanna Smolowitz, Bruce Lancaster and Carol L. Reinisch</i>	B-15
Cellular Alterations Preceding Neoplasia in <i>Pseudopleuronectes americanus</i> from Boston Harbor, MA, USA <i>Michael J. Moore, Roxanna Smolowitz and John J. Stegeman</i>	B-16
Feminization of the Hepatic Microsomal Cytochrome P-450 System in Brook Trout by Estradiol, Testosterone and Pituitary Factors <i>Ana M. Pajor, John J. Stegeman, Peter Thomas and Bruce Woodin</i>	B-16

Cellular Distribution of Cytochrome P450 in Winter Flounder Liver With Degenerative and Neoplastic Disease <i>Rozanna M. Smolowitz, Michael J. Moore and John J. Stegeman</i>	B-17
Cytochrome P450 Forms in Fish: Catalytic, Immunological and Sequence Similarities <i>John J. Stegeman</i>	B-17
Cytochrome P450 Monooxygenase Systems in Aquatic Species: Carcinogen Metabolism and Biomarkers for Carcinogen and Pollutant Exposure <i>John J. Stegeman and John J. Lech</i>	B-17
Experimental and Environmental Induction of Cytochrome P450E in Fish from Bermuda Waters <i>John J. Stegeman, Kenneth W. Renton, Bruce R. Woodin, Yu-Sheng Zhang and Richard F. Addison</i>	B-18
Structure, Function and Regulation of Cytochrome P450 Forms in Fish <i>John J. Stegeman, Bruce R. Woodin and Rozanna Smolowitz</i>	B-18
PHYTOPLANKTON	
Cysts as Factors in <i>Pyrodinium bahamense</i> Ecology <i>Donald M. Anderson</i>	B-19
Toxin Variability in <i>Alexandrium</i> Species <i>Donald M. Anderson</i>	B-19
Immunofluorescent Detection of the Brown Tide Organism, <i>Aureococcus anophagefferens</i> <i>Donald M. Anderson and David M. Kulis</i>	B-19
Toxin Composition Variations in the Dinoflagellate <i>Alexandrium fundyense</i> <i>D. M. Anderson, D. M. Kulis, J. J. Sullivan and S. Hall</i>	B-20
Dynamics and Physiology of Saxitoxin Production by the Dinoflagellates <i>Alexandrium</i> spp. <i>D. M. Anderson, D. M. Kulis, J. J. Sullivan, S. Hall and C. Lee</i>	B-20
Biochemical Composition and Metabolic Activity of <i>Scrippsiella trochoidea</i> (Dinophyceae) <i>Brian J. Binder and Donald M. Anderson</i>	B-21
Cell Cycle Studies of the Dinoflagellates <i>Gonyaulax polyedra</i> Stein and <i>Gyrodinium uncatenatum</i> Hulbert During Asexual and Sexual Reproduction <i>Catherine M. Cetta and Donald M. Anderson</i>	B-21
Cyst Formation in the Red Tide Dinoflagellate <i>Alexandrium tamarense</i> (Dinophyceae): Effects of Iron Stress <i>Gregory J. Doucette, Allan D. Cembella and Gregory L. Boyer</i>	B-22
Relative Effects of Nitrogen or Phosphorus Depletion and Light Intensity on the Pigmentation, Chemical Composition, and Volume of <i>Pyrenomonas salina</i> (Cryptophyceae) <i>Alan J. Lewitus and David A. Caron</i>	B-22
Changes in Cell Chemical Composition During the Life Cycle of <i>Scrippsiella trochoidea</i> (Dinophyceae) <i>Thaithaworn Lirdwitayaprasit, Tomotoshi Okaichi, Shigeru Montani, Tadashi Ochi and Donald M. Anderson</i>	B-22
PLANKTON ECOLOGY	
Behavioral Responses of the Marine Tintinnid <i>Favella</i> sp. to Phytoplankton: Influence of Chemical, Mechanical and Photic Stimuli <i>Edward J. Buskey and Diane K. Stoecker</i>	B-23

Effects of Gametogenesis on Test Structure and Dissolution of Some Spinose Planktonic Foraminifera and Implications for Test Preservation <i>David A. Caron, O. Roger Anderson, Judith L. Lindsey, Walter W. Faber, Jr. and Ee Lin Lim</i>	B-23
Carbon Utilization by the Omnivorous Flagellate <i>Paraphysomonas imperforata</i> <i>David A. Caron, Joel C. Goldman and Mark R. Dennett</i>	B-24
Trophic Interactions Between Nano- and Microzooplankton and the "Brown Tide" <i>David A. Caron, Ee Lin Lim, Holly Kunze, Elizabeth Cosper and Donald Anderson</i>	B-24
Composition and Degradation of Salp Fecal Pellets: Implications for Vertical Flux in Oceanic Environments <i>David A. Caron, Laurence P. Madin and Jonathan J. Cole</i>	B-25
Carbon, Nitrogen and Phosphorus Budgets for the Mixotrophic Phytoflagellate <i>Poterioochromonas malhamensis</i> (Chrysophyceae) During Bacterial Ingestion <i>David A. Caron, K. G. Porter and Robert W. Sanders</i>	B-25
The Ecology of Planktonic Sarcodines <i>David A. Caron and Neil R. Swanberg</i>	B-25
Effects of Fixation on Cell Volume of Marine Planktonic Protozoa <i>Joon W. Choi and Diane K. Stoecker</i>	B-26
Dynamics of Prey Selection by An Omnivorous Flagellate <i>Joel C. Goldman and Mark R. Dennett</i>	B-26
Abundance, Chlorophyll Content and Photosynthetic Rates of Ciliates in the Nordic Seas <i>Mary Putt</i>	B-26
Metabolism of Photosynthate in the Chloroplast Retaining Ciliate <i>Laboea strobila</i> <i>Mary Putt</i>	B-27
Relationship Between Phototrophy and Phagotrophy in the Mixotrophic Chrysophyte <i>Poterioochromonas malhamensis</i> <i>Robert W. Sanders, K. G. Porter and David A. Caron</i>	B-27
Predation on Protozoa: Its importance to Zooplankton <i>Diane Stoecker and Judith McDowell Capuzzo</i>	B-27
Chloroplast Replacement and Aging in <i>Strombidium capitatum</i> (Ciliata, Oligotrichida) <i>Diane Stoecker and M. W. Silver</i>	B-28
Oceanic Mixotrophic Flatworms <i>D. K. Stoecker, N. Swanberg and S. Tyler</i>	B-28
Submersible Incubation Device (SID), Autonomous Instrumentation for the In Situ Measurement of Primary Production and Other Microbial Rate Processes <i>Craig D. Taylor and Kenneth W. Doherty</i>	B-28
POPULATION ECOLOGY	
Growth of Two Species of Bacterivorous Microflagellates in Batch and Continuous Culture, and Implications for Their Planktonic Existence <i>David A. Caron</i>	B-29
Factors Responsible for the Differences in Cultural Estimates and Direct Microscopical Counts of Populations of Bacterivorous Nanoflagellates <i>David A. Caron, Paul G. Davis and John McN. Sieburth</i>	B-29

Communities in Patchy Environments: A Model of Disturbance, Competition, and Heterogeneity <i>Hal Caswell and Joel Cohen</i>	B-30
Density Effects in a Colonial Monoculture: Experimental Studies With a Marine Bryozoan (<i>Membranipora membranacea</i> L.) <i>C. Drew Harvell, Hal Caswell and Paul Simpson</i>	B-30
Demographic Analysis of Tropical Zooplankton Populations <i>Saran Twombly and Hal Caswell</i>	B-31
Demographic Consequences of <i>Chaoborus</i> -Induced Response and Food Availability in <i>Daphnia pulex</i> <i>Mari Walls, Hal Caswell and Matti Ketola</i>	B-31
ZOOPLANKTON	
Aspects of Jet Propulsion in Salps <i>Laurence P. Madin</i>	B-31

DEPARTMENT OF CHEMISTRY

GEOCHEMISTRY

- Cosmic Ray Exposure Dating With *In-Situ* Produced Cosmogenic ^3He : Results From Young Hawaiian Lava Flows
Mark D. Kurz, Debra Colodner, Thomas W. Trull, Richard B. Moore, and Keran O'Brien C-1
- Cumulate Gabbros From The Southwest Indian Ridge, 54°S-7°16'E: Implications for Magmatic Processes at a Slow Spreading Ridge
Peter S. Meyer, Henry J. B. Dick, and Geoffrey Thompson C-1

INSTRUMENTS

- The Seep Meter: A Benthic Chamber for the Sampling and Analysis of Low Velocity Hydrothermal Vents
F. L. Sayles and W. H. Dickinson C-2
- TG/Plus-A Pyrolysis Method for Following Maturation of Oil and Gas Generation Zones using Tmax of Methane
Jean Whelan, Robert M. Carangelo, and Peter Solomon C-2

ORGANIC AND BIOLOGICAL CHEMISTRY

- Temporal Variations in Nitrogen and Particle Dynamics in the Sargasso Sea: Interpretation of Isotopic Data
Mark A. Altabet C-2
- Organic C, N, and Stable Isotopic Composition of Particulate Matter Collected on Glass-Fiber and Aluminum Oxide Filters
Mark A. Altabet C-3
- Differences in Nitrogen Isotope Composition Between Particles Collected by Bottles and Large-Volume Pumps in Gulf Stream Warm-Core Rings and the Sargasso Sea
M. A. Altabet, J. K. B. Bishop, and J. J. McCarthy C-3
- Nitrogen Isotopic Ratios in Fecal Pellets Produced by Marine Zooplankton
Mark A. Altabet and Lawrence F. Small C-3
- Dissolved Fluorescence in the Black Sea
Paula Garfield Coble, Robert B. Gagosian, L. A. Codispoti, Gernot E. Friederich, and John P. Christensen C-4
- Reef-Building Corals and Identification of ENSO Warming Episodes
E. R. M. Druffel, R. B. Dunbar, G. M. Wellington, and S. A. Minnis C-4
- Radiocarbon in Dissolved Organic and Inorganic Carbon from the Central North Pacific
Ellen R. M. Druffel, Peter M. Williams, Ken Robertson, Sheila Griffin, A. J. Timothy Jull, Douglas Donahue, Lawrence Toolin, and Timothy W. Linick C-5
- Early Diagenesis of Organic Matter in Peru Upwelling Area Sediments
J. W. Farrington, M. A. McCaffrey, and J. Sulanowski C-5
- Impact of Phytoplankton-Generated Surfactants on Gas Exchange at the Air-Sea Interface
Nelson M. Frew, Joel C. Goldman, Mark R. Dennett, and A. Sherwood Johnson C-5
- Fluorescence Detection of Free Radicals by Nitroxide Scavenging
John L. Gerlock, P. J. Zacmanidis, David R. Bauer, Daniel J. Simpson, Neil V. Blough, and Irving T. Salmeen C-6

An Ocean Basin-Scale Model of Plankton Dynamics in the North Pacific During Oceanographic Spring <i>David M. Glover, J. S. Wroblewski, and Charles R. McClam</i>	C-6
Sources of Carbon to Deep-Sea Corals <i>Sheila Griffin and Ellen R. M. Druffel</i>	C-6
Generation and Migration of Petroleum from Abnormally Pressured Fluid Compartments <i>John M. Hunt</i>	C-6
Fluorescence Detection of Carbon-Centered Radicals in Aqueous Solution <i>David J. Kieber and Neil V. Blough</i>	C-7
The Organic Geochemistry of Peru Margin Surface Sediments-I. A Comparison of the C ₃₇ Alkenone and Historical El Niño Records <i>Mark A. McCaffrey, John W. Farrington, and Daniel J. Repeta</i>	C-7
An Investigation of Hydrogen Peroxide Chemistry in a Coastal Marine Environment Using H ₂ ¹⁸ O ₂ and ¹⁸ O ₂ <i>James W. Moffett and Oliver C. Zafriou</i>	C-8
Organic Geochemistry of Aerosols Over the Pacific Ocean <i>E. T. Peltzer and R. B. Gagosian</i>	C-8
Evidence for Anoxygenic Photosynthesis from the Distribution of Bacteriochlorophylls in the Black Sea <i>D. J. Repeta, D. J. Simpson, B. B. Jorgensen, and H. W. Jannasch</i>	C-8
Chemical Methods for Assessing Kerogen and Protokerogen Types and Maturity <i>Jean K. Whelan and Carolyn Thompson-Rizer</i>	C-9
RADIOCHEMISTRY	
Vertical Profiles of Some Natural Radionuclides Over the Alpha Ridge, Arctic Ocean <i>Michael P. Bacon, Chih-An Huh, and Robert M. Moore</i>	C-9
Scavenging and Particle Deposition in the Southwestern Black Sea—Evidence from Chernobyl Radio-tracers <i>K. O. Buesseler, H. D. Livingston, S. Honjo, B. J. Hay, T. Konuk, and S. Kempe</i>	C-10
²¹⁰ Pb Scavenging in the Open Ocean <i>J. Kirk Cochran, Thomas McKibbin-Vaughan, Mark M. Dornblaser, David Hirschberg, Hugh D. Livingston, and Ken O. Buesseler</i>	C-10
SEAWATER AND GEOCHEMISTRY	
Carbon Dioxide Transport by Ocean Currents at 25°N Latitude in the Atlantic Ocean <i>Peter G. Brewer, Catherine Goyet, and David Dyrssen</i>	C-10
Chlorofluorocarbons as Time-Dependent Tracers in the Ocean <i>John L. Bullister</i>	C-11
Polycyclic Aromatic Hydrocarbons in <i>Saccoglossus kowalewskyi</i> (Agassiz) <i>D. A. Carey and J. W. Farrington</i>	C-11
Mineralogy and Chemistry of Ocean Floor Hydrothermal Precipitates from Kolbeinsey and Reykjanes Ridges near Iceland: Scanning Electron Microscope (Energy-Dispersive X-ray) Analysis <i>Robert F. Commeau, Geoffrey Thompson, Frank T. Manheim, Jon Olafsson, and Sveinn P. Jakobsson</i>	C-12
Surface-Ocean Color and Deep-Ocean Carbon Flux: How Close A Connection? <i>W. G. Deuser, F. E. Muller-Karger, R. H. Evans, O. B. Brown, W. E. Esaias, and G. C. Feldman</i>	C-12

The Rare Earth Elements In Rivers, Estuaries and Coastal Seas And Their Significance To The Composition Of Sea Waters <i>H. Elderfield, R. Upstill-Goddard, and E. R. Sholkovitz</i>	C-12
Pb Isotopes In Surficial Pelagic Sediments From The North Atlantic <i>B. Hamelin, F. Grousset, and E. R. Sholkovitz</i>	C-13
Axial And Off-Axial Heterogeneity of Basaltic Rocks From The East Pacific Rise at 12°35'N-12°51'N and 11°26'N-11°30'N <i>Roger Hekinian, Geoffrey Thompson, and Daniel Bideau</i>	C-13
Alkenone Molecular Stratigraphy in an Oceanic Environment Affected by Glacial Freshwater Events <i>John P. Jasper and Robert B. Gagosian</i>	C-14
Glacial-Interglacial Climatically-Forced $\delta^{13}\text{C}$ Variations in Sedimentary Organic Matter <i>John P. Jasper and Robert B. Gagosian</i>	C-14
The Sources and Deposition of Organic Matter in the Late Quaternary Pigmy Basin <i>John P. Jasper and Robert B. Gagosian</i>	C-15
Temporal Variations in the Concentrations of Some Particulate Elements in the Surface Waters of the Sargasso Sea and their Relationship to Deep Sea Fluxes <i>T. D. Jickells, W. G. Deuser, and R. A. Belostock</i>	C-15
Variability of Some Elemental fluxes in the Western Tropical Atlantic Ocean <i>T. D. Jickells, W. G. Deuser, A. P. Fler, and C. Hemleben</i>	C-15
Geochronology of TAG and Snakepit Hydrothermal Fields, Mid-Atlantic Ridge: Witness to a Long and Complex Hydrothermal History <i>C. Lalou, G. Thompson, M. Arnold, E. Brichet, E. Druffel, and P. A. Rona</i>	C-15
Trace Metals in Contemporary and 17th-Century Galapagos Coral: Records of Seasonal and Annual Variations <i>L. J. Linn, M. L. Delaney, and E. R. M. Druffel</i>	C-16
Cerium Oxidation Rates and Mechanisms in Oligotrophic and Coastal Marine Waters <i>James W. Moffett</i>	C-16
Rare Earth Elements in Sediments Off Southern California: A New Anthropogenic Indicator <i>Ilhan Otmez, Edward R. Sholkovitz, Diane Hermann, and Robert P. Eganhouse</i>	C-17
Upward Fluxes of Particulate Organic Matter in the Deep North Pacific <i>K. L. Smith, Jr., P. M. Williams, and E. R. M. Druffel</i>	C-17
Hydrothermal Activity on the Mid-Atlantic Ridge <i>G. Thompson, S. E. Humphris, C. Lalou, and P. A. Rona</i>	C-17
Organic Matter in Peru Upwelling Sediments—Analysis by Pyrolysis, Pyrolysis-Gas Chromatography (PY-GC) and PY-GC Mass Spectrometry (PY-GCMS) <i>Jean K. Whelan, Zoltan Kanyo, Martha Tarafa, and Mark A. McCaffrey</i>	C-18
Chemistry of Superoxide (O_2^-) Ion-radical in Seawater I. pK_{asw}^* (HOO) and Uncatalyzed Dismutation Kinetics Studied by Pulse Radiolysis <i>O. C. Zafriou</i>	C-18

DEPARTMENT OF GEOLOGY AND GEOPHYSICS

GEOCHEMISTRY

- Melting in the Oceanic Upper Mantle: An Ion Microprobe Study of Diopsides in Abyssal Periodites
Kevin T. M. Johnson, Henry J. B. Dick and Nobumichi Shimizu GG-1

GEOLOGY

- The Late Early Eocene Montagnais Meteorite: No Impact on Biotic Diversity
Marie-Pierre Aubry, Felix M. Gradstein and Lubomir F. Jansa GG-1

- Evolution of Marine Geology During the Past Fifty Years
K. O. Emery and David A. Ross GG-1

- Structure and Topography of the Siqueiros Transform Fault System: Evidence for the Development of Intra-Transform Spreading Centers
Daniel J. Fornari, David G. Gallo, Margo H. Edwards, John A. Madsen, Michael R. Pefit, and Alexander N. Shor GG-2

- Particle Deposition in the Present and Holocene Black Sea
Bernward Hay and Susumu Honjo GG-2

- Interannual Variability in Particle Flux in the Southwestern Black Sea
B. J. Hay, S. Honjo, S. Kempe, V. A. Ittekkot, E. T. Degens, T. Konuk and E. I. dar GG-2

- A Finite Amplitude Necking Model of Rifting in Brittle Lithosphere
Jian Lin and E. M. Parmentier GG-3

- Sound Production by Hydrothermal Vents
Sarah A. Little and Keith D. Stolzenbach GG-3

- Genetic Global Geomorphology
Elazar Uchupi and K. O. Emery GG-3

- North Atlantic Ocean Basin: Aspects of Geologic Structure and Evolution
P. R. Vogt and B. E. Tucholke GG-4

- Microearthquake Evidence for Extension Across the Kane Transform Fault
W. S. D. Wilcock, G. M. Purdy and S. C. Solomon GG-4

- Accumulation of Holocene Banktop Sediment on the Western Margin of Great Bahama Bank: Modern Progradation of a Carbonate Megabank
R. Jude Wilber, John D. Milliman and Robert B. Halley GG-5

GEOPHYSICS

- Acoustic Waveform Logs, and the In-Situ Measurement of Permeability - A Review
Daniel R. Burns GG-5

- Three Dimensional Numerical Modelling of Geoacoustic Scattering from Seafloor Topography
Daniel R. Burns and Ralph A. Stephen GG-6

- Seismic Reflection Structure of the Upper Oceanic Crust: Implications from DSDP Site 504B, Panama Basin
J. A. Collins, T. M. Brocher and G. M. Purdy GG-6

- Seismic Velocity Structure at DSDP Site 504B, Panama Basin: Evidence for Thin Oceanic Crust
J. A. Collins, G. M. Purdy and T. M. Brocher GG-6

Comment on "The Geometry of Propagating Rifts" by D.P. McKenzie <i>Martin C. Kleinrock</i>	GG-7
Detailed Tectonics Near the Tip of the Galapagos 95.5°W Propagator: How the Lithosphere Tears and a Spreading Axis Develops <i>Martin C. Kleinrock and R. N. Hey</i>	GG-7
Migrating Transform Zone and Lithospheric Transfer at the Galapagos 95.5°W Propagator <i>Martin C. Kleinrock and R. N. Hey</i>	GG-8
Tectonics of the Failing Spreading System Associated with the 95.5°W Galapagos Propagator <i>Martin C. Kleinrock, Roger C. Searle and R. N. Hey</i>	GG-8
Evidence from Gravity Data for Focussed Magmatic Accretion Along the Mid-Atlantic Ridge <i>J. Lin, G. M. Purdy, H. Schouten, J.-C. Sempere and C. Zervas</i>	GG-9
Transform Zone Migration: Implications of Bookshelf Faulting at Oceanic and Icelandic Propagating Rifts <i>Jason Phipps-Morgan and Martin C. Kleinrock</i>	GG-9
Buoy Based Measurements of Ocean Heat Flux in the Fram Strait <i>Donald K. Perovich, Walter B. Tucker, III and Richard A. Krishfield</i>	GG-9
High-Resolution Inversion for South Atlantic Plate Kinematics Using Joint Altimeter and Magnetic Anomaly Data <i>Peter R. Shaw and Steven C. Cande</i>	GG-10
Using Topographic Slope Distributions to Infer Seafloor Patterns <i>D. K. Smith and P. R. Shaw</i>	GG-10
Solutions to Range Dependent Benchmark Problems by the Infinite Difference Method <i>Ralph A. Stephen</i>	GG-10
Seismic Stratigraphy in a Transverse Ridge, Atlantis II Fracture Zone <i>Stephen A. Swift, Hartley Hoskins and Ralph A. Stephen</i>	GG-11
The Magnetic Structure of Axial Seamount, Juan de Fuca Ridge <i>Maurice A. Tivey and H. Paul Johnson</i>	GG-11
Heat Flow and the Thermal Origin of Hot spot Swells: The Hawaiian Swell Revisited <i>R. P. Von Herzen, M. J. Cordery, R. S. Detrick, and C. Fang</i>	GG-12
OCEANOGRAPHY	
The Ocean Enterprise Concept <i>D. A. Ross, M. A. Champ, J. E. Dailey and C. E. McLain</i>	GG-12
The Spatial Distribution of Silicoflagellates in the Region of the Gulf Stream Warm Core Ring 82B: Application to Water Mass <i>K. Takahashi, P. L. Blackwelder and J. D. Billings</i>	GG-13
Historical Development and Use of Thousand-Year-Old Tide Prediction Tables <i>Yang Zuosheng, K. O. Emery and Xui Xui</i>	GG-13
PALEOCEANOGRAPHY	
The Influence of Microhabitats on the Carbon Isotopic Composition of Deep-Sea Benthic Foraminifera <i>Daniel C. McCorkle, Lloyd D. Keigwin, Bruce H. Corliss and Steven R. Emerson</i>	GG-13
Radiolarian from the Distal Bengal Fan in the Equatorial Indian Ocean ODP Leg 116 <i>Kozo Takahashi</i>	GG-14

PALEONTOLOGY

- Orbital Forcing, Calcareous Nannofossils and Stable Isotopes in Upper Miocene Sediments from the North Atlantic Ocean
Luc Beaufort and Marie-Pierre Aubry GG-14
- Cenozoic Bathyal and Abyssal Calcareous Benthic Foraminiferal Zonation
W. A. Berggren and Kenneth G. Miller GG-14
- Globorotalia truncatulinoides*' Growth and Chemistry as Probes of the Past Thermocline: 1. Shell Size
G. P. Lohmann and Peter N. Schweitzer GG-15
- Globorotalia truncatulinoides*' Growth and Chemistry as Probes of the Past Thermocline: 2. Shell Shape
G. P. Lohmann and Peter N. Schweitzer GG-15
- On Eigenshape Analysis
G. P. Lohmann and P. N. Schweitzer GG-16
- Life History and the Evolution of Ontogeny in the Ostracode Genus *Cyprideis*
P. N. Schweitzer and G. P. Lohmann GG-16

SEDIMENTOLOGY

- Morphology, Sediments and Structure of the Amirante Trench, Western Indian Ocean: Implications for Trench Origins
John E. Damuth and David A. Johnson GG-16
- KAIKO Project, A Preliminary Result (On Particle Sedimentation Study in Japan Trench at 8,798 m)
Susumu Honjo GG-17
- Discharge of Fluvial Sediment to the Oceans: Global, Temporal and Anthropogenic Implications
John D. Milliman GG-17
- Increased Particle Flux to the Deep Ocean Related to Monsoons
R. R. Nair, V. Ittekkot, S. J. Manganini, V. Ramaswamy, B. Haake, E. T. Degens, B. N. Desai and S. Honjo GG-17
- Gravels in the Atlantis II Fracture Zone
Stephen A. Swift GG-18
- Carbonate Platforms in Space and Time in the Atlantic
Elazar Uchupi GG-18

TECHNICAL REPORTS

- A Search for Layering in the Ocean Crust
John A. Collins GG-18
- Cruise Report: GOFS Leg 1 International Study of the North Atlantic Bloom, March-April 1989
Susumu Honjo, Steven J. Manganini and Richard Krishfield GG-19

DEPARTMENT OF APPLIED OCEAN PHYSICS AND ENGINEERING

Measurements of Tidal Flow Around a Headland with a Shipboard Acoustic Doppler Current Profiler <i>W. Rockwell Geyer and Richard Signell</i>	AOPE-1
Multisensor Modeling of Undersea Terrain <i>W. Kenneth Stewart</i>	AOPE-1
Second-Order Turbulence Model of a Couette Flow <i>Catherine Villaret</i>	AOPE-1
Energy Dissipation Just Beneath the Air Water Interface and Consequences for Gas Transfer <i>Nuri Merzi, Eugene A. Terray and Mark A. Donelan</i>	AOPE-1
Determination of Compressional Wave Speed Profiles Using Modal Inverse Techniques in a Range-Dependent Environment in Nantucket Sound <i>George V. Frisk, James F. Lynch and Subramaniam D. Rajan</i>	AOPE-2
Improvements in Three-Dimensional Raytracing Codes for Underwater Acoustics <i>A.E. Newhall, J.F. Lynch, C.S. Chiu and J.R. Daugherty</i>	AOPE-2
Numerical Simulations of Surface Wave Refraction in the North Sea Part 1: Kinematics <i>Hans C. Graber, Michael W. Byman and Wolfgang Rosenthal</i>	AOPE-3
Numerical Simulations of Surface Wave Refraction in the North Sea Part 2: Dynamics <i>Hans. C. Graber, Michael W. Byman and Heinz Günther</i>	AOPE-3
An Acoustic Telemetry System for Deep Ocean Mooring Data Acquisition and Control <i>Josko Catipovic, Maz Deffenbaugh, Lee Freitag and Dan Frye</i>	AOPE-3
Observation of Shear-Free Turbulence Beneath Whitecaps in the Marine Surface Layer <i>E.A. Terray, A.J. Williams III and B.H. Brumley</i>	AOPE-3
Implementation of a Third-Generation Ocean Wave Model on UNIX-Based Workstations <i>Hans C. Graber and Michael Caruso</i>	AOPE-4
A 200 KHz Deep Sea Interferometric Side Scan Sonar System <i>Christopher von Alt</i>	AOPE-4
Severe Environment Surface Mooring (Sesmoor) <i>Sean M. Kery</i>	AOPE-5
Cross Sections and Modulation Transfer Functions at L- and Ku-Bands Measured During the TO-WARD Experiment <i>William C. Keller and William J. Plant</i>	AOPE-5
Engineering Surface Oceanographic Mooring (ESOM) <i>Alessandro Bocconcelli</i>	AOPE-5
A Signal Processing System for Underwater Acoustic ROV Communication <i>Lee E. Freitag and Josko A. Catipovic</i>	AOPE-6
Three-Dimensional Modeling of Seafloor Backscatter from Sidescan Sonar for Autonomous Classification and Navigation <i>W. Kenneth Stewart</i>	AOPE-6
Numerical Simulation of Tidal Dispersion Around a Coastal Headland <i>Richard P. Signell and W. Rockwell Geyer</i>	AOPE-6
Diving in support of Buoy Engineering: The Ream Project <i>Sean M. Kery</i>	AOPE-7

Performance Limitations in Underwater Acoustic Telemetry <i>Josko A. Catipovic</i>	AOPE-7
Surface Wave, Internal Wave, and Moving Source Effects on Matched Field Processing Source Location Schemes <i>John R. Daugherty and James F. Lynch</i>	AOPE-7
Influence of Environmental Conditions on Acoustical Properties of Sea Ice <i>K.C. Jezek, T.K. Stanton, A.J. Gow and M.A. Lange</i>	AOPE-8
Application of Twersky's Boss Scattering Theory to Laboratory Measurements of Sound Scattered by a Rough Surface <i>D. Chu and T.K. Stanton</i>	AOPE-8
Sound Scattering by Spherical and Elongated Shelled Bodies <i>Timothy K. Stanton</i>	AOPE-8
Plane Wave Reflection from a Random Fluid Half-Space <i>Dajun Tang and George V. Frisk</i>	AOPE-9
A Technique for Making Unbiased Estimates of Current from a Wave-Follower <i>Markku J. Santala and Eugene A. Terray</i>	AOPE-9
Managing Computing Resources <i>Robert C. Groman</i>	AOPE-9
Measurements and Modeling of the Spatial Structure of Nonlinear Tidal Flow around a Headland <i>W. Rockwell Geyer and Richard Signell</i>	AOPE-9
An Experimental Investigation of the Quasi-Statics and Dynamics of a Long Vertical Tow Cable <i>Dana R. Yoerger, Mark A. Grosenbaugh, Michael S. Triantafyllou, Knut Engebretsen and James Burgess</i>	AOPE-10
A Full-Scale Experimental Study of the Effect of Shear Current on the Vortex-Induced Vibration and Quasi-Static Configuration of a Long Tow Cable <i>M.A. Grosenbaugh, D.R. Yoerger and M.S. Triantafyllou</i>	AOPE-10

DEPARTMENT OF PHYSICAL OCEANOGRAPHY

OCEAN CIRCULATION & LOW FREQUENCY VARIABILITY

Observations of Offshore Shelf Water Transport Induced by a Warm-Core Ring <i>Terrence M. Joyce, James K. B. Bishop and Otis B. Brown</i>	PO-1
Physical Structure and Temporal Evolution of Gulf Stream Warm-Core Ring 82B <i>Terrence M. Joyce and Trevor J. McDougall</i>	PO-1
Comparison of M_2 Tidal Currents Observed by Some Deep Moored Current Meters with Those of the Schwiderski and Laplace Models <i>James R. Luyten and Henry M. Stommel</i>	PO-1
A Deep Reaching Anticyclonic Eddy in the Subtropical Gyre of the Eastern South Atlantic <i>M. S. McCartney and M. E. Woodgate-Jones</i>	PO-2
Equatorial Deep Jets in the Atlantic Ocean <i>Rui M. Ponte, James Luyten and Philip L. Richardson</i>	PO-2
Evidence for Wind-Driven Current Fluctuations in the Eastern North Atlantic <i>R. M. Samelson</i>	PO-2
On the Sources of the Florida Current <i>William J. Schmitz, Jr. and Philip L. Richardson</i>	PO-2
Coupled Sea Ice - Mixed Layer Simulations for the Southern Ocean <i>Achim Stössel, Peter Lemke and W. Brechner Owens</i>	PO-3
Observations of the Pacific North Equatorial Current Bifurcation at the Philippine Coast <i>J. M. Toole, R. C. Millard, Z. Wang and S. Pu</i>	PO-3
Deep Circulation in the Eastern South Atlantic <i>Bruce A. Warren and Kevin S. Speer</i>	PO-4
Surges of Antarctic Bottom Water into the North Atlantic <i>John A. Whitehead</i>	PO-4
THEORETICAL & LABORATORY MODELS	
A Simple Kinematic Mechanism for Mixing Fluid Parcels across a Meandering Jet <i>Amy S. Bower</i>	PO-4
Solitary Waves on Conduits of Buoyant Fluid in a More Viscous Fluid <i>Karl R. Helfrich and John A. Whitehead</i>	PO-5
Maximizing Buoyancy Flux Across Layered Geostrophic Sections <i>Nelson G. Hogg and Henry M. Stommel</i>	PO-5
How Currents in the Upper Thermocline could Advect Meddies Deeper Down <i>Nelson G. Hogg and Henry M. Stommel</i>	PO-5
Performance of a Primitive-Equation Numerical Ocean Circulation Model on Loosely-Coupled Multiprocessor Systems <i>Hsiao-ming Hsu, Jih-Kwon Peir and Dale B. Haidvogel</i>	PO-6
On the Structure of Inertial Western Boundary Currents with Two Moving Layers <i>Rui Xin Huang</i>	PO-6

Sensitivity of a Multi-layered Oceanic General Circulation Model to the Sea Surface Thermal Boundary Condition <i>Rui Xin Huang</i>	PO-6
On the Three-Dimensional Structure of the Wind-Driven Circulation in the North Atlantic <i>Rui Xin Huang</i>	PO-7
Does Atmospheric Cooling Drive the Gulf Stream Recirculation? <i>Rui Xin Huang</i>	PO-7
Cross Sections of Two Layer Inertial Gulf Stream <i>Rui Xin Huang and Henry Stommel</i>	PO-7
Matching a Ventilated Thermocline Model with Inertial Western Boundary Currents <i>Rui Xin Huang</i>	PO-7
A Coupled Sea Ice - Mixed Layer - Pycnocline Model for the Weddell Sea <i>P. Lemke, W. B. Owens and W. D. Hibler III</i>	PO-8
On the Influence of the Continental Slope on the Western Boundary Layer - The Enhanced Transport and Recirculation <i>Zhengyu Liu</i>	PO-8
Sensitivity Studies with a Sea Ice - Mixed Layer - Pycnocline Model in the Weddell Sea <i>W. B. Owens and P. Lemke</i>	PO-8
On the Propagation of Velocity Discontinuities on Potential Vorticity Fronts <i>Joseph Pedlosky</i>	PO-8
The Dynamics of the Oceanic Subtropical Gyre <i>Joseph Pedlosky</i>	PO-9
The Nonlinear Behavior of Varicose Disturbances in a Simple Model of the Gulf Stream <i>L. J. Pratt, J. Earles, P. Cornillon and J.F. Cayula</i>	PO-9
Two-Layer Rotating Hydraulics: Strangulation, Remote and Virtual Controls <i>Larry Pratt and Larry Armi</i>	PO-9
Local Baroclinic Instability of Flow over Variable Topography <i>R. M. Samelson and J. Pedlosky</i>	PO-9
OCEAN MIXING AND SMALL SCALE PROCESSES	
On the Density Ratio Balance in the Central Water <i>Raymond W. Schmitt</i>	PO-10
Mesoscale Eddy Diffusion, Particle Sinking and the Interpretation of Sediment Trap Data <i>David A. Siegel, Timothy C. Granata, Anthony F. Michaels and Tommy D. Dickey</i>	PO-10
Meridional Variations of the Springtime Phytoplankton Community in the Sargasso Sea <i>D. A. Siegel, R. Iturriaga, R. R. Bibigare, R. C. Smith, H. Pak, T. D. Dickey, J. Marra, and K. S. Baker</i>	PO-10
Experimental Observations of Baroclinic Eddies on a Sloping Bottom <i>John A. Whitehead, Melvin E. Stern, Glenn R. Flierl and Barry Klinger</i>	PO-11
COASTAL CIRCULATION & DYNAMICS	
On the Damping of Free Coastal-Trapped Waves <i>K. H. Brink</i>	PO-11

Steady Two-Layer Exchange Through the Strait of Gibraltar <i>Harry L. Bryden and Thomas H. Kinder</i>	PO-11
Velocity and Hydrographic Structure of Subsurface Shelf Water at the Gulf Stream's Edge <i>James H. Churchill, Peter Cornillon and Peter Hamilton</i>	PO-11
Gulf Stream Water on the Shelf and Upper Slope North of Cape Hatteras <i>James H. Churchill and Peter C. Cornillon</i>	PO-12
Effect of Wave-Current Interaction on Wind-Driven Circulation in Narrow, Shallow Embayments <i>R. P. Signell, R. C. Beardsley, H. C. Graber and A. Capotondi</i>	PO-12
Scattering of Coastal-Trapped Waves by Irregularities in Coastline and Topography <i>John L. Wilkin and David C. Chapman</i>	PO-13
INSTRUMENTATION & EXPERIMENTAL METHODOLOGY	
Shipboard and Altimetric Studies of Rapid Gulf Stream Variability Between Cape Cod and Bermuda <i>Terrence M. Joyce, Kathryn A. Kelly, David M. Schubert and Michael J. Caruso</i>	PO-13
A Modified Objective Mapping Technique for Scatterometer Wind Data <i>Kathryn A. Kelly and Mike J. Caruso</i>	PO-14
Iodine Losses During Winkler Titrations <i>George P. Knapp, Marvel C. Stalcup and Robert J. Stanley</i>	PO-14
Observations of Ocean Ku-Band Radar Cross Section at Low Wind Speed During FASINEX <i>F. K. Li, G. Neumann and R. A. Weller</i>	PO-14
On the Calculation of the Brunt-Väisälä Frequency <i>R. Millard, W. B. Owens and N. P. Fofonoff</i>	PO-14
Improved Meteorological Measurements from Buoys and Ships for the World Ocean Circulation Experiment <i>Robert A. Weller and David S. Hosom</i>	PO-15
Measuring Near-Surface Meteorology over the Ocean from an Array of Surface Moorings in the Subtropical Convergence Zone <i>Robert A. Weller, Daniel L. Rudnick, Richard E. Payne, Jerome P. Dean, Nancy J. Pennington and Richard P. Trask</i>	PO-15
Measuring Upper Ocean Variability from an Array of Surface Moorings in the Subtropical Convergence Zone <i>R. A. Weller, D. L. Rudnick, N. J. Pennington, R. P. Trask and J. R. Valdes</i>	PO-16
TECHNICAL REPORTS	
Satellite Data Processing System Users Manual V1.0 (SDPS) <i>Michael Caruso, and Chris Dunn</i>	PO-16
Improved Meteorological Measurements from Buoys and Ships (IMET): Preliminary Comparison of Precipitation Sensors <i>Gennaro H. Crescenti and Robert A. Weller</i>	PO-16
Improved Meteorological Measurements from Buoys and Ships (IMET): Preliminary Analysis of Solar Radiation and Motion Data from IMET Test Buoy <i>Gennaro H. Crescenti, Robert A. Weller, David S. Hosom and Kenneth E. Prada</i>	PO-16
Improved Meteorological Measurements from Buoys and Ships (IMET): Preliminary Comparison of Solar Radiation Air Temperature Shields <i>Gennaro H. Crescenti, Richard E. Payne and Robert A. Weller</i>	PO-16

Improved Meteorological Measurements from Buoys and Ships (IMET): Preliminary Comparison of Pyranometers <i>Gennaro H. Crescenti, Richard E. Payne and Robert A. Weller</i>	PO-17
Dissolved Oxygen Measurements in Sea Water at the Woods Hole Oceanographic Institution <i>George P. Knapp, Marvel C. Stalcup and Robert J. Stanley</i>	PO-17
CTD Observations Off Northern California During the Shelf Mixed Layer Experiment, SMILE, November 1988 <i>Richard Limeburner and Robert C. Beardsley</i>	PO-17
CTD Observations Off Northern California During the Shelf Mixed Layer Experiment, SMILE, February/March 1989 <i>Richard Limeburner and Robert C. Beardsley</i>	PO-17
CTD Observations Off Northern California During the Shelf Mixed Layer Experiment, SMILE, May 1989 <i>Richard Limeburner and Robert C. Beardsley</i>	PO-18
CTD Observations in the Great South Channel During the South Channel Ocean Productivity Experiment, SCOPEX, May - June 1989 <i>Richard Limeburner and Robert C. Beardsley</i>	PO-18
CTD Observations on the North Brazil Shelf During A Multidisciplinary Amazon Shelf SEDiment Study, AMASSEDS, August 1989 <i>Richard Limeburner and Robert C. Beardsley</i>	PO-18
Improved Meteorological Measurements from Buoys and Ships (IMET): Preliminary Report on Barometric Pressure Sensors <i>Richard E. Payne, Gennaro H. Crescenti and Robert A. Weller</i>	PO-19
Surface Velocity in the Equatorial Oceans (20N -20S) Calculated from Historical Ship Drifts <i>Philip L. Richardson and Theresa K. McKee</i>	PO-19
FASINEX (Frontal Air-Sea Interaction Experiment) Moored Instrumentation <i>Richard P. Trask, Jerome P. Dean, James R. Valdes, Craig D. Marquette</i>	PO-19
Gulf Stream Recirculation Experiment - Part II <i>C. M. Wooding, W. B. Owens, M.E. Zemanovic and J. R. Valdes</i>	PO-19

MARINE POLICY CENTER

Biology and Conservation of Sea Turtles Nesting in Quintana Roo, Mexico, During 1988 <i>M. Tundi Agardy and Regna Gil Hernandez</i>	MP-1
Draft Guidelines for Coastal Biosphere Reserve Planning <i>M. Tundi Agardy</i>	MP-1
What Scientific Information is Critical for Management, and Why? <i>M. Tundi Agardy</i>	MP-1
Workshop on the Soviet Maritime Arctic <i>Lawson W. Brigham</i>	MP-1
Economizing Human Responses to Subsidence and Rising Relative Sea Level <i>James M. Broadus</i>	MP-2
Impacts of Future Sea Level Rise <i>James M. Broadus</i>	MP-2
Possible Impacts of and Adjustments to Sea Level Rise: The Cases of Bangladesh and Egypt <i>James M. Broadus</i>	MP-2
World Ocean Pollution Status Report <i>James M. Broadus</i>	MP-3
Marine Non-Fuel Minerals in the U.S. Exclusive Economic Zone: Managing Information as a Resource <i>James M. Broadus and Porter Hoagland</i>	MP-3
Defining a Key Industry: Marine Electronics Instrumentation <i>James M. Broadus, Porter Hoagland and Hauke L. Kite-Powell</i>	MP-3
Benefits and Incentives for Investment in Biosphere Reserves <i>James M. Broadus, John Wargo and Jane Robertson Vernhes</i>	MP-4
NEPA and the Conservation of Biological Diversity <i>Cynthia Carlson</i>	MP-4
An Evaluation of International Protection Offered to Caribbean Coral Reefs and Associated Systems <i>Lynn Davidson and Kristina Gjerde</i>	MP-4
Report of a Meeting of the Marine Biological Diversity Working Group <i>Mark E. Eiswerth</i>	MP-5
Does Analysis Matter? Economics, Litigation and Planning in the Department of the Interior <i>Scott Farrow</i>	MP-5
Financial Accounting for the OCS Leasing Program <i>Scott Farrow</i>	MP-5
Modeling the Importance of Oceans and Estuaries <i>Scott Farrow</i>	MP-5
Developing a National Marine Electronics Agenda, Massachusetts Centers of Excellence Corporation <i>Arthur G. Gaines</i>	MP-6
Edgartown Harbor Provides Model for Harbor Resources Management <i>Arthur G. Gaines and Richard M. Butler</i>	MP-6
Nitrogen Inputs to a Marine Embayment: The Importance of Groundwater <i>Anne E. Giblin and Arthur G. Games</i>	MP-6

Observations of Long-Term Tide-Gauge Records for Indications of Accelerated Sea-Level Rise <i>V. Gornitz and A. Solow</i>	MP-6
Iterative Techniques for Characterizing Marine Bird Habitats with Time-Series of Satellite Images <i>J. Christopher Haney</i>	MP-7
Remote Characterization of Marine Bird Habitats with Satellite Imagery <i>J. Christopher Haney</i>	MP-7
Winter Habitat of Common Loons on the Continental Shelf of the Southeastern United States <i>J. Christopher Haney</i>	MP-7
The 1988 IMO Convention on the Safety of Maritime Navigation: Towards a Legal Remedy for Terrorism at Sea <i>Christopher C. Joyner</i>	MP-8
The Antarctic Minerals Agreement: An Appraisal <i>Christopher C. Joyner</i>	MP-8
Ice-Covered Regions in International Law <i>Christopher C. Joyner</i>	MP-8
Review Article - The Evolving Antarctic Legal Regime <i>Christopher C. Joyner</i>	MP-9
Suppression of Terrorism on the High Seas: The 1988 IMO Convention on the Safety of Maritime Navigation <i>Christopher C. Joyner</i>	MP-9
Marketing, Ecological, and Policy Considerations Related to the New England Conch Fishery and <i>Hoploplana</i> <i>Ilene M. Kaplan, Barbara C. Boyer, and Daniela Hoffmann</i>	MP-9
Marine Policy Implications Related to the Commercial Value and Scientific Collecting of the Whelk <i>Busycon</i> . <i>Ilene M. Kaplan, Barbara C. Boyer, and Kristen A. Santos</i>	MP-9
Planning for the Galápagos Marine Resources Reserve <i>Richard A. Kenchington</i>	MP-10
Achieving Marine Conservation Through Biosphere Reserve Planning and Management <i>Richard A. Kenchington and M. T. Agardy</i>	MP-10
Coastal Area Management in Sri Lanka <i>Kem Lowry and H. J. M. Wickremeratne</i>	MP-10
Signals or Noise? Explaining the Variation in Recreation Benefit Estimates <i>V. Kerry Smith and Yoshiaki Kaoru</i>	MP-10
What Have We Learned Since Hotelling's Letter? A Meta Analysis <i>V. Kerry Smith and Yoshiaki Kaoru</i>	MP-11
Discriminating Between Models: An Application to Relative Sea Level at Brest <i>Andrew R. Solow</i>	MP-11
Geostatistical Cross-Validation: A Cautionary Note <i>Andrew R. Solow</i>	MP-11
On the Statistical Comparison of Climate Model Output and Climate Data <i>Andrew R. Solow</i>	MP-11

Reconstructing a Partially Observed Record of Tropical Cyclone Counts <i>Andrew R. Solow</i>	MP-11
Climatic Catastrophe: On the Horizon or Not? <i>Andrew R. Solow and James M. Broadus</i>	MP-12
On the Detection of Greenhouse Warming <i>Andrew R. Solow and James M. Broadus</i>	MP-12
Nonparametric Binary Regression: An Application to Particle Capture by a Ciliated Suspension Feeder <i>Andrew R. Solow and Scott M. Gallager</i>	MP-12
On the Relationship Between the Southern Oscillation and Tropical Cyclone Frequency in the Australian Region <i>Andrew R. Solow and Neville Nicholls</i>	MP-13
Inhomogeneity and Apparent Organization in Animal Behavior <i>Andrew R. Solow and Peter Tyack</i>	MP-13
The Ocean "Landscape" <i>John H. Steele</i>	MP-13

GRADUATE STUDENTS

Organic Nitrogen Utilization by Phytoplankton: the Role of Cell-Surface Deaminases <i>Brian P. Palenik</i>	GS-1
A Search for Layering in the Oceanic Crust <i>John A. Collins</i>	GS-1
An Investigation of the Marine Geochemistry of Gold <i>Kelly K. Falkner</i>	GS-2
Molecular Regulation of the Induction of Cytochrome P-450E in the Estuarine Fish <i>Fundulus heteroclitus</i> <i>Pamela J. Kloepper-Sams</i>	GS-3
Swimming Behavior and Energetics of Sharks <i>Jill V. Scharold</i>	GS-4
Efficient Representation of the Hydrographic Structure of the North Atlantic Ocean and Aspects of the Circulation from Objective Methods <i>Ichiro Fukumori</i>	GS-5
The Trace Metal Geochemistry of Suspended Oceanic Particulate Matter <i>Robert M. Sherrell</i>	GS-5
Rates of Vertical Mixing, Gas Exchange, and New Production: Estimates from Seasonal Gas Cycles in the Upper Ocean near Bermuda <i>William S. Spitzer</i>	GS-6
Diffusion of Helium Isotopes in Silicate Glasses and Minerals: Implications for Petrogenesis and Geochronology <i>Thomas W. Trull</i>	GS-7
Trace Metal Sources for the Atlantic Inflow to the Mediterranean Sea <i>Alexander F.M.J. van Geen</i>	GS-8
Ocean Bottom Seismic Scattering <i>Martin E. Dougherty</i>	GS-9
Tidal Dynamics and Dispersion around Coastal Headlands <i>Richard P. Signell</i>	GS-9
Acoustic Tomography in the Straits of Florida <i>David B. Chester</i>	GS-10
Collinear Analysis of Altimeter Data in the Bering Sea <i>Deborah K. Barber</i>	GS-10
The Structure of the Kuroshio West of Kyuchu <i>Changsheng Chen</i>	GS-10
A Numerical Model of Mixing and Convection Driven by Surface Buoyancy Flux <i>Xiaoming Wang</i>	GS-11
Deeply-Towed Underwater Vehicle Systems: A Verified Analytical Procedure for Creating Parameterized Dynamic Models <i>Franz S. Hover</i>	GS-12
A Control System Design Technique for Nonlinear Discrete Time Systems <i>David M. DeLonga</i>	GS-12

Acoustic Diffraction from a Semi-Infinite Elastic Plate under Arbitrary Fluid Loading with Application to Scattering from Arctic Ice Leads <i>Peter H. Dahl</i>	GS-12
Evolution of Icelandic Central Volcanoes: Evidence from the Austurhorn Plutonic and Vestmannaeyjar Volcanic Complexes <i>Tanya H. Furman</i>	GS-13
Modelling Bottom Stress in Depth-Averaged Flows <i>Harry L. Jenter, II</i>	GS-14
An Application of Ocean Wave-Current Refraction to the Gulf Stream Using SEASAT SAR Data <i>Michael W. Byman</i>	GS-15
Incorporating Thruster Dynamics in the Control of an Underwater Vehicle <i>John G. Cooke</i>	GS-15
Surface Wave, Internal Wave, and Source Motion Effects on Matched Field Processing in a Shallow Water Waveguide <i>John R. Daugherty</i>	GS-15
A Code-Division, Multiple Beam Sonar Imaging System <i>John M. Richardson</i>	GS-16
Inference of Ecology from the Ontogeny of Microfossils <i>Peter N. Schweitzer</i>	GS-16

DEPARTMENT OF BIOLOGY

Peter H. Wiebe, Chairman

BENTHOS

ABYSSOTHERMA PACIFICA N. GEN. N. SP., A RECENT REMANEICID (FORAMINIFERIDA: REMANEICACEA) FROM THE EAST PACIFIC RISE

Paul Brönnimann, Cindy Lee Van Dover and
John E. Whittaker

A new Recent remaneicid, *Abyssotherma pacifica*, is described from recruitment arrays placed in the vicinity of deep-sea (2,600) hydrothermal springs in the East Pacific. It is a close isomorph of the shallow, brackish-water species *Bruneica clypea* Brönnimann, Keij and Zaninetti, but differs in possessing two apertures per chamber in contrast to the single interiomarginal aperture of *Bruneica*.

Published in: *Micropaleontology*, 35(2), 142-149, 1989.

Supported by: Ocean Ventures; Education Office; and NSF Grants OCE81-17119 and OCE83-11029.

WHOI Contribution No. 7124.

BENTHIC MARICULTURE AND RESEARCH RIG DEVELOPED FOR DIVER OPERATIONS

George R. Hampson, Donald C. Rhoads and
Dan W. Clark

A benthic structure has been designed and deployed in 18 meters of water in the center of Buzzards Bay for two years for the purpose of growing mussels and other molluscs. This structure can also be used for settlement and growth studies of other marine species where long-term field experiments are required.

The structure is designed to be deployed on the bottom, and extends vertically 3.5 meters above the sediment surface. The food source consists of detritus suspended from the bottom by the tidal stream (Benthic Turbidity Zone).

The structure is based on a design that utilizes materials that are readily available, structurally stable in sea water, and are low in cost. Deployment and recovery of the structure can be done with vessels >7 meters in length.

Installation of grow-out ropes, cages, or experiments on the rig by SCUBA divers is facilitated by hooks and snaps which permit rapid attachment or recovery of deployed materials.

Supported by: Associated Scientists at Woods Hole (ASAWH); and NOAA Sea Grant NA86-AA-D-50G090, R/B-90-PD.

WHOI Contribution No. 7188.

ADAPTATIONS FOR REPRODUCTION AMONG DEEP-SEA MOLLUSCS: AN APPRAISAL OF EXISTING EVIDENCE

Rudolf S. Scheltema

Large regions of the deep sea underlying central oligotrophic waters of major ocean basins are presumed to be stable and physically monotonous areas with continuous darkness and constant temperature. However, regions of great depth, near the borders of oceans may include a variety of ephemeral habitats. Turbidity currents, intense eddy-driven currents or deep-sea "storms" are temporally unpredictable events related to the boundaries of oceans. Changes in surface productivity and the introduction of wood and other organic debris are most marked and seasonal near continental land masses. Moreover accretion and subduction along the margins of plates (i.e., the Mid-Atlantic Ridge) results in ephemeral habitats such as hydrothermal vents and areas of volcanism associated with tectonic activity. As might be anticipated deep-sea molluscs show adaptation in fecundity, periodicity and mode of development in relation to these varying environments. When more is known about their life history, reproduction of benthic deep-sea molluscs doubtlessly will prove to be fully as varied as that encountered in the more familiar shoal-water sublittoral environment.

Supported by: NSF Grant OCE84-10262.

WHOI Contribution No. 7223.

BEHAVIOR, SURVIVAL AND SEDIMENT SURFACE TRACES OF DEEP-SEA BENTHIC INVERTEBRATES IN THE LABORATORY

James R. Weinberg

Living bivalves (*Nucula*, *Thyasira*), gastropods (*Frigidoalvania*) and calcareous foraminifera (*Laticarinina*, *Lenticulina*), from 775 m depth in the northwest Atlantic, were maintained in the laboratory for 772 days to measure their survival, feeding behavior, movement, and effects of their movements on sediment characteristics. The organisms, < 4 mm in size, were maintained at 1 atm and at 5°C in cups containing sediment and sea water. Over the 772 day period, 46% of all bivalves survived. Minimum estimates for survival of *Laticarinina* in 6 containers ranged from 0-67% for a 1-2 year period. Survival of other species was not estimated either because they were rare or because I could not determine whether they were alive. Taxonomic groups differed in behavior and in their effects on sediments, and these are

demonstrated with time-lapse photographs. Bivalves burrowed down into the sediment and formed permanent burrows with openings to the surface, averaging 0.68 mm in diameter. In general, they did not move horizontally and rarely produced tracks or fissures across the sediment surface. In contrast, the gastropod produced numerous trails, and moved at the fastest rate across the sediment surface, averaging 150 mm day⁻¹. The gastropod crawled up the container sides and upside-down at the air-water interface, but did not burrow beneath the sediment surface. *Laticarinina* had the most diverse behavior. It 1) burrowed down and crawled beneath the sediment surface, creating fissures in the surface, 2) emerged from below the sediment surface and crawled across the surface in both vertical and flat positions, creating narrow or wide tracks, respectively, 3) crawled up the sides of containers, and 4) produced arc-shaped feeding traces in the sediment surface averaging 4.15 mm in length. To evaluate whether the conditions of foraminifera degenerated over time, rate of tract production on the surface was measured after the animals had been in the laboratory for one month, and again after 26 months. A degenerated condition was not indicated because average track length produced per day by *Laticarinina* was not significantly different between dates, 16.43 and 11.54 mm day⁻¹, respectively. This study demonstrates that it is feasible to study the ecology of continental slope fauna and their effects on sediments in the laboratory.

Supported by: WHOI Independent Study Award; and a NOAA/NURC Grant.

WHOI Contribution No. 7288.

BIOGEOGRAPHY AND SYSTEMATICS

THE APACOPHORA AS A TETHYAN SLOPE TAXON: EVIDENCE FROM THE PACIFIC

Amélie H. Scheltema

Recent aplacophoran collections from the Pacific yield information on global distributions of this class of Mollusca. A former Tethyan or pre-Tethyan distribution is suggested by the disjunct occurrence of five species which form a subgroup within the genus *Falcidens*, two from the western Atlantic and three from the western Pacific; by three species of the genus *Prochaetoderma* with a similar disjunct distribution; and by the broadly distributed family Pararrhopalidae. High diversity of species and less than 40% numerical dominance by any one species

typify samples from slope stations off southeast Australia, whereas low diversity and dominance greater than 60% typify the shelf in Bass Strait; the latter may reflect the disruptive effects of Pleistocene regression of sea level. Three species pairs with one of each pair occurring on the slope and the other on the shelf may indicate that shelf species evolved from slope species. A new genus with eight species, seven from slope and abyssal hydrothermal vents, is comprised of six species from slope depth and two from abyssal depths; the abyssal species have character states derived from the shallower species. The evidence from present-day distribution of species, genera, and families indicates that the Aplacophora were already widespread on continental slopes by Tethyan times.

In Press: *Bulletin of Marine Science*.

Supported by: Without Support.

WHOI Contribution No. 7072.

EVOLUTION

MORPHOLOGICAL DIVERGENCE OF EASTERN PACIFIC AND CARIBBEAN ISOPODS: EFFECTS OF A LAND BARRIER AND THE PANAMA CANAL

J. R. Weinberg and V. R. Starczak

The Isthmus of Panama rose approximately 3 million years before the present (mybp) and isolated biotas in the tropical eastern Pacific from those in the Caribbean Sea. Populations that were split by the Isthmus and have evolved in allopatry since that time are known as geminates. The surf zone/beach isopod *Excirolana braziliensis* Richardson was examined between 1984 and 1989 to test the hypothesis that divergence in geminate isopod morphology has occurred, and that geminate divergence is greater than divergence between local populations from the same coastline. Three morphs of *Excirolana braziliensis*, one in the Caribbean and two in the eastern Pacific, were discovered using numerical taxonomic methods that adjust for body size. The two Pacific morphs have overlapping large-scale distributions, but those morphs are segregated on a smaller scale by beach. We inferred that one Pacific morph and one Caribbean morph were geminates, based on their relative similarity in shape, their geographical ranges, and natural history information about the organism's dispersal capabilities. The origin of the third morph probably predates the Isthmus of Panama, given its relative dissimilarity from the geminate morphs. The presumed geminates differ primarily with respect to the rostrum, antennae

and one male reproductive structure. Divergence between geminates is greater than divergence between local populations of any morph along a coastline. Because only one morph occurs in the Caribbean, that region contains less morphological variation than the eastern Pacific, which contains two morphs. There was weak evidence that some introductions may have taken place in the last century from the Caribbean to the Pacific; however, introductions have not masked the pattern of divergence that has developed over millions of years.

Published in: *Marine Biology*, 103, 143-152, 1989.

Supported by: WHOI; and fellowships from the Smithsonian Institution.

WHOI Contribution No. 6969.

PREMATING ISOLATION AND CHROMOSOME VARIATION BETWEEN POPULATIONS OF A COASTAL MARINE POLYCHAETE

James R. Weinberg, Victoria R. Starczak,
Cornelia Mueller, Gerald G. Pesch and
Sara M. Lindsay

In theory, low gene flow between populations and sexual selection within populations enable populations to diverge and become reproductively isolated at the premating stage. Degrees of reproductive isolation should increase with geographical distance between populations due to reduced gene flow with greater distance. This prediction was tested using two Pacific and two Atlantic populations of the coastal marine polychaete *Nereis acuminata* (also known as *Neanthes arenaceodentata* and *N. caudata*). *N. acuminata* should have low gene flow between populations because adults live in sediment and the worm does not produce planktonic larvae. Furthermore, sexual selection affects individual fitness because both sexes use intrasexual aggression to obtain a mate, and males and females probably assess each other's identity with sex pheromones.

Results from pairing experiments between the four populations supported the "isolation with distance" hypothesis, expected for an organism with low dispersal and complex mating behavior. There was no evidence from 10-minute or 36-hour trials of premating isolation between the two Pacific populations, located approximately 25 km apart. Incomplete premating isolation was found between the two Atlantic populations, located approximately 110 km apart. Their incomplete isolation was represented in 10-minute trials by greater aggression between males and females than that measured in control (within population)

trials. There was no evidence from 36-hour trials that these Atlantic populations have any premating isolation, because they always paired to mate within 36 hours. Complete premating isolation was found between Atlantic and Pacific populations, which are 1000s of kilometers apart. During 10-minute trials, males and females from different oceans often attacked and then avoided each other, and they never paired to mate. Nor did they pair to mate in longer, 36-hour trials.

These populations were also compared with respect to karyotype and tolerance to cold water temperature. Atlantic populations studied had a diploid number of 22 acrocentric chromosomes while the Pacific populations had 18 metacentric or submetacentric chromosomes. Pacific individuals were less able to tolerate cold water than Atlantic individuals. These results suggest strongly that the Atlantic and Pacific populations have been allopatric for a long time, and are different species. This counters earlier suggestions that these Pacific populations may have been introduced around 1950 from the colder N. Atlantic. We conclude that the data support the "isolation with distance" model, but that additional populations need to be studied along each coastline, to better determine the geographical scale over which populations have diverged in karyotype and in mate recognition cues.

Supported by: WHOI; and USEPA CR-8143895-01-1.

WHOI Contribution No. 7218.

FISHES

SONIC SIGNATURES OF SPAWNING FISHES

Phillip S. Lobel

Two examples of fishes producing sounds while actually spawning are reported. The species are Caribbean coral reef fishes; a hamletfish, *Hypoplectrus unicolor* (Serranidae) and a parrotfish, *Scarus iserti* (Scaridae). The reproductive behaviors of these two species have been extensively studied by many scientists, but the association of sound with spawning is new. Both fishes produce distinctive sound patterns at the same time as broadcasting gametes in midwater: *H. unicolor* appears to use muscle stimulation of the swimbladder for its sound source, and the group fin movements themselves induce hydrodynamic noise in *S. iserti*. Both sounds are distinct and recognizable enough to allow counting and acoustic mapping of spawning events in these species.

Supported by: Island Foundation; The Kelley Foundation; Sippican Corporation; The Smith Special Studies Fund of WHOI; NOAA Sea Grant NA86-AA-D-SG090, R/B-97-RD; and NOAA National Undersea Research Program, 89-09-NA88-AAH-UR020.

WHOI Contribution No. 7250.

ANADROMOUS BEHAVIOR OF BROOK CHARR (*SALVELINUS FONTINALIS*) IN THE MOISIE RIVER, QUEBEC

W. Linn Montgomery, Stephen D. McCormick, Robert J. Naiman, Frederick G. Whoriskey and Geoff Black

During May-June 1980, brook charr migrated from Rivière à la Truite, a tributary of the Moisie River, to the Moisie River estuary. Charr >15 cm FL and ≥3 years of age entered saline waters of the estuary or the Gulf of St. Lawrence; smaller, younger charr remained in the surface layer of fresh water. Charr near the estuary's mouth fed on both marine and freshwater foods, while those upstream depended almost exclusively on insects. Growth averaged 4.3% of initial body weight per day for specimens at large for more than 30 days. Charr returning to Rivière à la Truite during August-September were dominated by females and showed a high frequency of maturation. Charr which migrate to coastal marine waters encounter supplementary marine foods, experience improved growth, and exhibit increased fecundity relative to trout remaining in the river.

In Press: *Polskie Archiwum Hydrobiologii*.

Supported by: WHOI Postdoctoral Fellowship; and the Matamek Research Program.

WHOI Contribution No. 7040.

GEOCHEMISTRY

A CONCEPTUAL FRAMEWORK FOR INTERPRETING LEAD IN MARINE PLANKTONIC ORGANISMS AND PELAGIC FOOD WEBS

Anthony F. Michaels and A. Russell Flegal

The bioaccumulation of lead in biological ecosystems traditionally has been interpreted in terms of the atomic ratio of lead to calcium. However, in marine planktonic ecosystems, most of the particulate calcium is found in the skeletons of a subset of all species and the amount of calcium present can be highly variable. The lead in

plankton can be partitioned between skeletal and non-skeletal components. In plankton samples collected in the equatorial Pacific Ocean, less than 0.5% of the lead was associated with CaCO₃ (primarily foraminiferan, coccolithophore and pteropod skeletons), while up to 54% of the lead in these samples may have been associated with the SrSO₄ skeletons and organic bodies of acantharia. Atomic ratios of lead to calcium were highly variable, principally because of the varying amounts of CaCO₃ in the samples. Therefore, normalizing lead concentrations to biomass rather than calcium is preferable for interpreting the bioactivity of lead in planktonic food webs. We develop a simple model based on the surface area to volume ratio of organisms to make predictions about the relative importance of organism size and food web interactions in the transfer of lead between trophic levels. For small organisms (less than 0.5 mm spherical diameter or the equivalent surface:volume ratio), the lead concentration is determined almost entirely by their surface area. For larger organisms, the total body lead will be a function of both the size of the prey and the distribution of lead within tissues. The role of food web interactions (e.g., grazing) in determining the amount of lead in plankton of different sizes will only be important for large plankton and nekton, where very little of the lead is absorbed on the animal surface.

Supported by: NSF Grant OCE86-12113.

WHOI Contribution No. 6988.

UNEXPECTED CHANGES IN THE OXIC/ANOXIC INTERFACE IN THE BLACK SEA

J. W. Murray, H. W. Jannasch, S. Honjo, R. F. Anderson, W. S. Reeburgh, Z. Top, G. E. Friederich, L. A. Codispoti and E. Izdar

The Black Sea is the largest anoxic marine basin in the world today. Below the layer of oxygenated surface water hydrogen sulfide builds up to concentrations as high as 500 μm in the deep water down to the maximum depth of 2200 m. The hydrographic regime is characterized by low salinity surface water of river origin overlying high salinity deep water of Mediterranean origin. A steep pycnocline, centered at about 50 m, is the primary physical barrier to mixing and is the origin of the stability of the anoxic (oxygen/hydrogen sulfide) interface. We report new observations that indicate dramatic changes in the oceanographic characteristics of the anoxic interface of the Black Sea over decadal or shorter time scales. The anoxic, sulfide containing interface has moved up in the water column since

the last U.S. cruises in 1969 and 1975. In addition, a suboxic zone overlays the sulfide containing deep water. The previously described overlap of oxygen and sulfide was not present. Horizontal mixing or flushing events provide a unified explanation for these observations.

Published in: *Nature*, 338(6214), 411-413, 1989.

Supported by: NSF Grant OCE86-08124.

WHOI Contribution No. 7010.

MINERALOGICAL AND CHEMICAL COMPOSITION OF HYDROTHERMAL DEPOSITS AT DEEP-SEA VENTS OF THE EAST PACIFIC RISE AND THE GULF OF CALIFORNIA

D. Rose, R. Huber and H. W. Jannasch

The mineralogical and chemical properties and the sequence of crystallization of 3 black smoker samples from the Guaymas Basin, Gulf of California (27°00'N, 111°24'W) and the East Pacific Rise (EPR, at 10°59'N, 103°41'W) was determined. In all samples a zonation in two or three concentric layers was detected which were described and identified by mineralogical and chemical compositions. Two smoker samples from the Guaymas Basin were characterized by an inner zone of sulfide minerals (wurtzite, pyrrhotite, chalcopyrite and galena) surrounded by a thick layer of sulfate- and carbonate-minerals. The sample from the EPR represented the "massive sulfide" type with mainly chalcopyrite, sphalerite + pyrite, and pyrite throughout the smoker wall.

Supported by: NSF Grant OCE87-00581.

WHOI Contribution No. 7055.

MARINE MAMMALS

REVIEW OF THE SIGNATURE-WHISTLE HYPOTHESIS FOR THE ATLANTIC BOTTLENOSE DOLPHIN

Melba C. Caldwell, David K. Caldwell and Peter L. Tyack

This paper summarizes 20 years of research on the signature whistles of bottlenose dolphins, *Tursiops truncatus*. We analyzed 22,278 whistles from 126 dolphins. Most of the dolphins produced 100% individually distinctive signature whistles; only 3 ranged below 51% and all of these were males. The percentage of each dolphin's whistles which were stereotyped signature whistles averaged

94%. For both sexes, there was a decrease in the percentage of signature whistles with age. Individual bottlenose dolphins also varied the percentage of signature whistles as a function of behavioral context, but each of 4 individuals tested had different individual-specific patterns of variation in this and other acoustic features across four behavioral conditions. Many whistles are made up of a variable number of repetitions of a component of the whistle, termed a loop. No differences between the sexes were noted in the average or maximum number of loops per whistle or in whistle durations, but there was a highly significant increase in both number of loops and whistle duration with age, with older dolphins producing more loops and longer whistles. The average whistle duration was 0.96 sec. The lowest frequency of whistles ranged from 1-9 kHz, and the mode was 5 kHz. The highest frequency ranged from 8- >24 kHz, with a mode of 13-15 kHz. There was no significant variation in these parameters with age or sex, but total frequency modulation of whistles did show a significant increase with age. The data summarized here is consistent with the hypothesis that each dolphin develops an individually distinctive whistle which is used to broadcast individual identity to other members of its group. While some acoustic features of these whistles are remarkably stable for periods of over a decade, other features vary with context and many communicate other forms of information, but even these context-specific variations appear to vary across individuals.

Supported by: ONR N00014-87-K-0236; and PHS Grant 1 R29 NS25290.

WHOI Contribution No. 7156.

HUMPBACK WHALES MEGAPTERA NOVAEANGLIAE FATALLY POISONED BY DINOFLAGELLATE TOXIN

Joseph A. Geraci, Donald M. Anderson, Ralph J. Timperi, David J. St. Aubin, Gregory A. Early, John H. Prescott and Charles A. Mayo

Between November 28, 1987 and January 3, 1988, 14 humpback whales (*Megaptera novaeangliae*) stranded dead along the beaches of Cape Cod Bay and northern Nantucket Sound, MA. While not unusual for toothed whales, group mortality of this kind is unprecedented for baleen whales, which come ashore rarely and singly. Based on the nature and timing of the episode, behavioral observations of a terminally-ill animal, condition of the carcasses, and laboratory analyses of food-fish and whale tissues, we conclude that the whales died by consuming mackerel (*Scomber*

scombrus) containing saxitoxin (STX). This neurotoxin, which is the cause of Paralytic Shellfish Poisoning (PSP) in humans, is produced by marine dinoflagellates and certain bacteria. This is the first report of STX accumulation and transfer through a living, commercially important pelagic fish, and of its role in killing marine mammals.

Published in: *Canadian Journal of Fisheries and Aquatic Sciences*, 46, 1895-1898, 1989.

Supported by: Natural Sciences and Engineering Research Council of Canada (A6130); Marine Mammal Commission; NSF Grant OCE86-14210; and the Coastal Research Center of WHOI.

WHOI Contribution No. 7071.

SIGNATURE WHISTLES OF FREE-RANGING BOTTLENOSE DOLPHINS *TURSIOPS TRUNCATUS*: STABILITY AND MOTHER-OFFSPRING COMPARISONS

*Laela S. Sayigh, Peter L. Tyack, Randall S. Wells
and Michael D. Scott*

Mother-calf whistle exchanges were recorded from temporarily captured free-ranging bottlenose dolphins from 1975 to 1989. This is part of a long-term research project studying social structure and behavior of a community of approximately 100 dolphins in waters near Sarasota, Florida. Analysis of whistle exchanges from 12 mother-calf pairs shows that signature whistles can remain stable for periods up to at least 12 years. We looked for effects of vocal learning on the development of the signature whistle by comparing whistles of calves to those of their mothers. Eight female calves produced whistles distinct from those of their mothers, while four male calves produced whistles similar to those of their mothers. Male calves appeared to produce a greater proportion of whistles other than the signature whistle (termed "variants"). We hypothesize that these sex differences in whistle vocalizations may reflect differences in the roles males and females play in the social structure of the community.

In Press: *Behavioral Ecology and Sociobiology*.

Supported by: Ocean Ventures Fund Award; ONR Grant N00014-87-K-0236; PHS Grant 5 R29 NS25290; Marine Mammal Commission; National Marine Fisheries Service; Earthwatch; and contribution of funds and equipment to Dolphin Biology Research Associates, Inc.

WHOI Contribution No. 7127.

AN ACOUSTIC MODEL DESCRIBING HOW MIGRATING GRAY WHALES *ESCHRICHTIUS ROBUSTUS* AVOID INDUSTRIAL NOISE

*Peter L. Tyack, Charles I. Malme,
Robert W. Pyle, Paul R. Miles,
Christopher W. Clark and James E. Bird*

Playback experiments were performed with gray whales, *Eschrichtius robustus*, off Big Sur, California during their southward migrations in January of 1983 and 1984. The objective of the experiments was to determine the degree of behavioral response of migrating gray whales to acoustic stimuli associated with oil and gas exploration and development activities. The playback sounds consisted of a single 100 cu. in. air gun and tape recordings of underwater acoustic signatures of a drilling platform, drillship, production platform, semisubmersible drilling rig and a helicopter overflight.

This paper establishes that gray whales respond to industrial waterborne sounds depending on the characteristics of the signal, its received level, and the signal-to-background noise conditions. Movement patterns of whales were quantified using theodolites on land stations. A computer-implemented track analysis program was established to analyze the theodolite data for any possible changes in speed, linearity of track, orientation toward the sound source, and distance from shore. The results of this program were cumulative track frequency distributions which were statistically analyzed to determine significant differences between experimental and control conditions.

Migrating whales responded to the presence of a noise source by slowing down and by small course changes as they approached the source. This "detection" reaction often occurred at ranges where the estimated level of the noise source was equal to the local ambient noise level. In the test area, this corresponded to ranges of 2 to 3 km. The result of these small course changes, as the whales approached the sound source, was an increase in the distance between the whales and the source at the closest point of approach (CPA). This "avoidance" behavior resulted in a lower sound level exposure than would have occurred had the whale maintained the original course.

The probability that whales would avoid a given sound level was calculated for each playback stimulus by comparing the difference in number of whale tracks at CPA for different distances to the source under control and experimental conditions. By converting the probability of avoidance distribution of range values to a distribution of sound exposure levels, using measured sound

propagation characteristics for the test area, a set of sound exposure characteristics were obtained which permitted prediction of the probability that migrating whales would avoid a region of high noise level. These sound exposure characteristics thus are specific for the industrial noise sources used in the experiments but are not site-specific.

The probability of avoidance analysis showed that avoidance behavior began at sound exposure levels of 164 dB (effective pulse pressure re 1 μPa) for the air gun. Whales showed nearly complete avoidance of the area ensounded at levels of 180 dB or more. For the other playback stimuli, which were continuous sounds, the threshold of avoidance behavior was around 110-120 dB (re 1 μPa). Avoidance was greater than 80% for regions with signal levels higher than 130 dB.

An estimate of the effective range of the original noise sources (from which the tape recorded signals were obtained) was made by assuming operation in the test area. The effective range for a 50% probability of avoidance for most of the playback sources was estimated as less than 100 m. The effective range for the drillship was estimated as 1.1 km and for the air gun, 400 m. Based on acoustic data obtained for a 4000 cu. in. seismic array, the effective range for broadside sound exposure is 2.5 km. Short-term behavioral response of migrating gray whales to the onset of air gun sounds was also observed at ranges of less than 5 km. These effective ranges are based on sound propagation in the test area off Soberanes Point, California, and are specific to this site. This same response model predicts that large ships may evoke avoidance at greater ranges than any of the industrial stimuli studied here.

Supported by: Minerals Management Service
Contract No. AA851-CT2-39 and
14-12-0001-29033.

WHOI Contribution No. 7155.

MARINE POLLUTION

POLYCHLORINATED BIPHENYL CONCENTRATION AND ALTERED CYTOCHROME P-450E EXPRESSION IN WINTER FLOUNDER FROM CONTAMINATED ENVIRONMENTS

Adria A. Elskus, Lucia C. Susani, Dianne Black,
Richard J. Pruell, Steven J. Fluck and
John J. Stegeman

Reproductively mature winter flounder (*Pseudopleuronectes americanus*) were collected from three northeastern U.S. sites with different degrees of polychlorinated biphenyl (PCB) and

polynuclear aromatic hydrocarbon (PAH) contamination. Liver PCB concentrations (measured by capillary electron capture-gas chromatography) in fish collected in 1987 and 1988 at New Bedford Harbor (NBH) ranged from 7.4-191 $\mu g/g$ dry wt.; at Gaspee Point (GP) 3.9-17.7 $\mu g/g$; and at Fox Island (FI) 1.6-15.1 $\mu g/g$. Levels of ethoxyresorufin O-deethylase (EROD) activity were similar in fish of the same reproductive status from the three sites; however, immunoquantitated P-450E homolog (the EROD catalyst) content was significantly higher in NBH fish. This suggests that P-450E catalytic activity is being suppressed in the livers of the NBH animals. Recent studies in our laboratory indicate competitive inhibition of the P-450E catalytic activity by specific PCB congeners is one likely mechanism of this suppression. Hepatic EROD activity and P-450E content were significantly lower in gravid females (EROD, 0.10 to 0.69 units per nmol P-450; P-450E, 8.4 to 19% of spectral P-450) than in spent females (EROD, 1.94 to 3.49; P-450E, 48 to 109%), and ripe males (EROD, 1.86 to 3.41; P-450E, 48 to 84%) at all sites. This is consistent with a hormonal effect on P-450E expression, and thus EROD activity, in gravid females. The data indicate a complex relationship between levels of EROD activity, or P-450E, and tissue PCB concentrations in highly contaminated fish. How these variables are linked to altered endocrine or gonadal function is not yet known.

In Press: *Marine Environmental Research*.

Supported by: EPA Grant CR-813155; and PHS Grant ES-04220.

WHOI Contribution No. 7082.

INDUCTION OF CYTOCHROME P450E (P450IA1) BY 2,3,7,8-TETRACHLORODIBENZOFURAN (2,3,7,8-TCDF) IN THE MARINE FISH SCUP (*STENOTOMUS CHRYSOPS*)

Mark E. Hahn, Bruce R. Woodin and
John J. Stegeman

The halogenated aromatic hydrocarbons (chlorinated biphenyls, dibenzofurans, and dibenzo-p-dioxins) are known to be potent inducers of P450IA1 in mammals. These compounds have been found in marine sediments and biota, but the ability of specific members of these groups of compounds to induce teleost P450IA1 is, with limited exceptions, unknown. Our recent studies have shown that the structure-activity relationship for induction of scup P450IA1 (P450E) by polychlorinated biphenyls (PCBs) may differ from that seen with mammalian species. We are now examining the induction of

P450E by chlorinated dibenzofurans. A single intraperitoneal dose (3.1 µg/kg; 10 nmol/kg) of 2,3,7,8-tetrachlorodibenzofuran (2,3,7,8-TCDF) produced a strong, sustained induction of P450E mRNA, protein, and ethoxyresorufin O-deethylase (EROD) activity in scup. Thus, this compound and other chlorinated dibenzofurans and chlorinated dibenzo-p-dioxins may contribute to the induction of P450IA1 observed in feral fish from contaminated environments.

In Press: *Marine Environmental Research*, 28, 1989.

Supported by: PHS Grant ES-04220; and a SURDNA Foundation Postdoctoral Fellowship in Marine Biomedical Research.

WHOI Contribution No. 7081.

THE RELATIONSHIP BETWEEN LIPID COMPOSITION AND SEASONAL DIFFERENCES IN THE DISTRIBUTION OF PCBs IN *MYTILUS EDULIS* L.

Judith McDowell Capuzzo, John H. Farrington,
Pirjo Rantamaki, C. Hovey Clifford,
Bruce A. Lancaster, Dale F. Leavitt and
Xiaoping Jia

The concentrations of individual chlorobiphenyl congeners were measured in the mussel *Mytilus edulis* transplanted to several stations in Buzzards Bay and Nantucket Sound, MA (USA). Individual stations represented a gradient of chemical contamination and the sampling period extended over a complete annual cycle. Fluctuations in concentrations of some chlorobiphenyl congeners were apparent at all stations during autumn; this pattern was correlated with the seasonal cycle of gametogenesis and spawning activity. Relative redistribution and release of individual chlorobiphenyl congeners associated with spawning is not consistent, suggesting differential partitioning of specific congeners in different tissues or lipid pools. These patterns are consistent with our general view of the bioconcentration of organic contaminants in marine organisms. The major factors controlling the distribution of PCBs in mussels are the relative concentration of individual contaminants in ambient waters, modified to some extent by differences in partitioning between organisms and water (as indicated by differences in K_{ow}), and seasonal variations in lipid content.

In Press: *Marine Environmental Research*.

Supported by: NOAA Sea Grant NA 86-AA-D-SG090, R/P-22 and R/P-17; and USEPA CR-814895-01-1.

WHOI Contribution No. 7076.

MICROBIOLOGY

DENITRIFICATION, NITROGEN-FIXATION AND NITROUS OXIDE CONCENTRATIONS THROUGH THE BLACK SEA OXIC-ANOXIC INTERFACE

Dennis A. Bazylinski, Brian L. Howes and
Holger W. Jannasch

Denitrification was measured as nitrous oxide accumulation using an acetylene block technique at Stations 2 and 3 (Leg 2), and Station 1 (Leg 5) of the R/V KNORR Black Sea Cruises in May and July 1988. Denitrification rates showed significant spatial variability on both horizontal and vertical scales. Maximum activity (0.1 µM/hr) was found at Station 2 being about four- to six-fold higher than that at the other two stations. Nitrous oxide production (under C₂H₂) showed distinct maxima in both oxic and anoxic zones, corresponding to the upper and lower boundaries of the nitrate zone. The data suggest that denitrification may be an important but variable biogeochemical process in the Black Sea.

Background nitrous oxide concentrations through the oxic/anoxic interface (0-140 m) showed no consistent differences among the three stations. Concentrations up to 30 nM were measured and were comparable to other oceanic environments. Nitrous oxide profiles showed no strong maxima although concentrations tended to decrease at the nitrate maxima and in the anoxic zone. Nitrogen-fixation, measured as ethylene production from acetylene, was undetectable at any site or depth even where ammonium and nitrate were apparently depleted or in low concentration. Parallel measurements in a seasonally stratified coastal salt pond were in strong contrast to those of the Black Sea. Although nitrous oxide concentrations were similar and declined below the oxic/anoxic interface, denitrification was negligible and nitrogen-fixation pronounced.

Supported by: NSF Grant OCE86-08124.

WHOI Contribution No. 7138.

MICROBIAL UTILIZATION OF NATURALLY-OCCURRING HYDROCARBONS AT THE GUAYMAS BASIN HYDROTHERMAL VENT SITE

Dennis A. Bazylinski, Carl O. Wirsen and
Holger W. Jannasch

The Guaymas Basin (Gulf of California, depth 2000 m) is a site of hydrothermal activity in which

petroliferous material is formed by thermal alteration of deposited planktonic and terrestrial organic matter. We investigated certain components of these naturally occurring hydrocarbons as potential carbon sources for a specific microflora at these deep-sea vent sites. Respiratory conversion of [1-¹⁴C]hexadecane and [1(4.5.8)-¹⁴C]naphthalene to ¹⁴CO₂ was observed at 4° and 25°C, some at 55°C, but none at 80°C. Bacterial isolates were capable of growing on both substrates as the sole carbon source. All isolates were aerobic and mesophilic with respect to growth on hydrocarbons but also grew at low temperatures (4-5°C). These results correlate well with previous geochemical analyses, indicating microbial hydrocarbon degradation, and show that at least some of the thermally-produced hydrocarbons at Guaymas Basin are significant carbon sources to vent microbiota.

Published in: *Applied Environmental Microbiology*, 55, 2832-2836, 1989.

Supported by: NSF Grant OCE87-00581; and ONR Contract 88-K-0386.

WHOI Contribution No. 7125.

STABLE ISOTOPE STUDIES OF THE CARBON, NITROGEN AND SULFUR CYCLES IN THE BLACK SEA AND THE CARIACO TRENCH

*Brian Fry, Holger W. Jannasch,
Stephen Molyneaux, Carl O. Wirsen,
Jo Ann Nicholson and Stagg King*

Samples for stable isotope studies of possible chemosynthesis in anoxic basins were collected in a 1986 cruise to the Cariaco Trench and a May 1988 cruise to the Black Sea. POM (particulate organic matter) collected in the oxic/anoxic interface regions of the water column showed no distinctive carbon or nitrogen isotopic compositions that could be associated with chemosynthetic bacteria. Carbon and nitrogen isotopic compositions at POM concentration maxima near the oxic/anoxic interface were -23 and 4.5 ‰ respectively, in both the Black Sea and the Cariaco Trench. Measurements of dissolved inorganic carbon (DIC) also indicated that carbon respired during decomposition at depth was isotopically similar to phytoplankton, with no distinctive component that could be attributed to chemosynthetic carbon. Respired carbon added to deep waters of the Black Sea averaged -23.1 ‰ and, as previously established by Deuser (1970a), -22 ‰ in the Cariaco Trench.

In the uppermost 150 m of anoxic bottom waters, sulfide isotopic compositions changed significantly in a region of sulfide oxidation,

increasing up to 14 ‰ vs. deep-water background values of -40.5 ‰ in the Black Sea and -31 ‰ in the Cariaco Trench. These increases in sulfide isotopic compositions are consistent with chemical oxidation of sulfides, but not consistent with sulfide oxidation by photosynthetic bacteria. Growth experiments with sulfate-reducing bacteria suggested that part of the increase in sulfide isotopic compositions could also be due to rapid rates of sulfate reduction in the oxic/anoxic interface regions.

Supported by: NSF Grant OCE86-08124.

WHOI Contribution No. 7121.

AMMONIUM REGENERATION AND CARBON UTILIZATION BY MARINE BACTERIA GROWN ON MIXED SUBSTRATES

J. C. Goldman and M. R. Dennett

In batch growth experiments we examined the impact of exposure of natural populations of marine bacteria to multiple nitrogen and carbon sources. The resulting substrate C:N ratio (C:N_s) was adjusted to span a range from 1.5:1 to 9:1 with equal amounts of different amino acids and NH₄⁺ supplemented with glucose to maintain the C:N_s ratio equal to that of the respective amino acid. We found that NH₄⁺ uptake was totally prevented in the presence of arginine and that catabolism of arginine led to a 70% NH₄⁺ regeneration efficiency; however, NH₄⁺ contributed 47 to 64% of the total nitrogen used for biosynthesis in the presence of alanine or glutamate, and >87% when the amino acid was aspartate or phenylalanine. Glucose utilization was complete for all treatments, being used solely as an energy source when arginine was present and as a combined energy and carbon source for the other treatments. In all experiments the gross growth efficiency based on total carbon utilization was ≈ 50%. Also, the C:N ratio of the bacterial biomass was fairly constant at 4.5:1 by atoms for all treatments. Thus it is evident that when a suitable carbon substrate is available, NH₄⁺ uptake will co-occur and in some situations dominate over amino acid uptake, thereby preventing catabolic regeneration of NH₄⁺. Key factors controlling the "source" or "sink" role for bacteria in marine waters clearly are the C:N_s ratio of the sum of available nitrogen and carbon substrates and the type of nitrogen (inorganic or organic) present. Since the dynamics of nitrogen cycling by bacteria is intimately connected to carbon uptake, the roles of both substrates must be evaluated.

Supported by: NSF Grant OCE87-16026.

WHOI Contribution No. 7287.

**A NOVEL GROUP OF ABYSSAL
METHANOGENIC ARCHAEBACTERIA
(METHANOPYRUS) GROWING AT
110°C**

*R. Huber, M. Kurr, H. W. Jannasch and
K. O. Stetter*

The organisms with the highest growth temperature known so far are members of the archaeobacterial genus *Pyrodictium*. These anaerobic sulfur reducers thrive at temperatures of up to 110°C within a shallow hydrothermal system off Vulcano, Italy. Here we describe a novel group of methanogenic archaeobacteria growing at least at 110°C which we were able to isolate recently from sediment samples taken by the research submersible ALVIN at the Guaymas Basin hot vents (Gulf of California). This finding demonstrates the unexpected biogenic methanogenesis at temperatures above 100°C. In view of biogeochemistry, it could explain isotope discrimination at temperatures which were thought to be unfavorable for biological methanogenesis.

Published in: *Nature*, 342, 833-834, 1989.

Supported by: NSF Grant OCE87-00581.

WHOI Contribution No. 7173.

**BAROPHILES AND THEIR POTENTIAL
IN BIOTECHNOLOGY**

Holger W. Jannasch

The origin of barophilic microorganisms in various deep-sea environments and their physiological and molecular characteristics are reviewed. Applications of barophiles in microbial enhancement of oil recovery and the biological gasification of lignite and agricultural crops are discussed. Bio- and technological problems related to barophilism have been encountered in the treatment of oil well souring, in food storage under hyperbaric conditions, and in the pressure-extension of thermostability in DNA cleaving enzymes.

Published in: *Journal of Chemical Technology and Biotechnology*, 42, 320-322, 1988.

Supported by: NSF Grant OCE87-00581.

WHOI Contribution No. 7075.

**CHEMOLITHOTROPHIC
PRODUCTIVITY AT DEEP-SEA
HYDROTHERMAL VENTS**

Holger W. Jannasch

The original observation of rich invertebrate

populations at newly discovered hydrothermal vents, 2550 m deep, initiated research on their possible chemolithoautotrophic sustenance. Today, 12 years later, many qualitative and quantitative studies have confirmed a highly efficient microbial transfer of geochemical to biochemical energy in the chemosynthetic production of organic carbon ($\text{CO}_2 + 3\text{H}_2\text{S} + 2\text{O}_2 \rightarrow [\text{CH}_2\text{O}] + 2\text{S}^0 + \text{H}_2\text{SO}_4 + \text{H}_2\text{O}$, -211 kJ/mol e^-). While free-living species of the genera *Thiomicrospira* and *Thiobacillus* contribute, the bulk production takes place within unique symbiotic associations between yet unidentified procaryotes and a number of hitherto unknown marine invertebrates. Anaerobic chemoautotrophy has also been found in connection with isolations of hyperthermophilic methanogens. Here the available energy for the reduction of CO_2 is independent of photosynthetic oxidants or reductants ($4\text{H}_2 + \text{CO}_2 \rightarrow \text{CH}_4 + 2\text{H}_2\text{O}$, -33.2 kJ/mol e^-). Based on geochemical calculations, the total chemosynthetic production in the deep sea might amount to 0.1% of the oceanic photosynthetic production. This almost negligible number becomes important, however, considering the fact that only about 1% of the surface production reaches the deep sea.

Published in: *Proceedings of the 5th ISME, Kyoto*, pp. 23-27, 1989.

Supported by: NSF Grant OCE87-00581.

WHOI Contribution No. 7200.

**MASSIVE NATURAL OCCURRENCE OF
UNUSUALLY LARGE BACTERIA
(*BEGGIATO*A SP.) AT A
HYDROTHERMAL DEEP-SEA VENT
SITE**

H. W. Jannasch, D. C. Nelson and C. O. Wirsen

White web-like mats of the filamentous sulphur-oxidizing bacterium *Beggiatoa* can commonly be observed on the surface of anoxic sediments. As a typical interface organism *Beggiatoa* requires a source of inorganic reduced sulphur and dissolved free oxygen. The first pure cultures of marine strains of *Beggiatoa* were recently obtained by artificially reconstructing an $\text{O}_2/\text{H}_2\text{O}$ interface in a semi-solid medium that supports the gliding mobility of the filaments. The maximal thickness of these *Beggiatoa* "mats" in culture was 1.0 mm. We now report the discovery of dense layers of *Beggiatoa* up to 3 cm thick on the sediment surface, and up to 30 cm thick between stands of vestimentiferan tube worms at the Guaymas Basin hydrothermal vent site in the Gulf of California. The mats are essentially monocultures of *Beggiatoa*-type organisms containing three filament width classes, the largest

116-122 μm in diameter. Freshly-collected filaments showed chemoautotrophic metabolism and active gliding motility. The phenomenon of a natural mass growth of a bacterium is of great physiological and ecological interest and could also be of biotechnical importance.

Published in: *Nature*, 342, 834-836, 1989.

Supported by: NSF Grant OCE87-00581; and ONR Contract N00014-88-K-0386.

WHOI Contribution No. 7248.

CHEMOAUTOTROPHIC SULFUR-OXIDIZING BACTERIA FROM THE BLACK SEA

*H. W. Jannasch, C. O. Wirsen and
S. J. Molyneaux*

In contrast to earlier attempts, we were able to isolate nine strains of obligately chemoautolithotrophic, sulfur-oxidizing bacteria from three offshore stations in the western basin of the Black Sea (R/V KNORR Cruise 134-9, Black Sea Leg 2). The isolates grew with doubling times up to 1.3 hours over a pH range of 6.5-9.0 in artificial seawater containing thiosulfate. They also oxidized hydrogen sulfide, elemental sulfur and tetrathionate. Although acid producing, growth of the isolates was neutrophilic (range pH 6.5-9.0, optimum pH 7.5). Nitrate or manganese and iron oxides were not utilized as alternate electron acceptors. If acetate was present, not more than 10% of the incorporated carbon was mixotrophically obtained from the organic source. With a DNA base composition range of 37-40 mol % G+C, the new isolates appear to belong to the genus *Thiomicrospira* (36-44 mol % G+C) rather than *Thiobacillus* (55-68 mol % G+C). Experimental studies on the potential sulfide oxidation by the new isolates under in situ conditions suggest that, above a certain density of active cells (*ca.* $10^4/\text{ml}$), bacterial oxidation of sulfide appears to be able to compete successfully with its spontaneous chemical oxidation.

Supported by: NSF Grant OCE86-08214.

WHOI Contribution No. 7126.

SULFIDE OXIDATION IN THE ANOXIC BLACK SEA CHEMOCLINE

*Bo Barker Jorgensen, Henrik Fossing,
Carl O. Wirsen and Holger W. Jannasch*

The depth distributions of O_2 and H_2S and of the activity of chemical or bacterial sulfide oxidation were studied in the chemocline of the

central Black Sea. Relative to measurements from earlier studies, the sulfide zone had moved upwards by 20-50 m and was now (May 1988) situated at a depth of 81-99 m. Oxygen in the water column immediately overlying the sulfide zone was depleted to undetectable levels resulting in a 20-30 m deep intermediate layer of O_2 and H_2S free water. Radiotracer studies with ^{35}S -labelled H_2S showed that high rates of sulfide oxidation, up to a few $\mu\text{M d}^{-1}$, occurred in anoxic water at the top of the sulfide zone concurrent with the highest rates of dark CO_2 assimilation. The main soluble oxidized products of sulfide were thiosulfate (68-82%) and sulfate. Indirect evidence was presented for the formation of elemental sulfur which accumulated to a maximum of 200 nM at the top of the sulfide zone. Sulfide oxidation was stimulated by particles suspended at the chemocline, probably by bacteria. Green phototrophic sulfur bacteria were abundant in the chemocline and suggested that photosynthetic H_2S oxidation took place. Flux calculations showed that the measured H_2S oxidation rates were 4-fold higher than could be explained by the downward flux of organic carbon and too high to balance the availability of electron acceptors such as oxidized iron or manganese. A nitrate maximum at the lower boundary of the O_2 zone did not extend down to the sulfide zone.

Supported by: NSF Grant OCE86-08124.

WHOI Contribution No. 7101.

BIOMINERALIZATION OF FERRIMAGNETIC GREIGITE (Fe_3S_4) AND IRON PYRITE (FeS_2) IN A MAGNETOTACTIC BACTERIUM

*Stephen Mann, Nicholas H. C. Sparks,
Richard B. Frankel, Dennis A. Bazylinski
and Holger W. Jannasch*

The ability of magnetotactic bacteria to orientate and navigate along geomagnetic field lines is due to the controlled intracellular deposition of the iron oxide mineral, magnetite (Fe_3O_4). The function and crystal chemical specificity of this mineral has been considered to be unique amongst the prokaryotes. Moreover, the bacterial production of magnetite may represent a significant contribution to the natural remanent magnetism of sediments. Here we report, for the first time, the intracellular biomineralization of single crystals of the ferrimagnetic iron sulphide greigite (Fe_3S_4), in a multicellular magnetotactic bacterium common in brackish, sulphide-rich water and sediment. We show that these crystals are often aligned in chains and associated with single crystals of the non-magnetic mineral, iron pyrite

(FeS₂). Our results have important implications for understanding biomineralization processes and magnetotaxis in micro-organisms inhabiting sulphidic environments. Furthermore, the biogenic production of magnetic iron sulphides should be considered as a possible source of remanent magnetization in sediments.

Supported by: NSF Grant OCE87-00581.

WHOI Contribution No. 7213.

COMPARISON OF MAGNETITE PARTICLES PRODUCED ANAEROBICALLY BY MAGNETOTACTIC AND DISSIMILATORY IRON-PRODUCING BACTERIA

Bruce M. Moskowitz, Richard B. Frankel,
Dennis A. Bazylinski, Holger W. Jannasch
and Derek R. Lovley

We compare the magnetic properties of fine-grained magnetite produced by two newly isolated anaerobic bacteria, a magnetotactic bacterium (MV-1) and a dissimilatory iron-reducing bacterium (GS-15). Although room-temperature magnetic properties are generally different between the two microorganisms, MV-1 and GS-15 magnetites can be most easily distinguished by the temperature variation of saturation remanence obtained at liquid helium temperatures. Magnetite produced by MV-1 displays a sharp discontinuity in intensity at 100 K related to the Verwey transition. Magnetite produced by GS-15 displays a gradual decrease in intensity with temperature due to the progressive unblocking of magnetization. This difference is due exclusively to different grain size distributions produced by these microorganisms. MV-1 produces magnetite with narrow grain size distribution that is within the stable single domain size range at room temperature and below. GS-15 produces magnetite with a wide grain size distribution extending into the superparamagnetic size range. Our results suggest that a substantial fraction of particles produced by GS-15 are superparamagnetic at room temperature.

Supported by: NSF Grant OCE87-00581.

WHOI Contribution No. 6989.

MASSIVE OCCURRENCE OF LARGE, AUTOTROPHIC BEGGIATOJA AT HYDROTHERMAL VENTS OF THE GUAYMAS BASIN

Douglas C. Nelson, Carl O. Wirsen and
Holger W. Jannasch

Filamentous bacteria, identified as members of the genus *Beggiatoja* by gliding motility and internal globules of elemental sulfur, occur in massive aggregations at the deep-sea hydrothermal vents of the Guaymas Basin (Gulf of California) at a depth of 2000 m. Cell aggregates covering the surface of sulfide-emanating sediments and rock chimneys were collected by DSRV/ALVIN and subjected to shipboard and laboratory experiments. Three discrete width classes of *Beggiatoja* were found usually accompanied by a small number of flexibacteria with a cell diameter of 1.5-4.0 μm (average width from 22-35, 35-45, and 116-122 μm). As indicated by electron microscopy and low cell volume/protein ratios, the dominant bacteria are "hollow" cells, i.e., a thin layer of cytoplasm surrounding a large central liquid vacuole. Activities of Calvin-cycle enzymes from very pure samples indicate that at least two of the strains were potentially autotrophic. Judging from temperature dependence of enzyme activities and whole cell CO₂ incorporation, the widest cells were mesophiles. A narrow strain (28-32 μm wide) was either moderately thermophilic or mesophilic with unusually thermotolerant enzymes. This was consistent with its occurrence on the flanks of "hot smoker" chimneys with highly variable exit temperatures. In situ CO₂ fixation rates, sulfide-stimulation of incorporation and autoradiographic studies suggest that these *Beggiatoja* strains are indeed autotrophic and contribute significantly as primary producers to the Guaymas Basin vent ecosystems.

Published in: *Applied and Environmental Microbiology*, 55(11), 2909-2917, 1989.

Supported by: NSF Grant OCE87-00581.

WHOI Contribution No. 7021.

THERMOCOCCUS LITORALIS SP. NOV.: A NOVEL SPECIES OF EXTREMELY THERMOPHILIC MARINE ARCHAEABACTERIA

Annemarie Neuner, Holger W. Jannasch and
Shimshon Belkin

By 16S rRNA sequence, the order *Thermococcales* represents the deepest branch-off within the group of methanogenic/halophilic archaeobacteria, although the members of this order

resemble the phenotype of the extremely thermophilic sulfur metabolizing archaeobacteria. At present two genera are evident within the *Thermococcales*: the genus *Pyrococcus*, consisting of the species *Pyrococcus furiosus* and *Pyrococcus woesei*, which grow at more than 100°C, and the genus *Thermococcus*, represented up to now by only one species, *Thermococcus celer*. *Thermococcus celer* is an organotrophic organism, growing up to 93°C within geothermally heated submarine sediments or hydrothermal systems by means of either sulfur respiration or fermentation.

Two new isolates were obtained from shallow submarine thermal springs in Italy: Strain NS-C was isolated from the beach near Lucrino, Naples, and strain A3 from Vulcano Island. The two isolates were found to represent a novel species within the genus *Thermococcus*, which is described in this paper.

Supported by: ONR Contract 88-K-0386; and NSF Grant OCE87-00581.

WHOI Contribution No. 7098.

**ERYTHROSPHAERA MARINA GEN. NOV.,
SP. NOV.: A DIAZOTROPHIC
UNICELLULAR CYANOBACTERIUM
CULTURED FROM THE TROPICAL
ATLANTIC OCEAN**

*S. W. Watson, F. W. Valois, D. Distel and
J. B. Waterbury*

A novel planktonic unicellular cyanobacterium capable of dinitrogen fixation in the presence of atmospheric concentrations of oxygen has been cultured from the western tropical Atlantic Ocean. It has been observed at concentrations up to 3×10^3 cells ml⁻¹ in surface waters warmer than 27°C, from 15°N to 30°S off the eastern coast of South America. Cell size varies from 2-5 μm in diameter both in cultures and natural samples. The coccoid to rod-shaped cells occur singly or in pairs, do not possess sheaths, and divide in two planes at right angles to one another. Like other cyanobacteria it contains chlorophyll *a* as its primary photosynthetic pigment. However, it is unusual in containing a predominance of phycoerythrin high in urobilin content as its major light-harvesting pigment. This cyanobacterium is obligately photoautotrophic and is incapable of growth using organic compounds as sole carbon sources. It is obligately marine requiring elevated concentrations of sodium, chloride, magnesium and calcium ions for growth. The temperature growth range is extremely narrow (26°-32°C) and is a primary determinant of the geographic distribution of this cyanobacterium. Photosynthesis and dinitrogen fixation are separated temporally with the latter

occurring during the dark portion of the diel light cycle. The DNA base ratios ranged from 30.6-31.0 mol % G+C. Its phylogenetic position determined by partial 16S rRNA sequence analysis showed that this organism is the sole representative of a deep branch within the *Synechocystis*-group of chroococcalean cyanobacteria. We propose to name this cyanobacterium *Erythrospira marina* gen. nov., sp. nov.

Supported by: NSF Grant OCE84-16960.

WHOI Contribution No. 6716.

PHYSIOLOGY AND BIOCHEMISTRY

**CHANGES IN DIGESTIVE ENZYME
ACTIVITIES DURING EARLY
DEVELOPMENT OF THE AMERICAN
LOBSTER *HOMARUS AMERICANUS*
MILNE-EDWARDS**

Patricia M. Biesiot and Judith McDowell Capuzzo

Activities of digestive protease, lipase, and amylase were measured during the course of early development in the American lobster *Homarus americanus*. Total enzyme activities per individual were very low among embryos sampled three days prior to hatching. Protease and amylase activities increased slightly at the time of hatching and again during larval Stage I; lipase activity did not change. Activity of the three enzymes more than doubled among Stage II larvae and although there were slight increases in enzyme activities during Stage III, they were not significant. Protease activity peaked during Stage IV whereas lipase and amylase activities were greatest among Stage V juveniles.

Different patterns were observed when specific enzyme activity (normalized on the basis of protein) are examined. Specific activities of the three enzymes were very low in embryos just prior to hatching and increased slightly during the hatching process. During Stage I, specific activities increased; protease activity doubled, lipase activity increased by a factor of ten, and amylase activity increased slightly. Activities of both protease and amylase more than doubled in Stage II larvae; in general, there were no significant differences in the specific activities measured in Stages II through V. Lipase specific activity did not change significantly among Stages I through V.

Lobster larvae normally hatch during early summer but embryonic development can be accelerated in the laboratory by maintenance at high (21°C) rather than ambient temperature. Temperature conditions during embryonic development, however, had no effect on digestive

enzyme activities of larvae that were induced to hatch out of season.

The increase in digestive enzyme activities among the hatching stages correlates well with morphological changes observed in the midgut gland (hepatopancreas), specifically in regard to the presence of digestive enzyme-producing B-cells. Changes in enzyme activities among the post-metamorphic Stages IV and V may be related to changes in body form, habit, or patterns of energy storage and utilization.

In Press: *Journal of Experimental Marine Biology and Ecology*.

Supported by: MIT/WHOI Joint Program in Oceanography; a Tai-Ping Foundation Predoctoral Fellowship; and NOAA Sea Grant NA80-AA-D-00077.

WHOI Contribution No. 6960.

DIGESTIVE PROTEASE, LIPASE AND AMYLASE ACTIVITIES IN STAGE I LARVAE OF THE AMERICAN LOBSTER *HOMARUS AMERICANUS*

Patricia M. Biesiot and Judith McDowell Capuzzo

1. Digestive protease, lipase, and amylase of stage I larvae of the American lobster *Homarus americanus* are characterized.
2. The pH optima for larval lobster proteases were 5.3 and 6.4 using Azocoll (10 mg/ml) as a substrate. Gastric fluid of young lobsters is ~pH 5.5, thus activity of the former protease was further characterized; activity increased with temperature from 25° to 50°C but ionic strengths between 0.1-0.7 did not significantly affect activity.
3. Larval lipase exhibited optimal activity at pH 5.5 and at a substrate concentration of 0.5 $\mu\text{g/ml}$ triolein; activity increased with temperature from 20°C to 45°C. Activity was greatest at an ionic strength of 0.5 but was not significantly different over the range 0.2 to 0.9.
4. Amylase showed a broad peak of activity at pH 6.5 through 7.0. Activity increased with temperature from 25° to 50°C; activity showed a slight peak at an ionic strength of 0.4 although there was little difference in activity from ~0.25 to 0.55.
5. A time course study was performed to determine the effect of feeding on the digestive enzyme activities of newly hatched larvae; a slight but not significant increase in protease and amylase activities occurred during the course of the first larval stage whether the larvae were fed or not, whereas lipase activity was constant.
6. A sensitive method to detect crustacean lipase was developed using an Iatroscan, which combines thin-layer chromatography (TLC) and

flame ionization detection (FID), to quantify free fatty acids (FFA) generated by lipase digestion.

In Press: *Comparative Biochemistry and Physiology*.

Supported by: A Tai-Ping Foundation Predoctoral Fellowship; and NOAA Sea Grant NA80-AA-D-00077.

WHOI Contribution No. 6961.

UPTAKE KINETICS OF PARALYTIC SHELLFISH TOXINS FROM THE DINOFLAGELLATE *ALEXANDRIUM FUNDYENSE* IN THE MUSSEL *MYTILUS EDULIS*

V. M. Bricelj, J. H. Lee, A. D. Cembella and D. M. Anderson

Laboratory experiments under controlled conditions were undertaken to investigate cell ingestion and PSP toxin incorporation by *Mytilus edulis* exposed to a high-toxicity isolate of the dinoflagellate *Alexandrium fundyense* (GtCA29). Rate of ingestion of toxic cells was maximized at 150-250 cells ml^{-1} , and declined at lower and higher concentrations. Clearance rates of dinoflagellate cells were significantly lower (by ca. 48%) than those on a non-toxic control diet of *Thalassiosira weissflogii*. Mussels exposed to a constant mean cell density of 256 *A. fundyense* cells ml^{-1} (toxicity = 66 pg cell^{-1}) over 17 d achieved a constant weight-specific ingestion rate of 0.8×10^6 cells g^{-1} tissue wet weight day^{-1} , and absorbed on the average 60-64% of the organic matter ingested. Although they had no prior PSP history, they experienced no mortality or sublethal adverse effects during intoxication. Toxin uptake followed Michaelis-Menten kinetics, attaining saturation levels of 4.5×10^4 $\mu\text{g STX eq/100 g}$ after 12-13 d. This toxicity is comparable to maximum values reported during severe red tides outbreaks in nature. Experimental results indicate that mussels can exceed the quarantine level (80 $\mu\text{g STX eq/100 g}$) in less than 1 h of exposure to this *A. fundyense* isolate, which is predominantly composed of highly potent carbamate toxins. At equilibrium, mussels incorporated 79% of the toxin ingested. This provides the first estimate of the efficiency of toxin incorporation at saturation by a bivalve species. The viscera accumulated 96% of total toxin, although they constitute only 30% of total tissue weight. The toxin profile of the muscle, mantle/gill and foot (determined by HPLC) differed significantly from that of ingested cells, showing enrichment in STX and relative reduction in GTX2+3 and neoSTX. The toxin composition of the viscera more closely resembled that of ingested cells, reflecting the presence of numerous intact cells in gut contents. Epimerization resulted

in an increase in the toxin ratio GTX3/GTX2 in mussel tissues over the course of intoxication.

Supported by: NOAA Sea Grant NA86AA-D-SG090, R/B-92.

WHOI Contribution No. 7217.

THE USE OF BIOCHEMICAL INDICATORS IN THE STUDY OF TROPHIC INTERACTIONS IN ANIMAL-BACTERIA SYMBIOSES: SOLEMYA VELUM, A CASE STUDY

Noellette Conway and Judith McDowell Capuzzo

Understanding trophic interactions between marine invertebrates and chemoautotrophic bacterial symbionts is difficult using techniques which require optimal animal and bacterial physiological condition, such as respirometry and enzyme kinetic studies. Deep-sea and hydrothermal vent symbioses are frequently damaged during collection; optimal laboratory conditions are not known, and the endosymbionts have only recently been cultured outside of the animal host. Consequently, in order to determine the contribution of the symbionts to host nutrition it is desirable to utilize parameters that are unaffected by damage to the animal during collection and storage.

In this paper we discuss the utility of biochemical markers such as stable isotope ratios and lipid composition profiles for the study of nutrition in animal-bacteria symbioses. The small protobranch bivalve *Solemya velum* is used as a general model of animal-bacteria symbioses, but the techniques discussed here are applicable to the study of other animal-bacteria and animal-plant symbioses.

In Press: *Proceedings of the 24th European Marine Biology Symposium*, Aberdeen University Press.

Supported by: Ocean Ventures Fund; Education Office at WHOI; and Summer Microbiology Course at the MBL.

WHOI Contribution No. 7210.

CHANGES IN THE BIOCHEMICAL COMPOSITION OF A SUBTROPICAL BIVALVE, ARCA ZEBRA, IN RESPONSE TO CONTAMINANT GRADIENTS NEAR BERMUDA

D. Leavitt, B. Lancaster, A. Lancaster and J. McDowell Capuzzo

To quantify the biochemical composition of a subtropical bivalve and to examine the changes in

biochemical composition in relation to contaminant gradients, the turkey wing mussel, *Arca zebra*, was deployed in cages along two contaminant gradients (Castle Harbor and Hamilton Harbor) in Bermuda for 12 days. Following exposure to the gradients, pooled homogenized samples of the mussel were analyzed for protein, ash, total lipid, and lipid class composition.

The resulting data indicated that the biochemical composition of *A. zebra* was similar to that observed in other bivalves that rely on glycogen as their primary energy substrate. Differences were noted in the lipid content and composition in mussels deployed in the two harbors. These differences suggested that Hamilton Harbor had higher food availability than Castle Harbor and consequently the *A. zebra* from Hamilton Harbor were in better physiological condition as indicated by higher lipid levels, primarily neutral lipids.

In evaluating the contaminant gradients, the biochemical composition of the mussels suggests that Castle Harbor is marginally impacted at a local dumpsite. Mussels deployed at Hamilton Harbor, on the other hand, demonstrated a response previously observed for bivalves impacted by anthropogenic inputs to the ecosystem. The *A. zebra* deployed in Hamilton Harbor had significantly increased levels of neutral lipids. An increase in the neutral lipid pool (primarily TG and FFA) may be the result of impaired mobilization of FFAs from the neutral to polar lipid pools. An alternate explanation may be the relationship of gonadal resorption following exposure to lipophilic contaminants.

Supported by: Mellon Senior Study Award.

WHOI Contribution No. 7286.

INCIDENCE OF HEMATOPOIETIC NEOPLASIA IN MYA ARENARIA: MONTHLY MONITORING OF PREVALENCE AND INDICES OF PHYSIOLOGICAL CONDITION

Dale F. Leavitt, Judith McDowell Capuzzo, Donna Miosky, Rozanna Smolowitz, Bruce Lancaster and Carol L. Reinisch

A field survey of hematopoietic neoplasia (Hn) in the soft shell clam *Mya arenaria* was undertaken using an immunoperoxidase diagnostic technique. Monthly collections of *M. arenaria* were made at two sites: Little Buttermilk Bay and New Bedford Harbor, both in Buzzards Bay, Massachusetts. Clams were diagnosed for leukemia and analyzed for soft tissue dry weight, condition index, and carbon and nitrogen content of the soft tissue. Prevalence of leukemia in *M. arenaria* exhibited a

seasonal fluctuation with a maximum prevalence in the fall and a minimum prevalence in the early summer. A second maximum peak in late winter was observed at one site. Leukemia primarily affected clams that were 3-4 years postsettlement. Lower prevalence levels were observed in both younger and older clams. Leukemic *M. arenaria* with advanced stages of the disease were in poorer physiological condition based on dry weight of the soft tissue, condition index, and carbon content of the tissue. Nitrogen metabolism appeared to be unimpaired. Significant differences were observed between the two sites with respect to prevalence of Hn and the physiological condition of the clams. Differences in disease prevalence between the two sites may be the result of unknown environmental factors that facilitate initialization of the disease or that compromise the defense mechanisms of the clams.

Supported by: NOAA Sea Grant
NA87-AA-O-OM093; and PHS Grant
1R01CA44307.

WHOI Contribution No. 6962.

CELLULAR ALTERATIONS PRECEDING NEOPLASIA IN *PSEUDOPLEURONECTES AMERICANUS* FROM BOSTON HARBOR, MA, USA

*Michael J. Moore, Rozanna Smolowitz and
John J. Stegeman*

Dysplastic and neoplastic liver disease has been described in adult winter flounder from Boston Harbor. In this study we examined the pathogenesis of the disease. Early changes, in fish of 100-300 mm, included biliary proliferation, abnormal vacuolation of biliary preductular epithelial cells, and macrophage aggregation. The identification of biliary preductular epithelial cells was based on nuclear morphology, numerous cellular junctions with adjacent hepatocyte apices, lack of contiguity with sinusoidal structures and central location in the hepatic tubule. Fish longer than 300 mm had progressively worsening pan-tubular changes in cholangiocytes and hepatocytes which culminated in grossly visible foci of vacuolation and associated neoplasia. Flounder from less contaminated sites showed occasional macrophage aggregations, but none of the other changes noted above. We suggest that the vacuolar change in Boston flounder occurs initially in preductular cells, which may be stem cells, extending later to fill entire hepatic tubules and intrahepatic portions of the biliary system. The involvement of the vacuolation process in the development of neoplasia is a question we are currently addressing.

In Press: *Marine Environmental Research*, 28, 1989.

Supported by: PHS Grant R01-CA44306;
MIT/WHOI Joint Program; Sea Grant New
Initiative Grant R/B-94-PD; and Ocean
Ventures Fund.

WHOI Contribution No. 7157.

FEMINIZATION OF THE HEPATIC MICROSOMAL CYTOCHROME P-450 SYSTEM IN BROOK TROUT BY ESTRADIOL, TESTOSTERONE AND PITUITARY FACTORS

*Ana M. Pajor, John J. Stegeman, Peter Thomas
and Bruce Woodin*

The effects of estradiol, testosterone, and pituitary extract on hepatic microsomal enzymes were studied in sham-operated and gonadectomized immature brook trout. Estradiol reduced the specific content of cytochromes P-450 and b₅ by 70% or more in both groups. Testosterone and pituitary extract also decreased the levels of total P-450 and b₅, but to a lesser extent. These latter effects were not evident when the contents of P-450 and b₅ were normalized per gm liver. Immunoblot analysis with antibodies to teleost (scup) P-450 forms showed the presence of cross-reacting proteins in control fish, presumed counterparts to the scup forms. Levels of a trout counterpart to P-450A (a putative testosterone 6 β -hydroxylase) were strongly suppressed in estradiol-treated fish. A trout P-450B counterpart was suppressed in estradiol-treated fish, but less strongly than was the P-450A counterpart. The trout orthologue of β -naphthoflavone-inducible P-450E (P-450IA1), the aryl hydrocarbon hydroxylase (AHH) catalyst, was undetectable in any group, consistent with very low levels of AHH activity in these fish. Estradiol or pituitary extract also decreased the levels of NADH-cytochrome b₅ and NADPH-cytochrome P-450 reductase activities, in sham-operated but not in gonadectomized fish. Gonadectomy alone also lowered the levels of reductase activities but not of total P-450 or b₅, suggesting an influence of gonads in maintaining normal levels of the reductases. The results support a prominent suppressive role for estrogens in producing the general sex differences in microsomal enzymes in fish liver, and indicate that there could be effects on several P-450 forms. The mechanism of action of the hormones in affecting microsomal enzymes is uncertain. The results also suggest the existence of unidentified gonadal factors which contribute to the regulation of reductases in teleost liver.

In Press: *Journal of Experimental Zoology*.

Supported by: PHS Grants ES-04220 and ES-04214.

**CELLULAR DISTRIBUTION OF
CYTOCHROME P450 IN WINTER
FLOUNDER LIVER WITH
DEGENERATIVE AND NEOPLASTIC
DISEASE**

*Rozanna M. Smolowitz, Michael J. Moore and
John J. Stegeman*

A characteristic hepatic pathology is highly prevalent in winter flounder (*Pseudopleuronectes americanus*) from Boston Harbor. Here we report initial evaluation of the cellular expression of a cytochrome P450E analogue in normal and diseased winter flounder liver using immunohistochemical analysis with MAb 1-12-3, a monoclonal antibody specific for P450E. Cytochrome P450E (P450IA1) is the polynuclear aromatic hydrocarbon (PAH) and polychlorinated biphenyl inducible form of P450 from scup (*Stenotomus chrysops*). MAb 1-12-3 was first applied to formalin-fixed, paraffin embedded sections of control and 3,3,4,4-tetrachlorobiphenyl-treated scup liver using an indirect peroxidase staining technique to visualize antibody binding. The results demonstrated specific positive staining of hepatocytes, bile and pancreatic duct epithelium and endothelium for P450E, confirming utility of MAb 1-12-3 in analysis of fixed tissue. Subsequent analysis of archival winter flounder liver also demonstrated positive staining of hepatocytes. No staining of abnormally vacuolated cells was present in any of the fish, however, nodules of such cells occasionally contained islands of intensely staining cells of unknown origin. The cellular distribution of P450E demonstrated here indicates a metabolic heterogeneity which could influence the responses of different cell types to subsequent or continued exposure to PAH or other hepatotoxins.

In Press: *Marine Environmental Research*, 26, 1990.

Supported by: PHS Grant ES-04220.

WHOI Contribution No. 7088.

**CYTOCHROME P450 FORMS IN FISH:
CATALYTIC, IMMUNOLOGICAL AND
SEQUENCE SIMILARITIES**

John J. Stegeman

1. Hepatic microsomal enzymes from teleost and elasmobranch fishes catalyze a diversity of monooxygenase reactions, consistent with the presence of multiple, distinct P450 forms. Protein purification and immunological studies have

confirmed that multiple microsomal P450s occur in teleosts.

2. A member of the aromatic hydrocarbon-inducible P450IA family is present in all fish species examined to date. This protein appears to be most closely related to P450IA1. Certain of the immunological probes for a teleost P450IA1 (scup P450E) appear to be reagent antibodies, recognizing the homologous protein in members of all vertebrate groups examined. The nature of the epitope recognized by such antibodies is not known.

3. Based on immunological and amino acid sequence comparisons, teleost P450IA1 appears to be orthologous to both P450IA1 and P450IA2 in mammals. Multiple P450IA genes may appear in teleosts, but divergence on separate lines from that involving mammalian P450IA2 could include additional, new members (P450IA3?) of the P450IA family.

4. There are marked similarities in the N-terminal amino acid sequence between different teleost (scup and trout) P450IA1 forms, as compared to the N-terminal sequence relationships found in P450IA1 of mammalian species. Whether this similarity extends to the rest of these teleost proteins is unknown.

5. The induction of P450IA1 in teleosts involves transcriptional and translational events. However, the temporal patterns involved in induction of mRNA or protein are different from those in mammalian species, suggesting additional aspects of the regulation in teleosts.

6. Relationships between other teleost and mammalian P450 forms, or between other P450 forms isolated from different teleosts, remain to be conclusively established. However, certain relationships are suggested, based on catalytic and other comparisons.

In Press: *Xenobiotica*, 19, 1989.

Supported by: PHS Grant ES-04220.

WHOI Contribution No. 7089.

**CYTOCHROME P450
MONOOXYGENASE SYSTEMS IN
AQUATIC SPECIES: CARCINOGEN
METABOLISM AND BIOMARKERS FOR
CARCINOGEN AND POLLUTANT
EXPOSURE**

John J. Stegeman and John J. Lech

High levels of polynuclear aromatic hydrocarbon (PAH) carcinogens commonly occur in aquatic systems where neoplasms arise in fish and other animals. Enzymes that transform PAH can act in initiating these diseases, and can indicate the contamination of fish by carcinogens

and other pollutants. Cytochrome P450 has similar roles in activating PAH carcinogens in fish and mammalian species. PAH and many chlorinated hydrocarbons, e.g., polychlorinated biphenyls (PCBs) induce a form of cytochrome P450 in fish that is the primary catalyst of PAH metabolism. The induction of this P450 in fish can accelerate the disposition of hydrocarbons, but can also enhance the formation of carcinogenic derivatives of PAH. Invertebrates have lower rates of PAH metabolism than fish. These rates are not obviously inducible by exposure to PAH or PCBs. The lower rates of foreign compound metabolism contribute to higher pollutant residue levels in bivalve molluscs, (clams, mussels, etc.) than in fish, and may limit the involvement of these compounds in disease processes in invertebrates.

The induction of P450 forms can indicate the exposure of fish to PAH, PCBs and other toxic compounds. Environmental induction has been detected in fish from contaminated areas by use of catalytic assay, antibodies to fish P450, and DNA probes that hybridize with P450 messenger RNA. Application of these methods can provide sensitive biological monitoring tools that can detect environmental contamination of fish by some carcinogens and tumor promoters. However, P450 potential for detecting the presence of direct acting carcinogens and non-inducing tumor promoters may be limited. Further study of the P450 genes in different species could identify biochemical features related to the presence and action of additional chemicals involved in carcinogenesis in fish, and will provide insight into the evolution and genetic regulation of this multigene family.

In Press: *Environmental Health Perspectives*.

Supported by: PHS Grants CA-44306, ES-04220 and ES-01080.

WHOI Contribution No. 7178.

EXPERIMENTAL AND ENVIRONMENTAL INDUCTION OF CYTOCHROME P450E IN FISH FROM BERMUDA WATERS

John J. Stegeman, Kenneth W. Renton,
Bruce R. Woodin, Yu-Sheng Zhang and
Richard F. Addison

The chemical induction of liver microsomal cytochrome in fish from Bermuda was evaluated by examining the rates of ethoxyresorufin O-deethylase (EROD) activity and the levels of protein recognized in Western blot by monoclonal antibody 1-12-3 to scup cytochrome P450E (P450E). Scup P450E is the EROD catalyst and a teleost representative of the hydrocarbon-inducible P450-IA gene family in vertebrates. Treatment of

blue-striped grunt (*Haemulon sciurus*) with β -naphthoflavone (BNF), an aromatic hydrocarbon-type inducer of P450E, resulted in a strong induction of total P450, EROD activity and the immunodetected P450E homologue, at doses greater than 1 mg/kg. The induction peaked at about 3 days, declining progressively after that. A P450E counterpart was also induced by BNF in squirrelfish (*Holocentrus rufus*). Analysis of freshly caught blue-striped grunt, squirrelfish, and four additional fish species, from sites in Hamilton Harbor, Castle Harbor and Ferry Reach, Bermuda, revealed appreciable levels of EROD activity and P450E in most of these fish. Two species, squirrelfish and tomtate (*Haemulon aurolineatum*) had unusually high levels of total microsomal P450 (up to 1.5 nmol/mg), of unknown isozymic composition. The levels of both EROD activity and P450E homologue in some species, notably blue-striped grunt, French grunt (*Haemulon flavolineatum*) and sergeant major (*Abudefduf saxatilis*) were significantly higher in fish taken at sites characterized by higher levels of sedimentary hydrocarbons and/or polychlorinated biphenyls. Association of EROD or P450E content with contaminant residues was strongest when comparison was with the levels of bioavailable PCBs, i.e., PCB content in the bivalve *Arca zebra* from the sampling sites. The results indicate that induction of P450E by environmental chemicals is occurring in many fish in Bermuda waters; the origin of these chemicals is not known. The results further support the utility of P450 induction as an indicator of chemical contamination in aquatic systems.

Supported by: PHS Grant ES-04220; EPA Grant CR183155; and the Intergovernmental Oceanographic Commission.

WHOI Contribution No. 7145.

STRUCTURE, FUNCTION AND REGULATION OF CYTOCHROME P450 FORMS IN FISH

John J. Stegeman, Bruce R. Woodin and
Rozanna Smolowitz

Cytochrome P450 plays key roles in determining the biological action including toxicity of pollutant chemicals, drugs and therapeutic agents, and many chemical carcinogens, catalyzing the activation and inactivation of these compounds. The extent to which these functions occur in different individuals or species exposed to various compounds will depend to a large degree on the complement of different P450 proteins present, their catalytic functions, and their regulation. The diverse structure and function of mammalian P450 proteins are well known from

studies with purified P450s, and with monoclonal and polyclonal antibodies of cDNA probes to the forms. These mammalian forms are well represented in a recently developed nomenclature based on gene sequence information for P450 forms, which describes a gene superfamily and organizes all sequences known at the time into P450 gene families and subfamilies.

Research on mammalian P450 continues to dominate the literature, but there is a growing recognition of the biological significance of P450 in other animals, and of our need to know the diversity and biochemistry of P450 proteins in these groups. The 20,000 species of fish extant, represent about one-half of the known vertebrate species. The fishes present extraordinary diversity, inhabiting virtually all of the world's aquatic environments. They also represent a significant source of protein for humans. The study of P450 forms in fish thus acquires importance from evolutionary and toxicological standpoints. In this paper we summarize information on cytochrome P450 proteins involved in xenobiotic metabolism in fish, drawing heavily on a more detailed review. We also present preliminary results of new studies on important aspects of relationships among P450 forms in fish.

In Press: *Biochemical Society Transactions (United Kingdom)*.

Supported by: PHS Grants ES-04220 and CA-44306.

WHOI Contribution No. 7165.

PHYTOPLANKTON

CYSTS AS FACTORS IN *PYRODINIUM BAHAMENSE* ECOLOGY

Donald M. Anderson

The resting cyst is an important factor in the ecology of many neritic dinoflagellates. These highly resistant cells can survive in the sediment for extended periods of time and then germinate to release vegetative cells that serve as an inoculum to initiate blooms. Cysts are considered important with respect to species dispersal, bloom timing, bloom location, survival through adverse conditions, and, for toxic species, as sources of toxin. Twenty years ago, Wall and Dale demonstrated that a microfossil called *Hemicystodinium zoharyi* was in fact the resting cyst of *Pyrodinium bahamense*. Aside from the preliminary germination experiments conducted by Wall and Dale, all other published work on the living form of this cyst has been taxonomic in nature. The objective of this paper is to describe the information that has been obtained for other

cyst-forming dinoflagellates and to discuss how such data can be useful in studies of *P. bahamense* bloom dynamics and distribution.

Supported by: NSF Grant OCE86-14210; and the Donaldson Charitable Trust.

WHOI Contribution No. 7128.

TOXIN VARIABILITY IN *ALEXANDRIUM* SPECIES

Donald M. Anderson

This paper reviews the results of experiments designed to quantify the net toxin production rate, the accumulation of toxin (toxin content), and the physiological state of *Alexandrium* cells as toxicity varied under different growth conditions. The conditions examined included N and P-limited growth in semi-continuous culture, and batch culture growth under nutrient replete, low temperature, high salinity, low P and low N conditions. Further details of the timing of toxin production were revealed in a cell cycle experiment which showed that toxin synthesis was not continuous but rather was limited to a discrete phase of the cell cycle, during DNA synthesis. Implications of these results with respect to the possible function of saxitoxin in the dinoflagellate are discussed.

Supported by: NSF Grant OCE86-14210; NOAA Sea Grant NA86AA-D-SG0090, R/B-76; and the Donaldson Charitable Trust.

WHOI Contribution No. 7158.

IMMUNOFLUORESCENT DETECTION OF THE BROWN TIDE ORGANISM, *AUREOCOCCUS ANOPHAGEFFERENS*

Donald M. Anderson and David M. Kulis

One of the major constraints to research on the causes, effects, dynamics and geographic distribution of the brown tide organism *Aureococcus anophagefferens* is the difficulty in identifying the tiny, nondescript cells in complex natural assemblages. In this study, the brown tide cells were grown in culture, preserved in a manner that maximized their structural rigidity and then injected into rabbits to obtain antibodies specific for the cell wall proteins. The resulting polyclonal antiserum was tested against 46 strains of phytoplankton from 5 algal classes. Twenty strains belong to the class Chrysophycophyta, which includes the genus *Aureococcus*. Using a 1:800 dilution of the antiserum and an indirect immunofluorescent technique with FITC-conjugated goat anti-rabbit IgG, only A.

anophagefferens exhibited visible fluorescence. At a 1:3200 dilution, immunofluorescence was still visible around the perimeter of the *A. anophagefferens* cells, resembling a green "halo". Excellent agreement was obtained between cell counts of laboratory cultures and natural bloom samples using phase contrast microscopy and the immunofluorescent technique. Cross-reactions in natural samples have been limited to some small bacteria and a few unidentified spherical "objects". In both instances, either the size of the cross-reacting particles or the manner in which they fluoresce make it easy to differentiate them from *A. anophagefferens*.

Supported by: Florence and John Schumann Foundation; NOAA Sea Grant NA86-AA-D-SG090, R/B-87-PD and R/B-91; Suffolk County Department of Health Services, Marine Sciences Research Center of the State University of New York; and the Living Resource Institute of the State of New York.

WHOI Contribution No. 6963.

TOXIN COMPOSITION VARIATIONS IN THE DINOFLAGELLATE *ALEXANDRIUM FUNDYENSE*

D. M. Anderson, D. M. Kulis, J. J. Sullivan and S. Hall

A commonly accepted paradigm in the study of saxitoxin-producing dinoflagellates is that the total concentration of all toxins (toxin content) in one isolate can vary with growth conditions, but that the relative abundance of each toxin (toxin composition) does not change. We demonstrate here that dramatic changes in toxin composition do occur in one isolate of *Alexandrium fundyense*. In nutrient limited semi-continuous culture, toxin composition varied systematically with growth rate; gradual increases in certain toxins were balanced by equally-steady decreases in others. Nitrogen limitation favored the production of toxins C 1,2 and GTX I,IV, whereas phosphorus limitation produced cells with high relative abundance of GTX II,III. STX reached its highest relative abundance when growth was most rapid. The lack of observed compositional changes in past studies is probably not due to inherent differences in toxin biosynthetic pathways between the strains of *Alexandrium* examined but instead reflects differences in the experimental protocols, methods of toxin analysis, and dominant toxins in the particular isolates examined. These findings have important implications in the areas of public health, chemotaxonomy, and toxin biosynthesis.

In Press: *Toxicon*.

Supported by: NSF Grant OCE86-14210; and NOAA Sea Grant NA86-AA-D-SG090, R/B-76.

WHOI Contribution No. 7038.

DYNAMICS AND PHYSIOLOGY OF SAXITOXIN PRODUCTION BY THE DINOFLAGELLATES *ALEXANDRIUM* SPP.

D. M. Anderson, D. M. Kulis, J. J. Sullivan, S. Hall and C. Lee

Toxin content (fmol cell^{-1}) and a suite of elemental and macromolecular variables were measured in batch cultures of the dinoflagellates *Alexandrium fundyense*, *A. tamarensis*, and *Alexandrium* sp. from the southern New England region, USA. A different perspective was provided by semicontinuous cultures which revealed sustained, steady-state physiological adaptations by cells to N and P limitation. Two types of variability were investigated. In batch culture, changes in nutrient availability with time caused growth stage variability in toxin content, which often peaked in mid-exponential growth. A second type of variability that could be superimposed on growth stage differences was best exemplified by the high toxin content of cells grown at suboptimal temperatures. Calculations of the net rate of toxin production (R_{tox} ; $\text{fmol cell}^{-1} \text{d}^{-1}$) for these different culture treatments and modes made it possible to separate the dynamics of toxin production from cell division. Over a wide range of growth rates, cells produced toxin at rates approximating those needed to replace "losses" to daughter cells during division. The exception to this direct proportionality was with P limitation, which was associated with a dramatic increase in the rate of toxin production as cells stopped dividing due to nutrient limitation in batch culture. Growth stage variability in batch culture thus reflects small imbalances (generally within a factor of two) between the specific rates of toxin production and cell division. N limitation and CO_2 depletion both affect pathways involved in toxin synthesis before those needed for cell division; P limitation does the opposite. The patterns of toxin accumulation were the same as for major cellular metabolites or elemental pools. The highest rates of toxin production appear to result from an increased availability of arginine (Arg) within the cell, due to either a lack of competition for this amino acid from pathways involved in cell division or to increased to novo synthesis. There were no significant changes in toxin content with either acclimated growth at elevated salinity, or with short term increases or decreases of salinity. These results demonstrate that toxin production is a complex process which, under some conditions, is closely coupled to growth rate; under other conditions, these processes are completely uncoupled. Explanations for the observed

variability probably relate to pool sizes of important metabolites and to the differential response of key biochemical reactions to these pool sizes and to environmental conditions.

In Press: *Marine Biology*, 104, 1990.

Supported by: NSF Grants OCE83-00018, OCE83-15262, OCE86-14210; and Sea Grant NA86-AA-D-SG090, R/B-76.

WHOI Contribution No. 6985.

BIOCHEMICAL COMPOSITION AND METABOLIC ACTIVITY OF *SCRIPPSIELLA TROCHOIDEA* (DINOPHYCEAE)

Brian J. Binder and Donald M. Anderson

The composition and metabolic activity of cysts of the marine dinoflagellate *Scrippsiella trochoidea* (Stein) Loeblich were examined during dormancy, quiescence, and germination. On a per cell basis, newly formed cysts contain an order of magnitude more carbohydrate, but significantly less protein and chlorophyll-*a* than do exponentially growing vegetative cells. Loss of lipid and carbohydrate from cysts during the initial dormancy period reflect a respiration rate estimated to be 10% of the respiratory activity in vegetative cells. Among older, quiescent cysts the calculated respiration rate decreases further to approximately 1.5% of the vegetative rate, and appears to proceed largely at the expense of carbohydrate reserves. These estimated rates of respiration are in good agreement with direct measurements of cyst oxygen consumption. The transfer of quiescent cysts to conditions permissive for germination results in a rapid increase in respiration rate, as evidenced by both carbohydrate loss and O₂ consumption. This increase in respiratory activity is followed by an increase in protein content and, later, by an increase in chlorophyll-*a* content and photosynthetic capacity. Just prior to germination the P/R ratio becomes greater than 1, and the estimated per-chlorophyll photosynthetic activity reaches 75% of the rate in vegetative cells. Complete restoration of photosynthetic and respiratory capacity apparently is not achieved until after encystment. Taken together, these data represent the first direct confirmation of the common assumption that dinoflagellate cysts represent true "resting" cells, containing extensive energy reserves and displaying greatly reduced metabolic activity.

In Press: *Journal of Phycology*.

Supported by: NSF Grant OCE84-00292; WHOI Education Program and Coastal Research Center; and the Donaldson Charitable Trust.

WHOI Contribution No. 7209.

CELL CYCLE STUDIES OF THE DINOFLAGELLATES *GONYAULAX POLYEDRA* STEIN AND *GYRODINIUM UNCATENATUM* HULBURT DURING ASEXUAL AND SEXUAL REPRODUCTION

Catherine M. Cetta and Donald M. Anderson

A microscope photometer system was used to quantify the relative DNA content of individual cells of the dinoflagellates *Gonyaulax polyedra* and *Gyrodinium uncatenum* during asexual reproduction and, for the latter species, during sexuality as well. The cell cycles of these two dinoflagellates are distinctly different, although both include discrete periods of DNA synthesis. In *G. polyedra*, DNA synthesis and cell division are tightly phased to restricted segments of the photocycle, separated in time by distinct gap phases. All cells that replicate their DNA and enter G₂ divide during the next division interval. G₁ is the stage occupied by the cells most of the time. In *G. uncatenum*, cell division is more broadly distributed and occurs throughout half the photocycle. Cell division is thus phased only to the extent that it is restricted to the same half of the photocycle each day. G₁ is very brief or absent, as DNA synthesis begins immediately after cell division. G₂ is the dominant stage through time, since it includes cells about to divide as well as those that just divided. *Gyrodinium uncatenum* is the first free-living photosynthetic dinoflagellate to exhibit a pattern of DNA synthesis immediately after mitosis. The tight phasing of *G. polyedra* division and the restriction of G₂ to cells that must divide at the end of the dark period should make it possible to calculate the growth rate of this species in mixed natural assemblages using these techniques. It should also be possible to distinguish sexual stages (zygotes) from vegetative cells. Since *G. uncatenum* vegetative cells often have 2 complements of DNA, as do zygotes following gamete fusion, these stages could not be distinguished from each other on the basis of DNA measurements alone. However, these data in combination with cell counts were used to define the onset of sexuality and to show that the gametes of this species result from two rapid divisions.

In Press: *Journal of Experimental Marine Biology and Ecology*.

Supported by: NSF Grants OCE84-00292 and OCE86-14210.

WHOI Contribution No. 7119.

**CYST FORMATION IN THE RED TIDE
DINOFLLAGELLATE *ALEXANDRIUM
TAMARENSE* (DINOPHYCEAE):
EFFECTS OF IRON STRESS**

Gregory J. Doucette, Allan D. Cembella and
Gregory L. Boyer

The toxic red tide dinoflagellate *Alexandrium tamarense* (Lebour) Balech [synonymous with *Protogonyaulax tamarensis* (Lebour) Taylor] was subjected to iron stress in batch culture over a 24-day time course. Monitoring of life history stages indicated that iron stress induced formation of both temporary (= pellicular) and resting (= hypnozygotic) cysts. Our experimental induction of sexuality appeared to be associated with iron limitation rather than the total depletion of biologically available iron. Degenerative changes in organelle (i.e., chloroplast, mitochondrion and chromosome) ultrastructure were largely restricted to pellicular cysts, suggesting that these temporary cysts were more susceptible to short-term iron stress effects than were hypnozygotes. These results are consistent with the hypothesized ecological roles of cysts in maintaining viability over brief (pellicular cysts) and extended (hypnozygotes) exposure to adverse environmental conditions.

Supported by: Natural Science and Engineering Research Council Postgraduate Scholarship and a Strategic grant; U.B.C. Graduate Fellowships; and a Florence and John Schumann Foundation grant.

WHOI Contribution No. 7149.

**RELATIVE EFFECTS OF NITROGEN OR
PHOSPHORUS DEPLETION AND LIGHT
INTENSITY ON THE PIGMENTATION,
CHEMICAL COMPOSITION, AND
VOLUME OF *PYRENOMONAS SALINA*
(CRYPTOPHYCEAE)**

Alan J. Lewitus and David A. Caron

The nitrogen-rich phycobiliproteins are efficient light-harvesting pigments of cryptophytes, cyanobacteria, and rhodophytes. Whereas it is well-established that certain cyanobacteria mobilize their phycobiliproteins in response to nitrogen deprivation, the effect of nitrogen stress on cryptophyte physiology has been studied only rarely. We compared the effects of nitrogen and phosphorus depletion on the biovolume, chemical composition, and pigment composition of the marine cryptophyte, *Pyrenomonas salina*, grown in batch cultures under light-limiting and light-saturating conditions. Cell phycoerythrin

content declined during the late exponential growth phase in nitrogen-depleted cultures, and the cells were nearly devoid of phycoerythrin (<3% of the phycoerythrin content of nitrogen-replete cells) at the beginning of stationary growth. Phycoerythrin content also decreased during late exponential phase in phosphorus-depleted cultures, but these latter cells contained more than 10 times the phycoerythrin concentration of nitrogen-depleted cells at the same growth stage. Chlorophyll *a* content declined in nitrogen-depleted cultures, but at a slower rate than the decrease in phycoerythrin, such that the phycoerythrin to chlorophyll *a* ratio decreased by more than 95% from the early exponential to early stationary growth phase. In nitrogen-depleted cultures grown at a low light intensity, the decline in phycoerythrin content preceded the decline in chlorophyll *a* content, and resulted in only slight changes in cell nitrogen content and volume. These data indicate that phycoerythrin is preferentially lost from *P. salina* during nitrogen deficiency, and support the hypothesis that, similar to certain cyanobacteria, *P. salina* responds to nitrogen deprivation by mobilizing phycoerythrin in order to help sustain cellular nitrogen requirements.

In Press: *Marine Ecology Progress Series*.

Supported by: Ocean Ventures Fund; NSF Grant BSR86-20443; and WHOI Education Program.

WHOI Contribution No. 7191.

**CHANGES IN CELL CHEMICAL
COMPOSITION DURING THE LIFE
CYCLE OF *SCRIPPSIELLA TROCHOIDEA*
(DINOPHYCEAE)**

Thaithaworn Lirdwitayaprasit, Tomotoshi Okaichi,
Shigeru Montani, Tadashi Ochi
and Donald M. Anderson

The cellular content of carbon, nitrogen, amino acids, polysaccharides, phosphorus and adenosine triphosphate (ATP) were determined at several stages during the life cycle of the dinoflagellate *Scrippsiella trochoidea*. Carbon per cell decreased slightly between exponential and stationary phase growth in vegetative cells whereas nitrogen per cell did not change. Both of these cellular components increased markedly on encystment and then decreased to vegetative cell levels during dormancy and germination. C/N ratios increased gradually during cyst dormancy and activation, reflecting a more rapid decrease in N than in C pools, even though both decreased through time. Amino acid composition was relatively constant during the vegetative cell stages, with glutamic acid as the dominant component. Arginine was notably higher in cysts than in vegetative cells, but decreased

significantly during germination, suggesting a role in nitrogen storage. The ratio of neutral amino acids to total amino acids (NAA/TAA) decreased as cysts were formed and then gradually increased during storage and germination. The ratio of basic amino acids to total amino acids (BAA/TAA) changed in the opposite direction of NAA/TAA, whereas the ratio of acidic acids to total amino acids (AAA/TAA) was generally invariant. Amino acid pools are not static during the resting state in the cysts - there is degradation or biosynthesis of certain, but not all, classes of these compounds. The monosaccharide composition of cold and hot water extracted polysaccharides was quite different between cells and cysts. A high percentage of glucose in cysts suggests that the storage carbohydrate is probably in the form of glucan. Total cellular phosphorus was higher in all cyst stages than in vegetative cells. However, ATP cell⁻¹ decreased as vegetative cell entered stationary phase and encysted, and continued to decrease in cysts during dark cold storage. ATP increased only as the cysts were activated at warm temperatures in the light and began to germinate. The above data demonstrate that dormancy and quiescence are not periods of inactive metabolism but instead are times when numerous biochemical transformations are occurring that permit prolonged survival in a resting state.

Supported by: NOAA Sea Grant
NA86-AA-D-SG090, R/B-92.

WHOI Contribution No. 7259.

PLANKTON ECOLOGY

BEHAVIORAL RESPONSES OF THE MARINE TINTINNID *FAVELLA* SP. TO PHYTOPLANKTON: INFLUENCE OF CHEMICAL, MECHANICAL AND PHOTIC STIMULI

Edward J. Buskey and Diane K. Stoecker

Videomicroscopy and computerized motion analyses were used to experimentally investigate the locomotory responses of a tintinnid, *Favella* sp., to phytoplankton and to chemosensory and mechano-sensory stimuli associated with the presence of phytoplankton. When exposed to increased concentrations of the dinoflagellate, *Heterocapsa triquetra*, *Favella* show transient change in behavior which result in a decrease in swimming speed, increase in turning rate and decrease in net to gross displacement ratio; this should result in the aggregation of *Favella* in patches of the dinoflagellate. Similar behavioral responses are elicited by exposure to exudates of

H. triquetra and to plastic beads of approximately the same size as the alga. When *Favella* was exposed to other phytoflagellates or their exudates, the behavioral responses were less pronounced or absent. *Favella* does not respond to beads smaller than 6 μ m; for larger beads, the response appears to depend on the concentration of beads. *Favella* do not exhibit a phototaxis or photokinesis, but they do have diel behavior patterns that may be entrained by the light cycle. We speculate that these diel changes in locomotory behavior increase the probability of encounter with food patches.

Published in: *Journal of Experimental Marine
Biology and Ecology*, 132, 1-6, 1989.

Supported by: NSF Subcontract OCE86-08395.

WHOI Contribution No. 7039.

EFFECTS OF GAMETOGENESIS ON TEST STRUCTURE AND DISSOLUTION OF SOME SPINOSE PLANKTONIC FORAMINIFERA AND IMPLICATIONS FOR TEST PRESERVATION

*David A. Caron, O. Roger Anderson,
Judith L. Lindsey, Walter W. Faber, Jr. and
Ee Lin Lim*

The process of gametogenesis observed in six species of laboratory reared spinose planktonic foraminifera was accompanied by significant changes in the calcite test. All species resorbed their spines prior to gamete release. In addition, a calcite crust was subsequently secreted over the outside of the test in three of the species (*Globigerinoides sacculifer*, *Globigerinoides conglobatus*, *Orbulina universa*), the test was decalcified in one species (*Hastigerina pelagica*), and there was little or no calcite crust deposited on the test in two species (*Globigerinella aequilateralis* and *Globigerinella ruber*), although the test weights of at least one of these species (*G. aequilateralis*) were greater in gametogenic specimens. Gametogenic calcification resulted in greater test weight per unit length for gametogenic specimens depositing a calcite crust, and slower dissolution rates in laboratory experiments than for specimens that did not undergo gametogenic calcification. Based on our results, we conclude that the species composition of planktonic foraminiferal test assemblages in deep-sea sediments will be affected by whether or not the species undergo gametogenic calcification or decalcification, and the proportion of these specimens that have attained reproductive maturity in the overlying waters.

In Press: *Marine Micropaleontology*.

Supported by: NSF Grant OCE81-17715.

WHOI Contribution No. 7016.

CARBON UTILIZATION BY THE OMNIVOROUS FLAGELLATE *PARAPHYSOMONAS IMPERFORATA*

David A. Caron, Joel C. Goldman and
Mark R. Dennett

Carbon utilization by the omnivorous microflagellate *Paraphysomonas imperforata* was examined when this protozoan was fed either of two species of algae grown to three degrees of nitrogen limitation and three degrees of phosphorus limitation. Carbon incorporation (retention in the particulate fraction) by the microflagellate differed slightly for the two prey species but was a constant percentage of the total carbon budget of the protozoan for each prey alga (i.e., the degrees of nitrogen or phosphorus deficiency of the algae did not affect carbon incorporation by the protozoan). The patterns of respiration in the size grazed cultures of each alga were also similar. Carbon and nutrient utilization by this protozoan apparently was uncoupled to achieve this result. Firm conclusions relating carbon to nutrient cycling by the microflagellate in these cultures are equivocal due to the possible dark uptake of nutrients by the algae. However, our results are consistent with a mathematical model in which the nutrient excretion rate is predicted from the respiration rate and gross growth efficiency of the protozoan, and the carbon:nutrient ratios of the protozoan and its prey.

In Press: *Limnology and Oceanography*.

Supported by: NSF Grants OCE83-08578 and OCE85-11283; and a WHOI Mellon Study Award.

WHOI Contribution No. 7017.

TROPHIC INTERACTIONS BETWEEN NANO- AND MICROZOOPLANKTON AND THE "BROWN TIDE"

David A. Caron, Ee Lin Lim, Holly Kunze,
Elizabeth Cosper and Donald Anderson

There has been very little work performed on the trophic interactions between algae that cause problem algal blooms in coastal marine ecosystems and the microconsumers present in these water masses. Experiments were carried out to determine the ability of planktonic protozoa to consume *Aureococcus anophagefferens*, the organism responsible for the Brown Tide, and to estimate the effect of the presence of this alga on microbial abundance and grazing in inshore waters around Long Island. Laboratory experiments were conducted in which cultured species of bacteria

and the Brown Tide alga were offered separately as food and in mixtures to cultured species of protozoa. *A. anophagefferens* supported rapid growth of a chrysoomonad microflagellate and a pleuronematid ciliate, moderate growth of a bodonid microflagellate, and no growth of a hypotrich ciliate and a scuticociliate. Whole seawater from Vineyard Sound, MA that was enriched with *A. anophagefferens* also developed high protozoan densities after 4 days. These experiments indicated an ability of at least some protozoa to tolerate and utilize Brown Tide biomass. Grazing experiments and microbial population estimates (bacteria, heterotrophic and phototrophic nanoplankton, heterotrophic microplankton, *A. anophagefferens*) were conducted on water samples collected from several sites in the Peconic Bay system and Great South Bay system on three separate dates during the summer of 1988. Population densities of potential microalgal consumers were not depressed as a result of the presence of the Brown Tide. In addition, an examination of grazing rates indicated that the presence of the Brown Tide in coastal waters did not inhibit all microbial grazing. Heterotrophic flagellates $>10 \mu\text{m}$ in size, predominantly dinoflagellates but also ebridians, were the major consumers of fluorescently-labeled algae in samples containing moderately high densities ($0.5-1.0 \times 10^5 \text{ ml}^{-1}$) of Brown Tide. Non-loricate choreotrich ciliates also consumed some fluorescently-labeled algae, but these protozoa (and other non-choreotrich ciliates) were more important as bacterivores than as herbivores. Our results indicate that the ability of *A. anophagefferens* to attain high densities in coastal ecosystems was not related to a complete cessation of protozoan grazing. We hypothesize that selectivity against this organism by consumers, or a reduction in the number of microbial consumers at the time of initiation of the bloom, may explain the occurrence of Brown Tides. These latter hypotheses remain to be tested.

In Press: *Novel Phytoplankton Blooms: Causes and Impacts of Recurrent Brown Tides and Other Unusual Blooms*, in the Series Lecture Notes on Coastal and Estuarine Studies, E. Carpenter, M. Bricelj and E. M. Cosper, eds. Springer-Verlag.

Supported by: Florence and John Schumann Foundation; and NOAA Sea Grant NA86-AA-D-SG090, R/B-87-PD and R/B-91.

WHOI Contribution No. 7019.

**COMPOSITION AND DEGRADATION
OF SALP FECAL PELLETS:
IMPLICATIONS FOR VERTICAL FLUX
IN OCEANIC ENVIRONMENTS**

*David A. Caron, Laurence P. Madin and
Jonathan J. Cole*

Changes in the sinking rates, ash-free dry weights, particulate carbon and nitrogen content, and carbon:nitrogen ratios from the fecal pellets of several species of oceanic salps were examined in ten-day decomposition studies. Although bacteria and protozoa became abundant in the incubation vessels, most of the fecal pellets remained physically intact throughout the study. Bacterial activity in the pellets (measured by the rate of uptake of ^3H -thymidine) increased, but microbial degradation had little effect on the sinking speeds of most of the fecal pellets. The average losses of ash-free dry weight and carbon and nitrogen content, along with changes in carbon:nitrogen ratio, were small compared to their initial values. We conclude that microbial degradation of large salp fecal pellets would not prevent the vertical flux to the deep ocean of a significant fraction of the particulate organic material contained in the pellets. The fecal pellets of oceanic salps provide a rapid, and potentially important, mechanism for the consolidation and vertical transport of organic and lithogenic material associated with minute particles in the open ocean.

In Press: *Journal of Marine Research*, 47.

Supported by: NSF Grants OCE80-24441,
OCE81-12991 and OCE86-00776.

WHOI Contribution No. 7013.

**CARBON, NITROGEN AND
PHOSPHORUS BUDGETS FOR THE
MIXOTROPHIC PHYTOFLAGELLATE
POTERIOCHROMONAS MALHAMENSIS
(CHRYSTOPHYCEAE) DURING
BACTERIAL INGESTION**

*David A. Caron, K. G. Porter and
Robert W. Sanders*

Growth, grazing, carbon incorporation and nutrient incorporation by the mixotrophic phytoflagellate *Poterochromonas malhamensis* were examined under a variety of different nutrient and light regimes in the presence of heat killed bacteria. *P. malhamensis* readily ingested bacteria in all culture treatments containing heat killed bacteria, and growth rates of the protist were much greater for heterotrophic (bacterivorous) growth than for phototrophic growth. Carbon incorporation efficiencies by the phytoflagellate

were virtually identical to phosphorus incorporation efficiencies during heterotrophic growth, but nitrogen incorporation efficiencies were somewhat lower than the latter two efficiencies in nearly all of the treatments. Algal growth in cultures with heat killed bacteria was similar in continuous darkness and in continuous light. Bacterial organic carbon was the primary source of protist cellular carbon for *P. malhamensis* during heterotrophic growth. Based on our observations, we conclude that *P. malhamensis* is primarily a heterotrophic, phagotrophic protist, and that it is highly competent in this mode of nutrition.

In Press: *Limnology and Oceanography*.

Supported by: NSF Grants BSR86-20441 and
BSR86-20443.

WHOI Contribution No. 7273.

**THE ECOLOGY OF PLANKTONIC
SARCODINES**

David A. Caron and Neil R. Swanberg

Planktonic sarcodines (amoebae, foraminifera, and actinopoda) are a taxonomically diverse and ecologically important component of oceanic plankton food webs. In addition, the fossilizable tests produced by many of these protist species have been, and continue to be extensively used as an important tool for reconstructing paleoclimatological conditions. Living planktonic sarcodines have not been as intensively studied as their non-living remains, however. Biologists have been slow to recognize the potential importance of planktonic sarcodines in the flow of energy and materials in the marine plankton because of their complex trophic status and fastidious nature in laboratory culture. Only recently has there been a realization that these organisms may contribute significantly to photosynthesis (via symbiotic algae sequestered within the cytoplasm), total grazing pressure in the plankton, and the total flux of material to the deep ocean. Based on a reevaluation of the existing data on their abundance, trophic interactions and grazing rates, it is suggested that planktonic sarcodines play a potentially important role in the cycling of energy and material in oceanic plankton communities.

In Press: *Critical Reviews in Marine Science*.

Supported by: NSF Grant OCE86-00510.

WHOI Contribution No. 7018.

EFFECTS OF FIXATION ON CELL VOLUME OF MARINE PLANKTONIC PROTOZOA

Joon W. Choi and Diane K. Stoecker

The effects of fixation on the cell volume of marine heterotrophic nanoflagellates and marine planktonic ciliates were investigated. Decreases in cell volume depend on combination of the protozoan taxa and on the particular fixative. For a particular fixative and protozoan species, degrees of shrinkage is independent of physiological state.

The volume of fixed cells is approximately 20-55% lower than the cell volume of live organisms. For the heterotrophic microflagellates, the fixatives ranked, in order of decreasing effect on cell volume, as glutaraldehyde, formaldehyde, acid Lugol's solution and modified van der Veer solution. With the oligotrichous ciliates and a tintinnid ciliate, formaldehyde caused less shrinkage than glutaraldehyde or acid Lugol's solution. With the aldehyde fixatives, the microflagellates shrunk more than did the ciliated protozoans. Differential effects of fixation on cell volumes may result in an underestimation of the biomass of certain protozoan taxa in natural samples.

Published in: *Applied and Environmental Microbiology*, 55, 1761-1765, 1989.

Supported by: NSF Grant OCE86-00765; and the WHOI Education Program.

WHOI Contribution No. 6996.

DYNAMICS OF PREY SELECTION BY AN OMNIVOROUS FLAGELLATE

Joel C. Goldman and Mark R. Dennett

The heterotrophic flagellate *Paraphysomonas imperforata*, a raptorial grazer, sustained maximum specific growth rates of $\approx 1.5^{-1}$ at 20°C when fed 3 phytoplankton species of different sizes and shapes (the relatively small diatom *Phaeodactylum tricoratum*, and haptophyte *Isochrysis galbana*), and the larger chlorophyte *Dunaliella tertiolecta*, either singularly or in combinations of 2 species. When prey combinations included *D. tertiolecta*, the chlorophyte was grazed only after a large fraction of the other species was first grazed. Diatom and haptophyte were grazed concurrently when offered in combination. Changing the relative proportions of starting biomass of the different species in combination had no effect on the order of grazing. However, in all cases the switch to the chlorophyte occurred rapidly and the maximum ingestion rate attained after the switch was proportional to the

contribution of the chlorophyte to total starting biomass. From a hydrodynamic standpoint, specific clearance rate C' increased as the ratio of predator to prey radii, $R:r$, decreases and C' increases as R decreases for a given value of $R:r$. We suspect that the preference for the two smaller species is governed by the ability of the flagellate to adjust its own size downward to accommodate the smaller prey while maintaining $R:r \approx 2:1$. When sized to graze these smaller species, the flagellate simply is too small to graze the chlorophyte. Thus, although there is clear evidence that the flagellate is a non-passive grazer and will not graze certain species at all, mechanoreception clearly plays a major role in the dynamics of grazing desired species. Raptorial grazers such as *P. imperforata*, by having the ability to graze prey almost as big as themselves, may be effective competitors with larger protozoa for nanoplankton-size food particles and also contribute to making the food chain (web) within the microbial loop long and complicated with high losses of energy and materials.

Published in: *Marine Ecology Progress Series*, 59, 183-184, 1990.

Supported by: NSF Grants OCE85-11283 and OCE87-16026.

WHOI Contribution No. 7091.

ABUNDANCE, CHLOROPHYLL CONTENT AND PHOTOSYNTHETIC RATES OF CILIATES IN THE NORDIC SEAS

Mary Putt

Plastidic and aplastidic oligotrichous ciliates, tintinnids and *Mesodinium rubrum* were enumerated in samples collected in July and August 1988 in the Iceland, Greenland and Barents Sea. Oligotrichs comprised 69-83% of ciliate numerical abundance both in surface waters and at 50 m. Chlorophyll containing ciliates (plastidic oligotrichs and *Mesodinium rubrum*) accounted for 58-65% and 14-28% of ciliate numerical abundance in surface waters and at 50 m respectively. At two stations in the Barents Sea, estimated daily photosynthetic rates for surface populations of *Strombidium* sp. A were equivalent to about 12-35% of ciliate body carbon/day. The estimated average contribution of the ciliate community to total chlorophyll was modest (4-15% of total chlorophyll). However, at stations where community chlorophyll was low ($\leq 0.2 \mu\text{g/liter}$), a single ciliate species (*Strombidium* sp. A) accounted for up to 24% of total chlorophyll. Maximum photosynthetic rates for *Strombidium* sp. A. (1.0-3.1 $\mu\text{g C}/\mu\text{g Chl/h}$) were similar to

previously reported values for polar communities. Chlorophyll containing ciliates may influence the size distribution of chlorophyll and primary production in oligotrophic polar waters. Because ciliates are a good food source for metazoans, higher trophic levels may benefit from enhanced production of ciliate biomass resulting from a mixotrophic mode of nutrition.

Supported by: WHOI Postdoctoral Scholarship; and NSF Grant OCE88-10235.

WHOI Contribution No. 7249.

METABOLISM OF PHOTOSYNTHATE IN THE CHLOROPLAST RETAINING CILIAE *LABOEA STROBILA*

Mary Putt

Assimilation of photosynthate into four chemical classes of compounds was compared in the chloroplast retaining ciliate *Laboea strobila* and the algae from which its chloroplasts were derived (*Isochrysis galbana* and *Pyrenomonas salina*). In laboratory cultures, the ratio of allocation of radiolabel into polysaccharide and protein was higher in *L. strobila* compared to microalgae following a 6h incubation at irradiances which were saturating or limiting to photosynthesis. In field populations collected in Vineyard Sound, Massachusetts and in laboratory cultures of *L. strobila*, maximum rates of polysaccharide production from photosynthate were equivalent to about 7-10%•h⁻¹ of body carbon. In contrast, maximum lipid and protein production from photosynthate were usually ≤1%•h⁻¹ of body carbon. About half of the radiolabel which accumulated during a 3h incubation in the light was respired or excreted when ciliates were placed in the light in the presence of the photosynthetic inhibitor DCMU, or in the dark for 18h. Net loss of radiolabel occurred largely from polysaccharide. Mixotrophic ciliates may have higher trophic efficiencies than heterotrophic ciliates because respiratory and excretory needs are supplemented by photosynthesis.

In Press: *Marine Ecology Progress Series*.

Supported by: NSF Grant OCE86-00684 and OCE88-10235; WHOI Postdoctoral Scholarship; and Natural Sciences and Engineering Research Council of Canada Postdoctoral Scholarship.

WHOI Contribution No. 7143.

RELATIONSHIP BETWEEN PHOTOTROPHY AND PHAGOTROPHY IN THE MIXOTROPHIC CHRYSTOPHYTE *POTERIOCHROMONAS MALHAMENSIS*

Robert W. Sanders, K. G. Porter and
David A. Caron

The time scales involved in the transition between phototrophic and phagotrophic modes of nutrition were examined in the mixotrophic chrystophyte *Poterioochromonas malhamensis*. Phagotrophy began almost immediately when bacteria were added to phototrophically growing cultures of the alga, and chlorophyll a concentration per cell in these cultures decreased over a period of 24 h. Chlorophyll concentrations per cell began to increase when bacteria were grazed to a density of approximately 10⁶ ml⁻¹, but after more than 24 h they had not returned to the higher chlorophyll concentrations observed in the phototrophically grown cultures. Bacterivory was the dominant mode of nutrition in all cultures containing heat killed bacteria. Photosynthesis did not contribute more than ≈ 7% of the total carbon budget of the alga when in the presence of abundant heat killed bacteria. Bacterial density was the primary factor influencing the ability of *P. malhamensis* to feed phagotrophically, while light intensity, pH, and the presence of dissolved organic matter had no effect on phagotrophy. We conclude that *P. malhamensis* is capable of phagotrophy at all times. In contrast, phototrophy is inducible in the light during starvation and is a long-term survival strategy for this mixotrophic alga (e.g., it operates on time scales greater than a diel cycle.)

In Press: *Microbial Ecology*.

Supported by: NSF Grant BSR86-20443.

WHOI Contribution No. 7274.

PREDATION ON PROTOZOA: ITS IMPORTANCE TO ZOOPLANKTON

Diane Stoecker and Judith McDowell Capuzzo

Protozoa are an important component of both the nano- and microplankton in marine and freshwater environments and are preyed upon by zooplankton, including suspension-feeding copepods, some gelatinous zooplankters and some first-feeding fish larvae. The clearance rates of suspension-feeding zooplankton for ciliates, in particular, are higher than for most phytoplankton. For at least some suspension-feeding zooplankton, protozoans are calculated to be quantitatively an important

component of the diet during certain seasons. In laboratory studies, protozoan components in the diet appear to enhance growth and survival of certain life history stages or enhance fecundity. These data suggest that protozoans are qualitatively as well as quantitatively important in the diets of marine zooplankton.

Most studies of predation on Protozoa have focused on the euphotic zone in nearshore waters. Predation on Protozoa, however, is expected to be particularly important both quantitatively and qualitatively in marine environments and seasons in which primary production is dominated by cells < 5 μm in size, such as nearshore environments after the spring phytoplankton bloom, in oligotrophic waters, and in environments dominated by detritus-dominated food webs, such as the deep sea. In detritus-dominated food webs, Protozoa may be a source of essential nutrients and may thus facilitate utilization of bacterial and detrital carbon by metazoan plankton.

Supported by: NSF Grant OCE86-00684 and NSF Subcontract OCE88-17399.

WHOI Contribution No. 7242.

CHLOROPLAST REPLACEMENT AND AGING IN *STROMBIDIUM CAPITATUM* (CILIATA, OLIGOTRICHIDA)

Diane Stoecker and M. W. Silver

The planktonic ciliate, *Strombidium capitatum*, retains functional chloroplasts derived from ingested algal cells. Chloroplast replacement and aging were experimentally investigated in cultured ciliates provided with a cryptophyte (*Pyrenomonas salina*), a prymnesiophyte (*Isochrysis galbana*) and a prasinophyte (*Pyramimonas* sp.) as sources of plastids. All three algae were ingested and chloroplasts from all were retained by the ciliate.

Within 15 minutes of exposure to the cryptophyte, this alga was taken up by the ciliates. Initially, most of the cryptophyte chloroplasts were in intact algal cells in ciliate vacuoles. By 2 h, cryptophyte plastids were mostly found free in the ciliate cytoplasm. When *S. capitatum* was switched from a diet containing cryptophytes to a non-cryptophyte diet, most cryptophyte chloroplasts were diluted out of the ciliates by cell division and/or replaced by non-cryptophyte chloroplasts within 9 hours.

When *S. capitatum* was deprived of algal food, chloroplasts were detected in the starving ciliates for as long as the ciliates survived (40 h or more). Under these conditions, cryptophyte chloroplasts were preferentially retained. Ultrastructural changes indicative of aging were observed in some of these chloroplasts. Chloroplasts, along with

ciliate mitochondria, were autophagocytized by starving ciliates.

Our observations suggest that chloroplast retention times in *S. capitatum*, depend on the type of chloroplast as well as the availability of phytoplankton containing suitable new chloroplasts, and probably also on the physiological states of the ingested algae and the ciliates. It is interesting that we were not able to grow this ciliate when we provided it only with prey that lacked chloroplasts.

Supported by: NSF Grants OCE86-00765 and OCE87-09961.

WHOI Contribution No. 7241.

OCEANIC MIXOTROPHIC FLATWORMS

D. K. Stoecker, N. Swanberg and S. Tyler

Most reports of photosynthetic flatworms are from benthic or littoral habitats, but small (<1 mm) acoel flatworms with algal endosymbionts are a widespread, though sporadic, component of the open-ocean plankton in warm waters. Among oceanic flatworms are specimens harboring prasinophyte or, less commonly, dinophyte endosymbionts. Photosynthesis was measured by ^{14}C uptake in flatworms from shelf/slope waters in the western north Atlantic and from the Sargasso Sea. Although these acoels were photosynthetic, they were also predatory on other plankton. These acoel-algal associations apparently depend on two sources of nutrition and are thus mixotrophic. Among the planktonic sarcodines, photosynthetic mixotrophy is a common nutritional strategy, it also appears to be common strategy among certain taxa of open ocean metazoa.

Published in: *Marine Ecology Progress Series*, 58, 41-51, 1989.

Supported by: NSF Grants OCE86-00765 and OCE88-00684.

WHOI Contribution No. 7099.

SUBMERSIBLE INCUBATION DEVICE (SID), AUTONOMOUS INSTRUMENTATION FOR THE IN SITU MEASUREMENT OF PRIMARY PRODUCTION AND OTHER MICROBIAL RATE PROCESSES

Craig D. Taylor and Kenneth W. Doherty

A Submersible Incubation Device (SID) is described that will conduct three sequential incubation experiments directly in situ. Each

incubation involves a cleaning cycle, procurement of a 400 ml sample at depth, with simultaneous introduction of fresh tracer, and the time course preservation of four subsamples for subsequent analysis upon retrieval of the instrument (12 subsamples total). The instrument records elapsed time, pressure (depth), light intensity, temperature, and battery voltage. The instrument has been successfully used for measurements of phytoplankton production in the open ocean and coastal waters. Three modes of operation have been employed: a) a mode for obtaining daily rate information by summation of data from multiple short-term incubations, b) a rapid profiling mode for measurement of microbial rate processes at several depths during a single deployment, and c) an unattended time series mode for obtaining representative short-term activity measurements at several day intervals. The described instrument is a prototype for a long-term (months) time series version deployable in the open ocean or in remote locations.

In Press: *Deep-Sea Research*, 1990.

Supported by: ONR Subcontract N00014-85-K-0155; NSF Grant OCE87-08958; and WHOI.

WHOI Contribution No. 7042.

POPULATION ECOLOGY

GROWTH OF TWO SPECIES OF BACTERIVOROUS MICROFLAGELLATES IN BATCH AND CONTINUOUS CULTURE, AND IMPLICATIONS FOR THEIR PLANKTONIC EXISTENCE

David A. Caron

The growth characteristics of the heterotrophic microflagellates *Monas* sp. and *Cryptobia* sp. were examined in batch and continuous culture. Batch cultures were used to establish the maximum growth rates (μ_{max}) and gross growth efficiencies at μ_{max} of the protozoa when fed the bacterium *Pseudomonas halodurans*. The microflagellates subsequently were grown in continuous culture on a non-growing population of *P. halodurans*, and the gross growth efficiencies, half-saturation constants (K_s , the bacterial density at which $\mu = \mu_{max}/2$), ingestion rates and clearance rates were determined at three steady states where $\mu < \mu_{max}$. The two microflagellates were capable of growth in continuous culture over a wide range of growth rates. Steady-state growth of *Monas* and *Cryptobia* was sustained at dilution rates equivalent to only 6% and 7%, respectively, of μ_{max} . These growth rates corresponded to ingestion rates of only 1-2

bacteria flagellate⁻¹ hr⁻¹. Gross growth efficiencies at the lowest growth rates were reduced by 15% for *Monas* and 51% for *Cryptobia* relative to efficiencies at μ_{max} . Bacterial biomass in the continuous cultures at the lowest dilution rates was comparable to published values for the bacterial biomass of oligotrophic oceanic ecosystems. An experiment was carried out in continuous culture in which *Monas* and *Cryptobia* competed for the same bacterial population. The results of this experiment (*Monas* outcompeted *Cryptobia*) were in agreement with predictions based on the growth parameters of the protozoa (μ_{max} , K_s) when grown separately in batch and continuous culture. The results of this study support the hypothesis that heterotrophic microflagellates are important consumers of suspended bacteria in oligotrophic plankton ecosystems, and may be the primary factor controlling bacterial densities in some of these ecosystems.

In Press: *Marine Microbial Food Webs*.

Supported by: NSF Grants OCE80-24441, OCE82-14928 and OCE86-00510; Ocean Industry Program Grant 4473; and WHOI Education Program.

WHOI Contribution No. 7014.

FACTORS RESPONSIBLE FOR THE DIFFERENCES IN CULTURAL ESTIMATES AND DIRECT MICROSCOPICAL COUNTS OF POPULATIONS OF BACTERIVOROUS NANOFLAGELLATES

David A. Caron, Paul G. Davis and John McN. Sieburth

Bacterivorous nanoflagellates (microflagellates) have been routinely enumerated in marine and freshwater samples using either a Most Probable Number culture method (MPN) or by a direct microscopical counting method (DC). These two techniques typically yield highly disparate estimates of the density of nanoflagellates in natural samples. We compared these methods with seawater and marine snow (macroscopic detrital aggregate) samples collected from surface waters throughout the North Atlantic and in freshwater samples collected at three stations in Lake Ontario. Densities of nanoflagellates determined by the two methods differed by as much as four orders of magnitude; the MPN estimate rarely exceeded 10% of the microscopical count, and averaged $\approx 1\%$ of this count. The MPN estimate constituted a higher percentage of the DC value in environments with high concentrations of nanoflagellates relative to environments with low concentrations of nanoflagellates. The ratio of the culture count to

the microscopical count (MPN:DC) increased along an environmental gradient from oligotrophy to eutrophy, and was positively correlated with the density of bacteria in the samples. In laboratory experiments with two species of bacterivorous nanoflagellates, the MPN count constituted a much greater percentage of the DC count during the exponential growth phase of the nanoflagellate than during the stationary growth phase. Differences in the estimates of nanoflagellate density obtained with these two techniques probably can be explained by the trophic mode of these protozoa, their growth stage, and the amenability of these species to laboratory culture.

Published in: *Microbial Ecology*, 18, 89-104, 1989.

Supported by: NSF Grants OCE80-24441, OCE81-21881, OCE82-14928, OCE85-11365, OCE86-00510, OCE87-10085, Doctoral Dissertation OCE81-12991; Ocean Industry Program Grant 4473; and WHOI Education Program.

WHOI Contribution No. 7015.

COMMUNITIES IN PATCHY ENVIRONMENTS: A MODEL OF DISTURBANCE, COMPETITION, AND HETEROGENEITY

Hal Caswell and Joel Cohen

All landscapes are to some extent patchy. The biological heterogeneity of communities on patchy landscapes reflects the time scales of local biotic interactions and abiotic disturbance, the time and space scales of dispersal, and (especially) the interaction of these scales. To investigate these factors, we will examine here a simple model which provides a framework for building models of patchy communities directly from hypotheses about time scales. Our model describes a landscape composed of an effectively infinite set of effectively identical patches. Species colonize these patches, interact, are affected by abiotic disturbance, and eventually become locally extinct. Each of these processes has a characteristic temporal scale, in terms of which we describe the stochastic dynamics of individual patches, and the resulting statistical properties of the landscape. Because we assume that all patches are identical, we are providing only the bare minimum *environmental* heterogeneity that produced by the independence of the patches. Our focus is on heterogeneity generated by the biological processes.

Supported by: NSF Grants OCE85-16177, BSR86-09395, BSR87-04936 and BSR87-05047.

WHOI Contribution No. 7214.

DENSITY EFFECTS IN A COLONIAL MONOCULTURE: EXPERIMENTAL STUDIES WITH A MARINE BRYOZOAN (*MEMBRANIPORA MEMBRANACEA* L.)

C. Drew Harvell, Hal Caswell and Paul Simpson

Naturally occurring monocultures of plants and animals are not common, despite recent emphasis on the analysis of density effects in artificial plant monocultures. In natural populations, *Membranipora membranacea*, an encrusting marine bryozoan, usually forms monospecific, nearly even-aged stands on kelp blades. We experimentally manipulated the density of *M. membranacea* colonies and monitored the responses of individual colonies on settling panels. Colonies undergo a sub-annual cycle of growth, stasis and reproduction, shrinkage, and death. However, crowding by conspecifics accelerates the transition to stasis, triggers early onset of reproduction, and results in increased stage-specific mortality. Unlike many interactions involving colonial invertebrates, overgrowth rarely occurs at boundaries of *M. membranacea* colonies. Instead, colonies stop growing when they contact conspecifics; therefore more dense assemblages are populated with smaller individual colonies. At the peak in colony size during August, the mean size among colonies grown at high population densities was 300 mm² less than of colonies grown at low densities or approximately 62% smaller. Mortality was concentrated in small size classes; at the end of the season colonies gradually shrank to the smallest size classes and then died. We summarized the demography of *M. membranacea* colonies on low- and high-density panels using size-classified transition matrices and used loglinear analysis to examine the effects of density and time on the transition patterns. As the amount of free space on panels declined, so did the frequency of upward size-class transitions. Our analysis revealed that free space declined more rapidly on panels in the high density treatment and that the transitional probabilities were sensitive to density of conspecifics and seasonal change, but only for some size classes and during some time periods.

Supported by: NSF Grants OCE85-16177, BSR86-09395; and NOAA WASC-83-00220.

WHOI Contribution No. 7261.

DEMOGRAPHIC ANALYSIS OF TROPICAL ZOOPLANKTON POPULATIONS

Saran Twombly and Hal Caswell

A first step in understanding patterns of zooplankton distribution and abundance is estimation of age- or stage-specific vital rates (survival, growth, fertility). These parameters account directly for changes in population size, in response to environmental (biotic or abiotic) fluctuations. For most copepod populations, demographic parameters are estimated from field samples using techniques (e.g., Rigler and Cooley 1974; Gehrs and Robertson 1975) that have unrealistic assumptions, yield inaccurate results (Hairston and Twombly 1985) and rely on the identification of discrete cohorts in field samples. Thus, demographic estimates obtained are imprecise and apply only to populations with discrete cohort structure. Using these methods, we cannot estimate vital rates when generations overlap, as they do in most tropical populations, and we remain unable to explain the dynamics of many copepod populations.

We are developing a demographic estimation procedure based on matrix models for complex life cycles (e.g., Lefkovich 1965; Caswell 1978, 1989) that is appropriate for all size or stage-classified populations when the time (sampling) interval $(t, t+1)$ is shorter than the duration of the shortest stage. We describe population dynamics at time t by the matrix projection equation $n(t+1) = A_t n(t)$, where $n(t)$ is a vector whose entries give the abundance of each stage at time t . A_t is a non-negative matrix whose entries incorporate demographic transitions (Caswell 1982) of individuals in the population: the first row contains stage-specific fertilities, F_i ; the subdiagonal contains probabilities G_i of surviving and growing from stage i to $i+1$; the diagonal contains probabilities P_i of surviving and remaining in the same stage. We estimate the vital rates (entries in A_t), given a sequence of stage distribution vectors $n(t)$. This model does not assume a stable stage distribution, and does not rely upon identification of cohorts. It provides a time series of demographic estimates for each stage, rather than single average values. We describe our model in detail elsewhere (Caswell and Twombly 1989); here, we illustrate this procedure with an analysis of a tropical copepod population.

Supported by: NSF Grant BSR86-09395.

WHOI Contribution No. 7176.

DEMOGRAPHIC CONSEQUENCES OF CHAOBORUS-INDUCED RESPONSE AND FOOD AVAILABILITY IN *DAPHNIA* *PULEX*

Mari Walls, Hal Caswell and Matti Ketola

The hypothesis that predator-induced spines affect the fitness of *Daphnia pulex* was tested in a life table experiment. *Chaoborus*-induced and non-induced *Daphnia pulex* morphotypes were cultured at normal and low food levels; we predicted that under low food conditions the costs of inducible defenses will be greater. We used matrix population models to quantify fitness, measured as population growth rate, and sensitivity analysis to quantify the effects of induction, food and their interaction on fitness. The results confirm the hypothesis that there are demographic costs of inducible defence. Fitness decreased 19.6% in the *Chaoborus*-exposed, low food population compared to non-exposed controls. The sensitivity analysis revealed that the fitness differences depend on treatment effects in the early instars (1-11) of *D. pulex*. The interaction between *Chaoborus* exposure and low food level was negative, and mediated through growth and fertility components. Both these components were reduced more in the *Chaoborus*-exposed, low food treatment than would be expected in the absence of interaction.

Supported by: Academy of Finland (under agreement 09/013); Maj and Tor Nessling Foundation; Turka University Foundation; NSF Grants OCE85-16177, BSR86-09395 and BSR87-04936; and EPA Cooperative Agreement CR-814895-01-1.

WHOI Contribution No. 7177.

ZOOPLANKTON

ASPECTS OF JET PROPULSION IN SALPS

Laurence P. Madin

Several morphological and functional characteristics which affect the jet propulsion of salps are described, based on observations of living animals in situ and in the laboratory. A velocity profile of water flowing through the salp and its feeding net is determined from video frames, and velocities of the jet efflux related to forward movement of the animal. Analysis of the site and spacing of vortices in the jet trail indicates the theoretical augmentation of thrust from a pulsed jet may indeed affect the locomotory efficiency of

salps. The external morphology of several species of solitary generation salps indicates selection for streamlining in most, while the architecture of the chains of aggregate generation individuals has a significant effect on their locomotory capabilities. Calculated cost of locomotion for several salp species are similar to literature values for other salps, and lower than for all other jet-propelled organisms. Differing locomotory capabilities and their consequences may be one of the main characteristics which isolate species of salps.

Supported by: NSF Grant OCE86-08961.

WHOI Contribution No. 6987.

DEPARTMENT OF CHEMISTRY

Frederick L. Sayles, Chairman

GEOCHEMISTRY

COSMIC RAY EXPOSURE DATING WITH *IN-SITU* PRODUCED COSMOGENIC ^3He : RESULTS FROM YOUNG HAWAIIAN LAVA FLOWS

Mark D. Kurz, Debra Colodner, Thomas W. Trull,
Richard B. Moore, and Keran O'Brien

In an effort to determine the *in situ* production rate of spallation-produced cosmogenic ^3He , and evaluate its use as a surface exposure chronometer, we have measured cosmogenic helium contents in a suite of Hawaiian radiocarbon-dated lava flows. The lava flows, ranging in age from 600 to 13,000 years, were collected from Hualalai and Mauna Loa volcanoes on the island of Hawaii. Because cosmic-ray surface-exposure dating requires the complete absence of erosion or soil cover, these lava flows were selected specifically for this purpose. The ^3He production rate, measured within olivine phenocrysts, was found to vary significantly, ranging from 47 to 150 atoms $\text{g}^{-1} \text{yr}^{-1}$ (normalized to sea level). Although there is considerable scatter in the data, the samples younger than 10,000 years are well-preserved and exposed, and the production rate variations are therefore not related to erosion or soil cover. Data averaged over the past 2000 years indicate a sea-level ^3He production rate of 125 ± 30 atoms $\text{g}^{-1} \text{yr}^{-1}$, which agrees well with previous estimates. The longer record suggests a minimum in sea level normalized ^3He production rate between 2000 and 7000 years (55 ± 15 atoms $\text{g}^{-1} \text{yr}^{-1}$), as compared to samples younger than 2000 years (125 ± 30 atoms $\text{g}^{-1} \text{yr}^{-1}$) and those between 7000 and 10000 years (127 ± 19 atoms $\text{g}^{-1} \text{yr}^{-1}$). The minimum in production rate is similar in age to that which would be produced by variations in geomagnetic field strength, as indicated by archeomagnetic data. However, the production rate variations (a factor of $2.3 \pm .8$) are poorly determined due to the large uncertainties in the youngest samples and questions of surface preservation for the older samples. Calculations using the atmospheric production model of O'Brien (1979), and the method of Lal and Peters (1987), predict smaller production rate variations for similar variation in dipole moment (a factor of 1.15 to 1.25). Because the production rate variations, archeomagnetic data, and theoretical estimates are not well determined at present, the relationship between dipole moment and production rate will require further study. Precise determination of the production rate is an important uncertainty in the surface-exposure technique, but the data demonstrate that it is feasible to date samples as young as 600 years of

age providing that there has been no erosion or soil cover. Therefore, the technique will have important applications for volcanology, glacial geology, geomorphology and archaeology.

Supported by: NSF Grant EAR88-3783 and NASA Grant NAG9-69.

WHOI Contribution No. 7257.

CUMULATE GABBROS FROM THE SOUTHWEST INDIAN RIDGE, 54°S-7°16'E: IMPLICATIONS FOR MAGMATIC PROCESSES AT A SLOW SPREADING RIDGE

Peter S. Meyer, Henry J. B. Dick, and
Geoffrey Thompson

A diverse volcanic and plutonic rock suite was recovered from the center of the 80 km long ridge segment of the Southwest Indian Ridge (54°S, 7°16'E) between the Islas Orcadas and Shaka Fracture Zones. The cumulus nature of the gabbroic rocks in the suite is indicated by phase, modal and cryptic layering, igneous lamination, and low incompatible element abundances. We present a mass-balance model for calculating the proportions and compositions of cumulus phases and crystallized intercumulus liquid from bulk-rock major element compositions. The model is based on the ability to define a compositional array of basaltic liquids and on the assumption that cumulus minerals are initially in equilibrium with trapped liquid. Calculated proportions of trapped liquid range from 3%-15%; values that are characteristic of adcumulates to mesocumulates. Models of postcumulus crystallization indicate significant enrichments of incompatible elements and buffering of compatible elements in residual trapped liquids, thus explaining the high TiCO_2 contents observed in magnesian clinopyroxenes. Cumulus phase assemblages and compositions suggest solidification in shallow level magma chambers, but disequilibrium plagioclase compositions suggest some crystallization at greater depth. Furthermore, basalt compositions projected onto the olivine-clinopyroxene-quartz pseudoternary suggest magma generation over a range of pressures (from less than 10 to greater than 20 kb), as well as polybaric fractional crystallization. We suggest that the Southwest Indian Ridge is characterized by low magma supply with small batches of melt that either ascend directly to the surface having undergone limited polybaric crystallization or are trapped in shallow crustal magma chambers where they evolve and solidify to form cumulate gabbros. The adcumulus nature of the gabbros investigated here suggests slow cooling rates typical of large

intrusions implying relatively large, but ephemeral magma chambers below segments of the Southwest Indian Ridge.

Published in: *Contributions to Mineralogy and Petrology*, 103, 44-63, 1989.

Supported by: NSF Grant DPP87-20002.

INSTRUMENTS

THE SEEP METER: A BENTHIC CHAMBER FOR THE SAMPLING AND ANALYSIS OF LOW VELOCITY HYDROTHERMAL VENTS

F. L. Sayles and W. H. Dickinson

A "seep meter" for the determination of flow rate and collection of samples from low velocity hot springs on the sea floor is described. The device is a benthic chamber designed for deployment from a research submersible. Temperature in the chamber is monitored in real time, providing information for the collection of samples and determination of flow rate. Samples of solution in the chamber are collected to provide a means of defining the composition of solutions emanating from the hot springs. The performance of the instrument has been evaluated in a series of laboratory experiments and in field deployments in hydrothermal areas of the Guaymas Basin.

In Press: *Deep-Sea Research*.

Supported by: NSF Grant OCE86-14387.

WHOI Contribution No. 7229.

TG/PLUS—A PYROLYSIS METHOD FOR FOLLOWING MATURATION OF OIL AND GAS GENERATION ZONES USING TMAX OF METHANE

Jean Whelan, Robert M. Carangelo, and Peter Solomon

Thermogravimetric Fourier transform infrared spectroscopy (TG-FTIR) analyses were carried out on two sets of isolated kerogens covering a wide maturity range from immature (0.2% Ro) through the end of oil and gas generation (maximum Ro = 5.8%). Data on weight percent and Tmax of methane, tars, ethylene, SO₂, NH₃, CO₂, and CO are reported. The Tmax of methane shows the most consistent response to increasing maturation in both sets of samples. Results are comparable to those of whole rocks from an Alaskan North Slope well analyzed previously. This collective data for both whole rocks and isolated kerogens is

consistent with a generally linear correlation between %Ro and Tmax of methane, with a deviation in two of the curves at Ro of about 2.0% where a phase change in kerogen is known to occur. The slope of correlation line was steeper for kerogens isolated from the Wilcox shale than for the other two sets of data, possibly indicative of a higher geothermal heating rate. These preliminary data indicate that Tmax of methane is a good maturation indicator for whole rocks and isolated kerogens up to an Ro of about 4%, which includes all of the wet gas and a considerable portion of the dry gas generation zones. This correlation was also observed for samples containing migrated bitumen, where it was not possible to measure a reliable Tmax of the tar (S2) peak.

In Press: *Organic Geochemistry*.

Supported by: DoE Grant DE-FCO2-86ER13466. A002.

WHOI Contribution No. 7237.

ORGANIC AND BIOLOGICAL CHEMISTRY

TEMPORAL VARIATIONS IN NITROGEN AND PARTICLE DYNAMICS IN THE SARGASSO SEA: INTERPRETATION OF ISOTOPIC DATA

Mark A. Allabet

Seasonal and interannual variations were observed for euphotic zone particulate nitrogen content and flux and their associated isotopic ratios at the OFP site off Bermuda. PN concentration and flux as sinking particles at 100 m tended to have minima in late-fall and maxima in late winter/early spring. Corresponding $\delta^{15}\text{N}$ values for suspended particles showed a similar seasonal pattern with an annual amplitude of 2 to 3‰. Only in one year, when wintertime euphotic zone NO₃⁻ concentrations remained undetectable, did $\delta^{15}\text{N}$ values for sinking particles exhibit a similar temporal pattern. Otherwise, values for sinking particles instead decreased by about 3‰ at the time of the wintertime maxima in NO₃⁻ concentration. This was also the period in which sinking and suspended particles were most similar in $\delta^{15}\text{N}$. During the rest of the year, sinking particles were typically 4‰ higher in $\delta^{15}\text{N}$.

Comparison of results from a simple nitrogen flux model for the euphotic zone shows at least three phenomena contribute to these temporal variations in $\delta^{15}\text{N}$: 1) Isotopic fractionation in the utilization of NO₃⁻ when it is present at elevated concentrations in the euphotic zone in the winter.

The signal appears to propagate into the deep ocean and may be used to trace other processes within the ocean's nitrogen cycle. 2) Seasonally non-steady conditions in the overall balance between nitrogen fluxes into and out of the euphotic zone which also produce variations in the ^{15}N budget. The euphotic zone is never in true steady state with respect to nitrogen fluxes but cycles about a mean state. 3) A decrease in the difference in $\delta^{15}\text{N}$ ($\Delta\delta^{15}\text{N}$) between sinking and suspended PN when NO_3^- is at elevated concentrations which also perturbs the ^{15}N budget for the euphotic zone. $\Delta\delta^{15}\text{N}$ may decrease due to fewer steps in the conversion of suspended particles into sinking ones under these conditions.

Supported by: NSF Grants OCE85-16296 and OCE87-17508.

WHOI Contribution No. 7029.

ORGANIC C, N, AND STABLE ISOTOPIC COMPOSITION OF PARTICULATE MATTER COLLECTED ON GLASS-FIBER AND ALUMINUM OXIDE FILTERS

Mark A. Altabet

The relative retention of particles from the upper ocean at a site near Bermuda were compared for organic C and N contents and for stable carbon and nitrogen isotopic ratios. Glass-fiber (Whatman GF/F, 0.7 μ ; QM-A, 1 μ ; and GF/D, 3 μ) and aluminum oxide filters (Anotec Anopore, 0.2 μ) filters were used. Most of the POC and PN passed the GF/D and QM-A filters. A majority was retained on the GF/F filter. However, an average of 35% of the PN and 40% of the POC passed the GF/F filter and was retained on the Anopore filter. This fraction would have been overlooked by previous studies employing GF/F filters. The fraction passing the QM-A filter but retained on the GF/F had distinctly lower C/N ratios perhaps due to a greater contribution from cyanobacteria. This size fraction and the one passing a GF/D filter but retained on a QM-A filter had lower $\delta^{15}\text{N}$ and $\delta^{13}\text{C}$ values which may be probably accounted for by a relatively high contribution from phytoplankton. Inclusion of the fraction retained by the Anopore filter resulted in slightly higher C/N and $\delta^{13}\text{C}$ values for the total particle pool. Bacteria are likely an important component of the particles passing GF/F filters and retained by Anopore filters, but future study is required to definitively identify the particles in this fraction.

In Press: *Limnology & Oceanography*.

Supported by: NSF Grant OCE87-17508.

WHOI Contribution No. 7137.

DIFFERENCES IN NITROGEN ISOTOPE COMPOSITION BETWEEN PARTICLES COLLECTED BY BOTTLES AND LARGE-VOLUME PUMPS IN GULF STREAM WARM-CORE RINGS AND THE SARGASSO SEA

M. A. Altabet, J. K. B. Bishop, and J. J. McCarthy

Nitrogen content and isotopic composition for particles collected by standard water-sampling bottles and *in-situ* large-volume pumps are compared. Data are presented for stations in warm-core ring 82-B in April and June 1982, newly formed warm-core ring 82-H in Sept./Oct. 1982, and the OFP site off Bermuda. For warm-core rings, relatively large differences in $\delta^{15}\text{N}$ and PN concentration are observed between the two techniques. For the OFP site, except for PN concentration in the upper 200 m, good agreement was observed. Consideration of the effects of different retention sizes for the filter types used by the two techniques and whether or not large particles were included in the samples brought the OFP results into even closer agreement. However, only a fraction of the discrepancies in the warm-core ring results could be accounted for. Possible explanations include artifacts associated with differences in the details of the sample collection and handling techniques or differences in the size distributions of submicron particles and their $\delta^{15}\text{N}$ values in rings. The much better agreement in $\delta^{15}\text{N}$ between pumps at the OFP site, bottles at the OFP site, and pumps in Ring 82-H suggests that minimal sample handling is desired. However, for measurement of PN concentrations the use of filters with the smallest available retention size is preferred. These difficulties underscore the need to evaluate carefully the limitations of any particle sampling technique regarding the specific measurements to be made.

Supported by: NSF Grants OCE87-17508 and OCE85-16296.

WHOI Contribution No. 7258.

NITROGEN ISOTOPIC RATIOS IN FECAL PELLETS PRODUCED BY MARINE ZOOPLANKTON

Mark A. Altabet and Lawrence F. Small

In the upper ocean, regardless of site or season, fecal pellets were consistently depleted in ^{15}N relative to the zooplankton that produced them. However, fecal pellets were also 2‰ enriched in $\delta^{15}\text{N}$ relative to the zooplankton's apparent food source. ^{14}N -containing molecules are evidently

preferentially assimilated in zooplankton intestinal tracts, but other metabolic processes must account for the widely observed enriched in ^{15}N of these organisms relative to their food. $\delta^{15}\text{N}$ values for sinking particles and fecal pellets are very similar, supporting the perspective that macrozooplankton are important factors in producing and processing particles that sink into the ocean's interior and sediments. In contrast, the relationship between fecal pellets and suspended particles in the euphotic zone is variable. Evidently, zooplankton can vary in their selection of food particles among components of the suspended particle pool which vary in $\delta^{15}\text{N}$. These results have important implications for the processes which determine the composition of sinking particulate matter in the ocean with respect to the suspended particle source in the euphotic zone.

In Press: *Geochimica et Cosmochimica Acta*.

Supported by: NSF Grant OCE87-17508.

WHOI Contribution No. 6994.

DISSOLVED FLUORESCENCE IN THE BLACK SEA

*Paula Garfield Coble, Robert B. Gagosian,
L. A. Codispoti, Gernot E. Friederich, and
John P. Christensen*

Subsurface *in-situ* fluorescence maxima have previously been found to occur in low oxygen waters below the bottom of the mixed layer at several locations in the Pacific Ocean. These fluorescence maxima coincide with maxima in nitrite, suspended particles, bacterial biomass and microbial activity, but are not associated with a pycnocline. While some of the fluorescence signal may be due to chlorophyll or its degradation products, it has also been suggested that fluorescent substances may be produced by the resident microbial populations. Our preliminary experiments with cultures of denitrifying bacteria isolated from the Cariaco Trench in March 1986 verify that they are capable of producing fluorescent pigments. These pigments could be part of the observed fluorescence signal in low oxygen waters and potentially could serve as "real time" indicators of bacterial aggregations in the water column.

We present here results from the Black Sea where we made continuous profiles of fluorescence in three channels (chlorophyll, dissolved organic matter (DOM) and flavin), simultaneously, using a pump profiling system. Other parameters measured on each pump cast included temperature, salinity, beam attenuation coefficient (c), nutrients, oxygen and hydrogen sulfide. Dissolved organic matter (DOM) and flavin

fluorescence increased with depth, while chlorophyll fluorescence showed two distinct maxima, one at the bottom of the euphotic zone, and one at the depth of the sulfide interface. This deeper maximum was associated with a particle maximum and a maximum in microbial activity (ETS), and is attributed to the presence of photosynthetic bacteria of the genus *Chlorobium*.

Supported by: NSF Grant OCE87-01386.

WHOI Contribution No. 7153.

REEF-BUILDING CORALS AND IDENTIFICATION OF ENSO WARMING EPISODES

*E. R. M. Druffel, R. B. Dunbar,
G. M. Wellington, and S. A. Minnis*

Many chemical and physical changes that occur in the atmosphere and surface ocean are recorded in coral skeletons. In this chapter, we discuss some of the physical, chemical and isotopic changes observed in coral skeletons and their relationships with various climate-related forcing functions. Among the specific factors affecting coral growth and the chemical and isotopic composition of the accreted aragonite are those encountered during ENSO events: abnormal temperature and salinity, reduced nutrient and zooplankton supply, and variation in light intensity. We also determine the usefulness of coral skeletons for reconstructing ENSO records in the eastern tropical Pacific. We present records of stable oxygen and carbon isotopes in corals from the Galapagos Islands and the coast of Panama. We conclude that stable isotopic studies are adequate for tracking most minor and major ENSO events, but are insufficient for unequivocally determining the occurrences of all events or of catastrophic events, such as that which occurred during 1982-83. The catastrophic environmental stresses imposed on corals during such events result in cessation of skeletal accretion, and thus an absence of a significant portion of the record.

In Press: Chapter for *Global Ecological Consequences of the 1982-83 El Niño-Southern Oscillation*.

Supported by: NSF Grants OCE83-15260 and OCE86-08263.

WHOI Contribution No. 6991.

RADIOCARBON IN DISSOLVED ORGANIC AND INORGANIC CARBON FROM THE CENTRAL NORTH PACIFIC

Ellen R. M. Druffel, Peter M. Williams, Ken Robertson, Sheila Griffin, A. J. Timothy Jull, Douglas Donahue, Lawrence Toolin, and Timothy W. Linick

Radiocarbon measurements are reported for dissolved organic carbon (DOC) and inorganic carbon (DIC) from sea water samples collected from the Alcoyne-5 cruise in the central North Pacific Ocean in 1985. Differences between the UV-radiation techniques used here and those reported by Williams, Oeschger and Kinney (1969) to oxidize and recover the DOC from sea water are presented. UV unoxidizable DOC in these samples is discussed in a separate publication (Druffel, Williams and Suzuki, 1989). We briefly discuss the penetration of the bomb radiocarbon signal into the DOC and DIC pools. The temporal variability of $\Delta^{14}\text{C}$ in DIC in surface samples taken every 2-3 days is presented. Concentrations of total dissolved free (FAA) plus combined (hydrolyzable) amino acids (THAA) and total dissolved carbohydrates (TCHO) measured in the same water samples are also reported. Our main aim is to present the chemical and isotopic data from samples collected during the Alcoyne-5 cruise. Detailed interpretation is published elsewhere.

In Press: *Radiocarbon*, Vol. 31, No.3, 1989.

Supported by: NSF Grants OCE84-16632 and OCE87-16590.

WHOI Contribution No. 6993.

EARLY DIAGENESIS OF ORGANIC MATTER IN PERU UPWELLING AREA SEDIMENTS

J. W. Farrington, M. A. McCaffrey, and J. Sulanowski

The early diagenesis of organic matter in the surface sediment of the Peru Upwelling area at 15°S has been investigated and is discussed. Previous data for organic carbon, nitrogen, pore water geochemistry, total hydrolyzable amino acids, and interstitial water amino acids are compared and contrasted with more recent data for lipid class compounds, such as long chain alkenones and fatty acids from two box cores collected in 1978. Detailed depth profiles of previously unpublished fatty acid data for these two box cores are reported and discussed. Despite substantial early diagenesis and remineralization of organic matter, it appears that historical records of fluctuations of periods of predominantly normal

productivity and periods of predominantly lower than normal productivity (ENSO events) are recorded via certain lipid class compound distributions in sediments.

In Press: *Facets of Modern Biogeochemistry*.

Supported by: NSF Grant OCE85-09859.

WHOI Contribution No. 7239.

IMPACT OF PHYTOPLANKTON-GENERATED SURFACTANTS ON GAS EXCHANGE AT THE AIR-SEA INTERFACE

Nelson M. Frew, Joel C. Goldman, Mark R. Dennett, and A. Sherwood Johnson

The effect of surface-active organic matter generated by seven common species of marine phytoplankton on gas exchange rates under turbulent conditions at the air-water interface was determined. Reductions in oxygen evasion rates ranging from 5-50% were observed relative to clean seawater controls. Relative oxygen exchange coefficients (expressed as $R = K_w[\text{sample}]/K_w[\text{control}]$) were shown to be sensitive to small changes in total dissolved carbohydrate (TDC) at concentrations $<1 \text{ mg Cl}^{-1}$ and to asymptotically decrease to a lower limit ($R = 55-70\%$) at concentrations between 2-6 mg Cl^{-1} . A similar relationship was observed in which R decreased with increasing relative surfactant amounts derived from surface pressure-area measurements. However, gas exchange reductions were significant for plankton exudate samples displaying surface pressures $\leq 1 \text{ mN m}^{-1}$. It thus seems that condensed monolayer films are not a prerequisite for reduced gas exchange and that relatively soluble surfactants derived from phytoplankton can strongly affect the dissipation of near-surface turbulence and thus, lead to changes in the Schmidt number dependency of K_w . Based on detailed analyses of carbohydrate-containing surface-active exudates isolated by solid phase extraction from one of the species, *Phaeodactylum tricornutum*, it appears that small glucans and heteropolysaccharides associated with proteins and possibly lipids were responsible for the observed reductions in R .

In Press: *Journal of Geophysical Research (Oceans)*.

Supported by: ONR Contract No. N00014-87-K-007 and NSF Grant OCE84-09169.

WHOI Contribution No. 7052.

FLUORESCENCE DETECTION OF FREE RADICALS BY NITROXIDE SCAVENGING

John L. Gerlock, P. J. Zacmanidis,
David R. Bauer, Daniel J. Simpson,
Neil V. Blough, and Irving T. Salmeen

The fluorescence quantum yields of 4-(1-naphthoxy)-2,2,6,6-tetramethylpiperidine-1-oxyl(I) in acetonitrile and hexane are ~55 and 30 fold lower than those of diamagnetic analogs. Experiments herein demonstrate that this property makes possible the fluorescence detection of radical scavenging reactions in which the paramagnetic nitroxide-substituted naphthalene is converted to a diamagnetic product. 2-cyanopropyl-free radicals were generated by the thermal decomposition of azobisisobutyronitrile (AIBN) in cyclohexane or in acetonitrile containing I. The fluorescence intensity of the sample increased proportionally to a decrease in the ESR signal intensity, indicating the conversion of the paramagnetic species to a diamagnetic product. The linear relationship between the increase in fluorescence intensity and decrease in ESR signal intensity shows that the changes in the fluorescence intensity can serve as a sensitive means for optically detecting radicals.

In Press: *Free Radical Research Communications*.

Supported by: ONR Contract N00014-87-K-007 and ONR Grant N00014-89-J-1260.

WHOI Contribution No. 7112.

AN OCEAN BASIN-SCALE MODEL OF PLANKTON DYNAMICS IN THE NORTH PACIFIC DURING OCEANOGRAPHIC SPRING

David M. Glover, J. S. Wroblewski, and
Charles R. McClain

A model of the concentration of phytoplankton, zooplankton and dissolved nutrient (nitrate) in the surface mixed layer of the ocean is applied to the North Pacific basin for the climatological conditions during oceanographic springtime (May, June, and July). The model is initialized with a $1^\circ \times 1^\circ$ gridded estimate of wintertime (February, March, and April) mixed layer nitrate concentrations calculated from an extensive nutrient database and a similarly gridded mixed layer depth data set. A transition zone in phytoplankton concentration running across the basin at 30° to 40° north latitude predicted by the model corresponds to a basin wide front in surface chlorophyll observed in a composite of Coastal Zone color Scanner images for May, June and July, 1979. Comparison of this model prediction with

CZCS data provides a means to evaluate certain biological parameter values used in the model. The geographical distribution of zooplankton biomass predicted by the model shows features similar to published maps of zooplankton abundance in the North Pacific. We conclude that wintertime vertical mixing determines the total nutrient available to the plankton ecosystem in the spring and thereby sets the stage for much of the biogeochemical cycling that occurs through the remainder of the year.

Supported by: NSF Grant OCE87-01461 and NASA Grant NAGW-1314.

WHOI Contribution No. 7268.

SOURCES OF CARBON TO DEEP-SEA CORALS

Sheila Griffin and Ellen R. M. Druffel

Radiocarbon measurements in deep-sea corals from the Little Bahama Bank was used to determine the source of carbon to the skeletal matrices. Specimens of *Lophelia*, *Gerardia*, *Paragorgia johnsoni*, and *Corallium niobe* were sectioned according to visible growth rings and/or stem diameter. We determined that the source of carbon to the corals accreting organic matter was primarily from surface-derived particulate organic matter. Those corals that accrete a calcareous skeleton were found to obtain their carbon solely from dissolved inorganic carbon (DIC) in sea water from the depths at which the corals grew. These results, in conjunction with growth rate studies using short-lived radioisotopes, support the use of deep-sea corals to reconstruct time histories of transient and non-transient tracers at depth in the oceans.

In Press: *Radiocarbon*, Vol. 31, No.3, 1989.

Supported by: NSF Grants OCE83-15260 and OCE86-08263.

WHOI Contribution No. 6992.

GENERATION AND MIGRATION OF PETROLEUM FROM ABNORMALLY PRESSURED FLUID COMPARTMENTS

John M. Hunt

Much of the world's oil and gas has been generated from source rocks inside deep (>3000 m or 9,840 ft) seal-bounded fluid compartments. The quantity and composition of the kerogen and the burial history of the source rocks determine the volumes of petroleum generated; however, the migration from the compartments during an oil

and gas phase, is a pressure driven process in which the flow direction is controlled by the configuration and internal pressures of the fluid compartments. Many sedimentary basins contain layers of two or more superimposed hydrogeological systems. The shallow systems are usually basin wide in extent and exhibit normal hydrostatic pressures. The deeper systems, where the oil is generated, are not basin wide and are abnormally overpressured. They generally consist of a series of individual fluid compartments that are not in hydraulic pressure communication with each other nor with the overlying hydrodynamic regime. Tops of fluid compartments in currently sinking basins do not always follow a specific stratigraphic horizon. They frequently have planar tops and subsurface temperatures ranging from 90° to 100°C (194° to 212°F). The tops in clastic sediments appear to be caused by carbonate mineralization along a thermocline. In the North Sea, the depth to the top of the deepest seal changes with the geothermal gradient. The seal is deeper where the gradient is lower.

The generation of oil and gas within the compartments, plus the thermal expansion of pore fluids, eventually causes fracturing of the top compartment seal during periods of basin sinking. Hydrocarbons and other pore fluids then move vertically into the overlying lower pressured sediments and accumulate in the nearest structural and stratigraphic traps. Seal fracturing causes a pressure drop with compartment fluids rushing to the breakout point. The compartment then reseals and pressure builds to another breakout. This episodic process continues with resealing and breakout cycles probably occurring in intervals of thousands of years in rapidly sinking basins such as the United States Gulf Coast. This concept of episodic dewatering of deep-basin fluid compartments needs to be considered in any basin-modeling program where the bulk of the oil generation occurs in the compartmented overpressured section of the basin and the oil moves vertically into the normally pressured rocks above.

Published in: *The American Association of Petroleum Geologists Bulletin*, 74(1), 1-12, 1990.

Supported by: Contract No. 5088-260-1746 of the Gas Research Institute.

WHOI Contribution No. 7110.

FLUORESCENCE DETECTION OF CARBON-CENTERED RADICALS IN AQUEOUS SOLUTION

David J. Kieber and Neil V. Blough

A simple, highly sensitive method for the simultaneous determination of arrays of

carbon-centered radicals in aqueous systems is described. Radicals are efficiently trapped by an amino-nitroxide to form stable products which are then reacted with fluorescamine to produce highly fluorescent adducts. The adducts are easily separated by reversed-phase high performance liquid chromatography. The detection limit for individual radical adducts (0.5 to 2 nM) is two to three orders of magnitude lower than those of current methods employing electron paramagnetic resonance detection. Results on the photolysis of ketones and α -keto acids demonstrate the potential of this technique. This approach should be widely applicable to the study of radical processes in biological and chemical systems.

In Press: *Free Radical Research Communications*.

Supported by: ONR Contract No. N00014-87-K-007 and Grant No. N00014-89-J-1260.

WHOI Contribution No. 7111.

THE ORGANIC GEOCHEMISTRY OF PERU MARGIN SURFACE SEDIMENTS—I. A COMPARISON OF THE C₃₇ ALKENONE AND HISTORICAL EL NIÑO RECORDS

Mark A. McCaffrey, John W. Farrington, and Daniel J. Repeta

The alkenone-U₃₇^k "paleothermometer" has potential as a sedimentary marker for El Niño/Southern Oscillation (ENSO) events in the Peru upwelling regime. We assess the utility of the U₃₇^k ratio as an indicator of ENSO depositional conditions by comparing the historical ENSO record with detailed U₃₇^k profiles for ²¹⁰Pb-dated cores from the Peru margin oxygen minimum zone (OMZ). Our data suggest that U₃₇^k profiles in Peru margin sediments may record the history of El Niño occurrences if (1) the sediments are collected from a stable portion of the OMZ where bioturbation is inhibited and (2) the core sectioning interval is ≤ the yearly sedimentation rate. Periods of frequent ENSO activity (i.e., 1870-1891) are more readily identified in the sediment record than isolated ENSO events in periods of less frequent ENSO activity. Detailed depth profiles of the C₃₇ alkenones in a core from ≈255 m (O₂ <0.1 ml/l bottom water) suggest significant alkenone remineralization (≈30%) in the 0-1 cm interval, despite the dysoxic depositional conditions. However, the similarity of the U₃₇^k values for the five 2 mm sections from 0-1 cm suggest that the U₃₇^k may be unaffected by the alkenone degradation. Correlation between the C₃₇ alkenone concentration profiles in two cores from ≈15°S collected nine years apart are consistent

with the use of these compounds for "molecular stratigraphy."

Supported by: NSF Grant OCE88-11409.

WHOI Contribution No. 7197.

AN INVESTIGATION OF HYDROGEN PEROXIDE CHEMISTRY IN A COASTAL MARINE ENVIRONMENT USING $H_2^{18}O_2$ AND $^{18}O_2$

James W. Moffett and Oliver C. Zafriou

^{18}O labelled hydrogen peroxide and O_2 have been used to determine absolute rates and pathways of peroxide formation and decay processes in surface waters of a coastal marine site. Reactions were followed by incubating seawater samples with labelled O_2 or H_2O_2 and following the chemical transformation of the isotope label.

Hydrogen peroxide chemistry was more dynamic than has been previously indicated by following changes in total H_2O_2 alone, with simultaneous formation and decay occurring under a variety of conditions. Photodecomposition of $H_2^{18}O_2$ in seawater led exclusively to the production of $^{18}O_2$, indicating oxidation by photochemically produced oxidants. These species are currently unknown and cannot be any of the previously identified oxidants in seawater.

In unfiltered seawater containing organisms, hydrogen peroxide decay was dominated by light independent biological decay processes. Decomposition of $H_2^{18}O_2$ led to the formation of $^{18}O_2$ and $H_2^{18}O$, and the product distribution indicates that 65-80% of the decay was due to catalase, and that 20-35% was due to peroxidase activity.

Particle dependent, light independent peroxide production was also observed in freshly collected samples, with rates ranging from 1.2-3.4 nMh^{-1} . These rates are low relative to daytime photochemical production rates in surface waters, but may be important under conditions of low light intensity. Experiments with a metabolic inhibitor suggest that at least some of this production was biologically mediated. However, there was no evidence for light dependent biological production.

The results demonstrate the usefulness of oxygen isotope labels in studies of redox processes in complex aqueous media such as natural waters.

Supported by: ONR Contract Nos. N0001-14-87-K-0007 and N000-14-85-C-0001.

WHOI Contribution No. 7275.

ORGANIC GEOCHEMISTRY OF AEROSOLS OVER THE PACIFIC OCEAN

E. T. Peltzer and R. B. Gagosian

For the past ten years, as part of the Sea-Air Exchange (SEAREX) Program, the authors have conducted studies on the organic geochemistry of aerosols over the Pacific Ocean. In order to quantify the air-sea exchange of materials and to understand the processes that control this exchange, it was felt necessary to identify the sources of the materials, their transport mechanisms over the ocean and the processes affecting their fluxes across the air-sea interface. Previous reports of these studies stressed the results from single sites (*e.g.*, Gagosian *et al.*, 1981, 1982; Schneider *et al.*, 1983; Schneider and Gagosian, 1985; Zafriou *et al.*, 1985; and Gagosian *et al.*, 1987). In this chapter, the authors will provide an overview and attempt to make a synthesis of the results.

Samples were collected using stringent anti-contamination protocols at five remote sites in the four major wind fields in the Pacific Ocean basin and the Peru coastal upwelling region. Enewetak Atoll and American Samoa were chosen as the sites for sampling the north and south tradewind regimes; the northern tip of New Zealand and a cruise track north of Hawaii were the sites for the southern and northern hemisphere westerlies. Samples collected at these sites were assayed for the major naturally occurring lipid classes of compounds. These compound classes were chosen because of their potential usefulness as tracers of meteorological processes and chemical phenomena.

Published in: *Chemical Oceanography*, Vol. 10, J. P. Riley, R. Chester and R. A. Duce, editors. Academic Press, London, pp. 281-338, 1989.

Supported by: NSF Grants OCE77-12914, OCE81-11947, OCE84-06666 and OCE87-16954.

WHOI Contribution No. 6995.

EVIDENCE FOR ANOXYGENIC PHOTOSYNTHESIS FROM THE DISTRIBUTION OF BACTERIOCHLOROPHYLLS IN THE BLACK SEA

D. J. Reaeta, D. J. Simpson, B. B. Jorgensen, and H. W. Jannasch

The contribution of anoxygenic photosynthesis to carbon cycling in the Black Sea, the world's largest body of anoxic marine water, has been vigorously investigated and debated for over four decades. Penetration of light into the

sulfide-containing deep water may result in a zone of anaerobic primary production by photosynthetic bacteria. We report here the results of analyses of photosynthetic pigments in samples of suspended particulate matter collected from two stations in the western basin of the Black Sea. Our data demonstrate high concentrations of a bacteriochlorophyll at the chemocline, and thus the potential for anoxygenic photosynthesis as a component of primary production in the carbon cycle of the Black Sea. More than 95% of the pigments in the bacteriochlorophyll-maximum are accounted for by a series of aromatic carotenoids and bacteriochlorophylls-*e*, including a previously unreported geranyl ester of 4-*i*-butyl bacteriochlorophyll-*e*. The distribution of pigments is characteristic of the obligate phototrophs *Chlorobium phaeobacteroides* and *C. phaeovibrioides*. Total depth-integrated bacteriochlorophyll at one station exceeded total chlorophyll-*a* in the overlying oxygenated portion of the euphotic zone. We suggest that anoxygenic photosynthesis is a relatively recent phenomenon in the Black Sea initiated by shallowing of the chemocline over the past decade and development of an anoxic layer devoid of O₂ and H₂S.

Published in: *Nature*, 342, 69-72, 1989.

Supported by: NSF Grant OCE88-14398.

WHOI Contribution No. 7198.

CHEMICAL METHODS FOR ASSESSING KEROGEN AND PROTOKEROGEN TYPES AND MATURITY

Jean K. Whelan and Carolyn Thompson-Rizer

Kerogen is the complex, high molecular weight, disseminated organic matter in sediments. It is operationally defined as the complex disseminated organic matter present in sedimentary rocks which is not soluble in either nonpolar organic solvents or via short treatment with cold or warm nonoxidizing mineral acids, most commonly HCl and HF. It is generally believed to be the major starting material for most oil and gas generation as sediments are subjected to geothermal heating in the subsurface and is the most abundant form of organic carbon on Earth—about 1000 times more abundant than coal which forms primarily from terrigenous higher plant remains. Kerogen forms from the remains of marine and lacustrine microorganisms, plants, and animals and variable amounts of terrigenous debris in sediments. The structured terrestrial (*e.g.*, woody- or cuticle-containing) portions of kerogen have elemental compositions similar to coal (Hunt, 1979, pp. 279-280). In the past, kerogen was sometimes pictured as a complex high molecular

weight material formed from random condensation of monomers generated by the initial breakdown of polymeric biological precursor molecules following sediment burial. However, microscopic and, increasingly, chemical evidence is more in accord with substantial incorporation of biological macromolecules which have undergone varying degrees of chemical alteration prior to and after burial, as summarized recently in Horsfield, 1989. Because it is formed from the remains of marine, lacustrine, and terrigenous microorganisms, plants and animals, it contains information about the depositional, geological and geothermal history of sediments.

This chapter reviews the current state of knowledge about how chemical properties of kerogen—including elemental analysis, pyrolytic, properties, spectral characteristics and isotopic composition—change as a function of sediment processes and thermal history.

In Press: *Organic Geochemistry*, M. Engel and S. Macko, Eds., Plenum Press.

Supported by: DoE Grant DE-FCO2-86ER13466. A002.

WHOI Contribution No. 7238.

RADIOCHEMISTRY

VERTICAL PROFILES OF SOME NATURAL RADIONUCLIDES OVER THE ALPHA RIDGE, ARCTIC OCEAN

Michael P. Bacon, Chih-An Huh, and
Robert M. Moore

Concentration profiles of ²²⁸Ra, ²³⁴Th, ²³⁰Th, ²³²Th, ²²⁸Th, and ²³¹Pa were measured in the CESAR Ice Camp water column (85°50'N, 108°50'W). Thorium isotopes were determined in both dissolved and particulate forms. The results show that rates of scavenging of the reactive nuclides are unusually low, even in comparison with other oligotrophic oceans. Application of a reversible exchange model to the Th isotope data suggests that Th cycling is measurably faster in the surface water than it is at depth.

Published in: *Earth and Planetary Science Letters*, 95, 15-22, 1989.

Supported by: NSF Grants OCE82-19583, OCE84-17910, and OCE88-00620.

WHOI Contribution No. 7152.

SCAVENGING AND PARTICLE DEPOSITION IN THE SOUTHWESTERN BLACK SEA—EVIDENCE FROM CHERNOBYL RADIOTRACERS

K. O. Buesseler, H. D. Livingston, S. Honjo, B. J. Hay, T. Konuk, and S. Kempe

The pulse of fallout tracers from the Chernobyl accident in April 1986 is used to examine scavenging and particle deposition in the southwestern Black Sea. Data on the distribution of ^{137}Cs , ^{134}Cs , ^{106}Ru and ^{144}Ce between the dissolved, suspended and sinking phases are presented. As expected by their differing chemistries, the more particle-reactive ^{106}Ru and ^{144}Ce tracers are preferentially removed from surface waters relative to Chernobyl Cs, a predominantly conservative tracer. By comparing the tracer isotopic ratios in suspended fine particulates and rapidly sinking large particulates caught in sediment traps, an indication of the sediment source can be obtained. During the spring and summer, biological blooms drive rapid vertical transport of particles and tracer to depth, while during the fall and winter months the lateral transport of shelf derived particulates dominates the sinking flux. By the end of this annual cycle, much of the Chernobyl ^{106}Ru and ^{144}Ce have been scavenged from surface waters and removed to depth on sinking particles; however, there is significant release of these tracers back into the mid-waters during this process.

In Press: *Deep-Sea Research*.

Supported by: NSF Grants OCE87-00715 and OCE84-17106, ONR Contract N000014-85-C-0007, The Coastal Research Center, The German Ministry for Research and Technology Grant No. MFU005438, and the Turkish Research Council.

WHOI Contribution No. 7168.

^{210}Pb SCAVENGING IN THE OPEN OCEAN

J. Kirk Cochran, Thomas McKibbin-Vaughan, Mark M. Dornblaser, David Hirschberg, Hugh D. Livingston, and Ken O. Buesseler

The radionuclide ^{210}Pb shows significant geographic variations in the extent of its removal from the open ocean water column. This "texture of scavenging" is defined by mapping (1) the deficiency of ^{210}Pb in the water column, relative to its supply from the atmosphere and from *in-situ* decay of dissolved ^{226}Ra , and (2) inventories of excess ^{210}Pb in deep-sea sediments. The ratio of ^{210}Pb deficiency to its supply, termed the

scavenging effectiveness, is only ~20% in the North Equatorial Pacific Ocean and ~50% in the North Atlantic (south of 50°N) and Indian Ocean. The highest values observed are 60-70% in the Nansen Basin of the Arctic Ocean and in the Bay of Bengal. This variation is related to the combined effects of uptake of ^{210}Pb onto sinking particles and lateral transport of ^{210}Pb to areas of more intense removal. Sediment inventories of excess ^{210}Pb , normalized to the ^{210}Pb deficiency in the overlying water column, permit evaluation of the relative importance of these effects. In the North Equatorial Pacific and Arctic virtually all of the ^{210}Pb removed from the water column is present in the underlying sediments but in the central North Atlantic, the sediments comprise only about 50% of the ^{210}Pb removed. The deficiencies of ^{210}Pb in the North Atlantic sediments south of 50°N are qualitatively accounted for by surpluses in high latitude sediments north of 50°N. Higher primary productivity and new production in the surface waters of the high latitude North Atlantic and North Equatorial Pacific, relative to the oligotrophic central North Atlantic, probably account for the greater importance of ^{210}Pb scavenging onto sinking particles in those areas.

In Press: *Earth and Planetary Science Letters*.

Supported by: NSF Grant OCE86-14545.

WHOI Contribution No. 7234.

SEAWATER AND GEOCHEMISTRY

CARBON DIOXIDE TRANSPORT BY OCEAN CURRENTS AT 25°N LATITUDE IN THE ATLANTIC OCEAN

Peter G. Brewer, Catherine Goyet, and David Dyrssen

Measured concentrations of CO_2 , O_2 , and related chemical species in a section across the Florida Straits and in the open Atlantic Ocean at approximately 25°N, have been combined with estimates of oceanic mass transport to estimate both the gross transport of CO_2 by the ocean at this latitude, and the net CO_2 flux from exchange with the atmosphere. The northward flux was 63.9×10^6 moles per second (mol/s); the southward flux was 64.6×10^6 mol/s. These values yield a net CO_2 flux of 0.7×10^6 mol/s (0.26 ± 0.03 gigaton of C per year) southward. The North Atlantic Ocean has been considered to be a strong sink for atmospheric CO_2 , yet these results show that the net flux in 1988 across 25°N was small. For O_2 the equivalent signal is 4.89×10^6 mol/s northward and 6.97×10^6 mol/s southward, and the net transport is 2.08×10^6 mol/s or three times the net

CO₂ flux. These data suggest that the North Atlantic Ocean is today a relatively small sink for atmospheric CO₂, in spite of its large heat loss, but a larger sink for O₂ because of the additive effects of chemical and thermal pumping on the O₂ cycle but their near equal and opposite effects on the CO₂ cycle.

Published in: *Science*, 246, 477-479, 1989.

Supported by: NSF Grant OCE87-1461.

WHOI Contribution No. 7109.

CHLOROFLUOROCARBONS AS TIME-DEPENDENT TRACERS IN THE OCEAN

John L. Bullister

Chlorofluorocarbons (CFCs) are a group of anthropogenic compounds which are widely used as refrigerants, aerosol propellants, plastic foam blowing agents and solvents. Although often popularly referred to by the Dupont tradename "freons," these compounds are produced worldwide by a number of manufacturers. CFCs have low toxicity, are not very reactive under normal conditions, and have a variety of useful physical properties. Production of two of these compounds, dichlorodifluoromethane (F-12) and trichlorofluoromethane (F-11), began in the early 1930's. Industrial production of F-11 and F-12 accelerated during the following three decades as demand for these compounds grew. CFCs are volatile, and most of the F-11 and F-12 produced eventually enters the atmosphere. In some applications, such as the use of F-11 and F-12 as aerosol propellants, the typical delay between production and release of the CFC to the atmosphere is relatively short, but for other uses, such as in hermetically sealed refrigeration systems, the average delay until release can be a decade or longer.

Sensitive analytical techniques for measuring CFCs in the environment were not available during the first four decades of release. Pioneering measurements of CFCs in the troposphere were made by Lovelock (1971) using electron-capture gas chromatography. Since then, a number of programs have been established to monitor the increases of F-11 and F-12 in the earth's atmosphere as a function of location and time. For the period prior to the start of monitoring programs, the increase of CFCs in the atmosphere can be modeled based on production records and release scenarios, with corrections for losses due to photolysis of these compounds in the stratosphere.

Published in: *Oceanography*, 2, 12-17, 1989.

Supported by: NSF Grants DPP86-19704 and OCE88-00957.

WHOI Contribution No. 7092.

POLYCYCLIC AROMATIC HYDROCARBONS IN *SACCOGLOSSUS* *KOWALEWSKYI* (AGASSIZ)

D. A. Carey and J. W. Farrington

Hydrocarbon extracts were analyzed from *Saccoglossus kowalewskyi*, a deposit-feeding enteropneust worm, and from surface sediments from Cape Cod, MA. Worms were held in experimental aquaria in sieved sediments and flowing seawater for four months and then fed sediments mixed with creosote, lampblack or clean sediment for two weeks as analogues of sediments containing degraded oil and pyrogenic compounds. Worms from all treatments contained polyaromatic hydrocarbons (PAHs) in amounts and composition that indicate that the worms were contaminated with weathered No. 2 fuel oil before our experimental treatment and that the contamination persisted for four months in clean conditions. The contamination was not detected in the clean sediments used in the experiment. The worms accumulated steroid transformation products in greater abundance than the odd chain n-alkanes that dominated the sediment extractions. This may indicate selective assimilation of algal detritus and microbial products over salt marsh detritus. Worms, actively feeding during the experiment, contained $1-3 \times 10^{-6} \text{ g g}^{-1}$ dry weight of unknown brominated compounds which were not detected in the sediments. These compounds are similar to bromopyrroles found elsewhere in enteropneusts, polychaetes and bacteria and may cause substantial interference in analyses for some industrial pollutants.

Published in: *Estuarine, Coastal and Shelf Sciences*, 29, 97-114, 1989.

Supported by: Grants from the Andrew W. Mellon Foundation.

WHOI Contribution No. 7150.

**MINERALOGY AND CHEMISTRY OF
OCEAN FLOOR HYDROTHERMAL
PRECIPITATES FROM KOLBEINSEY
AND REYKJANES RIDGES NEAR
ICELAND: SCANNING ELECTRON
MICROSCOPE (ENERGY-DISPERSIVE
X-RAY) ANALYSIS**

*Robert F. Commeau, Geoffrey Thompson,
Frank T. Manheim, Jon Olafsson, and
Sveinn P. Jakobsson*

This report describes the mineralogy and associated chemistry of ocean floor mineral precipitates recovered from areas of hydrothermal emission on Kolbeinsey and Reykjanes Ridges, which are located along the northern extension of the Mid-Atlantic Ridge near Iceland. Selected samples were examined in the scanning electron microscope (SEM) and analyzed using the energy-dispersive spectrometer (EDS) system.

The Kolbeinsey Ridge samples were dredged in June 1987 from an area of active hydrothermal emission. The site is 90 to 100 m deep, 110 km north of Iceland, and 6.6 km south of the island of Kolbeinsey (location marked on Index Map). The hydrothermal zone is located on a constructional volcanic edifice that is composed of tholeiitic basalts. The center of hydrothermal activity is denoted by boiling undersea springs emitting waters at temperatures of about 200 to 300°C, rising gas bubbles, and sub-boiling seeps. A dense bacterial mat (*Beggiatoa* community) covers most of the site along with colonies of tunicates and the hydroid *Cormorpha*. The dredge sample (B6/87-326) recovered mainly volcanic rocks, including some breccia samples (inventoried as rock group 3) imbedded in hydrothermal precipitates. The breccia is composed of volcanic clasts of fine-grained vesicular basalt cemented with hyaloclastite, glass shards, and basaltic debris. The basalt is similar in mineralogy to the described sample 2677 (J. Olafsson and others, manuscript in preparation, 1989) with extensive alteration of glass and olivine, and replacement by clays and opaline silica. The breccia is embedded in a matrix of gypsum and barite with minor quartz, aragonite and basaltic debris. Filaments of bacterial mat cover the surface. Sulfide minerals are not abundant but are present as fine granules in the matrix and as infillings or linings in small cavities and vesicles in the basaltic clasts. Based on optical and x-ray diffraction studies, the sulfide minerals include major amounts of pyrite, minor amounts of marcasite and sphalerite, and trace amounts of cubanite, covellite, and bornite. This assemblage of sulfide minerals, in association with Ca and Ba sulfates and silica, is typical of many deep ocean vents and indicates that the breccia is

in contact with relatively high temperature hydrothermal solutions. This report includes a descriptive study of the pyrite, silica, gypsum, barite, and sinectite contained in sample B6/87-326.

Published in: *USGS Open File Reports*, 89-480, pp. 1-18, 1989.

Supported by: NSF Grant OCE87-12136.

**SURFACE-OCEAN COLOR AND
DEEP-OCEAN CARBON FLUX: HOW
CLOSE A CONNECTION?**

*W. G. Deuser, F. E. Muller-Karger, R. H. Evans,
O. B. Brown, W. E. Esaias, and G. C. Feldman*

Seven years of simultaneous, quasi-continuous data collected by the Nimbus-7 Coastal Zone Color Scanner and by a deep-ocean sediment trap in the Sargasso Sea allow the derivation of empirical relationships between remotely sensed ocean color and the sinking of particulate carbon into the deep sea. In agreement with earlier observations, the results indicate a 1-1.5 month lag between surface-ocean events observed by the satellite and arrival of a record of those events, carried by sinking particles, at a depth of 3200 m. In addition, the results suggest that the sea-surface area most influential on particle-flux characteristics recorded by the sediment trap in the Sargasso Sea lies within a square, 200 km on its side, to the northeast of the trap's mooring site. The results point towards possible ways of quantifying the role of marine biota in the regulation of atmospheric carbon dioxide through use of satellite observations.

Supported by: NSF Grants OCE76-21280,
OCE78-19813, OCE80-24130, OCE82-19588,
OCE84-17909, OCE85-01955, and
OCE87-165189.

WHOI Contribution No. 7219.

**THE RARE EARTH ELEMENTS IN
RIVERS, ESTUARIES AND COASTAL
SEAS AND THEIR SIGNIFICANCE TO
THE COMPOSITION OF SEA WATERS**

*H. Elderfield, R. Upstill-Goddard, and
E. R. Sholkovitz*

The concentrations of the rare earth elements (REE) in samples from fifteen rivers, from six estuarine transects and of five coastal seawaters are reported and have been used with literature data to examine the continuity in average REE pattern between average continental crust and the dissolved input of REE to the oceans via estuaries.

undepleted basalts with the highest K/Ti (0.25-0.46), Zr (150-170 ppm) and Nb (8-16 ppm) contents, and the transitional basalts falling within compositions between these two extremes. These three basaltic groups occur within limited portions of the axial graben and its limbs in areas of less than 10 km in length and less than 3-4 km in width near 12°43'N-12°51'N on the E.P.R. Similar volcanic diversity in a more limited area (<3 km²) is observed on off-axial seamounts and other constructional features centered up to 6 km and 18 km from the rise axis. Depleted and undepleted melts are believed to have been formed during sequential batch melting of a composite mantle. The transitional basalts probably result from mixing of depleted and undepleted liquids which have undergone variable degrees of crystal fractionation. Two distinct mantle sources are distinguishable by their incompatible elements contents and their susceptibility to melting; we suggest that a chondritic mantle, with minerals having a variable behavior under partial melting, constitutes this type of composite mantle. Indeed, clinopyroxene, enriched in incompatible elements, will be consumed at an earlier stage of melting than the olivine plus orthopyroxene. Eruption of compositionally distinct magma batches in close proximity to axial and off-axial structures implies periods of quiescence between successive magmatic stages and cycles.

Published in: *Journal of Geophysical Research*, 94, 7,437-17,464, 1989.

Supported by: NSF Grant OCE87-12098.

ALKENONE MOLECULAR STRATIGRAPHY IN AN OCEANIC ENVIRONMENT AFFECTED BY GLACIAL FRESHWATER EVENTS

John P. Jasper and Robert B. Gagosian

The sedimentary record of a ratio (UK37) of long chain (C₃₇) unsaturated alkenones is a useful indicator of glacial-interglacial climatic change in the Late Quaternary northern Gulf of Mexico where a planktonic foraminiferal δ¹⁸O-CaCO₃ record is complicated by meltwater and/or fluvial events (Williams and Kohl, 1986). Application of a laboratory temperature calibration of the UK37 ratio (Prah and Wakeham, 1987) to a Pigmy Basin hydraulic piston core record (Deep Sea Drilling Project core 619) suggested that the minimum glacial surface mixed layer (SML) temperature was 8° ± 1°C colder than the Holocene high SML temperature of 25.6° ± 0.5°C. This predicted glacial-interglacial temperature difference was significantly larger than the differences predicted by either the foraminiferal δ¹⁸O or foraminiferal

assemblage temperature methods (0.8°- 2.0°C). This large difference may be caused by local *Prymnesiophyte* assemblage changes in response to climatically induced hydrographic changes. Interglacial periods may be dominated by pelagic *Prymnesiophyte* assemblages, while glacial periods may be dominated by neritic assemblages. A combined mechanism of both climatically varying *Prymnesiophyte* species assemblage and depth of alkenone biosynthesis may account for the large difference between the temperature methods.

Published in: *Paleoceanography*, 4(6), 603-614, 1989.

Supported by: NSF Grants OCE84-15720, MIT/WHOI Joint Program Fellowship, and an Andrew W. Mellon Foundation Grant from WHOI's Coastal Research Center.

WHOI Contribution No. 7202.

GLACIAL-INTERGLACIAL CLIMATICALLY-FORCED δ¹³C VARIATIONS IN SEDIMENTARY ORGANIC MATTER

John P. Jasper and Robert B. Gagosian

Sedimentary organic geochemical properties have long been used to characterize sedimentary organic matter sources, but the characterizations are often not unique. There are at least four plausible mechanisms to account for the large (~3-6‰) glacial-to-interglacial climatic variations in the sedimentary organic-carbon isotopic composition (δ¹³C_{org}) in the northern Gulf of Mexico. They are: temperature-dependent C isotopic fractionation by phytoplankton, mixing of C₃-photosynthetic terrigenous and marine organic matter, sedimentary mixing of C₃- and C₄-photosynthetic organic matter and diagenetic alteration of the originally sedimented material. In a 207.7-m Deep Sea Drilling Project hydraulic-piston core (DSDP 619) from the Pigmy Basin in the northern Gulf of Mexico, we find that paired analyses of δ¹³C_{org} and N/C are consistent with the hypothesis that the sedimentary organic carbon in the Pigmy Basin is a glacial-interglacial climatically determined mixture of C₃-photosynthetic terrigenous and marine organic matter, confirming the model of Sackett.

Published in: *Nature*, 342, 60-62, 1989.

Supported by: NSF Grants OCE84-15720, MIT/WHOI Joint Program Fellowship, and an Andrew W. Mellon Foundation Grant from WHOI's Coastal Research Center.

WHOI Contribution No. 7203.

Concentrations in river waters span a wide range (e.g., 120-3300 pmol kg⁻¹ Nd). REE patterns, normalised to average shale, are of 2 main types: all show heavy REE enrichment between La and Gd but either heavy REE enrichment or depletion between Gd and Lu. Some patterns showed negative cerium anomalies and these can be related to pH in a small suite of carbonate rivers. Different patterns were found in rivers draining different rock types had the same patterns, suggesting that the catchment rocks play a minor role in defining the REE chemistry of river waters. The results may be explained by the presence of two main pools for the REE in rivers, a colloidal pool of REE-rich particles <0.4 μm having a shale-like pattern and a dissolved pool characterised by heavy REE enrichment. Significant REE removal during the mixing of river water and sea water was measured for the Connecticut, Delaware, Mullica and, on two occasions, Tamar estuaries. This was confirmed by mixing experiments using radiotracers. Removal varied from about 30% to near-quantitative. In some cases, preferential removal of the light REE was associated with REE changing the proportions of the two REE pools. The REE concentrations and patterns of the coastal seawaters are intermediate between those for rivers and for ocean waters, reflecting the influence of continental drainage. The dissolved input of REE to the oceans is characterised by REE patterns in which the evolution of the characteristic oceanic REE pattern has started to develop. The same fundamental processes that define the oceanic pattern appear to operate for continental waters also, but the REE patterns are not as "evolved," i.e., fractionated relative to continental crust of lower pH and shorter water residence times.

In Press: *Geochimica et Cosmochimica Acta*.

Supported by: NSF Grants OCE85-15695 and OCE87-11032.

WHOI Contribution No. 7276.

PB ISOTOPES IN SURFICIAL PELAGIC SEDIMENTS FROM THE NORTH ATLANTIC

B. Hamelin, F. Grousset, and E. R. Sholkovitz

Stable Pb isotopic composition and concentration were measured in sediment samples close to the sea water interface in 6 box-cores from the NE Atlantic, 2 box-cores from the Sargasso Sea, and 1 from the U.S. continental shelf, in order to quantify the anthropogenic Pb input to marine sediments, due to the increase of Pb pollution during the last century. The results show that in the eastern part of the Atlantic, i.e., in regions

under aeolian influence from Europe, Pb pollution can be recognized using its distinctive unradiogenic composition, clearly different from the upper-crustal values commonly found in pre-Holocene sediments. In contrast, Pb pollution in the box-cores from regions under U.S. influence can be identified only in detailed concentration profiles, because the Pb pollution from American origin has an isotopic composition much closer to that of the natural detrital Pb input coming from weathering of the continental crust. Pb excess inventories are in good agreement with fluxes estimated from sediment traps data and with the time record of Pb pollution increase given by analyses in coral growth bands. Fluxes of Pb pollution to the sediments of the Mud Patch (American shelf) are tenfold higher than those to Hatteras and Bermuda abyssal plains.

In Press: *Geochimica et Cosmochimica Acta*.

Supported by: NSF Grant OCE85-05695.

WHOI Contribution No. 7049.

AXIAL AND OFF-AXIAL HETEROGENEITY OF BASALTIC ROCKS FROM THE EAST PACIFIC RISE AT 12°35'N-12°51'N AND 11°26'N-11°30'N

Roger Hekinian, Geoffrey Thompson, and Daniel Bideau

Surface ship operations and forty submersible dives have provided a large amount of field observations and rock samples from two segments of the E.P.R. at 12°35'N-12°51'N and at 11°26'N-11°30'N, and from four adjacent seamounts centered at less than 18 km from the rise axis. The basaltic samples show a great variety of morphological features and a diversity in the proportions of early formed mineral phases and chemical composition. There is no correlation between lava flow morphology, geological settings or compositions. Based on mineral and compatible element composition, these basalts were classified into three types. The least evolved olivine-basalts and highly phyrlic plagioclase-basalts (Type "A") have high Fo₈₇₋₈₉, high Mg# (66-70) and high Ni (>100) contents. The most evolved plagioclase-olivine basalts with or without pyroxene (Types "B" and "C") have relatively low Fo₇₈₋₈₆, low Mg# (55-65) and low Ni (60-100 ppm) content. Simple crystal fractionation (3-18%) account for some of the observed compositional range. However, based on their incompatible element contents, the above basalts are divided into three groups (the various types "A" to "C" are found in each group): depleted basalts with low K/Ti (0.04-0.15) ratios, low Zr (<100 ppm) and low Nb (<0.4 ppm) contents,

THE SOURCES AND DEPOSITION OF ORGANIC MATTER IN THE LATE QUATERNARY PIGMY BASIN

John P. Jasper and Robert B. Gagosian

The concentration and carbon isotopic composition ($\delta^{13}\text{C}$) of sedimentary organic carbon (C_{org}), N/C ratios, and terrigenous and marine $\delta^{13}\text{C}-\text{C}_{\text{org}}$ end-members form a basis from which to address problems of Late Quaternary glacial-interglacial climatic variability in a 208.7 m hydraulic piston core (DSDP 619) from the Pigmy Basin in the northern Gulf of Mexico. Paired analyses of $\delta^{13}\text{C}-\text{C}_{\text{org}}$ and N/C are consistent with the hypothesis that the sedimentary organic carbon in the Pigmy Basin is a climatically-determined mixture of C_3 -photosynthetic terrigenous and marine organic matter, confirming the model of Sackett (1964). A high resolution (~ 1.4 - 2.9 ky/sample) $\delta^{13}\text{C}-\text{C}_{\text{org}}$ record shows that sedimentary organic carbon in interglacial oxygen isotope (sub)stages 1 and 5a-b are enriched in ^{13}C (average $\pm 1\sigma$ values are $-24.2 \pm 1.2\text{‰}$ and $-22.9 \pm 0.7\text{‰}$ relative to PDP, respectively), while glacial isotope stage values 2 are relatively depleted ($-25.6 \pm 0.5\text{‰}$). Concentrations of terrigenous and marine sedimentary organic carbon are calculated using $\delta^{13}\text{C}-\text{C}_{\text{org}}$ end-members. The net accumulation rate of terrigenous organic carbon is 4.3 ± 2.6 times higher in isotope stages 2-4 than in (sub)stages 1 and 5a-b, recording higher erosion rates of terrigenous organic material in glacial times. The concentration and net accumulation rates of marine and terrigenous C_{org} suggest that the nutrient-bearing plume of the Mississippi River may have advanced and retreated across the Pigmy Basin as sea level fell and rose in response to glacial-interglacial sea level change.

In Press: *Geochimica et Cosmochimica Acta*.

Supported by: NSF Grants OCE84-15720, MIT/WHOI Joint Program Fellowship, and an Andrew W. Mellon Foundation Grant from WHOI's Coastal Research Center.

WHOI Contribution No. 7204.

TEMPORAL VARIATIONS IN THE CONCENTRATIONS OF SOME PARTICULATE ELEMENTS IN THE SURFACE WATERS OF THE SARGASSO SEA AND THEIR RELATIONSHIP TO DEEP SEA FLUXES

T. D. Jickells, W. G. Deuser, and R. A. Belastock

The concentrations of particulate Ca, Al, Ba, Sr, Mn, Mg, V and I have been measured in the

upper 200 m of the water column of the Sargasso Sea at approximately monthly intervals over a four-year period. Biogenic particles dominate the composition of the particulate matter and show a seasonality related to the cycle of primary productivity with concentration maxima in spring. Particulate aluminium concentrations (presumed to be associated with clays) in the shallowest samples show a maximum in summer which is suggested to be associated with aeolian inputs to a shallow mixed layer compared to inputs of similar magnitude to the deeper mixed layer in winter. The different seasonalities in calcium and aluminium concentrations lead to a seasonality in Ca/Al ratios which can also be seen in sediment trap material collected in this area. Particulate manganese shows a unique behaviour among the elements studied, which may be controlled by *in-situ* scavenging of dissolved manganese.

In Press: *Marine Chemistry*.

Supported by: NSF Grants OCE80-24130, OCE82-19588, OCE84-17909 and OCE85-09155.

WHOI Contribution No. 7074.

VARIABILITY OF SOME ELEMENTAL FLUXES IN THE WESTERN TROPICAL ATLANTIC OCEAN

T. D. Jickells, W. G. Deuser, A. P. Fleer, and C. Hemleben

Fluxes of selected major and trace elements into a deep-ocean sediment trap in the western tropical Atlantic were quite variable over a two-year period, with no apparent seasonality as observed in the Sargasso Sea. Fluxes of aluminium and other trace elements associated with abiogenic and biogenic material, correlate with organic carbon flux, suggesting that biogenic and abiogenic material are transported by the same mechanisms. Lead fluxes are higher than expected, presumably as a result of enhanced removal rates of lead close to ocean margins compared to central ocean areas.

In Press: *Oceanologica Acta*.

Supported by: NSF Grants OCE81-17002 and OCE85-09155.

WHOI Contribution No. 7263.

GEOCHRONOLOGY OF TAG AND SNAKEPIT HYDROTHERMAL FIELDS, MID-ATLANTIC RIDGE: WITNESS TO A LONG AND COMPLEX HYDROTHERMAL HISTORY

C. Lalou, G. Thompson, M. Arnold, E. Brichet, E. Druffel, and P. A. Rona

Geochronologic studies of a large number of

precipitates from the TAG hydrothermal field and of few samples from Snakepit hydrothermal field of the Mid-Atlantic Ridge show intermittent repeated hydrothermal events at both sites. $^{210}\text{Pb}/\text{Pb}$ and $^{230}\text{Th}/^{234}\text{U}$ measurements of sulfides, iron and manganese oxides, and ^{14}C measurements of carbonates combined with observations of hydrothermal events recorded as discrete layers in sediment cores provide the basis for unravelling the temporal history of the fields. The TAG field shows intermittent activity over the past 120,000 years as evidenced by ages of low temperature Mn oxides. The presently active black smoker mound first formed about 40 to 50,000 years ago with precipitation of massive sulfides. It has had intermittent, pulsed high temperature activity every 5 to 6,000 years over the past 20,000 years which may reflect renewed magmatic activity at the ridge axis. Fluid flow is focussed at the mound site by structural and tectonic control suggested by the intersection of N-S ridge parallel lystric normal faults and an E-W transfer fault. Periods of inactivity are marked by covering of the mound with pelagic carbonate ooze which is probably partially dissolved and reprecipitated as aragonite at the end of each high temperature event. The Snakepit field had an initial event about 4,000 years ago, probably shortly after the eruption of the volcanic ridge on which it sits. A recent renewal, still presently active, was probably initiated by recent fissuring of the volcanic pile.

In Press: *Earth and Planetary Science Letters*.

Supported by: NSF Grant OCE87-12136.

WHOI Contribution No. 7093.

TRACE METALS IN CONTEMPORARY AND 17TH-CENTURY GALAPAGOS CORAL: RECORDS OF SEASONAL AND ANNUAL VARIATIONS

L. J. Linn, M. L. Delaney, and E. R. M. Druffel

We report trace element/calcium ratios for modern (Cu/Ca, Mn/Ca, Cd/Ca, and Pb/Ca) and 17th-century (Cu/Ca, Mn/Ca, and Pb/Ca) specimens of *Pavona clavus* collected in the Galapagos Islands. These data include the first reliable measurements of Cu/Ca ratios in coralline aragonite. We estimate that the ratio of Cu/Ca in the lattice to that in seawater (*i.e.*, the effective distribution coefficient) is ~ 0.3 , lower than the value of 1 observed for several other divalent elements; we estimate the effective distribution coefficient for Mn is ~ 1 . In a modern Hood Island coral quarter-annually sampled from 1964-73, Cu/Ca ratios decrease twofold from the late 1960s to early 1970s. Mn/Ca and Cd/Ca ratios vary seasonally with upwelling and the generic El Niño.

The El Niño Southern Oscillation events of 1965, 1969, and 1972 are marked by suppression of Cd/Ca ratios by about 2.5 nmol/mol, while the Mn/Ca ratio is highest during the strong 1972 ENSO. Pb/Ca ratios were relatively constant throughout this period. From a Cu/Ca record for a 17th-century Urquina Bay coral annually sampled from 1600-1725 and the estimated Cu distribution coefficient, surface seawater Cu concentrations at Galapagos during the 17th century were similar to present day at 0.7-1.4 nmol/kg. Estimated Pb concentrations were lower at 5-20 pmol/kg, and Mn concentrations were slightly higher at 1.6-2.8 nmol/kg.

In Press: *Geochimica et Cosmochimica Acta*.

Supported by: NSF Grant RII86-20256.

WHOI Contribution No. 7285.

CERIUM OXIDATION RATES AND MECHANISMS IN OLIGOTROPHIC AND COASTAL MARINE WATERS

James W. Moffett

Cerium redox chemistry has long been of interest to geochemists because it leads to enrichment or depletion of Ce with respect to its non-redox reactive lanthanide neighbors. The resultant Ce anomaly is a potentially useful tracer of redox mediated transport in seawater and Ce anomaly data from the sediment record may provide useful information on changes in redox state of the ocean with time. However, lack of knowledge of the rates and mechanisms Ce oxidation and reduction in natural waters prevents a complete understanding of its geochemistry. In this study Ce oxidation rates were measured using radiotracers in seawater samples collected at a station in the Sargasso Sea at depth from 20-200 m and from the surface at a coastal site in Vineyard Sound, Massachusetts. Ce oxidation was exclusively microbial; no abiotic oxidation was detectable. In the Sargasso, rates increased from $0.02\% \text{ d}^{-1}$ at 20 m to $0.7\% \text{ d}^{-1}$ at 200 m. The data indicate that the negative Ce anomaly in seawater is due to microbial oxidation and preferential scavenging of Ce(IV). Furthermore, they are consistent with the hypothesis that sunlight inhibition of microbial oxidation of Ce and Mn contributes to the pronounced surface maxima observed for these elements, by inhibiting oxidative scavenging.

Supported by: NSF Grant OCE89-17401.

WHOI Contribution No. 7265.

RARE EARTH ELEMENTS IN SEDIMENTS OFF SOUTHERN CALIFORNIA: A NEW ANTHROPOGENIC INDICATOR

*Ilhan Olmez, Edward R. Sholkovitz,
Diane Hermann, and Robert P. Eganhouse*

The rare earth elements (REE) composition of dated sediment cores from the San Pedro Shelf (60 m) and the Santa Barbara basin (588 m) are contrasted. The Santa Barbara Basin core has relatively uniform REE concentrations throughout its 60 cm length and a REE composition similar to the crustal abundance. In contrast, the upper 20 cm of the 36 cm deep San Pedro Shelf core is enriched in the concentrations of the light REE (La, Ce, Nd and Sm) but not in the middle REE (Eu) and the heavy REE (Yb, Lu). These upper sediments have a REE signature which is very different from crustal material reflecting anthropogenic inputs beginning in the early 1960's delivered from the Joint Water Pollution Control Plant wastewater outfall located 6 km upcurrent from the San Pedro Shelf Core. The sources of the light REE enrichment are petroleum cracking catalysts and their products; these include emissions of bottom ash, fly ash and wastewater from oil-fired power plants and oil-refineries. Cracking catalysts, which are produced from mainly two REE ore minerals, bastnasite and monazite, are strongly enriched in the light REE. With their unique signature and source, light REE may be a new tool for tracing anthropogenic inputs to the Santa Monica and San Pedro Basins.

Submitted to: *Environmental Science and
Technology.*

Supported by: NSF Grant OCE85-15695.

WHOI Contribution No. 7264.

UPWARD FLUXES OF PARTICULATE ORGANIC MATTER IN THE DEEP NORTH PACIFIC

*K. L. Smith, Jr., P. M. Williams, and
E. R. M. Druffel*

The flux of particulate matter through the oceanic water column is a primary component in elemental cycling and is generally perceived as being in one direction: downward. The organic matter constituting these particles is produced through photosynthesis in surface waters and either sinks directly as phytoplankton and products or undergoes various trophic transformations through the water column. A large proportion of the particulate organic matter

produced in surface waters is regenerated in the euphotic zone. A fraction of this organic matter, however, leaves the surface waters and settles through the water column, generally decreasing in quantity and changing in quality with increasing distance from the surface. Although the net transport of organic matter must be downward to fuel the lower portions of the water column, there is also an upward component to transport.

Positively buoyant particles, including lipid-rich eggs, larvae and, possibly, carcasses of deep-sea animals are examples of particles which undergo upward transport. A previous attempt to quantify the upward mass flux indicated rates of 1-4% of the downward mass flux. Here we report the first evidence that there is a significant upward flux of particulate organic matter, up to 66.7% of the concurrently measured downward flux, at two stations in the deep North Pacific. Given this magnitude, the previously ignored upward flux of such organic matter must be considered in models of carbon and nitrogen cycling in the open ocean.

Published in: *Nature*, 337, 724-726, 1989.

Supported by: NSF Grant OCE87-16590.

WHOI Contribution No. 7284.

HYDROTHERMAL ACTIVITY ON THE MID-ATLANTIC RIDGE

*G. Thompson, S. E. Humphris, C. Lalou, and
P. A. Rona*

Two active hydrothermal vent sites are known on the Mid-Atlantic Ridge at 26°N (TAG) and 23°N (Snakepit). Both fields have high temperature sulfide deposits of pyrite, chalcopyrite and sphalerite, but the Snakepit site differs in having pyrrothite as a dominant phase. Secondary Cu-Fe sulfides, oxides, chlorides, native copper and gold, as well as aragonite, are abundant at TAG but absent at Snakepit. The TAG site has Mn-oxide deposits up to 120,000 years in age. High temperature sulfides range up to 40,000 years old and indicate a number of discrete, punctuated episodes of hydrothermal activity separated by periods of quiescence. Snakepit activity appears to have begun about 5000 years ago, followed by a new, recent active period. Fluid flow at both sites is controlled by tectonic faulting and is related to magmatic intrusions.

Published in: *Water Rock Interaction*, D. L. Miles, ed., Balkema, Rotterdam, pp. 679-682, 1989.

Supported by: NSF Grant OCE87-12136.

**ORGANIC MATTER IN PERU
UPWELLING SEDIMENTS—ANALYSIS
BY PYROLYSIS, PYROLYSIS-GAS
CHROMATOGRAPHY (PY-GC) AND
PY-GC MASS SPECTROMETRY
(PY-GCMS)**

*Jean K. Whelan, Zoltan Kanyo, Martha Tarafa,
and Mark A. McCaffrey*

Significant variations in the nature and content of total carbon and total organic carbon (TOC) in closely-spaced near-surface samples from Sites 681A, 686, and 683 are accompanied by changes in pyrolysis parameters. All the TOC, pyrolyzable carbon values (P_2), and hydrogen index (HI) values (*e.g.*, P_2 normalized to TOC) were found to be significantly higher in the 681A sediments, compared to those from Sites 686 and 683. The Site 681A samples contained almost no carbonate. The T_{max} values (*e.g.*, maximum temperature of P_2 evolution) were generally highest for the Site 683 sediments, possibly indicating a greater influx of more reworked or terrigenous organic matter at this site, which is situated on the slope, at the edge or outside of today's upwelling area. TOC and pyrolysis (P_2) values correlated in closely-spaced near-surface samples from 681A (correlation coefficient, $r = 0.78$) with correlation decreasing for holes 686A ($r = 0.5$) and 683A ($r = 0.22$). Based on comparison to data from surface cores obtained by Woods Hole Oceanographic Institution, we postulate that the lack of correlation of P_2 and organic carbon values in several Site 683 intervals may indicate intervals containing more terrigenous or more reworked marine organic carbon. P_1 values showed poor correlation with TOC values at all three sites. Variations in P_1 values, which generally fall in the immature range of 0.04 to 0.08, are thought to show the relative amounts of *in-situ* marine biogenic (rather than petrogenic) influence. Pyrolysis-gas chromatography mass spectrometry patterns for a few of the ODP samples were compared with those for an extensive set of Peru surface samples (from three Woods Hole Oceanographic Institution cruises to the same area). The results suggest that the three ODP sections examined here were most strongly influenced by organic matter derived from marine upwelling (rather than terrigenous) influx, even at Site 683. Minimal influence by terrigenous influx is consistent with the desert nature of the Peru coast which is only sparsely vegetated. Pyrolysis-GCMS data also suggest that *Thioploca* bacterial mats, diagnostic of suboxic bottom waters in this region, may be a source of the sporadic thiophene pyrolysis products observed in some Peru sediments.

In Press: Vol. 112, Proceedings, ODP, Scientific Results.

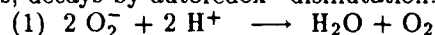
Supported by: NSF Grant OCE85-09859.

WHOI Contribution No. 7139.

**CHEMISTRY OF SUPEROXIDE (O_2^-)
ION-RADICAL IN SEAWATER I. pK_{ASW}^*
(HO_2) AND UNCATALYZED
DISMUTATION KINETICS STUDIED BY
PULSE RADIOLYSIS**

O. C. Zafriou

Superoxide, the one-electron reduction product of O_2 and an important transient in photochemical and possibly other redox processes in natural waters, decays by autoredox "dismutation."



The optical, acid-base, and self-decay properties of O_2^- in seawater were studied by electron pulse radiolysis-kinetic spectrophotometry, using added chelators to suppress transition metal catalysis. We find that:

$$(A) pK_a^* (HO_2) = 4.60 \pm 0.15,$$

(B) $[O_2^-]$ decay above pH 6 is strictly second-order and pH-dependent:

$$(2) -d[O_2^-]/dt = k_{dis} [O_2^-] [OOH] \approx 2k_2 [O_2^-]^2 [H^+]$$

(C) $k_{2sw} = 5 \pm 1 \times 10^{12} [H^+]$ ($S = 30-36\%$, assuming $\gamma_{H^+} = 1$).

The pK_a , rate law, and rate constant are extremely similar to those in pure water; theoretically predicted 3-5-fold slower rates in seawater were not confirmed. In non-coastal, high-salinity surface waters additional pseudo first-order O_2^- decay terms were undetectable ($<1.5 s^{-1}$); river and estuarine water samples exhibited pseudo first-order O_2^- decay terms of 1-5 s^{-1} . These additional paths could compete significantly with uncatalyzed dismutation in surface seawater even upon 1,000-fold dilution, suggesting that oceanic O_2^- decay may be controlled by unknown processes in addition to second-order dismutation.

Supported by: ONR Contract Nos.

N00014-87-K-0007 and N00014-89-J-1258.

WHOI Contribution No. 7142.

GEOCHEMISTRY

MELTING IN THE OCEANIC UPPER MANTLE: AN ION MICROPROBE STUDY OF DIOPSIDES IN ABYSSAL PERIODITES

Kevin T. M. Johnson, Henry J. B. Dick and Nobumichi Shimizu

A systematic study of rare earth and other trace elements in discrete diopsides from residual abyssal peridotites sampled from 5000 km of ocean ridge demonstrates that they are the residues of variable degrees of melting in the garnet and spinel peridotite fields. Further, the data clearly demonstrate that the peridotites are the residues of near-fractional melting, not batch melting, and that typical abyssal basalt can evolve from aggregated fractional melts. Ion microprobe analyses of diopsides in abyssal peridotites from fracture zones along the America-Antarctica and Southwest Indian Ridges reveal ubiquitous extreme fractionation of rare earth elements (REE) ($[(\text{Ce}/\text{Yb})_n=0.002-0.05]$; depletion of Ti (300-1600ppm); Zr (0.1-10ppm), and Sr (0.1-10ppm), and fractionation of Zr relative to Ti ($\text{Ti}/\text{Zr}=250-4000$). Ti and Zr in diopsides decrease with decreasing modal cpx in the peridotites, and samples dredged near hotspots are more depleted in incompatible elements than those dredged away from hotspots, consistent with higher degrees upper mantle melting in the former. All studied samples exhibit marked negative anomalies in Ti and Zr relative to REE. Incompatible element concentrations in peridotite clinopyroxenes are well modeled by repeated melting and segregation in $\leq 0.1\%$ increments to a total of 5-25% melting, a process very close to Rayleigh (fractional) melting; batch melting of a LREE-depleted source cannot account for the observed trace element concentrations in abyssal peridotites. The shapes of some REE patterns are consistent with variable degrees of melting initiated within the garnet stability field. Trace element concentrations in calculated integrated fractional liquids approximate the composition of primitive ocean floor basalts, consistent with postsegregation aggregation of small increments melts produced over a depth and melting interval.

In Press: *Journal of Geophysical Research - Solid Earth and Planets.*

Supported by: NSF Grant DPP87-20002.

WHOI Contribution No. 7211.

GEOLOGY

THE LATE EARLY EOCENE MONTAGNAIS METEORITE: NO IMPACT ON BIOTIC DIVERSITY

Marie-Pierre Aubry, Felix M. Gradstein and Lubomir F. Jansa

The suggestion that mass extinctions may have been triggered by extraterrestrial events has raised a significant controversy which may not be resolved until it can be shown that the timing of a mass extinction and that of an extraterrestrial event coincide precisely. There are great difficulties associated with the comparison of the record of mass extinctions with that of impact craters because, as Sepkoski and Raup (1986) pointed out, both are dated by totally independent means. There is also a question as to the size required for an impacting object to provoke mass extinction. The Montagnais impact crater is the first impact event which can be directly and precisely correlated to the marine stratigraphic record through biostratigraphic means. Its occurrence during the late early Eocene, between 52.6 and 53.4 Ma, at a time when Cenozoic diversity was at its peak, indicates that no global effect on biologic diversity can be expected from the impact in the ocean of a bolide 1.5 to 3 km in diameter.

In Press: *Micropaleontology.*

Supported by: A Consortium of Oil Companies.

WHOI Contribution No. 7192.

EVOLUTION OF MARINE GEOLOGY DURING THE PAST FIFTY YEARS

K. O. Emery and David A. Ross

An attempt is made to understand some of the ways that marine geology developed during the past fifty years, essentially the working lifespan of an active but venerable scientist. This interpretation is aided by comparing marine geology with the development of land geology during a longer period, and by attempting to understand the relative roles of science and technology in the field of marine geology. Excursions from a simple straight-line advance for all geology (and also for other fields) are provided by the unexpected appearances of broad generalizations, or paradigms, that commonly are developed by a few scientists and opposed by many at least for a time. These sudden advances await the accumulation of critical masses of knowledge that in turn depend upon exceptional opportunities, partly in the form of adequate funding and partly by transfer of technology. These unusual circumstances make accurate

prediction of future advances in marine geology (and in other scientific and technical fields) unreliable but still worthy of thought.

In Press: *Shepard Volume, Special Publication*
Society of Economic Paleontologists and Mineralogists.

Supported by: NOAA Sea Grant NA86-AA-D-SG090.

WHOI Contribution No. 7174.

STRUCTURE AND TOPOGRAPHY OF THE SIQUEIROS TRANSFORM FAULT SYSTEM: EVIDENCE FOR THE DEVELOPMENT OF INTRA-TRANSFORM SPREADING CENTERS

*Daniel J. Fornari, David G. Gallo,
Margo H. Edwards, John A. Madsen,
Michael R. Perfit, and Alexander N. Shor*

The Siqueiros transform fault system, which offsets the East Pacific Rise between 8°20'N-8°30'N, has been mapped with the Sea MARC II sonar system and is found to consist of four intra-transform spreading centers and five strike-slip faults. The bathymetric and side-looking sonar data define the total width of the transform domain to be ~20km. The transform domain includes prominent topographic features that are related to either seafloor spreading processes at the short spreading centers or shearing along the bounding faults. The spreading axes and the seafloor on the flanks of each small spreading center comprise morphological and structural features which suggest that the two western spreading centers are older than the eastern spreading centers. Structural data for the Clipperton, Orozco and Siqueiros transforms, indicate that the relative plate motion geometry of the Pacific-Cocos plate boundary has been stable for the past ~1.5 Ma. Because the seafloor spreading fabric on the flanks of the western spreading centers is ~500,000 years old and parallels the present EPR abyssal hill trend (350°) we conclude that a small change in plate motion was not the cause for intra-transform spreading center development in Siqueiros. We suggest that the impetus for the development of intra-transform spreading centers along the Siqueiros transform system was provided by the interaction of small melt anomalies in the mantle (SMAM) with deep-seated, throughgoing lithospheric fractures within the shear zone. Initially, eruption sites may have been preferentially located along strike-slip faults and/or along cross-faults that eventually developed into pull-apart basins. Spreading centers C and D in the eastern portion of Siqueiros are in this initial pull-apart stage. Continued intrusion

and volcanism along a short ridge within a pull-apart basin may lead to the formation of a stable, small intra-transform spreading center that creates a narrow swath of ridge-parallel structures within the transform domain. The morphology and structure of the axes and flanks of spreading centers A and B in the western and central portion of Siqueiros reflect this type of evolution and suggest that magmatism associated with these intra-transform spreading centers has been active for the past ~0.5-1.0 Ma.

In Press: *Marine Geophysical Researches.*

Supported by: NSF Grants OCE86-08489 and OCE87-16827.

WHOI Contribution No. 7240.

PARTICLE DEPOSITION IN THE PRESENT AND HOLOCENE BLACK SEA

Bernward Hay and Susumu Honjo

The Black Sea represents a fascinating environment for detailed particle deposition studies. The basin is comparatively small, yet over 2000 m deep. It is nearly completely enclosed and only connected through the shallow Bosphorus to the world's oceans. The hydrography and the sediment input parameters from the surrounding rivers are comparatively well-known. The seasonal changes in sedimentation are preserved in the bottom sediments in the form of laminated sequences, since the absence of oxygen in the deep water interface prohibits bioturbation. Once deposited, the sediments in the abyssal Black Sea remain in place; redistribution processes on the basin floor are comparatively insignificant.

Published in: *Oceanography Magazine.*

Supported by: NSF Grants OCE87-17106,
OCE86-14363 and ONR Contract
N00014-85-C-0001.

WHOI Contribution No. 6997.

INTERANNUAL VARIABILITY IN PARTICLE FLUX IN THE SOUTHWESTERN BLACK SEA

*B. J. Hay, S. Honjo, S. Kempe, V. A. Ittekkot,
E. T. Degens, T. Konuk and E. Izdar*

The vertical particle flux was measured at two sites in the southwestern Black Sea using automated time-series sediment traps over a period of 4.5 years. The particle flux was characteristically different between both sites. (1) Further offshore (site BSC), the dominant fraction

of the annual flux was deposited during short blooms; further nearshore (site BS), the particle flux was distributed more evenly throughout the entire year. (2) Further offshore, plankton blooms were the dominant cause for removal of suspended lithogenic matter through incorporation of the suspended matter in fecal pellets and "marine snow" aggregates; further nearshore, vertical transport of lithogenic matter was linked also to occurrence of storms and to high discharge periods of rivers. Suspended lithogenic particles may be transported over long distances, if intense plankton blooms also occur only sporadically in the open Black Sea. This mechanism could explain the basinwide correlation of individual laminae in recent sediments of the abyssal Black Sea.

In Press: *Deep-Sea Research*.

Supported by: NSF Grant OCE84-17106 and ONR Contract N00014-85-C-0001.

WHOI Contribution No. 7053.

A FINITE AMPLITUDE NECKING MODEL OF RIFTING IN BRITTLE LITHOSPHERE

Jian Lin and E. M. Parmentier

We formulate a mechanical model describing the formation of rifts as finite amplitude necking of an elastic-plastic layer overlying a fluid substrate. A perfectly plastic rheology is a continuum description of faulting in rift zones. Two important aspects of rift evolution are illustrated by this model: the evolution of the rift width as extension proceeds and the finite strain that occurs. A region at yield initially develops with a width determined by the thickness of the brittle layer, and the internal deformation within this yield zone is proportional to the topographic slope. As extension proceeds, the surface within the rift subsides and the width of the subsiding yield zone decreases. At any stage of rifting, material in regions just outside the yield zone is deformed but no longer deforming. The width of these deformed regions increases with increasing extension. Vertical forces due to the mass deficit of the rift depression will flex the elastic layer outside the yield zone, creating flanking uplifts. The external force required to maintain active rifting increases with the amount of lithospheric stretching, indicating that rifting is a quasi-static, stable process. Because the yield zone will revert to elastic behavior if the external force causing extension is removed, the model predicts that the rift depression and flanking uplifts will be preserved after extension stops. Our simple mechanical model demonstrates the inherent relationship among graben formation, crustal thinning and rift shoulder uplift in rift zones.

In Press: *Journal of Geophysical Research*.

Supported by: WHOI Culpeper Award.

WHOI Contribution No. 7151.

SOUND PRODUCTION BY HYDROTHERMAL VENTS

Sarah A. Little and Keith D. Stolzenbach

Theoretical examination of hot, turbulent, buoyant jets exiting from hydrothermal chimneys revealed acoustic source mechanisms capable of producing sound at levels higher than ambient ocean noise. Pressure levels and frequency generated by hydrothermal jets depend on chimney dimensions, fluid velocity and temperature and therefore could be used to monitor changes in these parameters over time.

A laboratory study of low Mach number jet noise and amplification by flow inhomogeneities confirmed theoretical predictions for homogeneous jet noise power and frequency. The increase in power due to convected flow inhomogeneities, however, was lower in the near field than expected.

Direct measurements of a hydrothermal vent sound field found frequency and power levels comparable to ambient ocean noise and consistent with jet quadrupole near-field sound which has been amplified by the dipole behavior of convected flow inhomogeneities. This near-field amplification is not as great as that predicted for the far-field but is consistent with theoretical considerations for near-field dipole and quadrupole behavior.

Indirect evidence of hydrothermal sound fields (Reidesel et al., 1982; Bibee and Jacobson, 1986) showing anomalous high power and low frequency noise associated with vents is due to processes other than jet noise.

Supported by: NOAA Sea Grant NA86-AA-D-SG090, ONR Contract N00014-87-K-0007, and NOAA Vents Program.

WHOI Contribution No. 7122.

GENETIC GLOBAL GEOMORPHOLOGY

Elazar Uchupi and K. O. Emery

Earth's surface morphology is primarily the result of the interaction between plates moved by seafloor spreading and/or intraplate tectonic/magmatic processes. Once the youthful endogenous (tectonic/magmatic) terranes are isolated from inter/intraplate influences as a result of long-continued lateral migration or changes in geometry, exogenetic processes (erosion and deposition) subdue and reduce the original relief. The rate of this modification and the nature of the

geologic processes involved in it are controlled by climate, which may change with time or with migration of the plates across climatic zones, and by oscillations in sea level. Whether a terrane can reach an old age stage in the geomorphic cycle depends upon its isolation from plate activity long enough for non-tectonic processes to complete its degradation. The low relief of ancient terranes in Precambrian shields is a clear indication that the geomorphic cycle can come to completion.

In Press: *Shepard Volume, Special Publication - Society of Economic Paleontologists and Mineralogists.*

WHOI Contribution No. 7186.

NORTH ATLANTIC OCEAN BASIN: ASPECTS OF GEOLOGIC STRUCTURE AND EVOLUTION

P. R. Vogt and B. E. Tucholke

In creating Volume M. the Western North Atlantic Region (Vogt and Tucholke, 1986) for the Geology of North America series, we deemed it best from both oceanographic and plate-tectonic viewpoints to deal with the entire North Atlantic spreading system from the equator to the Arctic (Figs. 1,2), rather than limiting treatment to the western half of the ocean basin. Even so, the scope in some places had to be expanded. The Atlantic, like other ocean basins, did not evolve in isolation from global changes in tectonic regime, oceanic circulation, or climate patterns (Fig. 3). The development of plate-tectonic theory since the late 1960s clearly has emphasized the importance of these large-scale linkages.

The present chapter continues this philosophy, summarizing the geology of the North Atlantic but noting linkages to areas outside this ocean basin. The synthesis is based largely on material presented in Volume M. The citation or lack of citation of Volume M references here, however, reflects only the thematic fabric of the present synthesis, not the scientific merit of the papers. We refer the reader to original sources in Volume M for more complete treatment. We begin this chapter by noting ties between Volume M and several other Geology of North America volumes, and we continue with some "vital statistics" which describe three basic components of the Atlantic - igneous crust, sediments, and ocean waters - in space and time. This is followed by a discussion of scales of spatial and temporal variability, with emphasis on the latter. The chapter concludes with a summary of some of the important advances that have occurred in the three years since Volume M was published.

The bare essence of North Atlantic geology is distilled in Plate 2, which provides a highly

condensed summary of many Atlantic and global parameters against time, starting at the Triassic-Jurassic boundary. Plate 3 shows basement topography along the Kane Fracture Zone corridor from North America to near Africa, and it also provides an index map for 1) numerous geologic features and geographic provinces discussed in this text, and 2) locations of sea-floor areas illustrated in figures. These plates and the text figures with their captions convey graphically a large amount of data that cannot be fully discussed in the limited space of this chapter. It should be kept in mind that Plate 2 has limitations: a) the Atlantic has strong asymmetries in oceanographic and geologic architecture across both latitude and longitude, b) for a given time slice, some properties such as sediment composition vary significantly with water depth across the ocean basin, c) for parameters like volcanism and seafloor erosion by bottom currents, only subjective estimates of intensity presently are available, d) high-frequency variability (e.g. Milankovitch cycles) cannot be displayed at this scale, and e) sampling of paleoenvironments still is very fragmentary because of wide spacing and limited penetration of drill sites, incomplete core recovery, and numerous hiatuses.

Published in: *The Geology of North America, Vol. A, The Geology of North America; An Overview.* eds. A.W. Bally and A.R. Palmer, Geol. Soc. America, Boulder, CO, p. 53-80, 1989.

Supported by: ONR Contract N00014-87-K-0007 and NSF Grant OCE87-16713.

WHOI Contribution No. 7041.

MICROEARTHQUAKE EVIDENCE FOR EXTENSION ACROSS THE KANE TRANSFORM FAULT

W. S. D. Wilcock, G. M. Purdy and S. C. Solomon

We report the results of a microearthquake experiment conducted in 1987 in the active transform portion of the Kane Fracture Zone. The Kane is a slow slipping (25 mm/yr), large-offset (150 km) transform delineated by a pronounced transform valley. The experiment site lies in the eastern half of the transform, 40 km west of the eastern ridge-transform intersection, in a region of marked transform-parallel topography. The network consisted of 12 ocean bottom hydrophones and seismometers and extended for 25 km along the transform and 10 km in width, spanning the transform valley and a narrow median ridge to the north. Hypocentral parameters were determined for 86 earthquakes. Epicenters within the network define a narrow transform-parallel trend along the steep southern wall of the transform valley.

DEPARTMENT OF GEOLOGY AND GEOPHYSICS

David A. Ross, Chairman

Maximum focal depths increase from 6 to 9 km from east to west across the network. Significant activity was also detected outside the transform tectonized zone. To the southeast this activity may be associated with the inside corner of the ridge transform intersection, while to the north about 20 events occurred on 7-Myr-old crust in a region of ridge-parallel bathymetry. Six focal mechanisms were obtained from P wave first motions for events within the transform valley. The best constrained solutions, for four earthquakes within the network, show normal faulting on fault planes subparallel to the trend of the transform. All the mechanisms indicate a tension axis perpendicular to the trend of the transform. These results together with a significant historical record of large earthquakes near the experiment site lead us to conclude that the principal transform displacement zone was inactive during our experiment and that the observed activity is the result of extension in the adjacent lithosphere. The observed focal mechanisms and the inference that the axis of least compressive stress is approximately perpendicular to the transform provide direct evidence that the transform fault is mechanically weak relative to the surrounding lithosphere. Potential sources of extension across the transform include thermal stress in the young oceanic lithosphere, topographic loading, a small component of plate divergence normal to the transform, and northward motion of the asthenosphere relative to the surface plate.

In Press: *Journal of Geophysical Research*.

Supported by: NSF Grant EAR85-17137.

WHOI Contribution No. 7280.

ACCUMULATION OF HOLOCENE BANKTOP SEDIMENT ON THE WESTERN MARGIN OF GREAT BAHAMA BANK: MODERN PROGRADATION OF A CARBONATE MEGABANK

*R. Jude Wilber, John D. Milliman and
Robert B. Halley*

High resolution seismic profiles and mini-submersible reconnaissance along the leeward margin of western Great Bahama Bank (GBB) reveal two wedge-shaped sedimentary sequences, separated from one another by a steep lithified slope. The shallow (10-50 m water depth) bank edge unit, as much as 25m thick, is composed primarily of sand. The deeper (140-600m) slope unit, up to 90 m thick, is composed primarily of needle aragonite mud. Sediments in both units are Holocene in age and appear to have been derived primarily from the GBB since flooding of the

platform interior 6-10 ka ago. The volume of sediment in the two units is approximately equal to the total sediment presently found across the bank top and may contain more than three times the amount of aragonite mud. The occurrence of analogous sequences in the pre-Holocene record suggests that slope deposition of exported mud during sea level high stands has been a major mechanism for the westward progradation of GBB throughout the Quaternary.

In Press: *Geology*.

Supported by: WHOI/USGS Cooperative Agreement.

WHOI Contribution No. 7243.

GEOPHYSICS

ACOUSTIC WAVEFORM LOGS, AND THE IN-SITU MEASUREMENT OF PERMEABILITY - A REVIEW

Daniel R. Burns

Full waveform acoustic logs are composed of two propagating head waves, the P and S waves, and two guided waves, the pseudo-Rayleigh and tube (Stoneley) waves. The measurement of P and S wave slowness provides information on the subsurface lithology as well as estimates of the in-situ dynamic compressibility and rigidity of those formations. Strong correlations exist between measured in-situ permeability and the slowness and attenuation of the tube wave. The tube wave slowness can provide a measure of relative permeability variations if corrections are made for any changes in the formation shear wave velocity and borehole radius, both of which also affect the tube wave slowness. The Biot model of wave propagation in a porous and permeable formation can be used to estimate absolute in-situ permeability values from tube wave attenuation measurements if all of the model parameters are accurately known. Permeability estimates obtained by both of these methods from field data sets in two different lithologies are in good agreement with smoothed core permeability measurements. Because heavy drilling fluids are not used in most geotechnical boreholes, there is no mudcake build up along the borehole wall, thereby removing one of the greatest causes of uncertainty in using tube waves to estimate in-situ permeability.

In Press: *ASTM Symposium on Geophysical Methods for Geotechnical Investigations*.

Supported by: NSF Grant OCE89-00316.

WHOI Contribution No. 7141.

THREE DIMENSIONAL NUMERICAL MODELLING OF GEOACOUSTIC SCATTERING FROM SEAFLOOR TOPOGRAPHY

Daniel R. Burns and Ralph A. Stephen

A three dimensional, second order finite difference method was used to create synthetic seismograms for wave propagation in heterogeneous media in order to investigate the scattering of elastic and acoustic energy due to topography on the seafloor. The method uses a fully staggered grid in cartesian coordinates as developed by Virieux. Numerical results were generated for two models: a linear fault scarp on the seafloor, and a flat seafloor containing a rectangular channel. Wavefront snapshots allow the scattering and focussing of different wave modes with direction to be visualized. Compressional and shear wave backscattering from the sides of the features can be seen together with the trapped compressional wave energy propagating inside the channel. The results illustrate the effects of out of the plane scattering due to simple seafloor topographic features.

Supported by: ONR Contract N00014-87-K-0007 and ONT Contract N00014-89-C-0179.

WHOI Contribution No. 7187.

SEISMIC REFLECTION STRUCTURE OF THE UPPER OCEANIC CRUST: IMPLICATIONS FROM DSDP SITE 504B, PANAMA BASIN

J. A. Collins, T. M. Brocher and G. M. Purdy

We investigate the seismic reflectivity of the upper oceanic crust by comparing multichannel seismic (MCS) reflection data collected at Deep Sea Drilling Project (DSDP) Site 504B to the results of downhole logging. At this site drilling shows a well-defined change in physical properties at depths within the basement of about 0.5-0.6 km, corresponding to the downward transition from volcanic rocks to dikes. Extensive processing of the MCS data, required to remove high-amplitude side-scattered arrivals, revealed no conclusive evidence for laterally coherent reflection events generated within the upper 1-2 km of the crust. The crustal traveltime to the volcanic/dike boundary (about 0.25 s) is similar to the traveltimes of shallow reflection events observed in other areas. In an attempt to understand the lack of reflectivity from the volcanic/dike boundary at Hole 504B, we calculated synthetic reflection seismograms for a series of velocity-depth profiles constructed from the logged downhole variations in

physical properties. These seismograms were calculated with the source signature of the 1785 in³ (29.3 l) airgun array used to acquire the MCS data. The synthetic seismograms demonstrate that the reflections from the shallow crust are low in amplitude and may be obscured by source reverberation and be sediment-column multiples. Nonetheless, the limited available data also suggest that the upper crustal structure at Hole 504B may in fact differ from that at other crustal sites where high-amplitude reflections from within the shallow crust have been observed.

In Press: ODP, Part B, Vol. III.

Supported by: NSF Grants OCE84-10658 and OCE87-00806.

WHOI Contribution No. 7070.

SEISMIC VELOCITY STRUCTURE AT DSDP SITE 504B, PANAMA BASIN: EVIDENCE FOR THIN OCEANIC CRUST

J. A. Collins, G. M. Purdy and T. M. Brocher

We present an analysis of wide-angle reflection/refraction data collected in the immediate vicinity of Deep Sea Drilling Project Hole 504B in the Panama Basin, currently the deepest drillhole (1.288 km) into oceanic crust. The data were acquired with a 1785 inch³ airgun array and fixed-gain sonobuoy receivers, and consist of four intersecting profiles shot along three different azimuths. Near-normal-incidence, multichannel seismic (MCS) reflection data were acquired simultaneously. Observed P- and S- wave arrivals out to maximum ranges of 30 km constrain the crustal velocity structure at basement depths of ~0.5-5 km. Comparison of the travel times and amplitudes of the P- and S-wave arrivals on all four profiles reveals important similarities. These common features were modeled using the reflectivity synthetic seismogram method, the emphasis of the analysis being on the determination of the velocity structure of the middle and lower crust. Forward modeling shows that in contrast to standard oceanic velocity models, a velocity-depth profile that better explains the observed data is characterized by high velocity gradients (up to 0.6 km s⁻¹ km⁻¹) immediately above Moho, and a total crustal thickness of only 5 km. Interpretation of the high velocity gradients in the middle crust, a 1.8 km thick low-velocity zone ($V_p=7.1-6.7$ km s⁻¹) immediately above Moho, and a total crustal thickness of only 5 km. Interpretation of the high velocity gradients in the middle crust is constrained by the observation of P-3-branch amplitude focusing at ranges of 16-19 km.

Although not as well developed in comparison to the P-wave arrivals, S3-branch arrivals show similar focusing. Total crustal thickness is constrained by the combined interpretation of a P-wave, wide-angle reflection event observed at a range of 16-28 km, and an MCS reflection event with a crustal travel time of 1.4-1.5 s. Although these events cannot be directly correlated, their travel times are consistent with the assumption that both have a common origin. Amplitude modeling of the wide-angle event demonstrates that these events are generated at the Moho.

Published in: *Journal of Geophysical Research*, 94, 9283-9302, 1989.

Supported by: NSF Grants OCE84-10658 and OCE87-00806.

WHOI Contribution No. 7068.

COMMENT ON "THE GEOMETRY OF PROPAGATING RIFTS" BY D.P. MCKENZIE

Martin C. Kleinrock

The ability to predict the geometry of structural elements associated with propagating rift systems is an important aspect of understanding accretion and deformation processes along midocean ridges. McKenzie contributed significantly by elegantly calculating the expected kinematics of tectonic elements and passive lithospheric markers for a continuously moving propagator system with evenly distributed simple shear occurring in a migrating broad transform zone (Table 1 and Figure 5 of McKenzie). This modelling predicts curvature of abyssal lineations similar to that found at the Galapagos 95.5°W propagator system. (Kleinrock and Hey and Phipps Morgan and Kleinrock extended this work by showing that several nonuniform shear distributions developed as perturbations to McKenzie's models also result in satisfactory geometric predictions; they used observed lineation trends to estimate the actual strain distribution.) McKenzie also addressed the pattern to be expected if the orientation of the transform zone is assumed to be oblique, rather than exactly parallel, to the spreading direction. In doing this, however, he erroneously assumed that the propagation, and therefore transform migration, direction was perpendicular to the transform zone orientation rather than perpendicular to the spreading direction. The overall process is controlled by propagation of the spreading axis parallel to its strike, and therefore the transform zone must migrate along the spreading system in a direction parallel to the axis and normal to the stable transform faults elsewhere along the plate

boundary. Thus, his analysis of the shape of markers in the transform zone is incorrect (reference his equations 44-45).

Published in: *Earth, Planetary and Science Letters*, 95, 180-182, 1989.

Supported by: ONR Contract N00014-87-K-0007, NSF Grants OCE81-09927, OCE83-15364, and OCE88-22199.

WHOI Contribution No. 7129.

DETAILED TECTONICS NEAR THE TIP OF THE GALAPAGOS 95.5°W PROPAGATOR: HOW THE LITHOSPHERE TEARS AND A SPREADING AXIS DEVELOPS

Martin C. Kleinrock and R. N. Hey

A model for propagation of an active spreading axis into preexisting lithosphere is presented based on extensive detailed studies using SeaMARC II, Sea Beam, Deep-Tow, and Alvin near the tip of the propagator which is growing westward at ~52 km/Ma along the east-west trending Galapagos spreading axis near 95.5°W. Initial lithospheric rifting appears to be accommodated along reactivated roughly east-west abyssal hill faults at the "tectonic tip". Extension leads to down-dropping of a keystone block which is pervasively cut by normal faults and fissures. The initial volcanism ("initial volcanic tip") occurs about 6.5 km behind the tectonic tip as basalt erupts through these fissures, covering most of the keystone block. The "neovolcanic axial tip" occurs another 4.5 km back at the western termination of a well-defined axial pillow ridge along which volcanism is localized. Spreading along the propagator axis accelerates to the full rate (29 mm/yr half-rate) at the "full rate tip", interpreted to be ~10 km behind the neovolcanic axial tip, or ~21 km behind the tectonic tip.

A complex pattern of strain in the tip area results from the interaction of plate spreading, transform shear stress, crack propagation, dynamic depression of the western end of the axial valley and the transform zone, and variations in the strength, thickness, heterogeneity, and anisotropy of the lithosphere. Southwesterly curvature of the neovolcanic axis near its tip is inferred to result primarily from the response of young, thin, weak, relatively homogeneous lithosphere to counterclockwise rotation of the maximum tensional stress direction relative to the spreading direction due to the influence of shear stress from the transform zone. Similar stress interactions likely occur at the tectonic tip but are inferred to be accommodated in this older, thick, strong, heterogeneous, and anisotropic lithosphere by

oblique slip along a set of left-stepping reactivated preexisting east-west abyssal hill structures.

Although on a time-scale of $\sim 10^6$ years the overall process of propagation is mostly continuous, rifting at the tectonic tip appears discontinuous at a scale of ~ 1500 m or 30,000 years, based on the east-west spacing of grabens formed as rifting begins. The scale of discontinuity of propagation of the neovolcanic axis is ~ 3 -5 km or $\sim 50,000$ -100,000 years, based on the distribution of northeast-trending features interpreted as beheaded western terminations of paleo-neovolcanic axes.

The extension involved in rifting is ~ 10 -20%, based on summing the horizontal normal separation of all normal faults and fissures integrated and averaged over the zone of rifting. These values are approximately doubled if simple shear listric faulting is dominant rather than pure shear normal faulting.

Published in: *Journal of Geophysical Research*, 94, 13,801-13,838, 1989.

Supported by: NSF Grants OCE81-09927, OCE83-15364, OCE88-22199, and ONR Contract N00014-81-K-0007.

WHOI Contribution No. 7130.

MIGRATING TRANSFORM ZONE AND LITHOSPHERIC TRANSFER AT THE GALAPAGOS 95.5°W PROPAGATOR

Martin C. Kleinrock and R. N. Hey

At the 95.5°W propagator system along the Cocos-Nazca plate boundary, the spreading axis is offset left-laterally about 35 km (~ 1 Ma). This offset migrates westward 52 km/Ma relative to points along the nearly east-west trending ridge axis, transferring lithosphere from the Cocos to the Nazca plate as it does so. The required 58 km/Ma of right-lateral motion across this migrating transform is apparently not accommodated by a through-going north-south transform fault, but rather by an approximately 15-20 km wide zone of shear deformation dominated by eastward curving of east-west structures to a northwest-southeast trend. This pattern of curvature, the coinciding zone of high seismicity, and the abundance of talus in the area suggest that shear is distributed over this entire zone. The deformation is inferred to be taken up by a "bookshelf" mechanism whereby faults oriented at high angles to the shear couple have left-lateral slip antithetic to the right-lateral shear couple, rotating individual blocks clockwise. These are interpreted as reactivated abyssal hill-bounding normal faults probably dipping ~ 45 -60°. Northeast-southwest shortening due to the rotation appears to be accommodated by

reverse slip on the faults and may account for the uplift of DeSteiguer Ridge in the zone of transferred lithosphere. These faults have had a very complex history: initially normal faults formed as abyssal hills were created at the spreading axis and subsequently they had left-lateral strike-slip motion in the transform zone and reverse motion uplifting DeSteiguer Ridge. Strain analysis based on observed structural curvature suggests that shear is distributed nonuniformly and lithospheric transfer requires ~ 0.4 Ma.

Published in: *Journal of Geophysical Research*, 94, 13,859-13,878, 1989.

Supported by: NSF Grants OCE81-09927, OCE83-15364, OCE88-22199, and ONR Contract N00014-81-K-0007.

WHOI Contribution No. 7132.

TECTONICS OF THE FAILING SPREADING SYSTEM ASSOCIATED WITH THE 95.5°W GALAPAGOS PROPAGATOR

Martin C. Kleinrock, Roger C. Searle and R. N. Hey

The failing spreading system associated with the Galapagos 95.5°W propagator system comprises a complex set of volcanic and structural provinces. Data from detailed surveys using GLORIA, SeaMARC II, Sea Beam, Deep-Tow, the submersible Alvin, magnetics, and bottom cameras constrain the plate boundary geometry and evolution of this area. Although the failing spreading system may involve diffuse spreading, the patterns of sedimentation, volcanism, and faulting suggest localization. The failed spreading axis, composed of a set of right-stepping en echelon basins, extends and ages southeastward from offset and overlapping doomed/failing axes. The failing axis is offset ~ 13 km left-laterally from the doomed axis. Although there may have been a preexisting offset in the doomed axis, lack of structural evidence for this and the lack of an offset of this magnitude in the Brunhes/Matuyama magnetic reversal argue against this possibility. A model whereby the offset is transient, does not explain the pattern of failed spreading basins which leads directly away from the currently failing axis. Detailed structural and volcanic patterns suggest that this offset may be caused by a westward progression of northward jumps in the location of the failing axis (like a secondary propagator), probably in association with the migrating strain/stress field of the migrating transform zone of the propagator system. This is modelled as a "migrating extensional relay zone"

(MERZ) similar to the relay zones observed at some fast-slipping transform faults except that it propagates westward with the overall system. Bathymetric and magnetic evidence for tectonic elements associated with the MERZ supports this model, although the expected extinct trace of the doomed axis is not obvious in the present, incomplete data set. Unlike other models for the plate boundary geometry, the MERZ model does not require extreme serendipity for temporal and spatial juxtaposition of the primary propagator and the offset within the failing spreading system. Observation of a similar geometry in the Lau Basin supports this preferred model. Present data from the Galapagos failing spreading system are inconclusive, however, and the MERZ model remains speculative. This model implies that in at least some cases paired propagators act together. The MERZ is too short and deep to drive its own propagation according to standard cracking models.

Published in: *Journal of Geophysical Research*, 94, 13-839-13,858, 1989.

Supported by: NSF Grants OCE81-09927, OCE83-15364, OCE88-22199, and ONR Contract N00014-81-K-0007.

WHOI Contribution No. 7131.

EVIDENCE FROM GRAVITY DATA FOR FOCUSED MAGMATIC ACCRETION ALONG THE MID-ATLANTIC RIDGE

J. Lin, G. M. Purdy, H. Schouten, J.-C. Sempere and C. Zervas

Analyses of newly collected gravity data at the Mid-Atlantic Ridge between latitudes 27°50'N and 30°40'N reveal that ridge magmatic accretion is highly focused at discrete centers along the spreading axis. Large negative gravity anomalies equivalent to more than 50% reduction in crustal thickness are observed over non-transform discontinuities bounding spreading segments.

In Press: *Nature*.

Supported by: NSF Grant OCE87-09615 and the WHOI Culpeper Award.

WHOI Contribution No. 7253.

TRANSFORM ZONE MIGRATION: IMPLICATIONS OF BOOKSHELF FAULTING AT OCEANIC AND ICELANDIC PROPAGATING RIFTS

Jason Phipps-Morgan and Martin C. Kleinrock

Ridge propagation necessitates the creation of a migrating transform zone (MTZ) that offsets the

propagating and retreating spreading axes. We examine several kinematic models of MTZ deformation to determine which models can generate observed seafloor fabric orientations, vertical tectonics, and faulting patterns within the 95.5°W Galapagos propagating ridge (PR) system. Models that involve transform parallel simple shear within the MTZ can fit observed seafloor fabric rotation patterns within the 95.5°W MTZ. However, these models predict pervasive transform parallel (strike-slip) faults within the MTZ that are not observed, and do not predict the dramatic shear-concurrent deepening and post-shear uplift that is seen in this PR system. Since we only measure the amount of structural rotation of the abyssal hill fabric within the MTZ, not abyssal hill parallel or normal extensional or compressional deformation, this information can only determine the rotational component of the finite strain tensor. Thus this simple-shear family of kinematic deformation models is actually only a small subset of MTZ deformation patterns that can produce the same finite rotation patterns, but with different abyssal hill parallel/perpendicular shortening and/or extension. There is strong seismic and surface fault-break evidence in Iceland that the South Iceland Seismic Zone MTZ propagates along an array of en-echelon, 'transform' perpendicular strike-slip faults. We next examine the kinematic consequences of finite MTZ deformation within this generalized 'Bookshelf Faulting' deformation scenario. We find that our kinematic realization of generalized bookshelf faulting predicts structural rotation and vertical tectonic patterns that are consistent with observations at the 95.5°W Galapagos PR system. Vertical tectonics are a by-product of bookshelf shearing because the geometric strain incompatibility associated with this mode of deformation causes local extension within the abyssal hills of the DeSteigneur Deep since these abyssal hills do not abut a spreading axis where this shear associated deformation would be preferably accommodated. We conclude that generalized bookshelf faulting is a promising candidate for the dominant deformation process within a MTZ.

Supported by: NSF Grant OCE88-22199.

WHOI Contribution No. 7133.

BUOY BASED MEASUREMENTS OF OCEAN HEAT FLUX IN THE FRAM STRAIT

Donald K. Perovich, Walter B. Tucker, III and Richard A. Krishfield

As one component of the Arctic Environmental Data Buoy two thermistor strings were installed

through the ice to measure ice temperatures and determine oceanic heat fluxes as the buoy drifted from the Arctic basin into the Greenland Sea. Ice temperature data between 14 Dec. 1987 and 2 Jan. 1988 were retrieved. During this period the AEDB progressed from approximately 81°N 4°E to 77°N 5°W. This constituted the most rapid displacement of the entire drift, coinciding with the entry of the floe into the marginal ice zone of Fram Strait. Once in the MIZ, water temperatures increased, most notably at a depth of 16 m, where values changed from -1.8°C to more than 2°C. Bottom ablation rates of 34 mm/day were observed between 21 and 28 Dec. During this excursion into warmer water, the oceanic heat flux increased by a factor of 18, from 7 W/m² to 128 W/m².

Published in: *Geophysical Research Letters*, 16(9), 995-998, 1989.

Supported by: ONR Contract N00014-87-K-0007.
WHOI Contribution No. 7046.

HIGH-RESOLUTION INVERSION FOR SOUTH ATLANTIC PLATE KINEMATICS USING JOINT ALTIMETER AND MAGNETIC ANOMALY DATA

Peter R. Shaw and Steven C. Cande

We present an inversion for plate kinematics that solves for finite rotation parameters using fracture zone (FZ) and magnetic anomaly location data jointly. We define misfit functions that incorporate properties unique to each data type; in particular, the FZ misfit function does not depend upon alignment of conjugate FZ traces in the same way as magnetic lineations under the finite rotations. This property is useful for FZ locations, in which the signals on conjugate sides of the ridge may include systematic differences, or where data from one side of the ridge are sparse or missing. Formal error bounds estimated for the pole parameters show that the magnetic and FZ data are complementary in their information content. Error bounds computed for the joint inversion are substantially smaller than for either the FZ or magnetics data used separately, indicating that simultaneous use of the data in an inversion is crucial. We apply this method to Seasat altimeter data and magnetic anomaly picks in the South Atlantic. We solve for finite poles corresponding to magnetic anomalies 5, 6, 8, 13, 21, 22, 25, 30, 33, 33r, and 34; these define a smooth path over the past 84 Ma indicating that the plate motions have not been as erratic as found previously.

In Press: *Journal of Geophysical Research*.

Supported by: NSF Grant OCE86-14512.

WHOI Contribution No. 7162.

USING TOPOGRAPHIC SLOPE DISTRIBUTIONS TO INFER SEAFLOOR PATTERNS

D. K. Smith and P. R. Shaw

At scales of tens to hundreds of kilometers, the most prevalent patterns on the seafloor are those formed by the succession of elongated abyssal hills. This seafloor fabric, generated at the ridge axis, and modified by sedimentation, mass wasting, and volcanism as it moves away from the ridge, is a record of geologic interest. In this report we describe the characteristics of abyssal-hill topography. The basic quantity that we use in our analysis is the distribution of topographic slopes in a region. A convenient means for parameterizing these slopes is through unit vectors that are normal to small patches of the seafloor. The normal vectors are decomposed into azimuthal and dip components. We find that the azimuthal distribution of the vectors provides a first-order indication of the dominant elongation directions in the topography, including multiple lineations when they are present. In addition, we find that the distributions of dip angles within a small window centered on the peaks of the azimuthal density function provide an indication of any asymmetry (i.e., transverse to the elongation direction), such as might result from back tilting of individual abyssal-hill blocks. Our investigations have shown that the slope statistics are relatively independent of long-wavelength depth variations, and are robust even if large anomalous features such as seamounts and fracture zones are included in the section of bathymetry analyzed. We apply the slope-analysis method to 3 regions in the Northeast Pacific and 2 regions in the Southwest Indian Ocean. We find that at the Sea Beam scale the abyssal-hill terrain is statistically symmetric in cross-section for four of these regions, the region with the largest topographic relief, formed at the slow-spreading Southwest Indian Ridge, shows evidence of asymmetry.

Published in: *IEEE Journal of Ocean Engineering*, 14(4), 338-347, 1989.

Supported by: ONR Contracts N00014-87-K-0087, N00014-K-0508 and N00014-89-J-0021.

WHOI Contribution No. 7135.

SOLUTIONS TO RANGE DEPENDENT BENCHMARK PROBLEMS BY THE INFINITE DIFFERENCE METHOD

Ralph A. Stephen

An explicit second order finite difference

scheme has been used to solve the elastic wave equation in the time domain. Solutions are presented for the perfect wedge and the plane parallel wave guide which have been proposed as benchmarks by the Acoustical Society of America. Good agreement with reference solutions is obtained if the media is discretized at twenty grid points per wavelength. The principle disadvantage of the technique is long computational times which are between ten and twenty hours on a minicomputer without an array processor. The method has the advantage of providing phase information and, when run for a pulse source, of providing insight into the evolution of the wavefield and energy partitioning. Arbitrarily more complex models including velocity gradients, strong lateral heterogeneities, and random media can be solved with no additional computational effort. The method has also been formulated to include shear wave effects.

In Press: *Journal of the Acoustical Society of America*.

Supported by: ONR Contract N00014-87-K-0007.

WHOI Contribution No. 7140.

SEISMIC STRATIGRAPHY IN A TRANSVERSE RIDGE, ATLANTIS II FRACTURE ZONE

*Stephen A. Swift, Hartley Hoskins and
Ralph A. Stephen*

On Ocean Drilling Program Leg 118, we made a vertical seismic profile in Hole 735B, a 0.5 km deep borehole in 720 m of water on the eastern wall of the Atlantis II fracture zone, Southwest Indian Ridge. Seismograms were collected at 20 borehole depths alternately using both a watergun and an airgun at each depth. The overall velocity is 6.5 km/s. The lowest interval velocities occur in the foliated gabbros (Unit I) and olivine gabbro-troctolite (Unit VI). We separated up- and down-going wave fields with frequency-wavenumber filtering and deconvolved the up-going field by spectral division using the down-going field at each receiver depth. The processed sections show irregular reflections from the base of the foliated gabbros (Unit I, 50-70 mbsf) and from the Fe-Ti rich gabbro (Unit IV, 200-250 mbsf). Coherent events at ~560 and 760-825 mbsf are interpreted as reflections from crustal lithologic or structural surfaces.

In Press: *Proceedings of the Ocean Drilling Program, Scientific Results*, Vol. 118.

Supported by: Ocean Drilling Program/Texas A&M.

WHOI Contribution No. 7171.

THE MAGNETIC STRUCTURE OF AXIAL SEAMOUNT, JUAN DE FUCA RIDGE

Maurice A. Tivey and H. Paul Johnson

Axial Seamount is a large, volcanically-active seamount located in the eastern Pacific on the central Juan de Fuca (JDF) ridge at 46°N, 130°W. Sea-surface magnetic anomaly data show that Axial lies completely within crust formed during the Brunhes normal polarity epoch. The edifice, however, does not produce a simple positive magnetic anomaly related to the excess mass above mean seafloor. Several pronounced negative magnetic anomalies are associated with the seamount, including both a circular-shaped low located west of the summit and an elongate low (trending NW) on the southeast flank of the volcano. These two anomalies form part of a NW-SE magnetic trough which extends across the seamount edifice oblique to the general JDF ridge trend of N20E. A third negative anomaly is observed on the northern flank of the seamount associated with North Helium Basin, a deep elongate basin which indents the northeast flank of the seamount. Both inversion of sea surface magnetics data and forward modelling of topography, constrained by magnetization values of dredged samples, show that bathymetric effects can explain the Helium Basin anomaly, but topography alone cannot produce the low magnetization values which extend across the seamount summit. Magnetization of crustal rocks does not vary spatially over the seamount, so that negative anomalies at the summit can be explained by variations in the effective thickness of the magnetic source layer. A simple forward model of uniform magnetization shows that the anomaly source layer would have to thin by 50% (to less than 700 meters thick) in order to generate the observed magnetic response. A thinned source layer is consistent with the presence of either a substantial magma chamber at depth beneath the summit of Axial or a zone of substantial crustal alteration. The shape of the anomaly implies the trend of either of these sources must be oriented obliquely to the general ridge trend but parallel to the direction of the absolute plate motion.

In Press: *Journal of Geophysical Research*.

Supported by: ONR Contracts N00014-87-K-0160 and N00014-89-J-1022 and NSF Grant OCE83-09812 and WHOI 4941.

WHOI Contribution No. 7277.

HEAT FLOW AND THE THERMAL ORIGIN OF HOT SPOT SWELLS: THE HAWAIIAN SWELL REVISITED

R. P. Von Herzen, M. J. Cordery, R. S. Detrick, and C. Fang

We present 150 new heat flow measurements obtained at eight sites along a 1230 km long profile across the Hawaiian Swell about 700 km ESE of Midway Island. Most of the measurements include in situ thermal conductivity determinations, which helped to reduce the statistical uncertainties (95% confidence) at all sites to $< \pm 2.1 \text{ mWm}^{-2}$. Surprisingly, there is no systematic variation in heat flow across the axis of the swell. With one exception, the mean heat flow (corrected for sedimentation) at each site is within +10% of the mean value of 57.7 ± 4.3 (S.D.) mWm^{-2} for all sites. At the two sites at either end of the profile, clearly located off the swell, the observed heat flow is $> 59 \text{ mWm}^{-2}$ about 20% higher than the predicted heat flow for 100 Ma sea floor based on simple lithospheric cooling models. Thus even though there is a small increase in heat flow with age along the swell, when compared with the off-swell heat flux the anomalous heat flow associated with the Hawaiian Swell is probably on the order of 5 to 10 mWm^{-2} , and arguably may not exist at all. A previous investigation (Von Herzen, et al., 1982) may have overestimated the magnitude of the heat flow anomaly associated with the Hawaiian Swell by comparing heat flux measurements on the swell with values expected for simple lithospheric cooling models. The heat flow anomalies associated with the Bermuda Rise and the Cape Verde rise may also be smaller than previously estimated, given the uncertainties in the heat flux on the normal sea floor surrounding these swells.

The lack of a significant heat flow anomaly associated with the bathymetric expression of the Hawaiian Swell is inconsistent with simple models of lithospheric reheating. Dynamic support, accompanied by modest temperature increases ($\leq 100\text{--}200^\circ\text{C}$) confined to the lower lithosphere, and underlying asthenosphere, appear to be required to explain both the height of the swell and its small heat flow anomaly. However, detailed modeling of the origin of mid-plate swells, and their associated heat flow anomalies, is hampered by our lack of understanding of the thermal evolution of old (≥ 80 Ma) oceanic lithosphere.

Published in: *Journal of Geophysical Research*, 94(B10), 13,783-13,799, 1989.

Supported by: NSF Grant OCE85-16298.

WHOI Contribution No. 7087.

OCEANOGRAPHY

THE OCEAN ENTERPRISE CONCEPT

D. A. Ross, M. A. Champ, J. E. Dailey and C. E. McLain

The Ocean Enterprise concept has been proposed as an exciting and challenging mechanism for launching a new era of awareness, practical development, and utilization of ocean resources beginning in the early 1990s. It is only through a cooperative 'pulling together' of government, academia, and industry that significant new areas of operational economic interest can be developed or current ones strongly bolstered in the oceans' sector. Great strides in the scientific understanding of the oceans have been made in some areas, yet no new major economic area has been developed in the ocean sector in twenty years and a strong well recognized constituency has not yet developed for the oceans.

This paper discusses the private sector environment and its necessary placement in bridging the No Man's Land gap between research and development. It defines an ocean enterprise using ocean platforms as an example and then discusses funding limitations and private sector incentives for oceans' development. An approach for the Ocean Enterprise concept is offered with the reminder that primary resources of basic ocean research lie within academia and the federal government, and that primary resources for development lie within the private sector. The model of a Research and Development Limited Partnership with government, academia and private industry in a 'triple alliance' is offered as a mechanism for launching Ocean Enterprises. In addition, an Ocean Economic Development Policy statement by the President is needed to follow up on the EEZ Proclamation of 1983, and a coalition of ocean resource states would be helpful in the development of a broader Congressional constituency as well.

An implementation strategy for the Ocean Enterprise concept would entail a team effort, with coordination by key federal agencies backed by specific White House approval, supporting major activities in five areas: policy development; constituency establishment; awareness enhancement; new enterprise initiation; and research and development direction and augmentation. The technology, ideas, and interest for Ocean Enterprises are present. The initiative can, if vigorously encouraged and coordinated, yield a strong turning point for the history of ocean research and enterprise.

Published in: *NSF Report on the Ocean Enterprise Workshop*, 12 pp.

Supported by: NSF Grant ENG88-06461 and NOAA
Sea Grant NA86-AA-D-SG090.

WHOI Contribution No. 7230.

THE SPATIAL DISTRIBUTION OF SILICOFLAGELLATES IN THE REGION OF THE GULF STREAM WARM CORE RING 82B: APPLICATION TO WATER MASS

K. Takahashi, P. L. Blackwelder and J. D. Billings

To delineate potential water mass affinities, we investigated silicoflagellates from the region of Gulf Stream warm core ring (WCR) 82B in the northwestern Atlantic. Silicoflagellates from 202 samples from N-S and an E-W transects across WCR 82B during late April were analyzed. Shelf to Sargasso Sea (SS) transects, one completed in early May and the other in June 1982 were also examined. Eight to eleven vertical profiles to 200 m comprised each of the transects. Six taxa of silicoflagellates were found in the samples studied and a total of more than 8000 specimens were encountered. Three major taxa dominated standing stocks: *Distephanus speculum*, *Dictyocha messanesis* (intermediate-sized form) and *D. mandrai*. *D. speculum*, considered a cold water taxon in the literature, showed a higher standing stock in the cooler high velocity region (HVR) of the warm core ring, continental shelf (SH), and slope (SL) waters. Fewer were present in the warmer ring center (RC), Gulf Stream (GS) and Sargasso Sea (SS). *D. mandrai* showed a similar distribution to that of *D. speculum*, but its preference for slightly warmer waters ($> \sim 10^{\circ}\text{C}$) was noted. In contrast, *Dictyocha messanesis* (intermediate) and *Distephanus pulchra*, known to be warm water taxa, were relatively abundant in the warm ring center. In contrast to standing stock data, ratios between cold and warm water taxa correlate well with temperature and salinity in the warm core ring. Since these ratios are not effected by convective loss, they are excellent water mass tracers in this system. Based on the silicoflagellate distribution, it can be concluded that the water mass in the ring center has higher affinity with the Sargasso Sea than the Gulf Stream.

Scores derived from factor analysis indicate that silicoflagellate species distributions are highly correlative with water masses. This was evident from correlations with temperature, salinity, and with distance from ring center. Nutrients were generally not correlated with species data. This may be due to keep vertical mixing in the ring center of 82B in April which resulted in loss of plankton cells below the euphotic zone which was responsible for low silicoflagellate standing stock. Silicoflagellate productivity, measured as % double

skeletons of *D. speculum*, were approximately the same in all water masses. This result is consistent with the hypothesized plankton population loss due to the convection.

In Press: *Deep-Sea Research*.

Supported by: WHOI Independent Study Award.

WHOI Contribution No. 6975.

HISTORICAL DEVELOPMENT AND USE OF THOUSAND-YEAR-OLD TIDE PREDICTION TABLES

Yang Zuosheng, K. O. Emery and Xui Xui

Tide-prediction tables require an understanding of the relation of tide to moon and sun, as expressed by correspondence of tide heights to phases of the moon and by the lag of high tide after local meridional transit of the moon. Such tables were compiled earlier in China than elsewhere—more to satisfy the interests of sightseers of spectacular river bores than for convenience of shipping. We used the earliest extant Chinese tables of A.D. 1056 to compare ancient predictions with those from modern tide tables for the Qiantang river bore near Hangzhou. The fit of hour and height is excellent for the ten days or so of highest (perigean) tides, but the ancient tables do not select the higher of the two daily apogean high tides during much of the rest of a month.

Published in: *Limnology and Oceanography*, 34,
953-957, 1988.

Supported by: Ocean Industry Program.

WHOI Contribution No. 7078.

PALEOCEANOGRAPHY

THE INFLUENCE OF MICROHABITATS ON THE CARBON ISOTOPIC COMPOSITION OF DEEP-SEA BENTHIC FORAMINIFERA

*Daniel C. McCorkle, Lloyd D. Keigwin,
Bruce H. Corliss and Steven R. Emerson*

We report $\delta^{13}\text{C}$ and $\delta^{18}\text{O}$ values for Rose Bengal-stained benthic foraminifera from a set of box cores from continental margin environments in the Atlantic and Pacific Oceans. These isotopic results are compared with foraminiferal distribution data and pore water $\delta^{13}\text{C}$ profiles to evaluate the importance of environmental (microhabitat) effects on the carbon isotopic composition of benthic foraminifera. The $\delta^{13}\text{C}$ values of infaunal taxa are consistently lower than

those of epifaunal taxa, suggesting that microhabitat effects on test composition do exist. The $\delta^{13}\text{C}$ differences between foraminiferal carbonate and bottom water dissolved inorganic carbon (DIC) are not correlated with the $\delta^{18}\text{O}$ differences between benthic foraminifera tests and equilibrium calcite, but they do correlate with variations in the chemistry of sediment pore waters. However, interspecific $\delta^{18}\text{O}$ differences as well as $\delta^{13}\text{C}$ differences between species with similar vertical distributions in the sediments indicate that taxon-specific "vital" effects also influence test composition.

In Press: *Paleoceanography*.

Supported by: NSF Grants OCE86-14496, OCE84-19595, OCE86-14162, OCE86-10043, and OCE86-14514.

WHOI Contribution No. 7201.

RADIOLARIAN FROM THE DISTAL BENGAL FAN IN THE EQUATORIAL INDIAN OCEAN ODP LEG 116

Kozo Takahashi

Cores recovered from three sites of Leg 116 were studied for radiolarians. Generally, radiolarians were absent from most samples prepared for examination. Moderate to well preserved radiolarian assemblages are found only in the uppermost one or two cores which were the focus of this study. All of the radiolarian assemblages in the upper cores belong to the *Buccinosphaera invaginata* Zone of latest Quaternary age. However, there is one horizon where a few Miocene radiolarians had been reworked into the modern assemblages. Local seamounts are suggested sources for the reworked radiolarians.

In Press: *Proceedings of the Ocean Drilling Program Leg 116*.

Supported by: Ocean Drilling Program, Texas A&M.

WHOI Contribution No. 7193.

PALEONTOLOGY

ORBITAL FORCING, CALCAREOUS NANNOFOSSILS AND STABLE ISOTOPES IN UPPER MIOCENE SEDIMENTS FROM THE NORTH ATLANTIC OCEAN

Luc Beaufort and Marie-Pierre Aubry

The ratio between the two most abundant calcareous nannofossil species (*Coccolithus*

pelagicus and *Reticulofenestra pseudoumbilica*) in the upper Miocene sediments at North Atlantic DSDP Site 552A display large fluctuations which are interpreted to reflect Milankovitch periodicities and are thought to be linked to climatic changes. The oxygen isotope records on benthic and planktonic foraminifera from the same site yield periods close to the tilt and the precession cycles. The two major $\delta^{18}\text{O}$ increases the latest Miocene described by Keigwin et al. (1986) and Keigwin (1987) and interpreted as reflecting glacial events, correlate exactly with two major abundance peaks in *C. pelagicus*. Longer term fluctuations seem to be correlated with the $\delta^{13}\text{C}$ record in benthic and planktonic foraminifera. We suggest that the composition of calcareous nannofossil assemblages varies as a function of the combined effects of temperature and nutrient variations.

In Press: *Paleoceanography*.

Supported by: Bureau de Recherches Géologiques et Minières, France and A Consortium of Oil Companies.

WHOI Contribution No. 7260.

CENOZOIC BATHYAL AND ABYSSAL CALCAREOUS BENTHIC FORAMINIFERAL ZONATION

W. A. Berggren and Kenneth G. Miller

Deep-sea (bathyal-abyssal) benthic foraminifera provide a potential supplement to planktonic biostratigraphy. Benthic foraminifera are more resistant to dissolution and are often found in upper bathyal, lower abyssal, and higher latitude sediments which contain impoverished planktonic faunas. The biostratigraphic utility of benthic foraminifera was previously limited by poor understanding of their taxonomy and paleobathymetric distributions. During the past ten years, study of deep-sea benthic foraminifera from Deep-Sea Drilling Project (DSDP) and industry wells has provided an improved taxonomic base and empirical observations of age-depth distributions. Building on this data base, we establish 14 bathyal and 12 abyssal zones for the Cenozoic deep sea. Biostratigraphic resolution is higher in the abyssal realm during the Neogene (3 abyssal versus 8 bathyal zones). During periods of accelerated taxonomic turnover (e.g., in the middle Miocene bathyal zone), deep-sea benthic foraminifera yield fairly refined zonations; in contrast, slow taxonomic turnover occurred during the Paleocene in the bathyal and abyssal realms and in the late Neogene in the abyssal realm, yielding few biostratigraphic subdivisions.

Published in: *Micropaleontology*, 35(4), 308-320. 1989.

Supported by: A Consortium of Oil Companies.

WHOI Contribution No. 7167.

**GLOBOROTALIA TRUNCATULINOIDES'
GROWTH AND CHEMISTRY AS
PROBES OF THE PAST THERMOCLINE:
1. SHELL SIZE**

G. P. Lohmann and Peter N. Schweitzer

This work identifies features of the life history of the deep-living planktonic foraminifer *G. truncatulinoides* that offer possibilities for reconstructing characteristics of the past ocean's main thermocline. First, Part I considers two aspects of variation in shell size: the predictability of growth-related size changes, which we need to calculate changes in shell chemistry, and a model for environmentally forced changes in shell size frequency, which suggests how shell size may be a direct source of paleoceanographic information. Even though size variation among shells of *G. truncatulinoides* at the same stage of growth (same number of chambers) exceeds the size difference between successive growth stages, growth-related size changes are predictable because shells tend to grow at the same rate. Variation in initial shell size is sufficient to account for the large size variation found among shells at the same stage of growth. Several lines of evidence suggest that *G. truncatulinoides* reproduces at ~600m in the water column, and it appears that vertical mixing to that depth is required to return juvenile shells to the surface. Anything that prevents this, such as shallowing of the thermocline, can interfere with *G. truncatulinoides*' life history in such a way that its shell size-frequency distributions are altered. Among shells falling to the seafloor from a reproducing population are large numbers of both juvenile and adult sizes and, if reproduction is inhibited, the frequencies of those sizes are reduced and the relative frequency of intermediate-sized shells increases. A paleoceanographically useful result of this is that the topography of the main thermocline tends to be reflected in the size-frequency distribution of *G. truncatulinoides*' shells from the underlying sediments: In areas where the top of the main thermocline is shallower than ~600m, production of juveniles (125-177 μm) and reproductive adults (>425 μm) is reduced, leaving predominantly intermediate-sized (212-355 μm) shells.

In Press: *Paleoceanography*.

Supported by: NSF Grants OCE84-17040,
BSR86-06701 and OCE89-12280.

WHOI Contribution No. 7045.

**GLOBOROTALIA TRUNCATULINOIDES'
GROWTH AND CHEMISTRY AS
PROBES OF THE PAST THERMOCLINE:
2. SHELL SHAPE**

G. P. Lohmann and Peter N. Schweitzer

Part 2 continues efforts outlined in Part 1 to use the growth and chemistry of the deep-living planktonic foraminifera *G. truncatulinoides* to reconstruct features of the past ocean's main thermocline. Here we show how changes in the shape of *G. truncatulinoides*' shell as chambers are added during growth, changes associated with its ontogeny, can be used as a size-independent measure of shell development. This permits comparisons between successive stages of development in spite of wide variation in size and it is a criterion for grouping together shells, within the same developmental stage, to obtain sufficient mass for isotopic analysis. With shell size, shell shape is the basis for tracking a population's "developmental pathway," the trajectory shells follow through size-shape space as they grow. Because of wide variability in size within developmental stages, anything that changes shell size frequency also shifts a population's developmental pathway. In particular, changes that select against development of larger, presumably faster sinking, shells shift sizes. Beyond a point where even "accelerated" development of the smallest shells is not sufficient for them to reach reproductive maturity, juvenile and adult stages disappear and only intermediate stages are present. These observations refine the pattern of changes seen in shell size frequency described in Part 1. Simple models are presented to show how this apparent "acceleration" in shell development can occur and developmental pathways are reconstructed for several different populations showing that it does occur in certain oceanographic settings, in particular where the main thermocline shallows. As developmental pathways are shifted toward smaller and smaller sizes, a residual subpopulation of larger, immature shells come to dominate the larger size range, their presence strongly distorts a population's apparent developmental pathway. Failure to recognize this would confuse interpretation of changes in *G. truncatulinoides*' shell chemistry.

In Press: *Paleoceanography*.

Supported by: NSF Grants OCE84-17040 and
BSR86-06701 and OCE89-12280.

WHOI Contribution No. 7044.

ON EIGENSHAPE ANALYSIS

G. P. Lohmann and P. N. Schweitzer

The term "eigenshape analysis" was originally coined to call attention to the fact that collections of observed shape functions can be represented by a set of orthogonal shape functions derived from an analysis of the observations themselves (Lohmann, 1983). This decomposition of data functions into empirical orthogonal functions has been usefully applied in many different fields (Lorenz, 1959; Davis, 1976; Aubrey, 1979; Lohmann and Carlson, 1981; Aubrey and Emery, 1986; Mix et al., 1986).

Since the term was introduced, "eigenshape analysis" has taken on a much broader meaning than was its original, limited intent. It has been misunderstood to include the choices, judgements, sampling strategies and technical details that were either required by the nature and aims of particular studies or dictated by equipment limitations. Here we consider all aspects of this extended definition of eigenshape analysis, of which eigenfunctions themselves play a small part.

The methods that follow were chosen from among many possible ways to solve particular research problems, problems whose primary concern was the description of growth histories and developmental pathways from measurements of fossil populations. The validity and suitability of these methods should be evaluated in that context.

In Press: *Proc. NSF Workshop on "Morphometrics in Systematic Biology"*.

Supported by: NSF Grant OCE84-17040.

WHOI Contribution No. 7048.

LIFE HISTORY AND THE EVOLUTION OF ONTOGENY IN THE OSTRACODE GENUS *CYPRIDEIS*

P. N. Schweitzer and G. P. Lohmann

Because of the nature of the fossil record, paleontologists have often had to view evolution as a process that selects animals strictly according to their morphology. In reality, of course, selection depends on behavioral traits as well, reproductive behaviors in particular. But fossils rarely show evidence of their life-history traits. Faced with only the form and distribution of fossils, paleontologists have striven to infer evolution of their life-history traits from the morphological changes that occurred during development. Our objective is to test the assumptions that underlie those inferences.

We studied four species of the salt-marsh ostracode genus *Cyprideis* to determine the relationships among size, shape, chronological age, and developmental events. Living populations were

sampled regularly to determine differences in seasonality among species and to estimate the duration of development. In addition, samples representative of the species' geographic and stratigraphic ranges were studied to assess the relative importance of these components of variation.

The changes in ontogeny that have occurred during the geological history of these species are insignificant in the statistical context of geographic and seasonal variation. Evolution of ontogeny occurs at the level of species in this group, but it is not simply related to differences in life-history. We find evidence of heterochrony where there is no difference in developmental timing, and a difference in developmental timing where there is no heterochrony. Size shows a similar pattern. Three of the four species show the expected positive correlation between size and age at maturity. The other species is relatively large yet matures rapidly. We conclude that *Cyprideis* does not support the generalization that life-history evolution causes heterochrony, and casts doubt on the inference of life-history evolution from heterochrony.

In Press: *Paleobiology*.

Supported by: NSF Grants OCE84-17040 and BSR86-06701.

WHOI Contribution No. 7047.

SEDIMENTOLOGY

MORPHOLOGY, SEDIMENTS AND STRUCTURE OF THE AMIRANTE TRENCH, WESTERN INDIAN OCEAN: IMPLICATIONS FOR TRENCH ORIGINS

John E. Damuth and David A. Johnson

The Amirante Trench is a 600 km long and up to 5200 m deep topographic depression whose origin has remained enigmatic. The trench contains >1 km of undisturbed, ponded turbidites and mass-transport deposits that have been periodically modified by northward flowing contour currents of the DWBC. Morphologically, the trench and adjacent Amirante Ridge resemble an arcuate oceanic arc-trench system and some investigators have suggested that this complex represents some type of subduction zone. However, our analysis of bathymetric and structural data indicate that the trench is not a single, continuous arcuate feature, but is actually a compound feature composed of three discrete, essentially linear segments of differing structural orientations and probable sea-floor spreading origins: (1) The northern segment (4°20'-6°20'S) trends northeast (~030°) and apparently represents a fracture zone

or transform-fault trend related to sea-floor spreading in the Mascarene Basin during the Late Cretaceous. (2) The central segment (6°20'-8°40'S) trends north-northwest (~350°) and appears to represent a fracture-zone lineament that is parallel to fracture zones and lineaments created by the opening of the Somali Basin during the Late Jurassic and Early Cretaceous. However, Somali Basin crust apparently does not extend eastward as far as this portion of the trench, so the origin of this segment remains uncertain. (3) The southern segment (8°40'-10°S) trends northwesterly (~310°) and may represent a tensional rift related to sea-floor spreading within the Mascarene Basin during the early Tertiary. Further, our data show no convincing evidence that any portion of this feature was a subduction zone at any time during its development. The data also essentially rule out an extraterrestrial impact origin for this region at the end of the Cretaceous.

Published in: *Marine and Petroleum Geology*, 6, 232-242, 1989.

Supported by: NSF Grant OCE87-15956.

WHOI Contribution No. 7079.

KAIKO PROJECT, A PRELIMINARY RESULT (ON PARTICLE SEDIMENTATION STUDY IN JAPAN TRENCH AT 8,798 M)

Susumu Honjo

A long mooring array with two time-series sediment traps were deployed at 9,100 m deep in the Japan Trench from August 30, 1986 to November 1, 1988. The deep trap was set at 8,798 m and the shallow one was at 4,260 m along a tautline. Each sediment trap was opened for 15 days for 12 times. There were two deployment recoveries in a year. Thus, there were 24 consecutive samples per year. The samples from the 4,260 m trap showed a normal pelagic sequence with a clear biogenic sedimentation in late May and early June. The deep trap samples were quite different from the shallow ones, showing a strong peak in lithogenic particles in November to January.

Published in: *Journal of Marine Science*, 21, 181-186, 1989.

Supported by: NSF Grant OCE84-17106.

WHOI Contribution No. 7012.

DISCHARGE OF FLUVIAL SEDIMENT TO THE OCEANS: GLOBAL, TEMPORAL AND ANTHROPOGENIC IMPLICATIONS

John D. Milliman

Rivers presently discharge about 15×10^9 tons of sediment and 33×10^3 km³ of water to the world oceans annually. About 70 percent of the sediment comes from southern Asia and Oceania, while northeastern south America (mostly the Amazon River), southern Asia and Oceania contribute about 65 percent of the water. Because the discharge values change dramatically with changes in climate and human land-use, these data are not applicable for forecasting nor can they be used for hindcasting. Since sea level reached its present position, about 5000 ka, most fluvial sediment has remained trapped in coastal environments and the inner shelf; large-scale escape of river-borne sediment to the deep sea seems to occur primarily during lower stands of sea level.

In Press: *Geological Fluxes to the Sea* National Academy of Sciences and National Research Council publication.

Supported by: NSF Grant OCE88-17626.

WHOI Contribution No. 7236.

INCREASED PARTICLE FLUX TO THE DEEP OCEAN RELATED TO MONSOONS

R. R. Nair, V. Ittekkot, S. J. Manganini, V. Ramaswamy, B. Haake, E. T. Degens, B. N. Desai and S. Honjo

Monsoons cause seasonal reversals in the surface circulation of the northern Indian Ocean. In the Arabian Sea this results in the upwelling of nutrient-rich water along the coasts, making it one of the highly productive regions of the world's oceans. In order to assess the impact of monsoon-driven processes on the downward particle flux variations to the deep Arabian Sea, 3 moored arrays consisting of 6 time-series sediment traps were continuously deployed at selected locations in the western (16°15' N, 60°28' E), central (14°29' N, 64°46' E), and eastern (15°28' N, 68°45' E) parts of the northern Arabian Sea. Strong seasonality was recorded in particle flux at all three sites with peaks during the SW and NE monsoons. High primary productivity during the monsoons resulting from wind induced mixed layer deepening and the associated nutrient injection to the euphotic zone appears to be the prime factor controlling the observed particle flux pattern.

Three mooring systems, each consisting of two time-series sediment traps - one 1000 m below the sea surface and the other 1000 m above the sea bottom - were deployed at three sites in the western, central and eastern Arabian Sea (Fig. 1). Prior to deployment the collecting cups were poisoned with mercuric chloride. The sediment traps were programmed to measure the flux of sinking particles at intervals of 12 to 13 days each over a duration of six months per deployment. They have been recovered and redeployed thrice since May 1986 using the research vessels R/V SONNE and the ORV SAGAR KANYA. Here we report the results obtained during the first year of deployment.

Published in: *Nature*, 338, 749-751, 1989.

Supported by: NSF Grant OCE89-14228.

WHOI Contribution No. 7080.

GRAVELS IN THE ATLANTIS II FRACTURE ZONE

Stephen A. Swift

The sedimentology of gravel intervals was studied in cores recovered at Ocean Drilling Program (ODP) Site 734 at ~3700m water depth on the eastern wall of Atlantis II Fracture Zone. At two holes, coring recovered single beds <1m long grading upwards from moderately well-sorted igneous gravel to foraminiferal ooze. The origin of the stratigraphy in the cores is problematic, but sedimentological arguments are used to infer that the recovered core is intact. The sediments are tentatively interpreted to be turbidity current deposits originating from a nearby cliff face. Lithology, particle size, and particle shape suggest that mass wasting of the cliff face was influenced as much by hydrothermal alteration and brecciation at depth as jointing and fracturing of the cliff face due to stress release.

In Press: *Proc. ODP, Scientific Results, Leg 118.*

Supported by: Ocean Drilling Program, Texas A&M.

WHOI Contribution No. 7247.

CARBONATE PLATFORMS IN SPACE AND TIME IN THE ATLANTIC

Elazar Uchupi

Carbonate deposition in the Atlantic Ocean was quite extensive during the past. In Late Jurassic, for example, carbonate platforms rimmed much of the Atlantic, and calcareous sediments blanketed the northwest European epicontinental

seas. As the continents migrated northward away from sites conducive to carbonate deposition and the input of terrigenous sediments increased, the extent of carbonate sediments slowly diminished. Today carbonate deposition in the Atlantic is found only in the Bahamas and the southern edge of the Florida platform.

Published in: *1989 Symposia of the XII Congreso Espanol de Sedimentologia*, 85-95.

WHOI Contribution No. 7077.

TECHNICAL REPORTS

A SEARCH FOR LAYERING IN THE OCEAN CRUST

John A. Collins

In Chapter 1, the geological structures that generate Moho reflections are investigated by calculating synthetic reflection profiles for laterally-varying velocity models appropriate to the fossil crust/mantle boundary exposed in the Bay of Islands Ophiolite. The similarities between the synthetic and observed data suggest that the complicated geological structures that comprise the fossil crust/mantle transition in ophiolites might also be characteristic of the oceanic crust. Analyses of the velocity and reflectivity structure at DSDP Site 504B are presented in Chapters 2 and 3. In contrast to standard oceanic models, a velocity-depth profile that better explains the observed data is characterized by high velocity gradients in the middle crust, a 1.8 km thick low-velocity zone immediately above Moho, and a total crustal thickness of only 5 km. The MCS data show no conclusive evidence for laterally coherent reflection events generated within the upper 1-2 km of the crust. This surprising observation is understandable on inspection of synthetic reflection seismograms calculated for velocity-depth profiles constructed from the logged downhole variations in physical properties. Low-amplitude reflections from the extrusives/sheeted-dike transition are obscured by sediment-column multiples and by source reverberation.

Supported by: NSF Grants OCE81-17210, EAR80-26445, EAR83-9535, OCE80-25206, OCE84-10658, and OCE87-00806.

WHOI Technical Report 89-4.

**CRUISE REPORT: GOFS LEG 1
INTERNATIONAL STUDY OF THE
NORTH ATLANTIC BLOOM,
MARCH-APRIL 1989**

*Susumu Honjo, Steven J. Manganini and
Richard Krishfield*

With the support of the National Science Foundation, we have completed the first cruise devoted to the GOFS and JGOFS program for the North Atlantic Bloom studies between March 28 and April 6 on board R/V ATLANTIS II. The major task of this cruise, to deploy bottom-tethered mooring arrays with time-series sediment traps along with current meters at two critical stations, 34°N and 47°N along 20°W, was accomplished. All 6 sediment traps, 3 on each array, were set at 14-day intervals for 13 periods from April 3 to September 26, 1989. Their opening and closing times were synchronized throughout the period of deployment. The arrays and instruments will be recovered and redeployed in September/October, 1989. Ancillary water column data, such as CTD, fluorometry, pigments, and major nutrient distribution, were also successfully completed (except for transmissometry profiling at the 47°N station) in order to understand the pre-bloom setting at JGOFS 34°N, 47°N, and 60°N stations. At the 47°N station on April 2, the mixed layer depth was 248 m.

Supported by: NSF Grant OCE88-14228.

WHOI Technical Report 89-22.

GG-20

DEPARTMENT OF APPLIED OCEAN PHYSICS & ENGINEERING

Albert J. Williams III, Chairman

MEASUREMENTS OF TIDAL FLOW AROUND A HEADLAND WITH A SHIPBOARD ACOUSTIC DOPPLER CURRENT PROFILER

W. Rockwell Geyer and Richard Signell

A shipboard acoustic current profiler (ADCP) and moored current meters were used to obtain detailed measurements of the spatial structure of the tidal flow around a headland in Vineyard Sound, Massachusetts, where tidal currents typically range from 50-70 cm s⁻¹. Eight shipboard surveys were conducted, each of which followed one of five trapezoidal tracks in the vicinity of the headland, completing 11-12 circuits in the course of the tidal cycle (12.4 hours). The measurements from the ADCP compare favorably with moored velocity measurements at two locations (rms deviations of ±3 cm s⁻¹), but the comparison showed more scatter at two other sites (rms deviations of ±7 cm s⁻¹). The ADCP measurements from separate cruises were merged to form a composite spatial representation of the tidal and residual currents, providing resolution of the spatial structure of the flow around the headland at scales from several hundred meters to 10 km. The semidiurnal tidal flow is relatively uniform in space, roughly following the bathymetry around the headland, while a residual current field consists of counter-rotating eddies on either side of the headland, with spatial scales of 5-8 km and velocities as high as 25 cm s⁻¹. The instantaneous current field indicates the formation of transient eddies on the downstream side of the headland during flood and ebb, with clear evidence of flow separation near the tip of the headland.

Supported by: NSF Grant No. OCE-8711031.

WHOI Contribution No. 7003.

MULTISENSOR MODELING OF UNDERSEA TERRAIN

W. Kenneth Stewart

This paper describes a method of constructing multidimensional models of the undersea environment with real-time multisensor data. The basis of this approach is to form a model as a three-dimensional spatial decomposition of cubical volume elements, or voxels. Associated with each voxel is a stochastic, multisensor feature vector that represents the properties within the small region. The model is an intermediate, numerical description that decouples low-level, high-bandwidth sensing from the higher-level, more asynchronous processes that extract deterministic information for operator displays,

obstacle avoidance, or path planning. As new sensor information is acquired, it is merged using a technique called *stochastic backprojection*; this is derived from an incremental adaptation of the summation method for image reconstruction. Error and ambiguity are accounted for by blurring a spatial projection of remote-sensor data before combining it stochastically with the model.

Published in: *Intervention '89 Conference and Exposition. Marine Technology Society*, pp. 160-169, 1989.

Supported by: Sea Grant Contract No. NA86AA-D-FG089.

WHOI Contribution No. 7004.

SECOND-ORDER TURBULENCE MODEL OF A COUETTE FLOW

Catherine Villaret

Reynolds stress equations are modeled as a function of a turbulent velocity ($q^2 = \overline{u'^2}$) and turbulence length scale Λ in a second-order turbulence model developed originally by Donaldson (1973). A dynamic equation for Λ introduces a set of empirical coefficients. We present a new method for determining some of these coefficients.

In the case of a one-dimensional Couette flow, we show that, in order for the length scale equation to admit a parabolic solution, two relations must be satisfied between its coefficients. Model equations can then be integrated, and the analytical solution compares well with Reichardt's (1959) experimental data.

The mean flow equation and the above length scale equation are solved for a one dimensional flow by using an implicit finite difference scheme. Simulations of Reichardt's Couette flow experiments show that a proposed new set of coefficients for the length scale equation significantly improves the numerical solutions.

Supported by: Ifremer Contract No. 852434000 DERO/EL.

WHOI Contribution No. 7011.

ENERGY DISSIPATION JUST BENEATH THE AIR WATER INTERFACE AND CONSEQUENCES FOR GAS TRANSFER

*Nuri Merzi, Eugene A. Terray and
Mark A. Donelan*

The effect of the breaking of short gravity and capillary waves on the sub-interfacial energy dissipation was explored in a wind-water tunnel.

The dissipation rate was estimated via the local instantaneous derivative of the streamwise velocity. Experiments with tap water resulted in a considerably higher dissipation rate compared with experiments using surfactant (which suppressed wave formation) and the energy flux to the water was much greater in the former case. The consequences of these results in interfacial gas transfer and oceanic forcing are explored.

Supported by: ONR Contract No. N00014-87-K-007
and NSF Grant No. OCE-8418711.

WHOI Contribution No. 7037.

DETERMINATION OF COMPRESSIONAL WAVE SPEED PROFILES USING MODAL INVERSE TECHNIQUES IN A RANGE-DEPENDENT ENVIRONMENT IN NANTUCKET SOUND

*George V. Frisk, James F. Lynch and
Subramaniam D. Rajan*

An inverse method for determining geoacoustic properties in a horizontally stratified, shallow water waveguide is extended to the case of a weakly range-dependent environment. The technique consists of estimating the local modal eigenvalues from the beamformed output of a horizontal array and using these data as input to modal inverse methods for obtaining the local bottom parameters. Specifically, the approach is applied to data at 140 Hz and 220 Hz obtained in a shallow water environment with a known abrupt change in bathymetry. First, a range-independent medium is assumed, and both iteration of forward models and perturbative inversion methods are applied to the modal data to obtain estimates of the bottom sound velocity profile. Although the perturbative inversion results are clearly superior, neither approach reproduces the full dependence with range of the observed pressure fields or the complete modal peak structure. In particular, the data exhibit an apparent splitting of the modal peaks which is interpreted, within the context of adiabatic mode theory, as the superposition of the modal contributions from the two segments of the waveguide with differing depths. When the assumption of the range-independent medium is relaxed, and the perturbative inverse technique is applied to the eigenvalue data from each portion of the waveguide, distinctly different bottom profiles are obtained for each part. These result in significantly improved agreement between theory and experiment, thereby demonstrating the effectiveness of the range-dependent inversion procedure.

Published in: *Journal of the Acoustical Society of America*, 86, 5, 1928-1939, 1989.

Supported by: ONR Contract No.
N00014-82-C-0152.

WHOI Contribution No. 7051.

IMPROVEMENTS IN THREE-DIMENSIONAL RAYTRACING CODES FOR UNDERWATER ACOUSTICS

*A.E. Newhall, J.F. Lynch, C.S. Chiu and
J.R. Daugherty*

Raytracing is a well established and insightful way of describing the propagation of energy through a medium, and has been very useful in its application to underwater acoustic propagation, which is our interest here. Until recent years only two-dimensional raytracing codes, which assume that the refraction and scattering of sound out of plane by ocean features are negligibly small, existed for ocean acoustic applications. With the development of the three dimensional Hamiltonian raytracing code HARPO^[1] by the Wave Propagation Laboratory group at NOAA, Colorado, researchers were able to explore out of plane ray refraction and scattering for nontrivial cases. It was found that, while three-dimensional effects were in general small, they were not insignificant and could have interesting consequences for acoustic tomography and source localization techniques.

The original HARPO routine could only handle canonical (analytic) ocean features and boundaries. This limitation was due to the fact that the integrator for the raypath equations requires a continuous first derivative of the soundspeed for the ocean and a continuous second derivative for the boundaries, and these can be obtained quickly if the derivatives are analytical expressions. But the forced assumption of straight line fronts, gaussian eddies, etc., is physically unsatisfying except for simple studies. To incorporate realistic oceanography such as the Gulf Stream and its meanders, one needs a more general framework.

Supplementary routines have been written recently to generalize HARPO to efficiently find eigenrays and include more realistic oceanography and boundary interactions. These routines include: 1) a multi-range eigenray routine, 2) a "generalized oceanographic data" input routine based on either empirical orthogonal functions or ocean quasigeostrophic modes (as one desires), 3) a Gauss-Markov interpolator for irregularly gridded ocean data, and 4) an inverse distance, nearest neighbors interpolator for bathymetry. These are the first routines in a package being developed for general ocean acoustics community use. In this paper, we discuss the physical, mathematical, and

computational bases of these routines, and give examples of their use in typical ocean applications.

In Press: *Computational Acoustics*.

Supported by: ONR Contract No.
N00014-88-K-0363.

WHOI Contribution No. 7065.

NUMERICAL SIMULATIONS OF SURFACE WAVE REFRACTION IN THE NORTH SEA PART 1: KINEMATICS

*Hans C. Graber, Michael W. Byman and
Wolfgang Rosenthal*

Numerical simulations of water wave refraction in the North Sea are used to determine the expected errors in travel time, angular deflection and lateral displacement of ray paths when (1) accounting for shoaling but neglecting refraction effects in deep water ray characteristics and (2) perturbing the initial swell frequency and direction of incidence.

The results show that depth refraction of swell waves is important and should properly be accounted for in numerical wave prediction models. It is shown that for the cases considered here, differences in travel time, angular deflection and lateral displacement exceed typical values for time step, grid spacing and directional resolution used in shallow water wave prediction models.

In Press: *Deutsche Hydrographische Zeitschrift*.

Supported by: ONR Contract No.
N00014-86-K-0751.

WHOI Contribution No. 7085.

NUMERICAL SIMULATIONS OF SURFACE WAVE REFRACTION IN THE NORTH SEA PART 2: DYNAMICS

*Hans C. Graber, Michael W. Byman and
Heinz Günther*

Numerical simulations of wave transformation due to shoaling and reflection are used to examine the distribution of wave energy, mean frequency and direction along the coastline. The variability in the directional distribution of typical swell events are calculated from reverse ray projections.

The results show that the German Bight divides the coastal wave climate and the directional characteristics of swell into a northern and southern domain and provides shelter to the Elbe and Weser estuaries from high sea states associated with swell when generation from local winds is negligible. This approach provides a more realistic description of the coastal wave climate

than has been possible with conventional techniques. Furthermore, it was found that the spatial variability in mean spectral parameters is considerable and depends on both near and far zone topographic features.

In Press: *Deutsche Hydrographische Zeitschrift*.

Supported by: ONR Contract No.
N00014-86-K-0751.

WHOI Contribution No. 7086.

AN ACOUSTIC TELEMETRY SYSTEM FOR DEEP OCEAN MOORING DATA ACQUISITION AND CONTROL

*Josko Catipovic, Max Deffenbaugh, Lee Freitag and
Dan Frye*

An acoustic telemetry system is being developed which will allow two-way communication between subsurface instruments and a near-surface receiver. A high-speed link allows data to be sent from instruments to the surface in real-time, and a slower down-link is available to send commands to the remote units. The objective is to develop a cost-efficient, reliable link which will allow real-time data from anywhere in the water column to be transmitted to the surface and then forwarded via satellite link to a user anywhere on the globe.

The system operates at 15-20 Khz and uses multiple frequency-shift keying (MFSK) modulation. Bit rates are adjustable, but 1200 bits per second has been selected for this application. The tones which make up the MFSK signal are decoded at the receiver with a Fourier transform implemented on a sophisticated signal processor. The processor can also be programmed to include an error-correction decoder, adaptive equalizer and data packet synchronizer. A simple, low baud rate, command link enables the use of an Automatic Repeat Request (ARQ) strategy which further increases the reliability of the link-up.

A prototype system has been successfully tested at 1200 bits per second over a 3000 meter vertical path. Additional development work on the receiver, command link, and the transmitter is ongoing.

Supported by: ONR Contract No. N00014-86-K-0751
and NSF Contract No. OCE-8612101.

WHOI Contribution No. 7090.

OBSERVATION OF SHEAR-FREE TURBULENCE BENEATH WHITECAPS IN THE MARINE SURFACE LAYER

E.A. Terray, A.J. Williams III and B.H. Brumley

We report new field observations of the

vertical distribution of mean shear, stress and turbulence intensity in the surface layer of a large lake under strong wind-forcing. Close to the surface, our data show a substantial departure from the wall-layer form, and indicate that the boundary layer has a two-part structure consisting of an energetic, intermittently forced layer characterized by negligible shear and high turbulence intensity overlying a region in which shear production dominates. The latter region has characteristics similar to a shear flow over a rigid boundary. We suggest that these features are a consequence of wave breaking.

Supported by: NSF Grant No. OCE-8418711 and
ONR Contract No. N00014-87-K-007.

WHOI Contribution No. 7094.

IMPLEMENTATION OF A THIRD-GENERATION OCEAN WAVE MODEL ON UNIX-BASED WORKSTATIONS

Hans C. Graber and Michael Caruso

The implementation of a third-generation ocean wave prediction model on a UNIX-based SUN microsystem workstation is described. The SUN modified wave model is validated with two test cases and compared with output of the same simulations on a CRAY-XMP computer. The results show that there is no degradation in accuracy of the model predictions when running on a 32-bit workstation. Timing benchmarks for different microcomputers are intercompared for the two test cases. Presently computation times are about 300 times slower than on a CRAY-XMP, but with additional changes in the code, run times can be considerably improved. Enhanced graphical capabilities of the SUN workstations are utilized in conjunction with an advanced data display and processing system SDPS to provide high-resolution color output and animated sequences of output fields. This feature renders the model as a powerful analysis tool for testing model source term physics.

Supported by: ONR Grant No. N00014-87-K-0007.

WHOI Contribution No. 7100.

A 200 KHZ DEEP SEA INTERFEROMETRIC SIDE SCAN SONAR SYSTEM

Christopher von All

A joint development effort was undertaken between the Deep Submergence Laboratory (DSL) of the Woods Hole Oceanographic Institution's Department of Ocean Engineering and the Applied

Physics Laboratory of the University of Washington. The program focussed on the development of a high resolution sonar system which would compliment and enhance the capabilities of towed, near bottom, visual imaging systems. The goal was to broaden the swath formed by visual imaging systems with a perspective view of the surrounding terrain. The merging of these visual and sonar swaths would permit an observer to look down and see the details directly beneath him, as well as to look to the sides and see the surrounding topography and objects in it. This paper describes a 200 KHz interferometric (split beam) sonar system which is rated to operate at full ocean depths. The system was taken to sea and successfully transmitted approximately 1.5 mega-bits per second of sonar data over a single mode optical link. Sonar images were viewed on a conventional paper graphic display and simultaneously recorded on half inch video tape.

Lower frequency phase comparison sonar systems have shown that data from an interferometric acoustic array may be used to compute the contours of the seafloor relative to the array. To compute the actual bathymetry of the seafloor, however, the location, velocity, attitude, and depth of the sonar platform must be known. Closed-loop computer control of the sonar platform in a precision acoustic navigation field, with a proper set of on-board sensors, will permit accurate repeatable bathymetric surveys to be performed in the deep ocean. The main obstacle preventing the development of deep ocean high frequency phase comparison systems of this nature has been the lack of available bandwidth on the standard oceanographic coaxial cable.

The broad band-width available on the single mode optical fibers on the new, deep ocean, electro-optic cable under development at DSL was used to simplify the sonar's subsea electronics in the following ways:

- (1) It permitted the acoustical wave-forms, received at the four subsea arrays, to be quadrature sampled at 16 bits, providing a potential of up to 96 dB of dynamic range and 10 KHz of bandwidth on all four channels;
- (2) The potential of 96 dB of dynamic range, coupled with three fixed levels of subsea gain, eliminates the need for subsea time varying gains and/or logarithmic signal compression techniques in medium swath width applications.

The quadrature sampling method permits the complete reconstruction of all acoustic wave-forms on the surface at data rates less than those demanded by conventional Nyquist sampling schemes. These reduced data rates permit the

sonar signals to be processed on the surface with conventional, off-the shelf equipment.

It is shown that a sonar system design which exploits the bandwidth available on an optical fiber will reduce the overall complexity of the system and thereby increase its reliability.

Published in: *Oceans '89*, pp. 1136-1141, 1989.

Supported by: ONR Contract No. N00014-86-C-0038
and NSF Contract No. OCE-8702836.

WHOI Contribution No. 7103.

SEVERE ENVIRONMENT SURFACE MOORING (SESMOOR)

Sean M. Kery

A Severe Environment Surface Mooring (SESMOOR) program has been initiated and pursued by the Woods Hole Oceanographic Institution to develop and demonstrate the capability to make long term meteorological and near surface oceanographic measurements in higher latitudes and areas where harsh environmental conditions prevail.

A SESMOOR prototype mooring was deployed from the R/V OCEANUS on Oct. 17, 1988 at 42° 33.17'N and 61° 14.00'W in 2984 m of water. The mooring was recovered with the help of the R/V ENDEAVOR on March 7, 1989. Valuable telemetered meteorological data were transmitted throughout the winter months, in support of the scientific ERICA program.

This paper describes the deviation from standard mooring design made both to the surface buoy and to the anchoring line, to ensure the survivability of the mooring and its instrumentation when deployed in extreme water conditions. A review is then made of the mooring performance while on station, and of the condition of the components after recovery. Recommendations for the design of similar moorings conclude the paper.

Published in: *Oceans '89*, pp. 1398-1405, 1989.

Supported by: ONR Contract No.
N00014-84-C-0134.

WHOI Contribution No. 7104.

CROSS SECTIONS AND MODULATION TRANSFER FUNCTIONS AT L- AND KU-BANDS MEASURED DURING THE TOWARD EXPERIMENT

William C. Keller and William J. Plant

Normalized radar cross sections and modulation transfer functions (MTFs) for

microwave backscattering from the sea surface have been measured at both L- and Ku-Bands during the TOWARD experiment. Long waves during the experiment were usually not generated by the local wind so a unique opportunity was afforded to investigate the effects of arbitrary wind, wave, and antenna angles on the backscatter. Data were collected using horizontal polarization at L-Band and vertical polarization at Ku-Band. Cross sections at L-Band are shown to be isotropic with respect to wind/antenna angle and nearly independent of wind speed except at the lowest wind speeds. Ku-Band cross sections, on the other hand, show the expected wind/antenna angle anisotropy and wind speed dependence. The Ku-Band cross sections agree well in magnitude with previous wavetank and satellite measurements casting doubt on the dependence of cross section on antenna height which has been suggested in the literature. At both frequencies the data suggest that cross sections may be lowered slightly when long waves propagate at large angles to the wind. Consistent with the cross section results, MTFs at L-Band are shown to depend little on wind speed while those at Ku-Band decrease with wind speed. These results agree with previous studies. At both frequencies, MTFs depend little on wind/antenna angle for a constant wave/antenna angle. On the other hand, for a constant wind/antenna angle, MTFs decrease with increasing wave/antenna angle. Implications of these results for radar imagery of the sea surface and for the theoretical interpretation of the origin of MTFs are discussed.

Supported by: NRL Project No. 83-1314-88.

WHOI Contribution No. 7106.

ENGINEERING SURFACE OCEANOGRAPHIC MOORING (ESOM)

Alessandro Bocconcelli

An Engineering Surface Oceanographic Mooring (ESOM) Program has been initiated and pursued by the Woods Hole Oceanographic Institution to permit the long term, on-site evaluation of prototype mooring components such as steel and Kevlar armored electro-mechanical cables, fairings, fishbite armor jackets and new surface buoys.

The first deep sea experimental mooring was deployed in March 1989, offshore Bermuda in 3000 meters of water depth. This mooring will remain on station at least two years. At the halfway mark of its deployment, it will be recovered and reset to evaluate components performance after a year and insert new samples as required.

This paper first describes the surface buoy, a novel, hemispherical, tuned buoy which uses

marine aluminum for its structure and SURLYN foam for its flotation. The buoy design stems from a semi-empirical study of hull motion conducted with the help of scale models in the Oregon State University wave tank (Ref. 1). Two main requirements are satisfied by this prototype: 1) increased mooring and payload capacity, 2) reduced dynamic response to wave motion.

The mooring design and components are next presented, with a detailed description of the candidate materials, the rationale for their selection, and the test method and instrumentation used for assessing and controlling their performance at sea.

The paper concludes with a description of the technique used for mooring deployment and servicing, and a review of the results so far obtained. Mention is also made of the buoy dynamics measurement program, which will take place in 1990.

Published in: *Oceans '89*, pp. 1381-1385, 1989.

Supported by: ONR Contract No.
N00014-84-C-0134.

WHOI Contribution No. 7107.

A SIGNAL PROCESSING SYSTEM FOR UNDERWATER ACOUSTIC ROV COMMUNICATION

Lee E. Freitag and Josko A. Catipovic

A new system for communication with untethered underwater vehicles is presented. The system is centered around sophisticated processing units which perform a variety of signal processing tasks. The processors are combined into an array using a flexible architecture designed for communication processing.

To combat the deleterious effects of the fluctuating ocean channel, a series of algorithms designed to produce low error rate communication is implemented on the array. The processing elements are INMOS T800 transputers and the number of transputers may be selected at deployment time to meet the requirements of a particular task. The result is a powerful and flexible architecture for underwater acoustic communication.

Using a multiprocessor system requires examination of interconnection methods and load allocation or sharing. Coarse grained multiprocessing for signal processing is discussed, then a specific incoherent modulation method for underwater acoustic communication is presented. The phenomena which affect the communication channel and algorithms to increase the reliability of the communication link are detailed together.

Supported by: ONR N00014-86-K-0751 and The Charles Stark Draper Lab.

WHOI Contribution No. 7116.

THREE-DIMENSIONAL MODELING OF SEAFLOOR BACKSCATTER FROM SIDESCAN SONAR FOR AUTONOMOUS CLASSIFICATION AND NAVIGATION

W. Kenneth Stewart

Sonars will continue to play an important role in world-modeling for autonomous underwater systems because of the greater range available to acoustic sensors compared with other sensing modalities. However, attempts to automate the interpretation of sidelook sonar data are typically based on two-dimensional image-processing and pattern-analysis techniques. Such sidelook "images" provide only indirect, qualitative, and view-dependent information, since the intensity of the returned signal is a function of both seafloor shape and scattering properties of the bottom materials.

This overview of work in progress at the Deep Submergence Laboratory describes several techniques for three-dimensional sonar processing in which seafloor shape information is used to reduce geometric and radiometric dependencies in the intensity signal. The approach is developed using Sea Beam bathymetry and Sea MARC I sidelook data. Preliminary results are also described for new splitbeam sidelook sonars designed for high-resolution seafloor characterization. Complex-domain processing of the quadrature-sampled signal gives amplitude and phase for three-dimensional modeling, and offers a measure of signal coherence and modeling certainty. The processed output is a quantitative model of three-dimensional shape and backscatter characteristics that will be applied to feature classification and terrain-relative navigation for intelligent underwater vehicles.

Published in: *Proceedings, Symposium on Unmanned Untethered Submersible Technology*, 21 pp., 1989.

Supported by: ONR Contract Nos. N00014-86-C-003 and N00014-87-J-1111.

WHOI Contribution No. 7120.

NUMERICAL SIMULATION OF TIDAL DISPERSION AROUND A COASTAL HEADLAND

Richard P. Signell and W. Rockwell Geyer

Tidal flows around headlands can exhibit strong spatial gradients in the Eulerian currents,

resulting in complex Lagrangian trajectories and effective dispersion of the vertically integrated flow. This typically occurs when the horizontal length scale of the headland is comparable to or smaller than the tidal excursion. The effects of these headlands on dispersion are investigated using a depth-averaged hydrodynamic model combined with a particle tracking model. The dispersion of patches of fluid is found to vary by more than an order of magnitude, depending both on position and tidal phase at the time release. This is due to the infrequent interaction of material with the strongly sheared flow at the tip of the headland, where flow separation occurs during times of maximum tidal flow. Spreading of these patches over many tidal cycles is not Gaussian, but rather shows a patchy, streaky structure.

Supported by: NSF Grant No. OCE87-11031 and the National Center for Atmospheric Research.

WHOI Contribution No. 7164.

DIVING IN SUPPORT OF BUOY ENGINEERING: THE REAM PROJECT

Sean M. Kery

Diving has been used as a valuable tool in the development of several key buoy systems. One application where diving was utilized is described in detail.

A Real Time Environmental Arctic Monitoring (REAM) system has been developed by the Woods Hole Oceanographic Institution. This mooring uses a variable buoyancy ascent module, connected to an instrumented cable to transmit data to a satellite. The module fills an internal ballast tank and rises to the surface once a day, transmits, and then vents the ballast tank and descends to a rest position.

Diving was used in the development phase to assess and fine tune the sea-keeping, ballasting and valve timing of the ascent module. The buoyancy and hydrodynamics of the module change continuously during the ascent and descent. Diving and underwater photography were used to identify and correct problems that developed during sea trials.

Published in: *Diving for Science ... 1989. Proceedings of the American Academy of Underwater Sciences Ninth Annual Scientific Diving Symposium.* Michael A. Lang and Walter C. Jaap eds., pp. 191-197, 1989.

Supported by: ONR Contract No. N00014-86-C-0135.

WHOI Contribution No. 7169.

PERFORMANCE LIMITATIONS IN UNDERWATER ACOUSTIC TELEMETRY

Josko A. Catipovic

This work addresses the current performance limitations in digital underwater acoustic telemetry. Recent increases in computational capabilities have led to a number of complex but practical solutions aimed at increasing the reliability of acoustic data links. These solutions span the problem from the ocean-basin scale data telemetry to video image transmission at a few hundred yards range. A common fact is the opportunity to implement highly complex tasks in real time on modest hardware. The data rates range from 1 kbit/sec to 100 kbits/sec and are much slower than, say, satellite channels, while acceptable system complexity is higher than virtually any other channel with comparable data throughput.

The basic performance bounds are currently the channel phase stability, available bandwidth, and the channel impulse response fluctuation rate. Phase stability, is of particular concern for long range telemetry, channel fluctuation characteristics drive equalizer/synchronizer design, and the bandwidth limitation is a direct constraint on data rate for a given signalling method.

Supported by: ONR U.R.I.P. Contract No. N00014-86-K-075 and Charles Stark Draper Lab.

WHOI Contribution No. 7224.

SURFACE WAVE, INTERNAL WAVE, AND MOVING SOURCE EFFECTS ON MATCHED FIELD PROCESSING SOURCE LOCATION SCHEMES

John R. Daugherty and James F. Lynch

Given well known environmental conditions, matched field processing has been shown to be a promising signal processing technique for the localization of acoustic sources. However, when environmental data are incomplete or inaccurate, a 'mismatch' occurs between the measured field and model field which can lead to a severe degradation of the localization estimator. We investigate the possible mismatch effects of surface and internal waves on matched field processing in a shallow water waveguides. We utilize a modified ray theory, based on the work of Tindle, to calculate the acoustic pressure field. This allows us to simply incorporate range dependent environmental conditions as well as to generalize our work to deeper waveguides. In general, the conventional (Bartlett) matched field beamformer does not

provide sufficient resolution to unambiguously locate a source, even in a perfectly matched environment. The maximum likelihood method (MLM) matched field beamformer has much better resolution but is extremely susceptible to mismatch. The mismatch due to surface roughness can result in a large reduction of the estimator peak. Part, but not all, of the peak can be regained by 1) using a model which induces incomplete reflection at the surface based on actual sea surface statistics and 2) short time averaging of the measured signal, with times on the order of the period of the surface waves. Mismatch due to internal waves can also result in a large degradation of the estimator. Averaging over the same time period as surface waves provides little improvement and leads one to surmise that internal waves may be a limiting constraint on matched field processing. Finally, we combine the surface and internal wave fields with a slowly moving source. This example highlights the necessity for the development of a beamformer which has a broader mainlobe while maintaining adequate sidelobe suppression, and we address this issue by looking at two such beamformers.

In Press: *Journal of the Acoustical Society of America*.

Supported by: ONR Contract No. N00014-87-K-0017.

WHOI Contribution No. 7225.

INFLUENCE OF ENVIRONMENTAL CONDITIONS ON ACOUSTICAL PROPERTIES OF SEA ICE

K.C. Jezek, T.K. Stanton, A.J. Gow and M.A. Lange

Sonar echo amplitude data have been collected at carrier frequencies of 188 and 120 kHz from the underside of different sea ice types. Histograms of normal incidence echo amplitudes were formed from over 90 samples of each ice type. Experiments were conducted on saline ice grown in an outdoor pond under relatively controlled conditions at CRREL and on the sea ice cover in the Fram Starit. Analysis shows marked variations (about a factor of 5) in the magnitude of the coherent reflection coefficients as congelation ice at the bottom of an ice sheet evolves from a growing dendritic interface to an ablating, thermally altered interface. Larger differences (about a factor of 10) are observed between growing congelation ice and slush ice, used to simulate frazil. These results indicate that important variations in acoustic regime exist in areas where different ice types are intermingled.

Supported by: ONR Contract No. N00014-89-J-1457.

WHOI Contribution No. 7226.

APPLICATION OF TWERSKY'S BOSS SCATTERING THEORY TO LABORATORY MEASUREMENTS OF SOUND SCATTERED BY A ROUGH SURFACE

D. Chu and T.K. Stanton

One of the many challenges in describing the scattering of sound by rough surfaces is to address the fact that most surfaces are three dimensional. Furthermore, only their statistical properties may be known. Twersky's model [V. Twersky, J. Acoust. Soc. Am. 29, 209-225 (1957)], by using a method of images and taking multiple scattering into account, established a general solution involving distributions of three dimensional "bosses" (protuberances) on a base plane. A prominent advantage of the theory over others is that it can describe bosses of arbitrary orientation. The purpose of the present article is to compare the theory with laboratory measurements of sound scattered by a continuously rough pressure-release surface. In the model, we use prolate hemi-spheroidal bosses oriented in a randomized range of directions and randomly packed to approximate the rough surface. The data were taken from Horton *et al.* [C.W. Horton, S.K. Mitchell and G.R. Barnard, J. Acoust. Soc. Am. 41, 635-643 (1967)] and Welton [P.J. Welton, report ARL-TR-75-30, University of Texas at Austin (1975)] and involve backscattered sound versus grazing angle for several frequencies. The comparisons of the numerical computations with Welton's data show a reasonable agreement with respect to not only the boss orientation parameters but also the surface statistical parameters (*rms* roughness and correlation length). An interesting phenomenon is that the number of spheroidal modes required to fit the data increases as the frequency of the incident plane wave increases.

In Press: *Journal of the Acoustical Society of America*.

Supported by: ONR Contract No. N00014-89-K-0044.

WHOI Contribution No. 7227.

SOUND SCATTERING BY SPHERICAL AND ELONGATED SHELLED BODIES

Timothy K. Stanton

Describing the scattering of sound by elongated objects with high aspect ratios (ratio of length to diameter) usually involves great

numerical difficulties. The recently developed deformed cylinder solution was shown to be increasingly accurate in the limit of very high aspect ratios ($\approx 5:1$) while requiring relatively low computation times and was applied to objects of constant composition [T.K. Stanton, "Sound scattering by cylinders of finite length. III. Deformed cylinders," *J. Acoust. Soc. Am.* 86, 691-705 (1989)]. In this article, the approximate formulation is used to describe scattering by prolate spheroids, straight finite cylinders, and uniformly bent cylinders where the objects are composed of an elastic shell surrounded by fluid and filled with either a fluid or gas. The calculations are compared with those involving spherical shells based on the formulations derived in R.R. Goodman and R. Stren, *J. Acoust. Soc. Am.* 34, 338-344 (1962). The calculations are made over a wide range of frequencies and shell thicknesses (ranging from solid elastic objects to thin-shelled objects). Since the deformed cylinder formulation is most accurate for angles of incidence normal or near-normal to the lengthwise axis, the calculations are limited to broadside incidence. The simulations show significant variations in the modal interference structure as the shell thickness and shape are varied. Comparisons are also made between predictions and laboratory data involving straight and bent finite-length cylindrical shells (stainless steel) with 3:1 aspect ratios and 52% shell thicknesses. The study not only shows reasonable agreement between the predictions and data, but also illustrates the dramatic change in scattering cross section due to the bend of the object (12 dB in this case).

Supported by: ONR Grant No. N00014-89-J-1729.

WHOI Contribution No. 7228.

PLANE WAVE REFLECTION FROM A RANDOM FLUID HALF-SPACE

Dajun Tang and George V. Frisk

The reflection of a monochromatic plane wave impinging from a homogeneous fluid half-space onto a random fluid half-space is studied using an integro-differential equation method. The coherent reflection coefficient is presented as a function of frequency and statistical parameters characterizing the random medium.

Supported by: ONR Contract No.
N00014-86-C-0338.

WHOI Contribution No. 7251.

A TECHNIQUE FOR MAKING UNBIASED ESTIMATES OF CURRENT FROM A WAVE-FOLLOWER

Markku J. Santala and Eugene A. Terray

Estimates of currents from velocity records measured in a surface-following reference frame are biased due to a correlation between the sensor motion and the orbital wave velocities. We demonstrate a technique that reduces this bias by an order of magnitude in cases where the motion of the current-meter is also known. The theory is verified both by numerical simulation and by application to data obtained from a fixed tower using a miniature acoustic current meter attached to a wave-follower.

Supported by: NSF OCE-87-16937, NSF
OCE-84-18711 and ONR N00014-85-C-0001.

WHOI Contribution No. 7256.

MANAGING COMPUTING RESOURCES

Robert C. Groman

This paper presents several issues in managing computing resources: distributed computing, the fast pace of technology, local and wide area networks and cost recovery. These issues impact all levels of an organization. For example, the computing "end user" must select his or her computing environment (PC, workstation, and/or central site) and deal with network accessibility. System managers must consider rapidly outdated hardware, support for multiple operating systems and the impact of new software such as X windows. Computer center and network managers must cope with the realities of distributed computing and the need to provide secure local and wide area network access. High level administrators/vice presidents look at training and software costs, hardware obsolescence and security issues.

Supported by: Funded by the Institution.

WHOI Contribution No. 7270.

MEASUREMENTS AND MODELING OF THE SPATIAL STRUCTURE OF NONLINEAR TIDAL FLOW AROUND A HEADLAND

W. Rockwell Geyer and Richard Signell

A shipboard acoustic current profiler (ADCP) was used to obtain detailed measurements of the horizontal structure of the tidal flow around a headland in Vineyard Sound, Massachusetts, where

the nonlinear generation of residual currents and overtides is pronounced. Repeated ship tracks extending through a tidal cycle provide information about the structure of the semidiurnal tide, the principal overtides (M4 and M6) and the residual circulation. The semidiurnal tidal flow was found to be relatively uniform in space, roughly following the bathymetry around the headland, while the overtides and residual flow showed considerable spatial structure, indicative of local nonlinear transfer of energy from the tidal flow. The vertical, relative vorticity was found to vary considerably during the tidal cycle from zero to several times the planetary vorticity.

A high-resolution, vertically integrated numerical model was used to simulate the tidal flow around a headland, to provide a comparison with the observations and to explore the sensitivity of the flow to variations in bottom friction, bathymetry and tidal velocity. The numerical results are consistent with the observations, showing similar tidal characteristics and vorticity variations. The numerical simulations indicate a pronounced flow separation and formation of a transient eddy at the tip of the headland, with a strong shear zone extending from the shore to the center of the eddy.

Supported by: NSF Grant OCE-8711031.

WHOI Contribution No. 7279.

AN EXPERIMENTAL INVESTIGATION OF THE QUASI-STATICS AND DYNAMICS OF A LONG VERTICAL TOW CABLE

*Dana R. Yoerger, Mark A. Grosenbaugh,
Michael S. Triantafyllou, Knut Engebretsen and
James Burgess*

This report presents preliminary results of a unique experiment examining the static and dynamic characteristics of long vertical tow cables. The experiment was conducted at the U.S. Navy's Atlantic Undersea Test and Evaluation Center (AUTECE) and combined acoustic tracking of cable position with simultaneous measurements of cable acceleration. The cable used was the 1.73 centimeter diameter steel-armored coaxial cable that has emerged as a standard in the oceanographic community. Cable lengths between 800 m and 1200 m at tow speeds up to 1 m/s were studied. Quasi-static configurations were measured by monitoring the position of acoustic pingers attached to the cable. A drag coefficient was estimated by comparing the measured cable shape to computed shapes. A value of 1.6 gives the best fit to the experimental data. Five self-recording instrument packages were attached to the cable to

observe high frequency cable motion. Spectral analysis shows large amounts of energy near the Strouhal frequency and its higher harmonics.

Published in: *ASME Proceedings of Offshore
Mechanics and Arctic Engineering*, 7 pp., 1988.

Supported by: ONR Grant N00014-87-G-0111 and
NSF OCE-8511431.

WHOI Contribution No. 7304.

A FULL-SCALE EXPERIMENTAL STUDY OF THE EFFECT OF SHEAR CURRENT ON THE VORTEX-INDUCED VIBRATION AND QUASI-STATIC CONFIGURATION OF A LONG TOW CABLE

*M.A. Grosenbaugh, D.R. Yoerger and
M.S. Triantafyllou*

The analysis of data of a unique experiment on the quasi-statics and vortex-induced dynamics of a long vertical tow cable is presented. The experiment consisted of measuring simultaneously the vortex-induced motions and the steady-state configuration of a long tow cable. The measured steady-state configuration of the cable was used to calculate the cable's average drag coefficient which was 2.2 ± 0.24 . It was observed during the sea trials that the vortex-induced motion of the cable was modulated by a beat due to the presence of a shear current. This is confirmed here by spectral and time domain analysis of the acceleration records. The modulated amplitude causes the RMS motion of the cable to be lower than that in a uniform flow. The modulation phenomenon that is caused by the presence of a shear current thus accounts for the lower drag amplification that is observed here and has been reported elsewhere by others. The RMS motion of the cable decreases with depth which indicates that the drag coefficient of the cable also decreases with depth.

Published in: *ASME Proceeding of Offshore
Mechanics and Arctic Engineering*, 8 pp., 1989.

Supported by: ONR Grant N00014-87-J-0111 and
NSF Grant OCE-8511431.

WHOI Contribution No. 7305.

DEPARTMENT OF PHYSICAL OCEANOGRAPHY

Robert C. Beardsley, Chairman

OCEAN CIRCULATION & LOW FREQUENCY VARIABILITY

OBSERVATIONS OF OFFSHORE SHELF WATER TRANSPORT INDUCED BY A WARM-CORE RING

*Terrence M. Joyce, James K. B. Bishop and Otis
B. Brown*

Gulf Stream warm-core rings often are observed to entrain water from the continental shelf and transport filaments of shelf water out over the continental slope. In June 1982 the R/V ENDEAVOR made a transect through one such shelf water "streamer" that was seen from satellite thermal imagery to the east of warm-core ring 82B. Acoustic Doppler current profiles together with repeated CTD stations were made through the streamer. The CTD system was also equipped with a dissolved oxygen sensor and transmissometer. We were able to make an unprecedented section of velocity and water mass structure of the shelf water filament. The offshore velocity structure was complicated with velocities ranging from 10-50 cm/s, temperatures, in a sub-surface temperature minimum, of less than 8°C, surface salinities less than 33‰, with high levels of suspended particulate matter and manganese, and with shelf water properties as deep as 100 m in the center of the streamer. Transports calculated in different temperatures and salinity classes showed a total volume transport of waters in the filament of $0.8-0.9 \times 10^6 \text{ m}^3$ for water with a salinity $< 35\text{‰}$. Thermal imagery showed that the streamer was not "wrapped around" the ring but was advected by the ring and deposited at the inshore edge of the Gulf Stream. Using adjacent stations not in the streamer, but in the Slope Water, as a reference for water that presumably replaced the above amount of shelf water, estimates have been made of the net exchange of heat, salt particulates, dissolved oxygen and Mn due to the offshore transport of shelf water by 82B. These estimates indicate that warm-core rings are capable of inducing significant exchange across the Shelf/Slope Water front off the Northeast coast of the U.S.

In Press: Deep-Sea Research.

Supported by: NSF Grants OCE85-01170,
OCE85-02126, OCE85-13420 and 8802773.

WHOI Contribution No. 7097.

PHYSICAL STRUCTURE AND TEMPORAL EVOLUTION OF GULF STREAM WARM-CORE RING 82B

Terrence M. Joyce and Trevor J. McDougall

The hydrographic properties of Warm-Core Ring 82B are shown from three cruises; April, June, and August 1982. The three-dimensional velocity field for each cruise is formed from the gradient-current relationship, the observed hydrography, and the near surface flow as measured by a ship-mounted Acoustic Doppler Current Profiler. The data for each cruise were sorted into radial bins 15 km apart, and into vertical bins based on potential density. The changes in salinity on isopycnals from April to June 1982 were modelled as being due to radial advection, and both diapycnal and isopycnal mixing processes. The diffusivities in the pycnocline were found from a least-squares fit to the data. Most of the observed changes in salinity were explained with a constant vertical diffusivity ($0.53 \times 10^{-4} \text{ m}^2 \text{ s}^{-1}$), while the required lateral diffusivity was only $26.5 \text{ m}^2 \text{ s}^{-1}$ at ring center, decaying to zero at a radius of 40 km.

In Press: Deep-Sea Research.

Supported by: NSF Grant OCE85-01176.

WHOI Contribution No. 7084.

COMPARISON OF M_2 TIDAL CURRENTS OBSERVED BY SOME DEEP MOORED CURRENT METERS WITH THOSE OF THE SCHWIDERSKI AND LAPLACE MODELS

James R. Luyten and Henry M. Stommel

M_2 tidal currents observed at 315 deep-sea locations (mostly in the northern hemisphere) confirm those computed by the numerical model of Schwiderski (1979). Together, they reveal large scale geographical coherences similar in form to those of the tide-generating potential and to those of the analytical Laplace model for tides on a globe completely covered with water of uniform depth.

By fitting the Laplace tidal ellipses to the array of current meters and to the velocities from Schwiderski's numerical model, we show that much of the M_2 tide is explicable in terms of Laplace's simple model-with friction.

Supported by: NSF Grants OCE87-15735,
OCE86-13810 and ONR Contracts
N00014-84-C-0134 and NR083-400.

WHOI Contribution No. 7067.

A DEEP REACHING ANTICYCLONIC EDDY IN THE SUBTROPICAL GYRE OF THE EASTERN SOUTH ATLANTIC

M. S. McCartney and M. E. Woodgate-Jones

A CTD transect of the South Atlantic at a nominal latitude of 23°S was made in early 1983. About two-thirds of the way from the Brazil Current in the west to the Benguela Current in the east, we encountered a large-diameter eddy (300-400 km). Its dynamic signature (bowl-shaped isopycnals) penetrated to over 4000 m, with the eddy anticyclonic transport relative to 4000 db over $30 \times 10^6 m^3 sec^{-1}$. Various origins for this eddy are conceivable. We feel that the most likely one is the Agulhas Retroflexion region: that the eddy was formed by a pinching off of this current elbow, and a subsequent northwest movement of more than 2500 km over a period spanning two winters. There was a superposed double thermostat in the core of the eddy interpreted to be the product to two successive winters' convective overturning. Main thermocline waters from the Agulhas Current, recognizable by the distribution of oxygen, were trapped in the eddy core and carried with it. This trapping could extend as deep as the Antarctic Intermediate Water (AAIW). The propagating eddy distorted the local property distributions. A ring of low-oxygen water from lower latitudes surrounded the core of the eddy at the thermocline levels. AAIW of the higher salinity and lower oxygen, and Deep Water of higher salinity and lower nutrients were observed at the eddy stations. These characteristics are also found to the North of the eddy. The kinematics of a drifting anticyclonic eddy provide a framework for understanding the trapping, the low-oxygen ring, and the pulling beneath the eddy of the AAIW and Deep Water.

In Press: *Joe Reid Volume, Deep-Sea Research.*

Supported by: NSF Grants OCE78-22223,
OCE86-14486 and ONR Contracts
N00014-82-C-0019 and NR 083-004.

WHOI Contribution No. 7182.

EQUATORIAL DEEP JETS IN THE ATLANTIC OCEAN

Rui M. Ponte, James Luyten and Philip L. Richardson

We report here a vertical profile of velocity measured in the equatorial Atlantic ($0^{\circ}00'N, 30^{\circ}22'W$) which reveals short vertical scale zonal jets with amplitudes of 10-20 cm/s over the upper 2500 m, alternating in the east-west direction with depth. Particularly prominent was

an eastward jet centered at a depth of 1000 m with an amplitude of 28 cm/s.

In Press: *Deep-Sea Research.*

Supported by: NSF Grants OCE87-21082 and
OCE85-00052.

WHOI Contribution No. 7117.

EVIDENCE FOR WIND-DRIVEN CURRENT FLUCTUATIONS IN THE EASTERN NORTH ATLANTIC

R. M. Samelson

Evidence is presented for local and remote wind-forcing of deep ocean currents in three frequency bands (corresponding to 3.7-8 day, 8-22 day, and 23-82 day periods) at a two-year mooring in the eastern North Atlantic. Coherence between current meter velocities and estimated wind stress curl is largest for the deepest instrument (3000 m) and decreases toward the surface. The strongest evidence is found at 3000 m depth in the high frequency (3.7-8 day) band, where both components of velocity are significantly coherent with wind stress curl. Meridional velocity at 3000 m is also significantly coherent with wind stress curl in the low frequency (23-82 day) band, while zonal velocity in the low frequency band and both velocity components in the intermediate frequency (8-22 day) band are only marginally coherent. The results are compared with a stochastically-forced linear quasi-geostrophic model that includes a simple representation of the mid-Atlantic Ridge. Good agreement between theory and observation is found for the 3000 m currents in the high frequency band. At lower frequencies, 3000 m energy levels are well predicted, but only partial agreement is found between predicted and observed coherence. For the shallower instruments (1100 m and 500 m), observed coherences are at most marginally significant and energy levels are considerably higher than the theory predicts. Including an upper-layer mean flow in the model improves the prediction of energy levels at the shallower instruments.

Supported by: ONR Contracts N00014-84-C-0134
and NR083-400.

WHOI Contribution No. 7262.

ON THE SOURCES OF THE FLORIDA CURRENT

William J. Schmitz, Jr. and Philip L. Richardson

In our opinion roughly 45% of the transport of the Florida Current is of South Atlantic origin, as

compensation for the cross-equatorial flow of North Atlantic Deep Water. 7.1 out of the 8.9 Sv. moving through the Straits of Florida with temperatures above 24°C in the upper 100 m of the water column is composed of comparatively fresh water coming through the southern Caribbean passages from the tropical South Atlantic. 1.8 Sv. of somewhat saltier surface water enters from the North Atlantic through Windward Passage as does much of the 18-degree Water in the Florida Current. A South Atlantic origin for the contribution from the uppermost layer is clear-cut because the surface water in the open Atlantic north of the Caribbean is comparatively cold and salty and intrudes south as Subtropical Underwater or Salinity-Maximum Water below a comparatively warm and fresh layer 50-100 m thick, which could hardly be transported from the North Atlantic. 13.0 out of 13.8 Sv. transported through the Caribbean in the 12-24°C temperature range is of North Atlantic origin, with about 0.8 Sv. of comparatively fresh South Atlantic water flowing on the western side of the Florida Straits, having entered the Caribbean on the southern side of St. Vincent and St. Lucia Passages. 5 out of 6 Sv. transported by the Florida Current in the 7-12°C temperature range appears to originate in the South Atlantic. Our estimate of 13 Sv. of South Atlantic and 16 Sv. of North Atlantic origin for the total transport of 29 Sv. for the Florida Current, along with partitioning in the aforementioned temperature ranges, is approximately consistent with open ocean sections along 24°N and with several previous investigations.

We have recomputed the transport into five key Caribbean passages to be 28.8 Sv. for the temperature range appropriate to the Straits of Florida off Miami, in close agreement with independent transport measurements for the Florida Current. These five passages and their contributions are: Grenada (7.7 Sv.), St. Vincent (7.9 Sv.), St. Lucia (3.8 Sv.), Dominica (2.6 Sv.), and Windward (6.8 Sv.). Breakdowns of these passage transport estimates into broad classes by temperature range agree to within about 2 Sv. in comparison with similar quantities for the Florida Current. Anegada Passage may transport 0.5 Sv. of water that exists through the upper 200 m or so of the Florida Current, and the mid-depth (5-12°C) flow in this passage, and in the general vicinity of the Caribbean, deserves further examination.

In Press: *Deep-Sea Research*.

Supported by: NSF Grants OCE81-09145, OCE86-00055 and ONR Contracts N00014-84-C-0134 and NR083-400.

WHOI Contribution No. 7020.

COUPLED SEA ICE - MIXED LAYER SIMULATIONS FOR THE SOUTHERN OCEAN

Achim Stössel, Peter Lemke and W. Brechner Owens

A coupled sea ice-mixed layer-pycnocline model for the Weddell Sea (Lemke et al., 1989; Owens & Lemke, 1989) is extended to the entire sea ice area around the Antarctic continent. The monthly atmospheric forcing and the annual oceanic forcing are specified from climatology. Sensitivity runs were performed with a fixed mixed layer, without snow cover, with different ice strength constants (P^*) and varying e-folding constants for the closing of leads (h_0), without dynamics, and without ocean currents. Since the atmospheric forcing fields, although derived from large, historical data sets, differ considerably depending on the analysis technique, alternative wind, temperature and precipitation forcing has been applied. Finally, the model has been forced with mean monthly winds supplemented by stochastic variations representing short term variability. The model results are compared with analyses of satellite data as well as with single measurements, and with simulation results from earlier models.

In Press: *Journal of Geophysical Research*.

Supported by: ONR Contract N00014-86-K-0751, and NSF Grant DPP85-18747.

WHOI Contribution No. 7220.

OBSERVATIONS OF THE PACIFIC NORTH EQUATORIAL CURRENT BIFURCATION AT THE PHILIPPINE COAST

J. M. Toole, R. C. Millard, Z. Wang and S. Pu

Hydrographic surveys were conducted off the Philippine coast in September 1987 and April 1988 as part of the United States/People's Republic of China cooperative research program. These cruises sampled the western Pacific Ocean where the North Equatorial Current (NEC) meets the western boundary and divides into the Kuroshio and Mindanao Currents. The requirement for mass conservation within a region enclosed by stations is utilized here to obtain absolute circulation fields for the two surveys. In both realizations, the surface flow of the NEC was observed to bifurcate near latitude 13°N; NEC flow poleward of this latitude turned north as the Kuroshio while flow to the south fed the Mindanao Current. Most striking was a twofold increase in the strength of the current system in spring 1988 as compared with

fall 1987. We note that the observations in fall 1987 were obtained during the height of the 1986/87 EL Niño, while those in spring 1988 were during a cold phase of the El Niño/Southern Oscillation. It is not clear how the observed current changes relate to the evolution of this event. The potential vorticity (Q) distributions of the surface waters were examined to explore the dynamics of the bifurcation. Within the NEC, Q was nearly constant (layer thickness change balanced meridional planetary vorticity variation). Within the Kuroshio and Mindanao currents, near constant Q (with magnitude comparable to that in the NEC) was also found with a balance between relative vorticity variation and layer depth change as would be expected for inertial boundary currents.

In Press: *Journal of Physical Oceanography*.

Supported by: NOAA NA85AA-D-AC117.

WHOI Contribution No. 7114.

DEEP CIRCULATION IN THE EASTERN SOUTH ATLANTIC

Bruce A. Warren and Kevin S. Speer

Tracer properties on sections of closely spaced hydrographic stations across the Angola Basin of the South Atlantic Ocean along Lats. 11°S and 24°S suggest a three-layer description of the deep circulation there. Below 4 km the basin is closed off in the south, so water enters only from the north; the interior flow is southward, and the western-boundary current (above the eastern flank of the Mid-Atlantic Ridge) is southward at 11°S but northward at 24°S, as required by the Stommel-Arons dynamics. At depths roughly between 2400 m and 4000 m the basin seems to be supplied only from the south, the western-boundary current is everywhere northward, and the interior flow is southward. Near the 2-km level the Mid-Atlantic Ridge is too deep to be an effective western boundary; the flow seems to be broadly southeastward across the full basin at 11°S, but at 24°S a topographically guided current flows northward above the ridge to supply southward interior flow. A hydrographic section along the Greenwich meridian illustrates an eastward jet at depths between 1300 m and 3200 m that extends near Lat. 22°S from the western-boundary current to a gap in the Walvis Ridge, through which the jet introduces water to the Cape Basin. Geostrophic estimates of the volume transports of these circulation elements, calculated with reference to zero-velocity surfaces construed from the tracer fields, are consistent in direction with the inferred flow patterns, but the

values may be somewhat erroneously high, as they imply dubiously large upward velocities.

A tongue of oxygen-poor, nutrient-rich water is found at depths between 3000 m and 4500 m at 11°S but not at 24°S. It is strongest at the African continental rise, and extends some 1000 km westward. Its origin is attributed to decay within the sediment of detritus originating mainly from the Congo River plume, and its form to the deep horizontal flow field.

In Press: *Deep-Sea Research*.

Supported by: NSF Grants OCE82-13967 and OCE78-22223.

WHOI Contribution No. 6984.

SURGES OF ANTARCTIC BOTTOM WATER INTO THE NORTH ATLANTIC

John A. Whitehead

Current meter records show that Antarctic Bottom Water surges into the western North Atlantic with roughly a sixty-day period. A time-dependent mass budget which incorporates estimated volume fluxes from geostrophic calculations, surges with a sixty-day period, a known time-average volume of the very coldest water in the North Atlantic, and a constant mixing coefficient predicts vertical excursions of 160-230 meters for the 1.1° isotherm and 45-60 meters for the 1.2° isotherm. Available data do not reveal such an excursion. The reason for the lack of the excursions, is that earlier estimates of volume of the very coldest water were too small. Corrected tables are presented. The disagreement between the current meter results and the geostrophic calculations remains.

Published in: *Journal of Physical Oceanography*, 19, (6), pp. 854-861, June, 1989.

Supported by: ONR Contracts N00014-87-K-0007 and NR 083-004.

WHOI Contribution No. 7036.

THEORETICAL & LABORATORY MODELS

A SIMPLE KINEMATIC MECHANISM FOR MIXING FLUID PARCELS ACROSS A MEANDERING JET

Amy S. Bower

Recent observations of fluid parcel pathways in the Gulf Stream using isopycnal RAFOS floats revealed a striking pattern of cross-stream and

vertical motion associated with meanders (Bower and Rossby, 1989). In an attempt to explain the observed pattern, a two-dimensional kinematic model of a meandering jet has been developed which enables us to examine the relationship between streamfunction patterns and fluid parcel trajectories. The streamfunction fields are displayed in a reference frame moving with the wave pattern so motions of fluid parcels *relative* to the jet can be seen more easily.

The results suggest that the observed pattern of cross-stream motion can be understood simply in terms of the downstream phase propagation of meanders. The model successfully reproduces several of the most distinctive features of the float observations: 1) entrainment of fluid into the Gulf Stream occurs at the leading edges of meander extrema while detrainment takes place at the trailing edges; 2) exchange between the Gulf Stream and its surroundings increases with a) increasing depth, b) increasing meander amplitude, and c) increasing wave phase speed.

Transport calculations from the model streamfunction fields indicate that for typical phase speeds and amplitudes, roughly 90% of the fluid in the surface layers of the Gulf Stream flows downstream in the jet while 10% continuously recirculates into the surroundings. In the deep main thermocline, where downstream speeds are less, only about 40% of the fluid is retained in the jet and 60% is trapped in the recirculating cells. It is concluded that this simple kinematic mechanism could be responsible for the homogenization of fluid in the deeper layers of the Gulf Stream.

Supported by: Postdoctoral Fellowship.

WHOI Contribution No. 7245.

SOLITARY WAVES ON CONDUITS OF BUOYANT FLUID IN A MORE VISCOUS FLUID

Karl R. Helfrich and John A. Whitehead

Fluid of a lower density and viscosity can buoyantly rise through a viscous fluid through conduits that support simple pipe flows. The conduits also support solitary waves which exhibit near soliton behavior. Laboratory experiments on the characteristics of the solitary waves and their interactions have been conducted and compared with theory. The observations of shape and phase speed of individual waves show good agreement with the theoretical predictions. Large amplitude waves traveled slightly faster than the theoretical predictions. The discrepancy is probably due to higher order effects associated with wave slope not accounted for in the theory. Individual wave characteristics (shape, amplitude and speed) were

very nearly preserved after collision with another wave. A phase jump of each wave was the main consequence of an interaction. The larger (faster) waves increased in amplitude by an average of 5 percent after collision and their phase speeds decreased by an average of 4 percent. The small wave was unchanged. Numerical solutions overpredicted the magnitude of the observed phase jumps by about 40 percent when compared to the experiments.

It is also shown theoretically and confirmed experimentally that the solitary waves have closed streamlines in a frame moving with the wave. Thus, transport of isolated packets of fluid over large distances will occur. Wave interactions result in the transfer of trapped fluid between the interacting waves.

In Press: *Geophysical and Astrophysical Fluid Dynamics*.

Supported by: NSF Grant EAR87-08033.

WHOI Contribution No. 6848.

MAXIMIZING BUOYANCY FLUX ACROSS LAYERED GEOSTROPHIC SECTIONS

Nelson G. Hogg and Henry M. Stommel

For layered analogues of the ocean stratification, the problem of maximizing heat flux across a section with zero mass flux is considered. The two layer situation on an f -plane is particularly simple and it is shown that the heat flux is related to a particular area integral on the h - D plane, h , and D being the depths of the upper and lower interfaces, respectively. The maximum heat flux maximizes this area while constraining the layers to have non-negative thickness. Extensions to a β -plane, meridional section, to three moving layers and to a moving bottom layer with a topography are discussed.

In Press: *Journal of Physical Oceanography*.

Supported by: ONR Contracts N00014-85-C-0001, NR 083-004 and NSF Grants OCE86-08258 and OCE87-15735.

WHOI Contribution No. 7083.

HOW CURRENTS IN THE UPPER THERMOCLINE COULD ADVECT MEDDIES DEEPER DOWN

Nelson G. Hogg and Henry M. Stommel

The high salinity anomalies that mark eddies (Meddies) of Mediterranean outflow origin lie well below the permanent currents in the upper

thermocline. Nevertheless they seem (Richardson et al., 1989; Rossby, 1988) to be advected by the currents. The nature of this coupling is modeled with a three-layer ocean in which the two upper layers each contain a baroclinic anticyclonic point vortex, and the top layer also has a steady current. The top vortex tends to move with the current, but also interacts with the lower vortex. Steady and oscillatory regimes exist in which the vortex pair remains coupled and advects with a fraction of the surface velocity. There is another regime in which the pair separate, the upper vortex drifts away, and the lower vortex (Meddy) is left behind.

In Press: *Journal of Physical Oceanography*.

Supported by: NSF Grants OCE86-08258,
OCE86-13810 and ONR Contracts
N00014-85-C-0001 and NR 83-004.

WHOI Contribution No. 6998.

PERFORMANCE OF A PRIMITIVE-EQUATION NUMERICAL OCEAN CIRCULATION MODEL ON LOOSELY-COUPLED MULTIPROCESSOR SYSTEMS

*Hsiao-ming Hsu, Jih-Kwon Peir and Dale B.
Haidvogel*

In the past decade, a large number of multiprocessor systems have been proposed to support parallel numeric computations. These systems seek to achieve efficiency with a significant speedup over uniprocessor machines. Amdahl's Law estimates the performance upper bound of a program running on multiprocessors in terms of the proportion of sequential and parallel parts of the program. However, an essential factor, the overhead associated with parallel computation; is often overlooked.

In this paper, we report performance measurements of an ocean circulation model on a loosely-coupled Array of Processors (ℓ CAP). Particular emphasis has been placed on quantifying the overheads for parallel computing on such a system. These overheads come primarily from data communication (sharing data), synchronization, and load balancing among processors. By carefully reducing these overheads, we are able to achieve a speedup of 6.9 on a 10-processor system, close to Amdahl's theoretical limit of 7.7.

In Press: *Parallel Computing*.

Supported by: ONR Contract N00014-86-K-0751.

WHOI Contribution No. 7001.

ON THE STRUCTURE OF INERTIAL WESTERN BOUNDARY CURRENTS WITH TWO MOVING LAYERS

Rui Xin Huang

The structure of inertial western boundary currents with two moving layers is studied using a streamfunction coordinate transformation. This transformation converts the equation system, a stiff system over a semi-infinite domain in physical coordinate, into a non-stiff system over a finite domain in streamfunction coordinate. For simplicity, the interfacial slopes of the interior solution are assumed constant. The structure of the solutions can be classified into three categories in a phase plane which consists of two regions joining along a critical line. Within each region solutions of the system appear in the form of two unconnected branches. As parameters approach values corresponding to those at the critical line, the two branches of the solutions join at a movable critical point to form a continuous solution. Although changes in the vorticity profile of the incoming flow or other parameters can alter the position and shape of the critical line, the general features of the system remain unchanged. Thus, requiring continuity of an inertial western boundary current through a critical point implies certain constraints on the structure of the mid-ocean thermocline.

In Press: *Tellus*.

Supported by: NSF Grant OCE88-08076.

WHOI Contribution No. 6999.

SENSITIVITY OF A MULTI-LAYERED OCEANIC GENERAL CIRCULATION MODEL TO THE SEA SURFACE THERMAL BOUNDARY CONDITION

Rui Xin Huang

Experiments with a low resolution, multi-layered model of the oceanic general circulation with wind and thermal forcing were carried out in order to identify processes controlling important aspects of the general circulation. Emphasis was placed on the sensitivity of the model's solution to the sea surface thermal boundary condition. For long restoring time scale, wind-driven circulation dominated the solution, resembling the circulation in the North Pacific. For short restoring time scale, strong thermohaline circulation driven by deep water formed at high latitude dominated the solution, resembling the circulation in the North Atlantic. Accordingly, other aspects of the circulation, such as the

baroclinic structure of the currents and the meridional mass flux partition, changed with the restoring time scale.

Published in: *Journal of Geophysical Research*, 94, (C12), 18011-18021, 1989.

Supported by: NSF Grant OCE86-14771.

WHOI Contribution No. 7146.

ON THE THREE-DIMENSIONAL STRUCTURE OF THE WIND-DRIVEN CIRCULATION IN THE NORTH ATLANTIC

Rui Xin Huang

The boundary value problem for the ideal-fluid thermocline equation has been revised to include a mixed layer which has a finite and horizontally varying depth and a zonal density gradient. A new eastern boundary condition applied in the model successfully overcomes the difficulties with the singularities existing in many previous models and leads to shadow zones in all ventilated isopycnal layers. The southern shoaling of the mixed layer base, the zonal density gradient in the mixed layer, and the new eastern boundary condition combine and substantially intensify the circulation in the shallow, ventilated thermocline at the expense of reducing the deep, unventilated thermocline pool.

The wind-driven circulation in the North Atlantic is calculated using realistic forcing boundary conditions taken from observations, including the background stratification, the wind-stress curl, and the annual maximum depth and surface density distribution of the mixed layer. The model's results show that the total meridional volume flux within the seasonal thermocline, the ventilated thermocline, and the unventilated thermocline is 6.5, 35.8, and 6.5 Sv respectively. The model results emphasize the dynamical importance of the coupling between the mixed layer and the interior geostrophic flow below and the fast communication between the atmosphere and the ventilated thermocline.

In Press: *Dynamics of Atmospheres and Oceans*.

Supported by: NSF Grants OCE86-14771 and OCE88-08076.

WHOI Contribution No. 6970.

DOES ATMOSPHERIC COOLING DRIVE THE GULF STREAM RECIRCULATION?

Rui Xin Huang

A two-layer model for the recirculation is studied. Initially, a narrow band of the upper layer

moves eastward with the lower layer remaining stagnant. When cold air flows over the narrow front region all moving water in the upper layer sinks to the lower layer with the momentum vertically well mixed within the lower layer. Thus, cooling creates an unbalanced velocity field in the second layer and an unbalanced pressure field at a vertical density front. After the geostrophic adjustment, a high pressure center south of the front and a low pressure center north of the front are established. These pressure centers drive a strong barotropic eastward current slightly north of the pressure center and slow westward return flow in the far field both south and north of the front. Thus, cooling over a narrow region can intensify an eastward jet and create recirculation gyres both north and south of the stream.

In Press: *Journal of Physical Oceanography*.

Supported by: NSF Grant OCE88-08076.

WHOI Contribution No. 7271.

CROSS SECTIONS OF TWO LAYER INERTIAL GULF STREAM

Rui Xin Huang and Henry Stommel

A two-moving-layer model for cross sections of the inertial flow in the Gulf Stream is studied. Potential vorticity is assumed uniform within each layer. With one or two layers outcropping, the model produces fronts associated with the outcropping isopycnals and the anticyclonic and cyclonic shear zone of the Gulf Stream. A three-moving-layer model successfully reproduced the main features of a cross section of the Gulf Stream observed at 68°W.

In Press: *Journal of Physical Oceanography*.

Supported by: NSF Grants OCE88-08076 and OCE88-16165.

WHOI Contribution No. 7185.

MATCHING A VENTILATED THERMOCLINE MODEL WITH INERTIAL WESTERN BOUNDARY CURRENTS

Rui Xin Huang

A two-layered ventilated thermocline model is matched with inertial western boundary currents in the southern part of the western boundary region. For general cases the western boundary currents break down much earlier than expected from general physical considerations. In fact, the boundary layer solutions appear in the form of two branches, i.e. the northern/southern or

upper/lower branches. However, as the parameters of the interior thermocline solution are altered, the distance between these two branches of the solution also changes. It is shown that for special values of parameters, these two branches join smoothly and form a solution extending continuously to high latitude. Thus, in terms of climatological mean circulation, the thermocline structure seems to have self-adjusted so as to avoid discontinuity in the circulation. In other words, the external parameters for wind-driven circulation of the interior ocean have to satisfy some intrinsic constraints imposed by western boundary currents.

Supported by: NSF Grant OCE88-08076.

WHOI Contribution No. 7148.

A COUPLED SEA ICE - MIXED LAYER - PYCNOCLINE MODEL FOR THE WEDDELL SEA

P. Lemke, W. B. Owens and W. D. Hibler III

A dynamic-thermodynamic sea ice model is coupled to a one-dimensional model of the oceanic mixed layer and pycnocline and is applied to the Weddell Sea. This model prognostically determines the vertical oceanic heatflux from the mixed layer dynamics in contrast to earlier sea ice modelling where the oceanic heatflux was prescribed. In addition to the standard simulation, polynya and paleoclimate experiments were performed to investigate the effects of sea ice dynamics. Furthermore, the mixed layer - pycnocline model is compared to the original Kraus-Turner approach.

In Press: *Journal of Geophysical Research.*

Supported by: ONR Contract N00014-86-K-0751.

WHOI Contribution No. 7073.

ON THE INFLUENCE OF THE CONTINENTAL SLOPE ON THE WESTERN BOUNDARY LAYER - THE ENHANCED TRANSPORT AND RECIRCULATION

Zhengyu Liu

Quasi-Geostrophic theory is used to study the effect of a continental slope on the western boundary layer. The compression of the relative vortex tubes by the slope results in a strong northward boundary current called the Continental Slope Boundary Current (hereafter CSBC). On the β -plane, for a reasonably high slope, we find a strong barotropic recirculation which enhances the total transport of the western boundary current significantly. The two layer model further shows

that the CSBC is trapped in the lower layer. In oceans with very deep lower layers, the CSBC transport increases dramatically. Consequently, even for a very weak lower layer incoming flow, we can still have a very strong barotropic CSBC transport compared to the Inertial Boundary Current. Additionally, for an ocean with a very deep lower layer, we can always have comparable total transport in both layers even when the lower layer incoming flow is very weak.

Supported by: NSF Grant ATM84-13515.

WHOI Contribution No. 7095.

SENSITIVITY STUDIES WITH A SEA ICE - MIXED LAYER - PYCNOCLINE MODEL IN THE WEDDELL SEA

W. B. Owens and P. Lemke

The sensitivity of a dynamic-thermodynamic sea ice model coupled to a one-dimensional mixed layer-pycnocline model to variations of dynamic and thermodynamic model parameters is investigated. Furthermore the modifications of the model results due to the inclusion of a prognostic snow cover and the implementation of simplified sea ice rheologies is investigated. In these comparisons special emphasis is placed upon the ice-ocean boundary conditions (buoyancy fluxes) and the mixed layer properties.

In Press: *Journal of Geophysical Research.*

Supported by: ONR Grant N00014-86-K-0751 and NSF Grant DPP-8518747.

WHOI Contribution No. 7222.

ON THE PROPAGATION OF VELOCITY DISCONTINUITIES ON POTENTIAL VORTICITY FRONTS

Joseph Pedlosky

The propagation of finite-length velocity discontinuities along a potential vorticity front is studied. The front is oriented in a fundamentally north-south direction on the β -plane. The potential vorticity on either side of the front is constant.

According to a semi-geostrophic theory, the shear disturbances propagate with a speed which depends on the *difference* of the deformation radius across the front and on the local depth, h_B , of the moving fluid layer at the front. The disturbance steepens as it propagates. Breaking is predicted by the semi-geostrophic theory at a time which depends inversely on the propagation speed and the initial steepness of the perturbation to the layer depth. Small velocity discontinuities will grow as they propagate.

In Press: *Journal of Physical Oceanography*.

Supported by: NSF Grant ATM89-03890.

WHOI Contribution No. 7196.

THE DYNAMICS OF THE OCEANIC SUBTROPICAL GYRE

Joseph Pedlosky

Recent theoretical advances in physical oceanography have produced plausible models for the structure of the circulation in the oceans' subtropical gyres. These theoretical ideas are reviewed and assessed in the light of present observational evidence. The dominant role of potential vorticity in both the theory and the observational analysis is emphasized. In particular, the complementary processes of subduction and recirculation are important determinants in the predicted and observed structures.

Supported by: NSF Grant ATM89-03890.

WHOI Contribution No. 7246.

THE NONLINEAR BEHAVIOR OF VARICOSE DISTURBANCES IN A SIMPLE MODEL OF THE GULF STREAM

L. J. Pratt, J. Earles, P. Cornillon and J.F. Cayula

The behavior of varicose (width-altering) disturbances to an equivalent barotropic, f -plane jet is examined using analytical and numerical techniques. Specifically, we show that long waves are subject to nonlinear steepening, and we follow the evolution of such disturbances past the point of wave-breaking using the model, quantified by a parameter, r , and on the amplitude of the initial wave, a variety of effects are produced including undular bores, ejected filaments, detaching eddies, and aneurisms. Most significantly, we show that r values in the range thought appropriate to the Gulf Stream produce detached eddies similar in appearance to 'warm outbreaks' (Cornillon *et al.*, 1986). Measurements of the propagation speed of Gulf Stream width values using satellite imagery support the prediction of wave steepening at long wavelengths.

In Press: *Deep-Sea Research*.

Supported by: ONR Contract N00014-87-K-0007 and NSF Grants OCE87-00601, OCE85-10828 and NASA NAGW-858.

WHOI Contribution No. 7221.

TWO-LAYER ROTATING HYDRAULICS: STRANGULATION, REMOTE AND VIRTUAL CONTROLS

Larry Pratt and Larry Armi

The hydraulics of two-layer, rotating channel flow is examined in the limit where the channel width is large compared to the internal Rossby radius of deformation, but small compared to the external deformation radius. In this limit the baroclinic flow is contained in boundary layers along each side wall, while the barotropic flow is distributed over the width of the channel. Width variations along the channel causes the strength of the barotropic flow to vary and the barotropic variations influence the baroclinic boundary layers in two independent ways. The dual nature of this forcing gives rise to a new type of critical condition which we refer to as a 'remote' control. 'Virtual' and 'true' controls also arise. Steady solutions can be obtained by solving a pair of simple quadratic equations and examples are given showing various combinations of controls.

Supported by: NSF Grant OCE87-00601 and ONR Contract N00614-98-K-1182.

WHOI Contribution No. 7252.

LOCAL BAROCLINIC INSTABILITY OF FLOW OVER VARIABLE TOPOGRAPHY

R. M. Samelson and J. Pedlosky

Local baroclinic instability is studied in a two-layer quasi-geostrophic model. Variable meridional bottom slope controls the local supercriticality of a uniform zonal flow. Solutions are found by matching pressure, velocity, and upper layer vorticity across longitudes where the bottom slope changes abruptly so as to destabilize the flow in a central interval of limited zonal extent. In contrast to previous results from heuristic models, an infinite number of modes exist for arbitrarily short intervals. For long intervals, modal growth rates and frequencies approach the numerical and WKB results for the most unstable mode. For intervals of length comparable to and smaller than the wavelengths of unstable waves in the homogeneous problem, the WKB results lose accuracy. The modes retain large growth rates (half maximum) for intervals as short as the internal deformation radius. Evidently, the deformation radius and not the homogeneous instability determines the fundamental scale for local instability. Maximum amplitudes occur near the downstream edge of the unstable interval. Lower layer amplitudes decay downstream more rapidly than upper layer amplitudes. For short

intervals, the instability couples motions with widely disparate horizontal scales in the upper and lower layers. Heat flux is more strictly confined than amplitude. Growth rates increase linearly with weak supercriticality.

Supported by: ONR Contracts N00014-84-C-0134,
NR 083-400 and NSF Grant ATM89-03890.

WHOI Contribution No. 7175.

OCEAN MIXING AND SMALL SCALE PROCESSES

ON THE DENSITY RATIO BALANCE IN THE CENTRAL WATER

Raymond W. Schmitt

An equation for the conservation of density ratio on isopycnal surfaces is derived. It is shown that a vertical shear can modify the density ratio if salinity (and temperature) gradients exist along isopycnals. The mixing processes of turbulence, salt fingering and lateral isopycnal mixing are evaluated for possible balances with the shear term in the " $R_\rho = \text{constant}$ " Central Waters. It is found that turbulence cannot provide a balance and that isopycnal mixing can balance only with a particular vertical variation in the mixing rate. Salt fingers, however, provide a simple balance between the shear term and the vertical variation of flux divergence, since heat and salt are transported at different rates. The "conservation of density ratio" should provide a useful constraint on mixing estimates from hydrographic data in both double-diffusive and non-double-diffusive regimes and could be applicable to modelling studies of the temperature-salinity relation in the thermocline.

In Press: *Journal of Physical Oceanography*.

Supported by: NSF Grant OCE88-13060.

WHOI Contribution No. 7136.

MESOSCALE EDDY DIFFUSION, PARTICLE SINKING AND THE INTERPRETATION OF SEDIMENT TRAP DATA

David A. Siegel, Timothy C. Granata, Anthony F. Michaels and Tommy D. Dickey

A Lagrangian analysis of a particle sinking through a random mesoscale eddy field is used to evaluate the effects of horizontal diffusion and particle sinking rates on particulate fluxes sampled by an idealized sediment trap. The analysis indicates that the spatial region where collected

particles are formed (L_x) is dependent upon the mean sinking rate of the collected particles and the mesoscale eddy advective field above the trap. This weighted spatial averaging creates difficulties in the interpretation of sediment trap data as fluxes of rapidly sinking particles ($> 200\text{md}^{-1}$) represent local processes ($L_x < 20\text{km}$) while fluxes of slower sinking particles ($< 10\text{md}^{-1}$) may be averaged over much larger scales ($L_x > 200\text{km}$) for a trap deployed at 1000 m. Several examples of the potential effects that this spatial averaging may have upon the ecological interpretation of the sediment trap collected particle fluxes are presented.

In Press: *Journal of Geophysical Research*.

Supported by: ONR Contract N00014-87-K-0084.

WHOI Contribution No. 7118.

MERIDIONAL VARIATIONS OF THE SPRINGTIME PHYTOPLANKTON COMMUNITY IN THE SARGASSO SEA

D. A. Siegel, R. Iturriaga, R. R. Bibigare, R. C. Smith, H. Pak, T. D. Dickey, J. Marra, and K. S. Baker

Meridional distributions of particle, pigment, optical, chemical and physical oceanographic properties and satellite sea surface temperature and color imagery are used to investigate phytoplankton community distributions and their relation to the near-surface water masses of the Sargasso Sea. Measurements were made during April of 1985 along a 1200 km meridional transect on 70°W (from 24°N to 35°N). The evolution of subtropical Mode water (18°water) is shown to be the primary factor controlling the spatial distribution and temporal evolution of the phytoplankton community in the northern Sargasso Sea (31° to 35°N). The springtime near-surface restratification of recently ventilated 18°water initiated a diatom-dominated phytoplankton bloom. As the bloom declined, the phytoplankton community evolved into a diverse assemblage. The consequences of these phytoplankton successions were observed both temporally and as distributional variations along the meridional transect. South of the region of 18°water wintertime ventilation (south of ~31°N), phytoplankton biomass concentrations were considerably less than those observed for the northern Sargasso Sea. The phytoplankton community for this region was regulated by different processes than the northern Sargasso Sea community. For the northern Sargasso Sea, the wintertime ventilation of 18°water is shown to be the primary new nutrient flux to the euphotic zone comprising nearly all of the annual new production.

Supported by: ONR Contract N00014-87-K-0084 and
Univ. of Southern California.

WHOI Contribution No. 7244.

EXPERIMENTAL OBSERVATIONS OF BAROCLINIC EDDIES ON A SLOPING BOTTOM

*John A. Whitehead, Melvin E.
Stern, Glenn R. Flierl and Barry Klinger*

Baroclinic eddies in a rotating box with a sloping bottom were produced by squirting dense salt water up the sloping bottom and along the "eastern" wall. The jet stagnated in shallow water and was ejected normal to the wall. For certain parameters (volume flux of jet, etc.), a coherent lense of dense bottom water formed and propagated west with an overlying *cyclonic* vortex. The circulation in the bottom lense, on the other hand, was relatively weak. No such eddy forms when the depth of fresh water is relatively deep, and a regime diagram is given for the formation of the coherent eddies. Thus a relatively simple structure emerges despite the complexity of the generating process. The pressure field determined from density measurements is discussed in terms of an integral theorem for coherent eddies, and the westward propagation is also related to previous theories. Several other techniques for generating such eddies are discussed.

In Press: *Journal of Geophysical Research.*

Supported by: NSF Grants OCE84-16100,
OCE87-14842 and ONR Contracts
N00014-87-K-0007 and NR 083-004.

WHOI Contribution No. 7054.

COASTAL CIRCULATION & DYNAMICS

ON THE DAMPING OF FREE COASTAL-TRAPPED WAVES

K. H. Brink

A perturbative method is presented for estimating the decay time of subinertial coastal-trapped waves under a wide range of conditions where damping is relatively weak. Bottom friction is generally much more important than "long-wave" results would suggest, even in the parameter range where the waves are approximately nondispersive. The presence of a mean flow can greatly change the effect of bottom friction. Specifically, if the mean flow over the shelf has positive (negative) relative vorticity in the

northern (southern) hemisphere, wave damping increases. This mean flow effect appears to account for the failure of coastal-trapped waves to propagate into the Agulhas between Port Elizabeth and Durban, South Africa.

Supported by: ONR Contracts N00014-C-0134 and
NR083-400.

WHOI Contribution No. 7033.

STEADY TWO-LAYER EXCHANGE THROUGH THE STRAIT OF GIBRALTAR

Harry L. Bryden and Thomas H. Kinder

Recent progress in steady hydraulic control modelling of the two-layer flow through the Strait of Gibraltar is reviewed. An application of the model is made to the specific physical configuration of the Strait using the most recent bathymetry. The maximal exchange solution resulting from the model must satisfy mass and salt conservation relations for the Mediterranean basin. Hence, it is not possible to specify arbitrarily the density difference between the inflowing and outflowing layers and the proper reservoir condition is a specification of the net evaporation over the Mediterranean basin. For a specified evaporation, both the magnitude of the maximum two-layer exchange and the density or salinity difference between the inflowing Atlantic water and outflowing Mediterranean water can be determined from the combination of the hydraulic control model and mass and salt conservation statements. For net evaporation values between 50 and 70 cm yr⁻¹, the predicted flow, outflow and salinity difference are in reasonable agreement with recent observations. In particular, for a net evaporation of 60 cm yr⁻¹, the steady hydraulic control model yields a predicted inflow of 2.0°/‰. For comparison, recent observations exhibit an inflow of $0.95 \times 10^6 \text{ m}^3 \text{ s}^{-1}$, an outflow of $0.79 \times 10^6 \text{ m}^3 \text{ s}^{-1}$ and an effective salinity difference of 2.1°/‰.

Supported by: ONR Contract N00014-87-K-0007.

WHOI Contribution No. 7194.

VELOCITY AND HYDROGRAPHIC STRUCTURE OF SUBSURFACE SHELF WATER AT THE GULF STREAM'S EDGE

*James H. Churchill, Peter Cornillon and Peter
Hamilton*

Relatively cool and fresh water, originating from the Middle Atlantic Bight continental shelf, has often been found along the northwestern

margin of the Gulf Stream. In this paper we present measurements of temperature, salinity, and velocity within subsurface filaments of entrained shelf water adjacent to the Gulf Stream. The data indicate that vertical mixing within and near these filaments is effected by double-diffusive processes and shear-induced turbulence. The measurements also reveal a complex velocity and hydrographic structure within the filaments and show that the character of individual filaments differed considerably. For example, the measured mean flow within two filaments was much slower than the current in the adjacent Gulf Stream, whereas a third filament appeared to be incorporated within the high-velocity region of the Gulf Stream. The most thoroughly sampled band of entrained shelf water exhibited temperature inversions and contained a slowly moving intrusion of warm water, presumably detached from the Gulf Stream. The estimated transport of shelf water within this band was roughly $7.2 \times 10^4 m^3 s^{-1}$, comparable with the rate at which water is transported over the southern Middle Atlantic Bight continental shelf as estimated by a previous study. However, the transport of individual entrained shelf water filaments may vary considerably because of the significant variation in their currents and hydrographic composition.

Published in: *Journal of Geophysical Research*, 94, (C8), 10,791-10,800, August 15, 1989.

Supported by: NSF Grants OCE88-12788, OCE85-10828, DoE Contract DE-AC0279EV10005 and 40-12-001-30066.

WHOI Contribution No. 6971.

GULF STREAM WATER ON THE SHELF AND UPPER SLOPE NORTH OF CAPE HATTERAS

James H. Churchill and Peter C. Cornillon

Although intrusions of water from the Gulf Stream have often been observed over the Carolina shelf, there has been no published report of Gulf Stream water near the continental margin north of Cape Hatteras. By examining sea surface temperature distributions and hydrographic data collected over an 11-year period we have found that water discharged from the Gulf Stream often appears over the shelf and upper slope north of Cape Hatteras. For example, between 36 and 39°N, roughly 80 to 400 km north of the tip of Cape Hatteras, Gulf Stream water was detected 3 to 24% of the time at hydrographic stations on the upper slope, and 3 to 8% of the time at locations on the shelf. In most instances, sea surface temperature distributions clearly reveal that the Gulf Stream water which appeared near the

continental margin was not part of the Gulf Stream's main current, but was expelled from the trailing edge of a meander. This discharged Gulf Stream water is relatively rich in nutrients which may promote biological productivity in the shelf and slope regions north of Cape Hatteras. Gulf Stream water found on the shelf had apparently given up a good deal of its kinetic and available potential energy. Its subtidal flow was largely driven by the along-shelf wind stress; and in most instances its vertical density profile nearly matched that of adjacent shelf water situated alongshore. In contrast, the discharged Gulf Stream water observed over the upper slope was significantly lighter than abutting fluid located along the slope to the northeast. The circulation associated with this density contrast often conveyed a large quantity of Middle Atlantic Bight shelf water seaward of the continental margin.

Supported by: NSF Grant OCE88-12778 and The Department of Energy DE-ACO2-79EV10005.

WHOI Contribution No. 7294.

EFFECT OF WAVE-CURRENT INTERACTION ON WIND-DRIVEN CIRCULATION IN NARROW, SHALLOW EMBAYMENTS

R. P. Signell, R. C. Beardsley, H. C. Graber and A. Capotondi

The effect of wave-current interaction on steady wind-driven circulation in a narrow, shallow bay is investigated with a simple two-dimensional (y, z) model similar to that of Hunter and Hearn (1987). A constant wind stress is applied in the along-channel x direction to a channel with a constant cross-sectional profile $h(y)$. The local eddy viscosity profile is cubic in z , with surface and bottom slopes set proportional to the surface and bottom friction velocities and the $u(y, z)$ velocity is computed through numerical integration of the x momentum equation. The along-channel pressure gradient is adjusted so that the net transport in the x direction vanishes, and the near-bottom current, bottom friction velocity, and surface wave field are consistent with the wave-current interaction model of Grant and Madsen (1979).

The wind-induced flushing of shallow bays is shown to be sensitive to both bottom topography and the effects of surface waves. The flushing increases with increasing h'/\bar{h} , where h' is the standard deviation of cross-channel depth and \bar{h} is the mean depth. This is consistent with the findings of Hearn et al. (1987). The flushing decreases, however, with the inclusion of surface wave effects which act to increase the bottom drag. Because there is a compensating effect of larger

wave influence in shallower water, the primary effect of wave-current interaction is to reduce the lateral circulation, while the set-up, bottom stress and vertical current structure remain nearly unchanged. An implication of the circulation dependence on wave-current interaction is that low-frequency oscillatory winds may drive a mean circulation when the wave field changes with wind direction.

In Press: *Journal of Geophysical Research*.

Supported by: NOAA NA86-AA-D-SG090, WHOI Sea Grant Project # R/m - 12 and NSF Grant OCE87-11031.

WHOI Contribution No. 7066.

SCATTERING OF COASTAL-TRAPPED WAVES BY IRREGULARITIES IN COASTLINE AND TOPOGRAPHY

John L. Wilkin and David C. Chapman

The scattering of freely-propagating coastal-trapped waves (CTWs) by large variations in coastline and topography is studied using a numerical model which accommodates arbitrary density stratification, bathymetry and coastline. Particular attention is paid to the role of stratification which in moderate amounts can eliminate backscattered free-waves which occur, theoretically, in a barotropic ocean.

Numerical simulations using widening and narrowing shelf topographies show that the strength of the forward-scattering into transmitted CTW modes is proportional to a topographic warp factor which estimates the severity of the topographic irregularities. The forward-scattering is further amplified by density stratification. Within the scattering region itself, the strengths of the scattered-wave-induced currents exhibit substantial variation over short spatial scales. There is generally a marked intensification of the flow within the scattering region, and rapid variations in phase. On narrowing shelves, the influence of the scattering can extend upstream into the region of uniform topography even when no freely-propagating backscattered waves exist.

A simulation is conducted of CTW scattering at a site on the East Coast of Australia where observations suggest the presence of scattered freely-propagating CTWs. The success of the model simulation in reproducing features of observations supports the notion that realistic shelf geometries can scatter significant levels of CTW energy, and that the scattered waves can have an appreciable signal in current-meter observations made on the continental shelf. This suggests that, along irregular coastlines, it is important to account for the possibility that CTW scattering

may be occurring if oceanographic observations are to be interpreted correctly.

In Press: *Journal of Physical Oceanography*.

Supported by: NSF Grant OCE85-21837.

WHOI Contribution No. 7115.

INSTRUMENTATION & EXPERIMENTAL METHODOLOGY

SHIPBOARD AND ALTIMETRIC STUDIES OF RAPID GULF STREAM VARIABILITY BETWEEN CAPE COD AND BERMUDA

Terrence M. Joyce, Kathryn A. Kelly, David M. Schubert and Michael J. Caruso

The temporal variability of the Gulf Stream between Cape Cod and Bermuda was examined using shipboard ADCP measurements satellite infrared (AVHRR) and altimeter (GEOSAT) data for a period of about 2 weeks in April 1989. Dominant changes were a southward shift and rotation of the Gulf Stream due to a meander, a westward translation of a warm-core ring and an eastward translation of a cold-core ring. Terms in the along-track (nearly cross-stream) and cross-track momentum balances from the ADCP data showed that horizontal advection of horizontal momentum was the principal ageostrophic term, exceeding both measured temporal changes and estimated vertical velocity terms by about a factor of five at a depth of 100m. Cross-track pressure gradients (not measured) needed to be about 20% higher than expected geostrophically and if not balanced by the horizontal advection terms, could force particles across and out of the Gulf Stream to the south at speeds of 0.1 m/s. Cross-track ADCP velocities agreed closely with those estimated from GEOSAT: both gave peak velocities in the Gulf Stream of about 2.0 ± 0.1 m/s. Errors were of the same order as the ageostrophic terms in the along-track momentum balance. Except near the Bermuda Rise, GEOSAT-derived absolute velocities could be quantitatively related to major oceanographic signals, such as the Gulf Stream and rings.

In Press: *Deep-Sea Research*.

Supported by: NASA NAGW-1666 and NSF Grant OCE88-17698.

WHOI Contribution No. 7231.

A MODIFIED OBJECTIVE MAPPING TECHNIQUE FOR SCATTEROMETER WIND DATA

Kathryn A. Kelly and Mike J. Caruso

An objective method to generate high resolution wind maps from the irregularly spaced scatterometer data was developed and tested on synthetic data for the Northeast Pacific Ocean. Current assimilation methods for atmospheric Global Circulation Models (GCMs) reproduce only the large-scale features ($> 600\text{km}$) of the wind field. In contrast, this method attempts to retain the high spatial resolution of the scatterometer where there are adequate measurements. To estimate the covariance function and to compute realistic error estimates for the method, a synthetic data set was constructed using wind fields from the European Center for Medium Range Weather Forecasting (ECMWF). The wavenumber spectrum of the synthetic data was based on an analysis of SEASAT scatterometer data. The patchiness of the scatterometer data caused discontinuities in the objective estimates, which would give unacceptable wind stress curl fields; thus the initial estimates were selectively smoothed using overdetermined biharmonic splines. A constraint on the horizontal divergence of the wind, applied only in regions of large estimated errors, improved the estimates. For the NASA scatterometer (NSCAT) this method would produce a wind map every 12 hours with spatial resolution that preserves the small-scale features of the original data over about half the mapped region and with somewhat decreased resolution and accuracy over the rest of the region.

In Press: *Journal of Geophysical Research.*

Supported by: Prime Contract NASA NAS7-918 and
JPL Subcontract # 957652.

WHOI Contribution No. 7102.

IODINE LOSSES DURING WINKLER TITRATIONS

*George P. Knapp, Marvel C. Stalcup and Robert J.
Stanley*

An experiment designed to measure iodine loss during the aliquot version of the Winkler titration for dissolved oxygen in sea water shows that none was lost in the method presently used. This result, contradicting an earlier report by Green and Carritt (1966), demonstrates that the whole-bottle method of oxygen titration is not to be preferred over the aliquot method.

Supported by: NSF Grant OCE87-16910.

WHOI Contribution No. 7161.

OBSERVATIONS OF OCEAN KU-BAND RADAR CROSS SECTION AT LOW WIND SPEED DURING FASINEX

F. K. Li, G. Neumann and R. A. Weller

14.6 GHz radar backscatter measurements from the ocean obtained during the Frontal Air-Sea Interaction Experiment over a wind speed range of 2 to 4 m/s are reported. Both horizontal and vertical polarization σ_0 were obtained over an incidence angle range of 20 to 30 degrees. They indicate that the change in the radar cross section in this wind speed range for horizontal polarization is substantially larger than that predicted empirical models, such as the SASS-1 model. However, the falloff in the backscatter cross section is less dramatic than those predicted by the model of Donelan and Pierson [1]. The data also indicate larger upwind-crosswind modulations for low winds than those predicted from the empirical models. We suggest that the use of radar scatterometry as a near surface wind remote sensing technique is viable with wind speed as low as 2 m/s over the incidence angles of 20 to 30 degrees.

Supported by: ONR Contracts N00014-84-C-0134
and NR083-400.

WHOI Contribution No. 7232.

ON THE CALCULATION OF THE BRUNT-VÄISÄLÄ FREQUENCY

R. Millard, W. B. Owens and N. P. Fofonoff

The three commonly used methods for estimating the Brunt-Väisälä frequency from vertical profiles of temperature and salinity are developed and results compared. These include intercomparisons for typical oceanographic values. The effects of errors in the temperature and salinity due to typical instrument errors are also considered.

In Press: *Deep-Sea Research.*

Supported by: NSF Grant OCE87-12087 and ONR
Contracts N00014-79-C-0071 and
N00014-86-K-0751.

WHOI Contribution No. 6990.

IMPROVED METEOROLOGICAL MEASUREMENTS FROM BUOYS AND SHIPS FOR THE WORLD OCEAN CIRCULATION EXPERIMENT

Robert A. Weller and David S. Hosom

The World Ocean Circulation Experiment (WOCE) is directed at understanding ocean circulation and its interrelation to climate. During WOCE, moored buoys and ships will provide attractive platforms from which to make accurate in-situ measurements of the basic observables— sea surface temperature, air temperature, wind velocity, barometric pressure, solar and longwave radiation, humidity and precipitation. From these measurements accurate estimates of the air-sea fluxes can be made. Drifting or moored air-sea interaction buoys will also be needed in WOCE for the verification of the surface data collected by remote sensing.

The overall goal of the "Improved Meteorological Measurements from Ships and Buoys" (MET) effort is to develop accurate and reliable means of making during WOCE. Work being done at the University of Southern California concentrates on improving longwave radiation sensors. The work at Woods Hole Oceanographic Institution includes development and evaluation of improved sensors, development of prototype data loggers capable of supporting intelligent data acquisition algorithms that reduce measurement error, and testing of sensors and data loggers on local moorings and on research ships.

Prototype buoy and ship data loggers are complete. Prototypes of some of the sensor modules are also complete. An optical WORM (Write Once, Read Many times) disc for storage has been working well even during rough weather testing on OCEANUS (1). Test buoy deployments began in January 1989 and test ship installations will be in operation later in 1989. Sensors for all variables are under test on land. Testing of the most promising of these will be continued on the test buoy and ship installations beginning in 1989.

Published in: *Oceans '89, Proceedings of Marine Technical Society*, pp. 1410-1415, September 18-21, 1989.

Supported by: NSF Grant OCE87-09614.

WHOI Contribution No. 7096.

MEASURING NEAR-SURFACE METEOROLOGY OVER THE OCEAN FROM AN ARRAY OF SURFACE MOORINGS IN THE SUBTROPICAL CONVERGENCE ZONE

Robert A. Weller, Daniel L. Rudnick, Richard E. Payne, Jerome P. Dean, Nancy J. Pennington and Richard P. Trask

An array of five surface moorings was set in the subtropical convergence zone southwest of Bermuda with spacings of 16 to 53 km. Meteorological instrumentation on each of the surface buoys recorded wind velocity, barometric pressure, solar radiation, air temperature, sea temperature, and relative humidity. One objective of the deployment was to look for horizontal variability in the meteorological fields on the scale of the array. In support of that objective, both a high data return from the instruments and a quantitative evaluation of the quality of the measurements were sought. To increase data return rates, two meteorological instruments were placed on each buoy. To determine the accuracy of the measurements, careful pre-deployment and post-deployment calibrations of all instruments were carried out, and, during the experiment, meteorological data were collected from ships stationed near the buoys. From the two redundant instruments it was possible to construct one complete data set for each mooring. The results of the calibrations and intercomparisons provide estimates of the errors in the measurements. Significant horizontal variability was occasionally observed in some of the surface meteorological variables and in the wind stress and air-sea heat flux fields. More often, observed spatial gradients in the meteorological fields were not significantly larger than the experimental uncertainty in those gradients. Larger than anticipated errors were encountered in measuring wind speed and barometric pressure; and the performance of anemometers, barometers, relative humidity sensors, and other sensors for use on buoys could be improved.

In Press: *Journal of Atmospheric and Oceanic Technology*.

Supported by: ONR Contracts N00014-84-C-0134 and NR 083-400.

WHOI Contribution No. 7159.

MEASURING UPPER OCEAN VARIABILITY FROM AN ARRAY OF SURFACE MOORINGS IN THE SUBTROPICAL CONVERGENCE ZONE

*R. A. Weller, D. L. Rudnick, N. J. Pennington,
R. P. Trask and J. R. Valdes*

Measurements of upper ocean variability were made in the subtropical convergence zone southwest of Bermuda from an array of five surface moorings set with spacings of 16 to 53 km. The intent was to observe oceanic fronts and to quantify the spatial gradients associated with them. Vector Measuring Current Meters (VMCMs) and Vector Averaging Current Meters (VACMs) were attached to the mooring lines beneath the surface buoys to measure velocities and temperatures. Modifications were made to the VMCMs in an attempt to improve data return. The performance and accuracy of these moored instruments are examined. Pre-deployment and post-deployment calibrations were carried out; and other sources of error, such as mooring motion, are considered. A number of oceanic fronts passed through the moored array during the experiment, and the horizontal gradients observed in the velocity and temperature fields were significantly larger than the uncertainties in measuring those gradients.

In Press: Journal of Atmospheric and Oceanic Technology.

Supported by: ONR Contracts N00014-84-C-0134, NR 083-400 and NSF Grant OCE87-09614.

WHOI Contribution No. 7002.

TECHNICAL REPORTS

SATELLITE DATA PROCESSING SYSTEM USERS MANUAL V1.0 (SDPS)

Michael Caruso, and Chris Dunn

SDPS was written to allow users to quickly and easily display image and line-based data on inexpensive Sun workstations. The primary purpose of the program is for assimilating oceanographic data that may be generated from a satellite, a ship or a buoy. This manual describes the various options available and examples of how to use them. Also discussed are several additional programs for managing data external to SDPS.

Supported by: ONR Contract N00014-86-K-0751 and NASA Contract 957652.

WHOI Technical Report 89-13.

IMPROVED METEOROLOGICAL MEASUREMENTS FROM BUOYS AND SHIPS (IMET): PRELIMINARY COMPARISON OF PRECIPITATION SENSORS

Gennaro H. Crescenti and Robert A. Weller

Rainfall data obtained from an optical rain gauge and a capacitive siphon rain gauge are analyzed and discussed. These sensors were developed for unattended use and are being considered for use at sea on ships and buoys.

Supported by: NSF Grant OCE87-09614.

WHOI Technical Report 89-44.

IMPROVED METEOROLOGICAL MEASUREMENTS FROM BUOYS AND SHIPS (IMET): PRELIMINARY ANALYSIS OF SOLAR RADIATION AND MOTION DATA FROM IMET TEST BUOY

Gennaro H. Crescenti, Robert A. Weller, David S. Hosom and Kenneth E. Prada

Data are analyzed from a test buoy equipped with a motion sensor (Hippy) and two different pyranometers in order to understand and quantify motion induced errors in meteorological data. The Hippy measures pitch, roll heave and acceleration of the buoy. Probability density functions and spectra buoy motion and insolation are constructed and discussed.

Supported by: NSF Grant OCE87-06914.

WHOI Technical Report 89-45.

IMPROVED METEOROLOGICAL MEASUREMENTS FROM BUOYS AND SHIPS (IMET): PRELIMINARY COMPARISON OF SOLAR RADIATION AIR TEMPERATURE SHIELDS

Gennaro H. Crescenti, Richard E. Payne and Robert A. Weller

Several different types of solar radiation air temperature shields are evaluated for use at sea on ships and buoys. They include three types of static or Thaller shields, two vane oriented shields, and two fan ventilated shields. A preliminary data analysis is presented and discussed.

Supported by: NSF Grant OCE87-09614.

WHOI Technical Report 89-46.

IMPROVED METEOROLOGICAL MEASUREMENTS FROM BUOYS AND SHIPS (IMET): PRELIMINARY COMPARISON OF PYRANOMETERS

Gennaro H. Crescenti, Richard E. Payne and Robert A. Weller

Three different types of pyranometers (two of each) are tested and evaluated. The sensors include the Eppley Precision Spectral Pyranometer (PSP) which meets the World Meteorological Organization (1965) criteria for a first class pyranometer, the Eppley 8-48 Black and White Pyranometer (second class) and the Hollis MR-5 Silicon Photovoltaic Pyranometer (third class).

Supported by: NSF Grant OCE87-09614.

WHOI Technical Report 89-47.

DISSOLVED OXYGEN MEASUREMENTS IN SEA WATER AT THE WOODS HOLE OCEANOGRAPHIC INSTITUTION

George P. Knapp, Marvel C. Stalcup and Robert J. Stanley

This report describes a modified Winkler titration technique that has been used for the past 25 years at the Woods Hole Oceanographic Institution (WHOI). During this time most of the dissolved oxygen measurements made at sea by WHOI personnel have been analyzed with this technique and only relatively minor, evolutionary changes in the procedures and equipment have occurred. These changes, however, have improved the precision and accuracy of deep-sea dissolved oxygen measurements to 0.005 ml/l and 0.02 ml/l respectively.

Supported by: NSF Grant OCE87-16910.

WHOI Technical Report 89-23.

CTD OBSERVATIONS OFF NORTHERN CALIFORNIA DURING THE SHELF MIXED LAYER EXPERIMENT, SMILE, NOVEMBER 1988

Richard Limeburner and Robert C. Beardsley

CTD observations on the R/V *Wecoma* cruise W8811 were made off the northern California coast November 13-24, 1988 as part of the Shelf Mixed Layer Experiment (SMILE). The survey consisted of repeated mappings of the central transect (C) through the SMILE moored array, and two synoptic sampling surveys - a large-scale grid of four cross-shelf transects extending to both sides of

Point Arena and Point Reyes, and a small-scale grid of five cross-shelf transects located near the central SMILE mooring site. The small-scale hydrographic survey had a much higher spatial resolution of CTD stations than the large-scale survey. The primary objectives of the hydrographic measurement program were to observe and characterize the temperature, salinity, density, and light transmission fields and their temporal and spatial variability in the surface boundary layer along the continental shelf and slope near the SMILE moored array, and to acquire an estimate of the cross-shelf and along-shelf scales over which the mixed-layer depth varies. All of the cross-shelf transects extended beyond the shelf break and the maximum sampling depth at each station was near-bottom or 600 m. This report presents a summary in graphic and tabular form of the hydrographic observations made during cruise W8811 on the R/V *Wecoma*.

Supported by: NSF Grant OCE87-16937.

WHOI Technical Report 89-25.

CTD OBSERVATIONS OFF NORTHERN CALIFORNIA DURING THE SHELF MIXED LAYER EXPERIMENT, SMILE, FEBRUARY/MARCH 1989

Richard Limeburner and Robert C. Beardsley

CTD observations were made off the northern California coast during R/V *Wecoma* cruise W8902 February 22 - March 10, 1989 as part of the Shelf Mixed Layer Experiment (SMILE). The surveys consisted of three sampling plans - a large-scale grid of four cross-shelf transects extending to both sides of Point Arena and Point Reyes, a small-scale grid of five cross-shelf transects located near the central SMILE mooring site, and an expanded small-scale grid of nine cross-shelf transects. All of the cross-shelf transects extended beyond the shelf break and the maximum sampling depth at each station was near-bottom or 1000 m. The average along-shelf separation between cross-shelf transects was about 15 km for the small-scale surveys and 50 km for the large-scale grid.

The primary objectives of the hydrographic measurement program were to observe and characterize the temperature, salinity, density, and light transmission fields and their temporal and spatial variability in the surface boundary layer along the continental shelf and slope near the SMILE moored array, and to acquire estimates of the cross- and along-shelf scales over which the mixed-layer depth varies. This report presents a summary in graphic and tabular form of the hydrographic observations made during cruise W8902 on the R/V *Wecoma*.

Supported by: NSF Grant OCE87-16937.

WHOI Technical Report 89-41.

CTD OBSERVATIONS OFF NORTHERN CALIFORNIA DURING THE SHELF MIXED LAYER EXPERIMENT, SMILE, MAY 1989

Richard Limeburner and Robert C. Beardsley

CTD observations were made off the northern California coast during R/V *Wecoma* cruise W8905 May 5-14, 1989 as part of the Shelf Mixed Layer Experiment (SMILE). The surveys consisted of two sampling plans - a large-scale grid of four cross-shelf transects extending to both sides of Point Arena and Point Reyes, and a small-scale grid of six cross-shelf transects located near the central SMILE mooring site. All of the cross-shelf transects extended beyond the shelf break and the maximum sampling depth at each station was near-bottom or 1500 m. The average along-shelf separation between cross-shelf transects was about 15 km for the small-scale surveys and 50 km for the large-scale grid.

The primary objectives of the hydrographic measurement program were to observe and characterize the temperature, salinity, density, and light transmission fields and their temporal and spatial variability in the surface boundary layer along the continental shelf and slope near SMILE moored array, and to acquire estimates of the cross- and along-shelf scales over which the mixed-layer depth varies. This report presents a summary in graphic and tabular form of the hydrographic observations made during cruise W8905 on the R/V *Wecoma*.

Supported by: NSF Grant OCE87-16937.

WHOI Technical Report 89-42.

CTD OBSERVATIONS IN THE GREAT SOUTH CHANNEL DURING THE SOUTH CHANNEL OCEAN PRODUCTIVITY EXPERIMENT, SCOPEX, MAY - JUNE 1989

Richard Limeburner and Robert C. Beardsley

CTD and acoustic Doppler current profiler (ADCP) observations were made in the Great South Channel (GSC) off the New England coast during R/V *Endeavor* cruise EN196 May 18 to June 12, 1989 as part of the South Channel Ocean Productivity Experiment (SCOPEX). These observations were obtained using several sampling plans - a series of small-scale surveys in support of

biological sampling and a large-scale survey of five cross-channel transects extending from Nantucket Shoals and the coast of Cape Cod to Georges Bank. The maximum sampling depth at each station was within a few meters of the bottom.

The primary objectives of the hydrographic measurement program were to a) observe and characterize the temperature, salinity, oxygen, fluorescence and light transmission fields and their spatial variability in the Great South Channel off the New England coast, (b) resolve the low salinity surface plume-like structure usually observed east of Cape Cod in late spring, (c) define the front or boundary between the vertically well-mixed water over Nantucket Shoals, the GSC, Georges Bank, and the stratified water in the deeper southwestern Gulf of Maine, and (d) characterize water properties in regions of enhanced biological productivity. This report presents a summary in graphic and tabular form of the hydrographic observations made during cruise EN196 on the R/V *Endeavor*.

Supported by: NSF Grant 87-13988.

WHOI Technical Report 89-51.

CTD OBSERVATIONS ON THE NORTH BRAZIL SHELF DURING A MULTIDISCIPLINARY AMAZON SHELF SEDIMENT STUDY, AMASSEDS, AUGUST 1989

Richard Limeburner and Robert C. Beardsley

CTD and acoustic Doppler current profiler (ADCP) observations were made on the North Brazil shelf adjacent to the mouth of the Amazon River during R/V *Iselin* cruise I8909 August 3-14, 1989 as part of A Multidisciplinary Amazon Shelf Sediment Study (AMASSEDS). These observations were obtained during a large-scale survey in support of geological and geochemical sampling, an anchored time series station consisting of 26 hourly CTD casts, and one transect which was repeated off the mouth of the Amazon River. The maximum sampling depth at each station was within two meters of the bottom.

The primary objectives of the AMASSEDS hydrographic measurement program were to (a) observe and characterize the temperature, salinity, density, oxygen, fluorescence and light transmission fields and their spatial variability on the north Brazilian shelf directly influenced by the Amazon River Discharge, (b) resolve the seaward extent and vertical structure of the surface plume of low salinity Amazon River water during different stages of river discharge, (c) describe the spatial structure of the turbidity and associated suspended sediment distributions across the shelf, (d) characterize the

properties of the Amazon shelf water beneath the surface plume and their seasonal variability, and (e) describe the landward penetration of the North Brazil Current (NBC) with respect to water properties and shelf currents. This report represents a summary in graphic and tabular form of the hydrographic observations made during the first AMASSEDS cruise (I8909) on the R/V *Iselin*.

Supported by: NSF Grant OCE88-12917.

WHOI Technical Report 89-53.

IMPROVED METEOROLOGICAL MEASUREMENTS FROM BUOYS AND SHIPS (IMET): PRELIMINARY REPORT ON BAROMETRIC PRESSURE SENSORS

Richard E. Payne, Gennaro H. Crescenti and Robert A. Weller

Stability tests over periods ranging from 3 to 19 months have been carried out on Paroscientific models 215-AT and 760-15A, AIR DB-1A, Rosemount 1201F1B, Setra 270 and Heise 623 electronic barometers. The paroscientific barometers had the highest accuracy, stability, and price, and the lowest power consumption. The Rosemount 1201F1B had excellent stability but high power consumption as well as price. The AIR DB-1A and Setra 270 gave good stability and moderate power consumption and price. The tests are being expanded to include inexpensive sensors.

Supported by: NSF Grant OCE87-09614.

WHOI Technical Report 89-49.

SURFACE VELOCITY IN THE EQUATORIAL OCEANS (20N -20S) CALCULATED FROM HISTORICAL SHIP DRIFTS

Philip L. Richardson and Theresa K. McKee

Ship drift velocity observations were used to calculate and plot monthly mean and yearly mean velocities in 2°latitude by 5°longitude boxes for the Atlantic, Pacific, and Indian Oceans. The vector maps shown here provide a visualization of the mean and seasonally varying currents.

Supported by: NSF Grant OCE87-16509.

WHOI Technical Report 89-9.

FASINEX (FRONTAL AIR-SEA INTERACTION EXPERIMENT) MOORED INSTRUMENTATION

Richard P. Trask, Jerome P. Dean, James R. Valdes, Craig D. Marquette

In 1986, FASINEX, a Frontal Air Sea Interaction Experiment, a multi-investigator cooperative experiment, was conducted to study the role of horizontal variability in air-sea interaction in the persistent front formed in the subtropical convergence zone south of Bermuda. Aimed at investigating all aspects of the atmospheric and oceanic variables related to the formation and maintenance of the front, an array of meteorological and current meter moorings was deployed by the Woods Hole Oceanographic Institution Buoy Group in 5400 meters of water. Two subsurface current meter moorings were deployed in October, 1984; five surface meteorological and current meter moorings and four Profiling Current Meter (PCM) moorings were set in January 1986. All except one PCM mooring, which was lost, were recovered in June 1986. This report discusses the extensive preparations of, and modifications to, the Woods Hole Oceanographic Institution Buoy Group instruments placed on the five surface moorings. The equipment included 30 vector measuring current meters, ten vector averaging current meters and five vector averaging wind recorders.

Supported by: ONR Contract N00014-84-C-0134.

WHOI Technical Report 89-3.

GULF STREAM RECIRCULATION EXPERIMENT - PART II

C. M. Wooding, W. B. Owens, M.E. Zemanovic and J. R. Valdes

This report presents trajectories and time series of velocity, pressure, and temperature for twelve neutrally-buoyant floats launched during the Gulf Stream Recirculation EXperiment (GUSREX) and two from earlier experiments, that continued to operate after May 1982. These float data were obtained from Autonomous Listening Stations (ALSs) deployed from May 1982 to August 1985.

Supported by: NSF Grants OCE81-09145 and OCE81-17467.

WHOI Technical Report 89-37.

MARINE POLICY CENTER
James M. Broadus III, Director

BIOLOGY AND CONSERVATION OF SEA TURTLES NESTING IN QUINTANA ROO, MEXICO, DURING 1988

M. Tundi Agardy and Reyna Gil Hernandez

The Caribbean beaches of the state of Quintana Roo, Mexico, provide important nesting sites for the green (*Chelonia mydas*) and loggerhead (*Caretta caretta*) sea turtles, and associated waters are important foraging habitat for subadult and adult hawksbill turtles (*Eretmochelys imbricata*). In addition to these three species which occur in large numbers, the leatherback (*Dermochelys coriacea*) and Kemp's ridley (*Lepidochelys kempi*) turtles have also been found in the area, although only sporadically and in low numbers. Recent surveys by personnel from the state para-governmental research agency CIQRO indicate that ten beaches on the Yucatan Peninsula's east coast are utilized by these species.

Published in: *U.S. Fish and Wildlife Service Report, NOAA Memorandum, 199-200, 1988.*

Supported by: *U.S. Fish and Wildlife Service and The Pew Charitable Trusts.*

DRAFT GUIDELINES FOR COASTAL BIOSPHERE RESERVE PLANNING

M. Tundi Agardy

These guidelines provide background on the Biosphere Reserve Programme, discuss the need to include coastal areas in the Reserve network and the difficulties in translating terrestrial models into useful tools for coastal management, and describe the planning, design and implementation potential for coastal biosphere reserves. In providing general guidelines for subsequent adaptation of the concept and design to meet specific needs in specific areas, no generic model is given, since it would be useful in only a limited number of conditions. Instead, these guidelines suggest the kinds of considerations which must be explored before viable coastal biosphere reserves can be designed and designated.

In Press: *MAB Publication Series.*

Supported by: *IUCN/Unesco, The Pew Charitable Trusts, and the Marine Policy Center.*

WHAT SCIENTIFIC INFORMATION IS CRITICAL FOR MANAGEMENT, AND WHY?

M. Tundi Agardy

Development of coordinated and comprehensive management plans for sea turtles,

in contrast to the usual crisis management approach, requires sound science to justify policy. Given the inherent constraints of time and money, complete knowledge about the species and its requirements is not a realistic prerequisite for undertaking sound management. What is required is a rigorous examination of population structure and dynamics, and a consideration of how demographic trends might be influenced by external factors like changing environments and socioeconomics.

The critical scientific questions that must be addressed before management of sea turtles can truly be efficient are:

1. What is the size and extent of the population to be managed (i.e., what is the management unit)?
2. What is the intrinsic rate of increase in this unit in its "undisturbed" state?
3. What are the natural and anthropogenic factors interfering with this intrinsic rate?
4. Which of the above factors can be controlled through management measures and which of those measures will yield the fastest results?

Once these basic scientific issues have been addressed, policy options can be evaluated according to their potential efficacy and political tractability.

Published in: *NOAA Technical Memorandum, NMFS-232, 1989.*

Supported by: *The Pew Charitable Trusts and the Marine Policy Center.*

WORKSHOP ON THE SOVIET MARITIME ARCTIC

Lawson W. Brigham

The Marine Policy Center of the Woods Hole Oceanographic Institution initiated studies focussing on Soviet policies affecting the use of the Soviet Maritime Arctic with an international workshop in May 1987. The workshop was divided into six sessions addressing a spectrum of interests — historical, cultural, legal, strategic, geopolitical, transportation, scientific, technological and resource development. Scholars from the U.K., Norway, Canada and the U.S. attended. A final summary session addressed the future of the maritime Arctic in terms of its importance to the Soviet Union.

Published in: *Arctic Research of the United States, 2, 46-49, 1988.*

Supported by: *The John D. and Catherine T. MacArthur Foundation and the Marine Policy Center.*

ECONOMIZING HUMAN RESPONSES TO SUBSIDENCE AND RISING RELATIVE SEA LEVEL

James M. Broadus

To help guide public responses to potential land subsidence and rising sea level in low-lying coastal areas, and to anticipate the ways in which the problems will affect and be affected by people, potential socio-economic impacts and human adjustments are examined. Economic impact assessments are a form of benefit-cost analysis to estimate the expected cost of an event in the absence of mitigation. Crude characterizations of the scale of potential impact in Egypt and Bangladesh are developed on the basis of inundation scenarios to the year 2050. Using strong assumptions about economic growth rates, land rent shares of national product, intertemporal discount rate, and rate of inundation, a method is demonstrated for extending this characterization to an even cruder estimate of potential economic loss. This is a certainty-equivalent value confined to land inundation and, aside from obvious sources of imprecision, underestimates lost capital structures, increased exposure to storm damage and interior flooding, and such secondary effects as saline intrusion, crowding and factor reallocation costs. Even so, it is probably an overestimate since it is not likelihood-weighted, assumes a linear rate of land loss, and, most important, ignores cost reductions arising from human responses. Five economic topics involved in such responses receive special attention. These are: (1) the advantages of incremental responses to gradual change; (2) principles for managing uncertainty; (3) the "retrofit" problem and capital durability; (4) economic discounting of future values; and (5) the nature and implications of common property, spillover, transboundary and informational effects.

In Press: *Rising Sea Level and Subsiding Coastal Areas.*

Supported by: The Pew Charitable Trusts, U.S. Environmental Protection Agency and Scientific Committee on Problems of the Environment.

WHOI Contribution No. 7190.

IMPACTS OF FUTURE SEA LEVEL RISE

James M. Broadus

Humankind has long experience in suffering from and dealing with coastal flooding and related natural disasters from the sea. In most cases these have had nothing to do with changing sea level, but we do have some historical experience with that problem too. This paper reviews our state of

knowledge about expected sea level rise from greenhouse warming and about methods employed to characterize potential impacts. These methods include benefit-cost projections from inundation scenarios, the so-called "coloring book" approach, holistic modeling, micro-simulation, and "policy analogues." Major potential physical and natural impacts are enumerated, and existing estimates of economic costs are critically summarized. An important obstacle to economic impact assessment is incorporation of future human responses to sea level change and other economic adaptations over time. Perhaps the greatest need is for scientific probabilistic forecasts of future sea level rather than the disparate array of "scenarios" used thus far.

Published in: *Global Change and Our Common Future: Papers from a Forum*, pp. 125-138, 1989.

Supported by: The Pew Charitable Trusts, the National Academy of Sciences, and the Smithsonian Institution.

WHOI Contribution No. 7181.

POSSIBLE IMPACTS OF AND ADJUSTMENTS TO SEA LEVEL RISE: THE CASES OF BANGLADESH AND EGYPT

James M. Broadus

The potential economic implications of relative sea level rise scenarios developed by physical scientists are examined for Egypt and Bangladesh for the years 2050 and 2100. Several reasons are noted for caution in the interpretation of these scenarios. The methods used to indicate the potential scale of economic effects is very coarse and simplistic, but its results suggest that relatively large economic values are at stake in both cases. As a first-order indication of these economic stakes, estimates are made of the current economic output generated in the areas affected by future sea level in each scenario. A 1 m. rise, for example, would cover areas currently accounting for about 7% of habitable land and 5% of population in Bangladesh and 12% of habitable land and 14% of population in Egypt. To demonstrate how this can be extended to an estimate of potential loss, one of the Bangladesh scenarios is developed further using strong but reasonable parametric assumptions. The result suggests that, absent mitigating adjustments, a "worst case" relative sea level rise of 1 m. by 2050 could impose a cumulative loss in present value terms at between 1 and 3% of the nation's current gross domestic product. It is shown further, however, that human adjustments would tend to reduce this loss; so it should be seen as a bounding

value. Potential adjustments discussed are: defensive measures, recombinations of productive factors, and technological adaptation. In the near term these might include such institutional adaptations as insurance, share markets, contracts and futures markets, mergers, and governmental risk-sharing schemes.

In Press: *The Effects of Climate Change on Sea Level, Severe Tropical Storms and their Associated Impacts.*

Supported by: The Pew Charitable Trusts, U.S. Environmental Protection Agency, and the Climatic Research Unit of East Anglia University.

WHOI Contribution No. 7147.

WORLD OCEAN POLLUTION STATUS REPORT

James M. Broadus

This report, based on the author's work in GESAMP, provides a brief and very general overview of the major forms of marine pollution currently identified in the world's ocean, along with "thumbnail" reviews of selected oceanic and coastal regions and a short suggested list of research issues for priority attention. Incidental attention is devoted to the policymaking process of States, taking special note of economic conditions and processes. The overall conclusion is quite clear. Open ocean areas of the world are still in good shape and largely free from marine pollution. Growing problems of marine pollution are found in a number of the world's poorly-mixed coastal waters, especially those associated with population centers, industrial activity and river inputs. The most pressing problems are associated with disposal of untreated or poorly-treated sewage, industrial effluents, and nutrients and sediment runoff from agricultural and development activities.

Published in: *Expert's Report to United Nations*, April, 1989.

Supported by: United Nations Office of Ocean Affairs and Law of the Sea and The Pew Charitable Trusts.

MARINE NON-FUEL MINERALS IN THE U.S. EXCLUSIVE ECONOMIC ZONE: MANAGING INFORMATION AS A RESOURCE

James M. Broadus and Porter Hoagland

Substantial quantities of marine nonfuel minerals are known to exist in the U.S. exclusive

economic zone (EEZ), but most of these are not yet close to production or even to being properly classified as economic resources. Nonfuel mineral prospecting, discovery and exploration activity in the EEZ is part of a long-range process of resource development. The product of this activity in the near-term is not mineral commodities such as metals, however, but rather information about the resource potential. We examine the role of investment in information in the resource development process, briefly discuss the economics of information, characterize the problems faced and the methods employed by public agencies in managing information, and highlight several critical policy issues concerning the management of information about EEZ nonfuel minerals. These issues concern the distribution of research effort, exclusive rights, confidentiality provisions, performance requirements, and national security classification.

In Press: *Ocean and Shoreline Management.*

Supported by: Department of Commerce, NOAA, National Sea Grant Program under Grant No. NA86-AA-D-SG090 (R/S-9), and the Marine Policy Center.

WHOI Contribution No. 7144.

DEFINING A KEY INDUSTRY: MARINE ELECTRONICS INSTRUMENTATION

James M. Broadus, Porter Hoagland and Hauke L. Kite-Powell

The article describes research sponsored by the Massachusetts Centers of Excellence Corporation to enhance understanding of industrial organization in the field of marine electronic instrumentation (MEI), a broadly defined "industry," which until now has received little systematic, scholarly attention. Over 350 firms in the U.S. industry annually earn a total estimated gross revenue of approximately \$5 billion. These firms fall into three largely distinct industry groups: (1) defense systems contractors; (2) commercial marine electronics; and (3) scientific instrumentation. The first group is by far the largest in sales volume and is oligopolistic in structure, consisting of a few large rivals for infrequent and complex defense systems contracts. The other groups are more purely competitive. Four major customer groups are distinguished: (1) military; (2) commercial and recreational shipping and boating; (3) offshore oil and gas; and (4) oceanographic/environmental. Most of the firms in the industry face international competition. The importance of marine electronic instrumentation to technological advance and economic activity in the world's oceans is strongly apparent. Institutional

factors affecting the international competitiveness of these firms in this industry include sponsored research, procurement, intellectual property rights, tax allowances, antitrust enforcement, small business encouragements, export controls, import restrictions, and exchange rates.

Published in: *Sea Technology*, 30, 59-64, 1989.

Supported by: Department of Commerce, NOAA, National Ocean Service, Office of Marine Operations through a grant to the Massachusetts Centers of Excellence Corporation, grant number NA87-AA-D-M0037.

BENEFITS AND INCENTIVES FOR INVESTMENT IN BIOSPHERE RESERVES

James M. Broadus, John Wargo and Jane Robertson Vernhes

This paper addresses the problem of mobilizing investment of organizational resources for effective implementation of the international Man and the Biosphere (MAB) Programme's coastal Biosphere Reserves. The achievement of MAB's objectives depends on the investments of agencies and other organizations in carrying out MAB functions. The degree to which an organization will commit extra resources to this investment depends on its own mission, the extent to which MAB can support that mission, and other incentives seen by the organization's managers. Experience with MAB at the international level suggests that the variety of motives includes financial returns, cooperative linkages, expression of cultural identity, enhanced land use and landscape protection, and altruism. Results of an international survey are reported. These indicate that soil and water conservation and tourism and recreation are the most widely-reported classes of benefit from biosphere reserves. The survey also suggests that MAB managers see little relationship between intensity of management and resulting benefits. An apparent problem for MAB is that designated biosphere sites are too readily accepted into a loosely managed network, lacking the structure for effective integration of research and management. Understanding the "objective functions" of organizations, and applying economic principles to identify incentives for organizational investments in MAB, can help to direct scarce MAB resources more effectively and to link effort more closely to intended benefits.

In Press: *Bioscience*.

Supported by: UNESCO, the U.S. National Park Service, the U.S. Man and the Biosphere Program, The J.N. Pew, Jr. Charitable Trust and the Marine Policy Center.

WHOI Contribution No. 7278.

NEPA AND THE CONSERVATION OF BIOLOGICAL DIVERSITY

Cynthia Carlson

For the past several years, there has been widespread interest in the concept of biological diversity, particularly among scientists and members of environmental groups. The conservation of biological diversity is particularly important in tropical regions, where forests, coral reefs, and other areas are believed to support as much as eighty percent of the world's species.

This article first reviews some of the scientific issues concerning the conservation and promotion of biological diversity as well as some of the policy measures that have been crafted in response. The article next focuses on the proposed amendments to NEPA and on NEPA as a mechanism for federal agency environmental decision making. The article concludes by recommending the review and revision of NEPA regulations as a less radical and perhaps more effective means of addressing biological diversity conservation needs.

Published in: *Environmental Law*, 19, 15-36, 1988.

Supported by: The J.N. Pew, Jr. Charitable Trust.

WHOI Contribution No. 6954.

AN EVALUATION OF INTERNATIONAL PROTECTION OFFERED TO CARIBBEAN CORAL REEFS AND ASSOCIATED SYSTEMS

Lynn Davidson and Kristina Gjerde

The emerging trend for a broader, systemic approach in conservation is positive and important. While there continues to be a need to protect specific natural areas and specific animals and plant species, there is a far greater need to expand the focus of conservation to look at entire ecosystems. Unless care is taken to reduce or eliminate the general stress on an ecosystem, the result will be a much lower standard of life not only for its animal and plant inhabitants but also for the many human communities currently enjoying its benefits.

Published in: *Greenpeace*, 90 pages, 1989.

Supported by: The J.N. Pew, Jr. Charitable Trust and Greenpeace International.

REPORT OF A MEETING OF THE MARINE BIOLOGICAL DIVERSITY WORKING GROUP

Mark E. Eiswerth

On August 3-4, 1989, the Marine Policy Center of the Woods Hole Oceanographic Institution hosted the initial meeting of the Marine Biological Diversity Working Group. The formation of this working group was fostered as part of an ongoing program of research concerning the oceans and biological diversity. Participants in the working group include professionals from the fields of biology, ecology, economics, statistics, law, environmental management, and international assistance, all of whom have expressed an interest in issues surrounding the conservation of marine biological resources. The proposed goals of the working group are to initiate an ongoing interdisciplinary dialogue on the topic, to establish a mechanism for two-way transfer of theory and empirical results between natural and social science, and to provide a source of authoritative and timely information to policy-makers. This report contains information about the working group and the motivations for its formation, a description of the format of the initial meeting, key points from each of the sessions, abstracts of research/issue briefings delivered at the meeting by participants, selected excerpts from group discussions, and an amended version of a draft working group statement that was introduced to the group for purposes of discussion. The appendices contain the agenda of the meeting, a list of the names and addresses of working group participants, and a list of key questions and issues submitted before the meeting by the working group.

In Press: WHOI Technical Report, 1990.

Supported by: The Pew Charitable Trusts and the Marine Policy Center.

DOES ANALYSIS MATTER? ECONOMICS, LITIGATION AND PLANNING IN THE DEPARTMENT OF THE INTERIOR

Scott Farrow

Economic theory and quantitative methods are the basis of a substantial portion of the formal policy analyses conducted in government. Repeat decision making with a common set of inputs seldom occurs so that statistical tests of the significance of policy analysis is rare. The Five-Year Offshore Leasing Plan of the Department of the Interior does provide a sample

of repeat decisions with a common set of inputs. The outcome of the plan, the number of auctions to hold in each of 26 planning areas in the next five years, are statistically related to the input data using a Poisson regression. The conclusion is that the input data are statistically related to the number of sales but estimated coefficients are of such small size that the analysis was irrelevant to planning the number of sales.

In Press: *The Review of Economics and Statistics*.

Supported by: The Marine Policy Center, The J.N. Pew, Jr. Charitable Trust and Carnegie-Mellon University.

WHOI Contribution No. 6834.

FINANCIAL ACCOUNTING FOR THE OCS LEASING PROGRAM

Scott Farrow

The Federal Outer Continental Shelf (OCS) leasing program implements an important shift of long-term Government assets into income producing property. The Government's accounting method, called fund accounting, differs from that of private business, but developing private business statements for the OCS can improve our understanding of Government policy. A balance sheet and an income statement are presented based on annual and periodic reports of the Minerals Management Service. In addition, the use of the funds received by the Government are followed to their uses in the Federal Government, including disbursements to the states as a result of section 8(g) settlements and from the Land and Water Conservation Fund.

Published in: *Oceans '89*, 2, pp. 500-504, 1989.

Supported by: The Pew Charitable Trusts and the Marine Policy Center.

MODELING THE IMPORTANCE OF OCEANS AND ESTUARIES

Scott Farrow

Analyzing the contribution of the ocean sector has advanced little since the pathbreaking work of Giulio Pontecorvo and his co-authors in "Contribution of the Ocean Sector to the United States Economy" in 1980. In the meantime, increasing controversy surrounding marine sanctuaries, national estuaries and offshore leasing has generated new demands for evaluating the services provided by the ocean environment. This paper utilizes recent advances in the economics of multiple output organizations to model the

tradeoffs of service and production oriented industries and their dependence, or lack of it, on the quality of the ocean environment. In effect, this is regional economic modeling that is conditional on the quality of the ocean environment.

Published in: *Oceans '89*, 1, pp. 130-132, 1989.

Supported by: The Pew Charitable Trusts and the Marine Policy Center.

DEVELOPING A NATIONAL MARINE ELECTRONICS AGENDA, MASSACHUSETTS CENTERS OF EXCELLENCE CORPORATION

Arthur G. Gaines

High technology products are important to the economic strength of the U.S., as R&D-intensive products continue to show the best performance of any U.S. foreign trade sector. It is a matter of national concern, therefore, that the U.S. share of world high technology manufacturers exports has been declining since 1982. Our three year program, sponsored by NOAA/NOS, has been examining the structure of the U.S. and world marine electronic instrumentation industries as well as existing and potential markets in selected marine and maritime areas, to identify measures to mitigate obstacles and enhance opportunities for these industries.

Published in: *Oceans '89*, 1, pp. 202, 1989.

Supported by: Department of Commerce, NOAA, National Ocean Service, Office of Marine Operations through a grant to the Massachusetts Centers of Excellence Corporation, grant number NA87-AA-D-M0037.

EDGARTOWN HARBOR PROVIDES MODEL FOR HARBOR RESOURCES MANAGEMENT

Arthur G. Gaines and Richard M. Butler

This article describes a cooperative program between ENDECO/YSI and the Marine Policy Center of the Woods Hole Oceanographic Institution to determine what kinds of information are most relevant to harbor management, and how electronic instruments can help provide it.

Published in: *Sea Technology*, 30, 10, 19-23, 1989.

Supported by: The Edgartown Harbor Association and the Marine Policy Center.

NITROGEN INPUTS TO A MARINE EMBAYMENT: THE IMPORTANCE OF GROUNDWATER

Anne E. Giblin and Arthur G. Gaines

We examined the importance of nitrogen inputs from groundwater and runoff in a small coastal marine cove on Cape Cod, MA. We evaluated groundwater inputs by three different methods: a water budget, assuming discharge equals recharge; direct measurements of discharge using bell jars; and a budget of water and salt at the mouth of the Cove over several tidal cycles. The lowest estimates were obtained by using a water budget and the highest estimates were obtained using a budget of water and salt at the Cove mouth. Overall there was more than a five fold difference in the freshwater inputs calculated by using these methods.

Nitrogen in groundwater appears to be largely derived from on site septic systems. Average nitrate concentrations were highest in the region where building density was greatest. Nitrate in groundwater appeared to behave conservatively in sandy sediments where groundwater flow rates were high ($>1 \text{ m}^2/\text{hr}$), indicating that denitrification was not substantially reducing external nitrogen loading to the Cove.

Nitrogen inputs from groundwater were approximately $300 \text{ mmol-N/m}^3/\text{y}$ of Cove water. Road runoff contributed an additional $60 \text{ mmol/m}^3/\text{y}$. Total nitrogen inputs from groundwater and road runoff to this Cove were similar in magnitude to river dominated estuaries in urbanized areas in the United States.

In Press: *Biogeochemistry*.

Supported by: WHOI Education Office, Town of Orleans, MA and the Marine Policy Center.

WHOI Contribution No. 7321.

OBSERVATIONS OF LONG-TERM TIDE-GAUGE RECORDS FOR INDICATIONS OF ACCELERATED SEA-LEVEL RISE

V. Gornitz and A. Solow

Long-term tide-gauge records have been examined for indications of accelerated sea-level rise. An initial evaluation of 21 records was made, using least squares linear regression. Four of the longest records were selected for more formal statistical analysis.

The regional mean sea-level curve for west-central Europe displays an upswing after 1900. However, individual stations vary considerably over short distances. Results from

other regions are less conclusive. Application of univariate and multivariate techniques to the four longest records yields strong evidence for the presence of a non-global, non-linear component. However, the three longest European records show some non-linear features in common, implying the presence of a regional component. There is some weak statistical evidence for a common changepoint around 1895, in the long-term European records (particularly for Amsterdam and Brest).

In Press: *Proceedings of the Department of Energy Workshop on Greenhouse Gas Induced Climate Change.*

Supported by: The Pew Charitable Trusts and the U.S. Department of Energy, Office of Energy Research, Contract DE-ACO5-84OR21400 with Martin Marietta Energy Systems Subcontract MRETTA 19X-91348V, NASA Cooperative Agreement NCC 5-29 with Columbia University.

WHOI Contribution No. 7328.

ITERATIVE TECHNIQUES FOR CHARACTERIZING MARINE BIRD HABITATS WITH TIME-SERIES OF SATELLITE IMAGES

J. Christopher Haney

Demonstrating long-term use of marine habitats by seabirds is often complicated by short-term changes in habitat location, persistence, and age. This paper describes iterative techniques for characterizing non-static habitats, such as meso-scale (10-100 km) ocean eddies and fronts, using time-series of satellite images that define sea surface conditions. Seabird use of satellite-detected habitats was compared using survey data and imagery from the Gulf of Alaska and southeastern United States. Time-series examination of satellite images combined with long-term seabird censuses slow (1) estimation of the successional stage (age) of some marine habitats, (2) detection of recurring habitats, (3) geographically-referenced measurement of habitat location and areal extent, (4) identification of consistently-used habitats, and (5) demonstration of time-dependent use by seabirds associated with seasonal or annual variation in habitat availability.

Published in: *Colonial Waterbirds*, 12, 1, 78-89, 1989.

Supported by: Burleigh-Stoddard Fund, Sheldon Fund, University of Georgia, Skidaway Institute of Oceanography, National Science Foundation grants OCE81-10707, OCE81-17761 and OCE84-15963; and The Pew Charitable Trusts.

REMOTE CHARACTERIZATION OF MARINE BIRD HABITATS WITH SATELLITE IMAGERY

J. Christopher Haney

Remote sensing techniques such as radar altimetry, synthetic aperture radar, coastal zone color scanning, and infrared radiometry provide effective, instantaneous, and relatively inexpensive means for characterizing critical habitats of marine birds. In order to make optimal use of satellite-derived data, the rationale for marine habitat classification is presented, and advantages and limitations of different remote sensing techniques are discussed. An application of remote characterization is used to test for short-term habitat use and selection by the Black-capped Petrel (*Pterodroma hasitata*). By combining synoptic satellite mapping (e.g., infrared radiometry) with ship-board censusing, it was possible to demonstrate that petrels did not use all marine habitats equally, nor did petrels use habitats in proportion to their availability (areal extent).

Published in: *Colonial Waterbirds*, 12, 1, 67-77, 1989.

Supported by: Burleigh-Stoddard Fund, Sheldon Fund, University of Georgia, Skidaway Institute of Oceanography, National Science Foundation grant OCE81-10707 and The Pew Charitable Trusts.

WINTER HABITAT OF COMMON LOONS ON THE CONTINENTAL SHELF OF THE SOUTHEASTERN UNITED STATES

J. Christopher Haney

Population size, habitat use, and habitat selection of wintering Common Loons (*Gavia immer*) were studied on the southeastern U.S. continental shelf. Winter population estimates ranged from 8,700 to 20,000 individuals for the shelf between 29° and 35°N latitude. Loons used shelf waters up to 100 m in depth and 100 km from land. Significant differences in habitat use and selection were found among four shelf habitats differentiated by water depth, distance from land, and water mass properties. Loons selected for waters 0-19 m deep, but avoided highly-turbid waters within 5-15 km of shore. Loon distribution shifted further offshore during midwinter as the areal extent of turbid water increased nearshore due to seasonal peaks in river discharge.

In Press: *The Wilson Bulletin*, 102(2), 1990.

Supported by: The Pew Charitable Trusts and
National Science Foundation grants
OCE81-10707 and OCE81-17761.

WHOI Contribution No. 7215.

THE 1988 IMO CONVENTION ON THE SAFETY OF MARITIME NAVIGATION: TOWARDS A LEGAL REMEDY FOR TERRORISM AT SEA

Christopher C. Joyner

The threat of international terrorism has become real, pervasive and ever-present. However, one domain that has remained largely free from terrorist activities has been international shipping sailing the high seas. Attacks on the *ACHILLE LAURO* in October 1985 and the Greek cruise ferry *CITY OF POROS* in July 1988 indicate that freedom from maritime terrorism no longer can be comfortably taken for granted. The terrorist threat to maritime navigation and transport facilities has become a crime waiting to happen.

The principal international effort organized to deal with maritime terrorism has been a series of negotiations sponsored by the International Maritime Organization (IMO). In March 1988, these negotiations successfully culminated in adopting the Convention for the Suppression of Unlawful Acts Against the Safety of Maritime Navigation, the first major international co-operative attempt to cope with terrorism threatening international shipping on the high seas.

The object of this study is to analyze and interpret key provisions of the Convention, with particular attention to the legal implications they create for dealing with impermissible activities on the high seas. Beyond the Convention itself, the study seeks to examine the quality of international criminal law-making when States confront a serious, immediate threat to their common welfare.

Published in: *German Yearbook of International Law*, 31, 230-262, 1988.

Supported by: The George Washington University
and the Marine Policy Center.

THE ANTARCTIC MINERALS AGREEMENT: AN APPRAISAL

Christopher C. Joyner

This paper has three aims. First, it discusses certain political and legal implications arising from the Antarctic Mineral Convention's adoption. Second, it points out some lingering questions about the regime's operation, its purpose and its portents for Antarctica's environmental situation.

And finally, to offer a few brief conclusions about the implications that the regime presents for the international community.

In Press: *Proceedings, 83rd Annual Meeting of The American Society of International Law.*

Supported by: The George Washington University
and the Marine Policy Center.

WHOI Contribution No. 7163.

ICE-COVERED REGIONS IN INTERNATIONAL LAW

Christopher C. Joyner

Ice occurs on the earth's continents in various forms. Most notable are the continental glaciers that cover Antarctica and Greenland, though smaller perennial ice masses are also found in parts of Canada and Alaska. Ice also occurs on land as ground ice, or permafrost, which is permanently frozen soil.

In an era of dwindling fresh water resources, the fact that more than three-fourths of all the world's fresh water is locked up in ice formations, principally those in the polar regions, assumes ever-increasing importance. No less significant is that for those ice resources to be managed prudently, an appropriate international legal regime should be in order. Nevertheless, the international law concerning ice remains incomplete and unclear. No international legal regime is yet in place which comprehensively sets out the legal status of ice in its various forms or specifically assigns jurisdictional competence over its use.

This paper modestly aims to improve upon that legal gap by undertaking a three-fold analytical approach. First, a brief assessment is made of the political regimes overseeing activities in ice-covered regions; second, various forms of ice are analyzed with a view to distinguishing their distinct features and geophysical status; and third, the status of different ice forms is appraised under contemporary international law and implications posed for jurisdiction over and use of ice resources are assessed.

In Press: *Natural Resources Journal.*

Supported by: The George Washington University
Faculty Development Research Grant and the
Marine Policy Center.

WHOI Contribution No. 7170.

REVIEW ARTICLE - THE EVOLVING ANTARCTIC LEGAL REGIME

Christopher C. Joyner

National activities and international interest in Antarctica heightened dramatically during the 1980s. Coordination of planning among governments has become increasingly necessary not only for making sound management decisions in the region, but also for conserving Antarctica's environmental integrity. This response to pressing circumpolar concerns suggests the need for greater understanding of the process of formation of the Antarctic legal regime and its evolutionary course. The three works under review contribute mightily to mitigating that need.

Published in: *The American Journal of International Law*, 83, 3, 605-626, 1989.

Supported by: The George Washington University and the Marine Policy Center.

SUPPRESSION OF TERRORISM ON THE HIGH SEAS: THE 1988 IMO CONVENTION ON THE SAFETY OF MARITIME NAVIGATION

Christopher C. Joyner

Maritime terrorism involves the threat or use of violence against shipping on the high seas. Until recently, the oceans have been relatively free from terrorist activities.

The international community's legal response to terrorism at sea came in 1988 through promulgation by the International Maritime Organization (IMO) of a new global treaty, the International Convention for the Suppression of Unlawful Acts against the Safety of Maritime Navigation. This paper analyzes the provisions of that international instrument, with a view toward assessing its contributions to establishing counter-terrorist norms and policies under international criminal law.

In Press: *Israel Yearbook of Human Rights*.

Supported by: The George Washington University and the Marine Policy Center.

WHOI Contribution No. 7154.

MARKETING, ECOLOGICAL, AND POLICY CONSIDERATIONS RELATED TO THE NEW ENGLAND CONCH FISHERY AND *HOPLOPLANA*

*Ilene M. Kaplan, Barbara C. Boyer, and
Daniela Hoffmann*

Marketing procedures and ecological factors associated with the New England conch (*Busycon*) fishery, and related changes in *Hoploplana*, a turbellarian flatworm commensal in the mantle cavity of *Busycon*, are examined. Conch and pot fishermen were observed at sea on a regular basis, and interviews with fishermen, seafood buyers, processors, and fish market and restaurant owners were conducted. Data on size, width, weight, sex, and number of worms in the conch also were collected.

Further monitoring of the conch fishery is suggested for future research and policy considerations.

Published in: *The Biological Bulletin*, 177, 2, 327, 1989.

Supported by: Earthwatch, Union College/Dana Fellowships, the Marine Policy Center and the Marine Biological Laboratory.

MARINE POLICY IMPLICATIONS RELATED TO THE COMMERCIAL VALUE AND SCIENTIFIC COLLECTING OF THE WHELK *BUSYCON*.

*Ilene M. Kaplan, Barbara C. Boyer, and
Kristen A. Santos*

This study examines socio-economic and ecological trends associated with fluctuations in the commercial value of the whelk *Busycon*, the basis of the New England conch fishery, and evaluates relevant marine policies. Interviews of fishermen, seafood buyers, and marine policy officials were conducted; information was also collected by setting our own conch traps for monitoring and research purposes. Results indicate a small but active conch industry in New England that has undergone significant price fluctuations and technological diversification.

Ecological problems involving the possible depletion of the New England fishery and scientific collecting problems associated with scarcity and rising costs as well as changes and confusions regarding recent marine policies regulating the New England conch fishery are also examined.

Published in: *The Biological Bulletin*, 175, 312, 1988.

Supported by: The Marine Policy Center, the Marine Biological Laboratory and Union College/Dana Fellowships.

PLANNING FOR THE GALÁPAGOS MARINE RESOURCES RESERVE

Richard A. Kenchington

The Galápagos Marine Resources Reserve was proclaimed by the Government of Ecuador in May 1986. Planning for its management has involved a high degree of international collaboration. By late 1987 a draft zoning plan, regulations and management strategy had been developed. These provide for conservation and for sustainable use for the purposes of artisanal fishing, tourism, local recreation and scientific research. Successful implementation of management will depend upon the identification of sustainable funding devoted to day-to-day management of the Galápagos archipelago.

Published in: *Ocean and Shoreline Management*, 12, 47-59, 1989.

Supported by: The Heritage Division of UNESCO and The Pew Charitable Trusts.

ACHIEVING MARINE CONSERVATION THROUGH BIOSPHERE RESERVE PLANNING AND MANAGEMENT

Richard A. Kenchington and M. T. Agardy

Environmental concern, a matter of minority interest and fitful protest in the past two decades, has become a factor of mainstream political and economic planning as the extent of global environmental crises has entered public understanding. In the marine realm, the physical and biological importance of ocean processes in the functioning of the global ecosystem are being recognized. It is clear that conservation and management of the systems which cover 72% of the surface of the planet is of primary importance.

In this paper the authors seek to explain why the biosphere reserve philosophy is applicable to marine management, to discuss difficulties inherent in extrapolating its terrestrially-derived management practices to marine environments, and to suggest an approach which may lead to the development of criteria for application of the biosphere reserve concept to marine environments.

In Press: *Environmental Conservation*.

Supported by: The Pew Charitable Trusts, Tinker Foundation, and Great Barrier Reef Marine Park Authority.

COASTAL AREA MANAGEMENT IN SRI LANKA

Kem Lowry and H. J. M. Wickremeratne

There is a growing interest in coastal area management among governmental and nongovernmental officials in developing countries. This interest is evident in the increasing number of management programs, in international financial assistance in support of such programs, and in national and international seminars, workshops, and training institutes devoted to various aspects of the topic.

Most coastal countries manage their coastal areas to some degree, although they vary greatly with regard to the number and types of coastal issues they address, the types of management strategies they employ, their intensity of management, and a host of other factors.

Sri Lanka has a strong and vigorous coastal management program. The case of the development of Sri Lanka's coastal zone management program is not necessarily a blueprint for other developing countries. Nevertheless, it is interesting and perhaps instructive to see how the Sri Lankans constructed their program, the challenges they confronted (and continue to face), the alternatives they considered, the choices they made, and the consequences of those choices.

Published in: *Ocean Yearbook*, 7, 263-293.

Supported by: The University of Rhode Island's International Coastal Management Project funded by the U.S. Agency for International Development and the Marine Policy Center.

SIGNALS OR NOISE? EXPLAINING THE VARIATION IN RECREATION BENEFIT ESTIMATES

V. Kerry Smith and Yoshiaki Kaoru

This paper uses meta-analysis to summarize the benefit estimates derived from travel cost recreation demand models. After reviewing approximately 200 published and unpublished studies prepared from 1970 to 1986, 77 were found to report either consumer surplus estimates or sufficient information to derive them. Using these estimates of the consumer surplus per unit of use from each study, it was possible to evaluate the influence of variables describing the site characteristics, the activities undertaken at each site, the behavioral assumptions, and the specification decisions. The findings provide clear support for using econometric methods to summarize results from diverse empirical studies. They highlight the important research issues in

model development and may well offer a consistency check to the procedures used in benefit transfer analyses for policy evaluations.

In Press: *American Journal of Agricultural Economics*.

Supported by: U.S. Environmental Protection Agency, The Pew Charitable Trusts and the Marine Policy Center.

WHOI Contribution No. 7255.

WHAT HAVE WE LEARNED SINCE HOTELLING'S LETTER? A META ANALYSIS

V. Kerry Smith and Yoshiaki Kaoru

This paper reports the results of a meta-analysis of the estimates of the price elasticity of demand for recreation sites using the travel cost method. By using econometric methods to summarize empirical literature, meta-analysis assists in identifying research conclusions despite the non-experimental nature of most empirical research in economics. In this application, the results suggest that modeling decisions based on theory, as well as those relying on fitting criteria, were important influences to the estimated price elasticities across studies.

In Press: *Economics Letters*.

Supported by: U.S. Environmental Protection Agency, The Pew Charitable Trusts and the Marine Policy Center.

WHOI Contribution No. 7254.

DISCRIMINATING BETWEEN MODELS: AN APPLICATION TO RELATIVE SEA LEVEL AT BREST

Andrew R. Solow

A simple, informal method is presented for discriminating between competing models of trend in a climate record. The method is applied to a tide gauge record of relative sea level at Brest for the period 1807-1970. Although relative sea level at Brest appears to have accelerated over this period, it is not possible to distinguish between a smooth acceleration and one that occurred over a relatively short period of time.

In Press: *Journal of Climate*.

Supported by: The Pew Charitable Trusts, the Marine Policy Center and NOAA, National Sea Grant College Program under Grant No. NA86-AA-D-SG090 (R/O-4).

WHOI Contribution No. 7233.

GEOSTATISTICAL CROSS-VALIDATION: A CAUTIONARY NOTE

Andrew R. Solow

The spatial covariance function is the basic tool of geostatistical analysis. Typically, this function is unknown and must be estimated from available data. This usually entails estimating the covariance function at several lags (e.g., at integer multiples of the unit grid spacing in the case of gridded data) and fitting a continuous parametric model to these estimates. Once a covariance model is fit, it is common to evaluate the model by geostatistical cross-validation (e.g., Davis (1987), Russo and Jury (1987), Starks and Sparks (1987)). In geostatistical cross-validation, the data are suppressed and estimated by kriging one at a time. Reduced estimation errors are formed by dividing the ordinary estimation errors by the square roots of the corresponding estimation variances calculated from the covariance model. The covariance model is judged to be acceptable if the sample mean and sample variance of the reduced errors are near zero and one, respectively. The purpose of this note is to use an extremely simple example to suggest that geostatistical cross-validation may be of limited use.

In Press: *Mathematical Geology*.

Supported by: The Pew Charitable Trusts.

WHOI Contribution No. 7267.

ON THE STATISTICAL COMPARISON OF CLIMATE MODEL OUTPUT AND CLIMATE DATA

Andrew R. Solow

Some broad issues arising in the statistical comparison of the output of climate models and the corresponding climate data are reviewed. Particular attention is paid to the question of detecting climate change.

In Press: *Proceedings of the Department of Energy Workshop on Greenhouse Gas Induced Climate Change*.

Supported by: The Pew Charitable Trusts.

WHOI Contribution No. 7327.

RECONSTRUCTING A PARTIALLY OBSERVED RECORD OF TROPICAL CYCLONE COUNTS

Andrew R. Solow

An approach to reconstructing a partially observed annual time series of tropical cyclone

counts is presented. The approach is based on a simple model of the time series of true counts and on a simple model of the way in which this time series is observed through time. The approach is applied to a record of observed tropical cyclone counts for the Australian region for the period 1910-88. Some diagnostics are presented that indicate the model performs fairly well at reproducing the behavior of the observed counts.

Published in: *Journal of Climate*, 2, 1253-1257, 1989.

Supported by: Dept. of Commerce, NOAA, National Sea Grant College Program under Grant No. NA86-AA-D-SG090 (R/O-4).

WHOI Contribution No. 7050.

CLIMATIC CATASTROPHE: ON THE HORIZON OR NOT?

Andrew R. Solow and James M. Broadus

The greenhouse effect refers to the process by which trace gases like carbon dioxide trap reflected long-wave solar radiation and warm the atmosphere. This connection between atmospheric composition and climate has been known since the last century. The possibility that human activity could alter atmospheric composition enough to enhance the natural greenhouse effect and cause climate change has been recognized for at least fifty years. The level of carbon dioxide in the atmosphere has increased by about 15 percent since monitoring began thirty years ago, and by about 25 percent since the beginning of the Industrial Revolution. This increase is due, in large part, to human activities like the consumption of fossil fuels and large-scale deforestation. In addition to carbon dioxide, a number of other trace gases - including chlorofluorocarbons and methane - have also been identified as greenhouse gases. Their levels also are rising, in some cases much more rapidly than carbon dioxide. The connection between atmospheric composition and climate, and the documented changes in atmospheric composition, have led to justifiable concern about the possibility of significant global warming and its possible consequences.

It is clear that the appropriate human response to the possibility of climate change depends on many factors including the timing, nature, and magnitude of the change; the impacts of the change on human and other biological populations; and the benefits and costs of the response itself. A response that would be efficient under a rapid change of large magnitude could be a costly mistake under a slow change of more modest magnitude. Unfortunately, there is a great deal of uncertainty about future climate. This uncertainty complicates the discussion of climate

change in general and the choice of policy response in particular. It is on this uncertainty and its implications for policy that this article focuses.

Published in: *Oceanus*, 32, 61-64, 1989.

Supported by: The Pew Charitable Trusts.

ON THE DETECTION OF GREENHOUSE WARMING

Andrew R. Solow and James M. Broadus

Two facts that have been cited as evidence of the onset of greenhouse warming are the extent to which the most recent value in a global temperature series is unusually warm and the observation that the four warmest years on record occurred in the 1980s. We examine these results in more detail, and we address the question as to whether these facts constitute evidence in favor of the detection of greenhouse warming. We conclude that they do not support unless we are prepared to attribute all warming in the data to the greenhouse effect.

Published in: *Climatic Change*, 15, 449-453, 1989.

Supported by: The Pew Charitable Trusts.

WHOI Contribution No. 7183.

NONPARAMETRIC BINARY REGRESSION: AN APPLICATION TO PARTICLE CAPTURE BY A CILIATED SUSPENSION FEEDER

Andrew R. Solow and Scott M. Gallager

A nonparametric approach to binary regression is described and applied to the estimation of capture efficiency along the length of cilia in suspension feeders. A simulation procedure is proposed for testing the significance of differences in capture efficiency for two cilia. In an illustrative example, the significance of effects due to experiment duration, surface charge, and particle size are assessed. No significant dependence on duration is found. Both surface charge and particle size are found to have significant effects on capture efficiency.

In Press: *Journal of Experimental Marine Biology and Ecology*.

Supported by: National Science Foundation Grant OCE-8711386 and the Marine Policy Center.

WHOI Contribution No. 7269.

**ON THE RELATIONSHIP BETWEEN
THE SOUTHERN OSCILLATION AND
TROPICAL CYCLONE FREQUENCY IN
THE AUSTRALIAN REGION**

Andrew R. Solow and Neville Nicholls

A statistical model of the relationship between tropical cyclone frequency in the Australian region and an index of the strength and phase of the Southern Oscillation is developed for the period 1910-88. The modeling is non-standard, because the cyclone record is incomplete early in this period. The fitted model indicates that the mean annual number of cyclones during a major cold event is twice that during a major warm event.

In Press: *Journal of Climate*.

Supported by: The Pew Charitable Trusts and the Dept. of Commerce, NOAA, National Sea Grant Program under Grant No. NA86-AA-D-SG090 (R/0-4).

WHOI Contribution No. 7291.

**INHOMOGENEITY AND APPARENT
ORGANIZATION IN ANIMAL
BEHAVIOR**

Andrew R. Solow and Peter Tyack

Sequences of animal behavior are commonly characterized by their order of dependence. A sequence with a high order of dependence is felt to be more organized than one with a low order of dependence. We present a simple model of animal behavior in which apparent organization arises from a simple form of inhomogeneity in the sequence. We apply this model to a short sequence of dolphin vocalizations.

In Press: *Biometrics*.

Supported by: Penzance Foundation Fund, Office of Naval Research, and the National Institutes of Health.

WHOI Contribution No. 7195.

THE OCEAN "LANDSCAPE"

John H. Steele

The ocean has a complex physical structure at all scales in space and time, with "peaks" at certain wave numbers and frequencies. Pelagic ecosystems show regular progressions in size of organisms, life cycle, spatial ambit, and trophic status. Thus, physiological and ecological parameters are closely coupled to spatial and temporal physical scales.

Published in: *Landscape Ecology*, 3, 3/4, 185-192, 1989.

Supported by: Woods Hole Oceanographic Institution.

GRADUATE STUDENTS

Abstracts of papers of theses submitted in 1989 by graduate students of the Woods Hole Oceanographic Institution Doctoral Degree Program and the Woods Hole Oceanographic Institution/Massachusetts Institute of Technology Joint Program in Oceanography/Oceanographic Engineering. Other papers authored or coauthored by graduate students are included in the departmental sections.

ORGANIC NITROGEN UTILIZATION BY PHYTOPLANKTON: THE ROLE OF CELL-SURFACE DEAMINASES

Brian P. Palenik

Many phytoplankton can catalyze the decomposition of organic phosphates using cell-surface phosphatases and subsequently take up the phosphorus for growth. The nitrogen analogs, cell-surface deaminases, have not been reported in phytoplankton, except for a low affinity asparaginase. In fact, high affinity cell-surface L-amino acid and amine deaminases (oxidases) exist in at least three phytoplankton genera: Amphidinium, Pleurochrysis, and Prymnesium. One type of enzyme oxidizes L-amino acids, a second type primary amines; the endproducts are hydrogen peroxide, an organic product (an α ketoacid or an aldehyde), and NH_4^+ which is assimilated by the cell.

The amino acid oxidases have half-saturation constants of about $0.2\mu\text{M}$ ($0.1\text{--}0.45\mu\text{M}$ range) for many L-amino acids. They do not oxidize D-amino acids, while glycine and L-serine, two amino acids commonly found in the environment, are not effective substrates. The amine oxidases studied both utilize ethanolamine, but differ in their specificity for other amines. The regulation of the amino acid and amine oxidases under different growth conditions and their inhibition by various reagents are discussed.

A method was developed for measuring H_2O_2 in seawater samples and was subsequently used to obtain field data showing dark production of H_2O_2 . This phenomenon may have been due to the presence of organisms with cell-surface oxidases. Since cell-surface deaminases would not have been detected by standard field methods used to study amino acid and primary amine cycling, the existence of these enzymes suggests that phytoplankton may have a more important role in recycling organic nitrogen than currently believed. These results thus have wide-ranging implications for understanding nitrogen cycling; primary production; the geochemistry of H_2O_2 , organic acids and aldehydes; and algal-invertebrate symbioses in aquatic environments.

Supported by: ONR Contract N-00014-80-C-0273
and NSF Grant OCE 83-17532.

A SEARCH FOR LAYERING IN THE OCEANIC CRUST

John A. Collins

The results of numerous seismic refraction and reflection experiments have shown that the seismic structure of the oceanic crust can be usefully

parameterized by a small number of locally horizontal layers within which the rates of change of velocity and impedance as a function of depth are approximately constant. Layer boundaries are defined by changes in velocity and/or impedance gradient. This dissertation discusses the structure of seismic layer boundaries within the oceanic crust, and investigates the relationships between the seismic characteristics of these boundaries and the geological structure of the crust.

The seismic signature of the crust/mantle boundary (Moho) is a prominent event on multichannel seismic (MCS) reflection data. In the Western North Atlantic, the character of the Moho reflection event varies from a single well-defined phase of up to 1.0 s total duration. In Chapter 1 of this dissertation, the geological structures generating Moho reflections are investigated by calculating synthetic reflection profiles for three laterally varying velocity models totaling 64 km in length. These velocity models were derived from the observed distribution of lithologies that comprise the inferred fossil crust/mantle transition found in the Bay of Islands Ophiolite. Along the synthetic profiles, the Moho reflection is characterized by both single-phase and multi-phase events, the geometry and durations of the latter being similar to those observed on MCS data from the Western North Atlantic. In addition, the lateral variation in Moho travel time, up to 0.25 s over distances of less than 10 km, is similar to that observed on MCS data. The similarities between the observed and synthetic data suggest that the complicated interlayered sequences of mafic and ultramafic rocks that comprise the inferred crust/mantle transition in ophiolites might also be characteristic of the oceanic crust.

Although ophiolites provide a useful model of the lithological structure of the oceanic crust, the unambiguous correlation of geologic and seismic structures can only be achieved by conducting seismic experiments in the vicinity of deep crustal drillholes. Chapters 2 and 3 of this dissertation present analyses of the velocity and reflectivity structure of the crust in the immediate vicinity of Deep Sea Drilling Project Hole 504B in the Panama Basin, currently the deepest drillhole (1.288 km) into oceanic igneous crust.

Reflectivity synthetic seismogram modeling of amplitude features common to four sonobuoy profiles collected in the immediate vicinity of Site 504B shows that crustal thickness at the drillsite is only 5 km. A critical constraint on this interpretation is the observation, on four MCS profiles passing through the drillsite, of a near-normal-incidence reflection event with a crustal travel time of 1.4-1.5 s. This event is assumed to correlate with a wide-angle reflection/refraction event observed at ranges of 16-28 km on the sonobuoy profiles. Seismic

modeling demonstrates that both of these events are generated at the Moho. The crustal velocity-depth profile at Site 504B is unusual in comparison to typical oceanic profiles in having high velocity gradients (up to $0.6 \text{ km s}^{-1} \text{ km}^{-1}$) in the middle crust and a 1.8 km thick low-velocity zone ($V_p=7.1-6.7 \text{ km s}^{-1}$) immediately above Moho. A simple explanation for this unusual profile is that the velocity of the middle crust has been increased by the addition of a high-velocity mineral component such as olivine. The olivine concentration of the middle crust need be no greater than 34-37%.

Hole 504B is the only site where the volcanics/sheeted-dike boundary, predicted by the ophiolite model to be a fundamental feature of oceanic crust, has been drilled. The downward change in rock type coincides with changes in a variety of logged physical properties. The normal-incidence travel time to this boundary is similar to the travel times of shallow reflection events observed in other areas. Accordingly, Site 504B is an ideal location to test the hypothesis that shallow reflection events correlate with the extrusive/dike boundary.

Despite extensive processing, MCS data collected in the immediate vicinity of Hole 504B show no conclusive evidence for a laterally coherent reflection event generated within the upper crust. The lack of a detectable reflection event from the upper crust is consistent with the results of synthetic seismogram modeling of velocity-depth profiles constructed from the logged downhole variation in physical properties. On these normal-incidence synthetic seismograms, low-amplitude reflections from the volcanic/dike contact are obscured by the high-amplitude basement reflection and by sediment-column multiples. In contrast to the synthetic reflection data, the seismic signature wide-angle reflection/refraction profile. The change in velocity across this boundary causes focusing of refracted arrivals in the range window 6-7 km. High-amplitude arrivals are observed at similar ranges on the sonobuoy profiles collected near the drillsite, suggesting that at Site 504B, variations in depth to this layer boundary are more easily mapped with the wide-angle reflector/refraction method.

Supported by: The National Science Foundation through grant Numbers OCE-81-17210, EAR-80-26445, EAR-83-9535, OCE 80-25206, OCE-84-10658, and OCE 87-00806.

AN INVESTIGATION OF THE MARINE GEOCHEMISTRY OF GOLD

Kelly K. Falkner

An analytical method has been developed for the analysis of gold (Au) in seawater and was applied to a suite of samples in order to conduct a preliminary assessment of the marine geochemical behavior of Au. The method involved preconcentration by anion exchange of Au complexed with cyanide ion and detection by flow injection-inductively coupled plasma quadrupole mass spectrometry (FI-ICPMS). An aliquot of a radiotracer (Au-195, $t_{1/2}=183 \text{ d}$) was added to each sample to monitor recoveries. Preconcentration of two to eight liters of seawater into one milliliter was carried out nearly quantitatively under the conditions specified. Analysis by FI-ICPMS resulted in a practical detection limit, expressed as the concentration of Au in seawater, of about 10 fmol/liter for a four liter preconcentrate. Corrections for the stable Au in the radiotracer and that contributed by reagents were significant, constituting up to 60% of the overall signals measured. Reproducibility, based in the analysis of five four-liter samples of Mediterranean seawater obtained from a single 30-liter Niskin bottle, was about 15% at the 140 fmol/liter level.

Gold profiles from the Atlantic Gulf Stream, Northeast Pacific, Mediterranean and Black Seas and hydrothermal fluids from 21°N , on the East Pacific Rise were analyzed. In general, the concentrations of Au in seawater (20-200 fmol/l) are nearly three orders of magnitude less than reported in the literature prior to 1988. This does not reflect a decrease in the Au concentrations with time, rather it indicated contamination problems with the earlier data. Gold is a non-conservative element in seawater. It does not appear to undergo appreciable recycling in the water column under oxic conditions as is evidenced by its fairly homogeneous distribution over the water column and similar average values in the Atlantic ($53 \pm 22 \text{ fmol/l}$) and Pacific ($55 \pm 36 \text{ fmol/l}$). Further data is required to be certain of this since relatively large errors in the Pacific data leave open the possibility of an enrichment or depletion by up to a factor of 2.5 between the deep Atlantic and deep Pacific.

The surface Mediterranean contains about the same Au concentrations as North Atlantic waters ($=50 \text{ fmol/l}$) whereas the deeper Mediterranean is enriched (100-150 fmol/l) with respect to North Atlantic waters. The source of this enrichment may be due to atmospheric dust which has been shown by other workers to be enriched in Au in this region or less likely to riverine inputs. In the Black Sea, Au concentrations decrease from 200 fmol/l in

the surface water to about 20 fmol/l in the deep anoxic waters. A plot of Au versus salinity suggests that the decrease from the surface is due to mixing with depleted deeper water with no abrupt changes at the redox boundary. Removal of Au is occurring either under the reducing conditions in the deeper waters which have a relatively long residence time (900-2000 years) or at the sediments. Upper limit calculations indicate that the Au removed in the deep Black Sea would contribute negligibly to the sedimentary inventory which is dominated by detrital materials.

Budget considerations suggest that rivers and atmospheric dust are likely to provide the bulk of Au to the oceans and may be equally important, although their fluxes are presently ill-constrained. While Au is enriched in hydrothermal fluids (30-250 pmol/l) with respect to ambient seawater (=50 fmol/l), hydrothermal Au is not likely to be widely disseminated in the oceans. Accordingly, its influence on the oceanic budget of dissolved Au is probably limited. The data would suggest an overall residence time for Au in the oceans on the order of a few hundred to a few thousand years.

Supported by: The Office of Naval Research and the National Science Foundation through the Massachusetts Institute of Technology.

MOLECULAR REGULATION OF THE INDUCTION OF CYTOCHROME P-450E IN THE ESTUARINE FISH *FUNDULUS HETEROCLITUS*

Pamela J. Kloepper-Sams

Induction of the aryl hydrocarbon hydroxylase (AHH) P450IA1 occurs in many organisms following exposure to polycyclic aromatic hydrocarbons (PAH). Regulation of induction of P450IA1 (called P-450E) was examined in the estuarine teleost *Fundulus heteroclitus*. Antibodies were a primary tool in this work; their specificity and cross reactivity with other species were investigated by immunoblot and catalytic inhibition studies. Scup (*Stenotomus chrysops*) P-450E protein had been previously purified (Klotz et al., 83) and antibodies generated against it (Park et al., 86a). Monoclonal antibody (MAb) 1-12-3 reacted only with P-450E when tested in immunoblot analysis with five scup P-450 fractions. This and six other MAbs recognized purified P-450E, as well as a single comigrating band in microsomes from β -naphthoflavone- (BNF) treated scup. Polyclonal antibodies (PAb) reacted with P-450E but not with other scup P-450 fractions, and reacted strongly with the BNF-induced, comigrating band. PAb also faintly recognized other microsomal proteins, which were not changed in intensity by xenobiotic treatment.

MAb 1-12-3 recognized P-450E induced by 3,4,5,3',4',5'-hexachlorobiphenyl and Aroclor treatment and the P-450E orthologue in teleost species including rainbow and brook trout, winter flounder, and *Fundulus*. P-450E was induced in these fish by BNF and other xenobiotics. P-450E protein content in all fish analyzed correlated with ethoxyresorufin O-deethylase (EROD) activity. EROD was strongly inhibited by MAb 1-12-3 in scup and trout. PAb inhibited AHH and EROD more than 90%, inhibited ethoxycoumarin O-deethylase by about 60%, and did not inhibit aminopyrine N-demethylase, confirming the identity of P-450E as the major inducible EROD and AHH catalyst in these fish. Several MAbs and the PAb recognized purified rat P450IA1 and a BNF-induced, comigrating band in microsomes. MAb 1-12-3 and the PAb also recognized a second band, which comigrates with P450IA2, in microsomes from BNF-treated rats. These results establish the identity of P-450E in scup and other fish and the immunochemical relationship of P-450E with rat P450IA1.

The mode of PAH-type induction was investigated by examining hepatic P-450E content, catalytic activity, and mRNA levels in *Fundulus* after exposure to a single dose of BNF. In a 20 day experiment, EROD was elevated in BNF-treated animals from Day 4 through Day 20. Increases in immunodetectable P-450E showed the same trend, with low control values and at least a 19-fold increase in the BNF-treated fish. Teleost RNA was used in *in vitro* translation reactions in the presence of [³H]-leucine. Precipitation of *Fundulus* liver RNA translation products with anti-P-450E PAb gave no detectable signal from control fish, while the BNF-treated animals showed incorporation of [³H]-leucine in a single 56,000 M_r band. In a 48 hour experiment, EROD and P-450E levels were again coordinately increased in response to BNF treatment, and immunoprecipitation of translation products showed increased signal at all times 6 hours or more post-treatment. cDNA pP1450-3', which encodes trout P450IA1 (Heilmann et al., 88), yielded unique bands on Southern blots with scup, trout and *Fundulus* DNA. A Northern blot of RNA from BNF-treated *Fundulus* showed increases in a single band with time when probed with the trout cDNA. P-450E mRNA increases preceded P-450E protein and EROD increases by about 25 hr, supporting the hypothesis that transcriptional activation is involved in induction of P-450E in fish. In another BNF study, *Fundulus* P-450E mRNA levels declined rapidly, returning to control levels by 5 days, while protein and activity levels remained elevated for at least 13 days. Thus, P-450E expression also appears to be under other forms of regulatory control.

Microsomal protein, P-450E protein, and

P-450E heme half-lives ($t_{1/2}$) were examined in *Fundulus* during elevated P-450E expression. Decay in incorporated radiolabel ($[^3\text{H}]$ -leucine and $[^{14}\text{C}]$ -ALA) was followed over time. The immunoprecipitation method used for RNA translation products was modified for precipitation of P-450E protein from microsomes. A preliminary experiment indicated the *Fundulus* microsomes contained no free labeled amino acid at 2 or 23 hr after injection, and that specific radioactivity was higher at 2 than 23 hr. In a longer experiment, $[^{14}\text{C}]$ counts were not detectable in total microsomes, but peak $[^3\text{H}]$ incorporation into microsomal protein was observed at 1.5 hr after injection, followed by a rapid decrease and stabilization at 30 hr. A calculation of the "rapid" and "slow" phases indicated that microsomal proteins had a "fast" $t_{1/2}$ of 9.3 hr and a "slow" $t_{1/2}$ of 190 hr. Both $[^{14}\text{C}]$ and $[^3\text{H}]$ were detectable in PAB-precipitated P-450E. Leucine incorporation peaked at 1.5 hr, with a second peak at 190 hr. Using only the early time points, P-450E protein was calculated to have a $t_{1/2}$ of 32 hr. This was consistent with the 43 hr calculated from the time for P-450E to reach half the induced steady state. $[^{14}\text{C}]$ incorporation peaked at 8 hr, indicating a lag between leucine and ALA incorporation into the holoenzyme. The subsequent decline in $[^{14}\text{C}]$ was relatively slow, leading to a calculated heme $t_{1/2}$ of 104 hr. Further studies of heme and apoprotein turnover will be needed to firmly establish the roles of these players in the regulation of P-450E expression.

This study addressed, on a molecular level, how xenobiotics in the marine environment elicit a biochemical response-induction of P-450E - in marine teleosts.

Supported by: The National Science Foundation through grant Number OCE-83-10505; the United States Public Health Service through contract Number ES-4220; and the United States Environmental Protection Agency through contract Numbers CR-813155-01-0 and CX-813567-01-1.

SWIMMING BEHAVIOR AND ENERGETICS OF SHARKS

Jill V. Scharold

In a field study of blue shark swimming behavior, acoustic telemetry was used to record depth, swimming speed and tailbeat frequency from free-ranging blue sharks (*Prionace glauca*) in northwestern Atlantic slope waters. Records obtained from five sharks show a consistent pattern of vertical migration between the surface and depths as great as 450 meters, with the deepest dives occurring during the daytime and

shallower dives at night. Mean swimming speed was 44.5 ± 1.6 ($X \pm S.E.$) $\text{cm} \cdot \text{s}^{-1}$ (0.179 ± 0.014 $\text{lengths} \cdot \text{s}^{-1}$) for three sharks, with short bursts up to $180 \text{ cm} \cdot \text{s}^{-1}$. Mean tailbeat frequency was 0.335 ± 0.021 $\text{beats} \cdot \text{s}^{-1}$. Measurement of swimming speed and rate of vertical movement during dives permits calculation of angles of ascent and descent. For 84 dives deeper than 50 m, the descent angle averaged 8.0 ± 0.7 degrees from the horizontal while the ascent angle was 6.4 ± 0.5 degrees. Tailbeat records indicate that blue sharks actively swam downward during most of the descent, with brief periods of gliding which appear to be associated with the most rapid descent rates. The observed diving behavior does not match that predicted by theory to be energetically optimal for migration, and may instead represent a strategy for encountering and capturing prey.

Heart rate, metabolic rate and activity were simultaneously recorded in the laboratory from lemon sharks (*Negaprion brevirostris*) during rest and spontaneous exercise, and from leopard sharks (*Triakis semifasciata*) during steady swimming at controlled speeds to evaluate the usefulness of heart rate as a measure of field metabolic rate. Heart rate was monitored by acoustic telemetry using a frequency modulated ECG transmitter, and metabolic rate was measured as oxygen consumption rate. For seven lemon sharks at 25°C , mean resting values for heart rate and oxygen consumption rate were 52.0 ± 0.4 (S.E.) $\text{beats} \cdot \text{min}^{-1}$ and 162.0 ± 2.0 (S.E.) $\text{mg O}_2 \cdot \text{kg}^{-1} \cdot \text{hr}^{-1}$, respectively. Both parameters increased significantly ($p < .001$) during swimming, to means of 55.9 ± 0.2 $\text{beats} \cdot \text{min}^{-1}$ and 233.6 ± 2.3 $\text{mg O}_2 \cdot \text{kg}^{-1} \cdot \text{hr}^{-1}$, at a mean swimming speed of 0.400 ± 0.003 $\text{body lengths} \cdot \text{s}^{-1}$. For seven leopard sharks at 16°C , mean resting heart rate and oxygen consumption rate were 36.6 ± 1.8 $\text{beats} \cdot \text{min}^{-1}$ and 15.3 ± 35.6 $\text{mg O}_2 \cdot \text{kg}^{-1} \cdot \text{hr}^{-1}$. While swimming at the maximum sustained speed (0.84 ± 0.03 $\text{lengths} \cdot \text{s}^{-1}$) for 30-60 minutes, these rates were 46.9 ± 0.9 $\text{beats} \cdot \text{min}^{-1}$ and 229.3 ± 13.2 $\text{mg O}_2 \cdot \text{kg}^{-1} \cdot \text{hr}^{-1}$. The observed elevations in heart rate from rest to exercise account for 20% of the increase in oxygen uptake in the lemon shark and 32% in the leopard shark, leaving the remainder to be brought about by increases in stroke volume and/or arteriovenous oxygen difference. Significant linear regressions of oxygen consumption rate on heart rate were obtained for both lemon sharks and leopard sharks; separate regressions were obtained for individual lemon sharks. Heart rate was approximately as closely correlated to oxygen consumption rate as was swimming speed.

Supported by: National Science Foundation through grant Numbers OCE-83-11512, and OCE 87-43949.

EFFICIENT REPRESENTATION OF THE HYDROGRAPHIC STRUCTURE OF THE NORTH ATLANTIC OCEAN AND ASPECTS OF THE CIRCULATION FROM OBJECTIVE METHODS

Ichiro Fukumori

The general theme of this thesis is the study of systematic mathematical techniques for determining the ocean circulation from classical hydrographic data. Two aspects of this theme are analyzed. The first is finding an efficient representation of hydrographic structure so as to make it most useful and informative. The second is application of inverse methods to the data to determine ocean circulation. Both subjects are examined in the North Atlantic Ocean.

The efficient representation is examined in terms of empirical orthogonal functions (EOFs) among the variations in vertical hydrographic profiles. The data used are of a new set of high quality hydrography, all obtained in the early 1980s. Common EOFs are examined among temperature, salinity, oxygen, phosphate, silicate, and nitrate. The EOFs identify a fundamental simplicity in the spatial distributions of these properties. Although the volume of numbers involved in the raw data is large, the significant degrees of freedom are only six in space and two among the six properties; temperature and salinity are represented by one mode, while the nutrients by another. The modal structure reflects some underlying simplicity in ocean physics. EOFs form a quantitative basis from which models of the ocean's hydrographic structure can be constructed for various degrees of complexities.

As for the second aspect, two applications of inverse methods are explored on small regional scales. The first problem addressed concerns the circulation inside a 12° square located in the eastern basin over the axis of the Mediterranean Water tongue. The study is based on an ocean model constructed by mapping the modes identified in the first half of the thesis over the entire North Atlantic Ocean. A combination of a box model inverse and β -spiral method is used to determine the geostrophic reference level velocities. The circulation consists of an anticyclonic circulation near the surface, which is part of the eastern half of the wind-driven subtropical gyre. The flow at depth is weak, and is a cyclonic circulation around the core of the mediterranean Water tongue.

In the second inverse problem, we examine a decaying warm-core ring. Observations of a warm-core ring are used to formulate a model for diagnosing the physics of ring change over a two month period. About 30 hydrographic casts and

acoustic doppler current measurements are used to generate estimates of an equivalent radially symmetric ring with radial contrasts of stratification, temperature, salinity, azimuthal velocity, angular momentum, and potential vorticity. A series of related models are inverted for the ring circulation and mixing coefficients. The circulation is insensitive to the model details, is well-resolved, and is a radial outflow and upwelling. Eddy coefficients are only partially resolved; determining the mixing with any degree of confidence appears to require a much more elaborate data set than the one available.

Supported by: The Office of Naval Research (Secretary of the Navy Chair) and the National Science Foundation through grant Number OCE-85-21685 through the Massachusetts Institute of Technology.

THE TRACE METAL GEOCHEMISTRY OF SUSPENDED OCEANIC PARTICULATE MATTER

Robert M. Sherrell

Vertical profiles of suspended particulate trace metals were measured in the Sargasso Sea near Bermuda and in the California Current, northwest Pacific. Using a new *in situ* pump, sufficiently large samples of particulate matter (order 10mg) were collected to allow measurement of a suite of trace metals as well as major component elements, using several different leaching techniques on separate subsamples.

Concentrations of particulate Cu, Zn, Co, Cd, Ni, and Pb near Bermuda were determined to be substantially lower than estimates based on previously published work. Concentrations of the more abundant elements Al, Fe, and Mn were similar to previous estimates.

Vertical profiles of Mn, Co, Pb, Zn, Cu, and Ni (mol/l) at Bermuda displayed similar features: a relative depletion in surface waters, a relative maximum in the upper thermocline, and relatively constant deep water concentrations. The similarity in the vertical variations of dissolved/particulate fractionation for these metals may be caused by interaction of dissolved metals with authigenic Mn phases; the fractionation is anti-correlated with other major particle components (organic carbon, calcium carbonate, opal, and aluminosilicate). The vertical profile of particulate Cd displayed a different form; enrichment at the surface and decreasing concentrations through the thermocline to constant deep water values.

These measurements were incorporated into a steady-state two-box flux model for the Bermuda station. Estimates of the residence time of small suspended particles suggest that metals associated

with these particles contribute less than half of the total flux observed in deep ocean sediment traps. This result held for metals displaying a wide variety of behaviors in their dissolved profiles, and suggests that processes occurring in the upper ocean and more important determinants of metal removal from the open ocean environment than dissolved/particulate interactions in the deep ocean.

The interactions between suspended particulate and dissolved Pb were investigated further by an analysis of the isotopic composition of Pb in each pool. Profiles of particulate $Pb/^{210}Pb$ and $^{206}Pb/^{207}Pb$ were virtually identical to contemporaneous seawater profiles for the same tracer ratios in the upper 2000m at Bermuda, indicating isotopic equilibration on a time scale which is rapid relative to the residence time of suspended particles in the water column (a few years), and to the time rate of change of the non-steady state dissolved profiles (years-decades). Analysis of the relative contribution of deep suspended particles to the total deep ocean downward flux suggests that the Pb isotopic composition of material delivered to the sediments will increasingly resemble that of deep ocean suspended matter as the anthropogenic input of Pb to the surface decreases over the next few years-decades. These results support a relatively rapid and reversible exchange of Pb between solution and particles.

The particulate metal distribution in the Sargasso Sea were compared with those observed at a station in the California Current, characterized by higher productivity, closer proximity to continental and hydrothermal particle sources, and the distinct dissolved metal distributions of the northwest Pacific. This provided an opportunity to observe the effect of bulk particle composition and dissolved metal concentration on dissolved/particulate metal fractionation. Although concentrations of non-aluminosilicate particulate metals were of the same order (generally within a factor of two) at the two stations, the differences are significant and are not generally proportional to differences in the dissolved distributions. Particulate contents of Mn, Co, Cu are lower by a factor of 2-3 in mid-waters at the Pacific site, despite similar dissolved concentrations. In contrast, particulate concentrations of the nutrient-type elements Zn, Ni, and Cd were less than 50% greater at the Pacific station, although dissolved metal concentrations are several times higher. Of the metals investigated, only Pb showed similar dissolved/particulate fractionation at both stations. The evidence indicated that metal partitioning in the open ocean water column varies in response to factors which are outside the predictive capability of simple chemical exchange

models.

Supported by: The Office of Naval Research and the National Science Foundation through the Massachusetts Institute of Technology.

RATES OF VERTICAL MIXING, GAS EXCHANGE, AND NEW PRODUCTION: ESTIMATES FROM SEASONAL GAS CYCLES IN THE UPPER OCEAN NEAR BERMUDA

William S. Spitzer

Argon measurements, obtained from three years of monthly detailed vertical profiles near Bermuda (Station S, 32°N 64°W), show a maximum in argon supersaturation of about 4% in the seasonal thermocline in late summer. Since the argon supersaturation is 3-4 times smaller than that of oxygen, most of the oxygen supersaturation is not of physical origin and hence must result from biological production.

In the winter mixed layer, air injection produces argon supersaturation despite high gas exchange rates. During spring and summer, radiative heating, air injection, and an upward argon flux create an even larger supersaturation in the mixed layer. In the seasonal thermocline, radiative heating creates argon supersaturation that persist in spite of vertical mixing.

The observed seasonal cycles of temperature, argon, helium, and oxygen are simulated with an upper ocean model. I linearize the model's response to variations in vertical diffusivity, air injection, gas exchange rate, and new production and then use an inverse technique (singular value decomposition) to determine the values of these parameters that best fit the data. Results for the 1985-1987 average are as follows: A vertical turbulent diffusivity of $1.0 \pm 0.1 \times 10^{-4} \text{ m}^2 \text{ s}^{-1}$ is consistent with both the thermal history of subsurface argon distribution. The rate of air injection, determined to $\pm 15\%$, is similar to previous estimates. The seasonally-averaged gas exchange rate, determined to $\pm 11\%$, is consistent within errors with that predicted by Liss and Merlivat (1986). I estimate a lower limit to depth-integrated new production below the mixed layer of $5.0 \pm 1.0 \text{ moles O}_2 \text{ m}^{-2} \text{ yr}^{-1}$, and obtain an estimate of $6.2 \pm 0.9 \text{ moles O}_2 \text{ m}^{-2} \text{ yr}^{-1}$ if new production in the mixed layer is fixed at zero. The period 1985-1987 appears to be typical of the climatological mean conditions at Station S and comparable to the 1960-1970 average period analyzed by Jenkins & Goldman (1985) and Musgrave *et al.* (1988).

I propose that a mesoscale anticyclonic eddy is responsible for excess ^3He and nitrate in the euphotic zone observed at a July, 1986 occupation

by Brundage & Dugan (1986), characterized by an unusually thick lens of subtropical mode (18°C) water. Analysis of the 35 year hydrographic record suggests that such eddies may arrive at Station S with an average frequency of 2-6 times per year, mostly during the summer and in years of vigorous 18°C water formation. Their timing and character suggest that they may be formed during winter convection events in the northeastern Sargasso Sea, advected southwestward by the gyre-scale circulation, and eventually absorbed by the Gulf Stream. Their magnitude and frequency indicate that they may supply a significant portion of the ^3He and nutrient flux into the euphotic zone near Bermuda, and suggest a mechanism by which newly formed subtropical mode water is incorporated within the gyre interior. However, enhanced new production in such eddies could account for only a small portion of the new production integrated over the Sargasso Sea.

Supported by: The National Science Foundation through grant Number OCE 85-01171.

DIFFUSION OF HELIUM ISOTOPES IN SILICATE GLASSES AND MINERALS: IMPLICATIONS FOR PETROGENESIS AND GEOCHRONOLOGY

Thomas W. Trull

Helium mobility in geologic materials is a fundamental constraint on the petrogenetic origins of helium isotopic variability and on the application of radiogenic and cosmogenic helium geochronology.

^3He and ^4He volume diffusivities determined at 25-600°C in basaltic glasses by incremental-heating and powder storage experiments (using a diffusion model incorporating grain size and shape information to obtain high precision) are three to four orders of magnitude greater than for common cations. Diffusion in tholeiitic glass can be described by an Arrhenius relation with activation energy = 16.85 ± 1.3 Kcal/mole and $\log D_0 = -2.37 \pm 0.06$, although low temperature data are better described by a distribution of activation energies model. The best estimate for D at 0°C in tholeiitic glass is $5 \pm 2 \times 10^{-16}$ cm²/s, an order of magnitude higher than the results of Kurz and Jenkins (1981) but lower than suggested by Jambon, Weber and Begemann (1985). Measurements in an alkali basalt show that helium diffusion is composition dependent ($E_a = 14.4 \pm 5$ Kcal/mole; $\log D = -3.24 \pm 2$), and roughly five times faster than in tholeiites at seafloor temperatures. The corresponding timescales for 50% helium loss or exchange with seawater (1 cm spheres) are about one million years for mid-ocean-ridge-basalts, and about

100,000 years in seamount alkali basalts. Radiogenic ^4He diffusion has a higher activation energy (27 ± 2 Kcal/mole; $\log D = +2.4 \pm 1.0$) than inherited (magmatic) helium, suggesting very low mobility ($D = 3 \times 10^{-19}$ cm²/s at 0°C; factor of 5 uncertainty) and that U+Th/ ^4He geochronology of fresh seafloor basalt glasses is unlikely to be hampered by helium loss.

Measured isotopic diffusivity ratios, $D^3\text{He}/D^4\text{He}$, are not composition dependent, average 1.08 ± 0.02 , and very slightly with temperature, consistent with an activation energy difference of 60 ± 20 cal/mole. This result differs from the inverse-square-root of mass prediction of 1.15, and may be explained by quantization of helium vibrational energies. These results suggest preferential loss of ^3He will be minimal at low temperature ($D^3\text{He}/D^4\text{He} = 1.02 \pm 0.03$ at 0°C). Therefore, alteration of magmatic $^3\text{He}/^4\text{He}$ ratios in basaltic glasses on the seafloor will occur only by helium exchange with seawater, and be important only for samples with low helium contents ($< 10^{-8}$ ccSTP/g), such as those found in island arc environments. Extrapolating the glass results to magmatic temperatures yields diffusivities similar to melt values, and suggests $D^3\text{He}/D^4\text{He}$ approaches 1.15 at these and higher temperatures.

Helium diffusivities in olivine and pyroxene at magmatic and mantle temperatures (900-1400°C) are higher than for cations, ($E_a = 100 \pm 5$ Kcal/mole, $\log D_0 = +5.1 \pm 7$; and 70 ± 10 Kcal/mole, $\log D_0 = +2.1 \pm 1.2$, respectively), but are still too low to transport or homogenize helium in the mantle or even in magma chambers. However, diffusion equilibrates melts and mantle minerals within decades, and interaction with wall-rocks may be enhanced for helium in comparison to other isotopic tracers because of its greater mobility. Rapid exchange of helium within xenoliths and with their host magmas set limits on origin depths and transport times for xenoliths which exhibit helium isotopic disequilibrium between minerals, or between the magma and the xenolith. Phenocrysts equilibrate helium too rapidly to exhibit zoned isotopic compositions, and are likely to retain magmatic helium quantitatively in rapidly cooled volcanic extrusives. The 100-fold higher He diffusivity in pyroxene than olivine at 1000°C allows diffusive loss effects to be evaluated in more slowly cooled rocks, when cogenetic minerals can be measured.

Diffusivities of cosmic-ray produced ^3He in surface exposed rocks are several orders of magnitude higher than for inherited helium. However, activation energies for olivine and quartz, 25 ± 4 Kcal/mole ($\log D_0 = -3.7 \pm 8$) and 25.2 ± 9 Kcal/mole ($\log D_0 = +2 \pm 4$) respectively, still suggest low diffusivities at surface temperatures of approximately 10^{-22} and 10^{-20} cm²/s. Equations for simultaneous helium production and diffusive

loss allow model ages for surface exposure to be corrected for helium loss, and demonstrate that cosmogenic ^3He geochronology will not be limited by helium loss for timescales of approximately 1 million years in quartz and 10 million years or more in olivine. The measurements also suggest that radiogenic ^4He produced by U and Th decay may be useful dating method in quartz.

Application of the diffusion measurements demonstrates that part of the wide range of $^3\text{He}/^4\text{He}$ ratios (.01 to $9 R_a$) of a suite of dredged basalts and andesites from the Woodlark Basin, (western Pacific) reflects post-eruptive helium addition, from seawater in glasses with low He contents and from U and Th decay in mafic mineral separates. In unaltered samples, $^3\text{He}/^4\text{He}$ ratios for tholeiites from the Woodlark Spreading Center are $8-9 R_a$, similar to mid-ocean-ridges, but distinctly different than the ratio of $6.9 \pm 2 R_a$ observed in Kavachi submarine volcano basaltic andesites. Helium isotopic systematics in cogenetic pyroxenes and olivines from these samples demonstrate that this is a magmatic signature, and not the result of preferential ^3He loss by diffusion. Coupled Sr and He isotopic systematics in these and other samples from the region suggest the sub-arc mantle has been enriched in radiogenic helium supplied by subducted Pacific lithosphere.

Supported by: The National Science Foundation through grant Numbers OCE 85-16082; OCE 87-16970, and EAR 88-3783.

TRACE METAL SOURCES FOR THE ATLANTIC INFLOW TO THE MEDITERRANEAN SEA

Alexander F.M.J. van Geen

Cu, Cd and Zn concentrations over a 40 km long portion of the Spanish continental shelf are an order of magnitude higher than enrichments generally found in coastal water. All samples were analyzed with a simple device which automates the pre-concentration of Cu, Ni, Cd, Zn and from seawater and fresh water by bis (2-hydroxyethyl) - dithiocarbamate-metal complex retention on a hydrophobic column. Enrichments observed over the Spanish shelf are sufficient to influence the composition of the Mediterranean because Spanish coastal water is entrained in the inflow to the Alboran Sea. Trace metal and ancillary data for 172 samples from the Gulf of Cadiz collected in April and October '86 confirm that Spanish shelf water dominates Cu, Cd and Zn fluxes through the Strait of Gibraltar. Following a review of alternative explanations, a shelf "metal-trap" mechanism is presented in order to reconcile the magnitude of observed metal enrichments with their geographical distribution and seasonal

variability. A simple box model of the metal-trap indicates this mechanism must be operating over the whole length of the Iberian Atlantic coast (rather than the Gulf of Cadiz only) in order to support the important metal sink through the Strait of Gibraltar.

The three water masses originating in the Atlantic and entering the Alboran Sea through the Strait of Gibraltar are (1) Atlantic surface water, (2) North Atlantic Central Water and (3) Spanish shelf water, based on salinity and Cu, Ni, Cd and Zn concentrations. A conservative mixing model of these end-members is solved by weighted least-squares and shown to be consistent with tracer data for 43 surface stations in the Strait of Gibraltar. Spanish shelf water is restricted to the northern half of the Strait and can be traced as a plume in the Alboran Sea. On three occasions (April '86, June '82 and October '86), salinity, Cu, Ni, Cd and Zn distributions in the surface Alboran Sea are consistent in most cases with conservative mixing of the three previously defined end-members with Mediterranean water. A metal enriched plume originating from the Spanish shelf was present in the Alboran Sea during all three sampling periods, but was significantly stronger in June '82.

Cu, Cd and Zn flux estimates at the Strait of Gibraltar for the Atlantic inflow and the saline outflow confirm that Spanish shelf water influences the composition of a basin as large as the Mediterranean. In- and outflow are roughly in balance for these elements. In contrast to Cu, Cd and Zn, Ni concentrations for the inflow are a factor of two lower than the Mediterranean outflow. Estimates of metal sources within the basin indicate the difference may be due to river input. Estimates of atmospheric input of Cu, Cd, Ni and Zn are an order of magnitude higher than either the uncertainty in the difference between in- and outflow concentrations, or the east-west gradient in surface water concentrations of the Mediterranean. This is true when aerosol input of these elements is scaled to the observed change in dissolved Al concentration in the water column and enrichment factors in aerosols relative to the crust from either the remote Pacific ocean, the Atlantic ocean or the Mediterranean Sea. The discrepancy may indicate either significant scavenging of trace elements in the Mediterranean, or that enrichment factors measured in aerosols are not representative of the composition of the dust input which dissolved in the water column.

Supported by: The Office of Naval Research through the Massachusetts Institute of Technology.

OCEAN BOTTOM SEISMIC SCATTERING

Martin E. Dougherty

Seismic studies of the oceanic crust, both experimental and theoretical, often assume a flat seafloor and laterally homogeneous crust. This is done regardless of the appearance in seismic data of obvious effects due to scattering from lateral heterogeneities both on and in the seafloor. Detailed fine scale surveys of mid-ocean ridges, where the upper oceanic crust is exposed, have revealed the presence of lateral heterogeneities in the form of complicated topography, extrusive volcanic structure, and abundant fracturing and faulting. These heterogeneities have a significant affect on the propagation of seismo/acoustic energy through the crust, especially in the immediate vicinity of the seafloor. This thesis deals with the problem of scattering of seismo/acoustic energy from a number of forms of lateral heterogeneity in the upper oceanic crust.

A common theme throughout this work is that the size of the heterogeneity on or in the seafloor is of the same order of magnitude as the seismo/acoustic wavelength. This is the realm of scattering theory where the wave-like characteristics of seismic energy have a particularly large influence on the outcome of interaction with structure in the media. The work presented here involves the application of the finite difference modeling technique to problems concerning laterally heterogeneous elastic media. This method is a full wave solution to the elastic wave equation and as such includes all wave interactions with the media. The finite difference formulation is used to study four distinct phenomena; scattering from discrete deterministic seafloor features; wave propagation through continuous randomly heterogeneous upper oceanic crust; scattering from more complicated topographic profiles and the limitations of the method for the rough seafloor problem; and the problem of plane acoustic wave scattering from an infinite elastic cylinder.

The principal finding of this work is that lateral heterogeneities in the upper oceanic crust can have a dramatic affect on seismo/acoustic wave propagation. Scattering from rough seafloors and/or volume heterogeneities is often quite similar and causes the occurrence of signal generated "noise" (coda), decorrelation of primary arrivals, and anomalies in arrival travel time and amplitude. Topographic and volume scatterers acting as secondary sources of seismic energy can cause a resonant coupling of body wave energy into interface (Stoneley) waves at the seafloor. This is possibly one mechanism by which natural seismic and storm generated acoustic energy can be

coupled into seafloor noise.

The applicability of the use of the finite difference method for non-planar water-solid interfaces is also discussed. Models were calculated which approximate sinusoidal seafloors and plane acoustic wave scattering from an infinite elastic cylinder. The discretization of a rectangular difference grid must be extremely fine to accurately accommodate a smoothly varying water-solid interface which does not align with the grid. Regardless of the discretization concerns, the rough seafloor models presented here demonstrate the arrivals expected from larger scale sinusoidal topography as well as the importance of considering quite small ($\lambda/15$ wavelength) topographic features in the scattering problem. Also, steep topography will allow seismo/acoustic energy to enter the seafloor at very large ranges because the angle of incidence can repeatedly fall below the critical angle for transmitted energy, especially for converted shear energy. Ray theoretical shadow zones do not occur in these models (or in the real world) because of Franz-type waves diffracting into areas where the grazing angle is less than zero.

Supported by: Office of Naval Research under Contract Number N00014-85-C0001 and the National Science Foundation through grant Number OCE 8761132.

TIDAL DYNAMICS AND DISPERSION AROUND COASTAL HEADLANDS

Richard P. Signell

This thesis concerns the dynamics of tidal currents and tide-induced dispersion around coastal headlands. The depth-averaged shallow water equations forced by a oscillatory x -directed current with amplitude U_0 and frequency σ are solved numerically for a Gaussian headland described by $\zeta(y) = b \exp[-1/2(x/a)^2]$. The water depth H is constant except for a shoaling region along the boundary which is narrow compared to the headland width b .

Solutions to this idealized tidal flow around a headland reveal a wide range of dynamical behavior, from quasi-linear, non-separating flow to strongly nonlinear, separating flow with transient eddy formation. During each half tidal cycle, transient eddies are formed when vorticity generated in the narrow shoaling region along the headland separates from the coast and wraps up to form a large scale transient eddy. For a fixed headland shape, the structure of the flow depends primarily on the relative sizes of the tidal excursion $[2U_0/\sigma]$, the frictional decay length scale $[H/2C_D]$ (where C_D is the depth-averaged drag coefficient), and the length scale of the headland a

frictional Reynolds number $Re_f = [H/C_D a]$. If the frictional length scale is much longer than the tidal excursion, then the flow is controlled by $K_c = [U_o/\sigma a]$. In many tidal flows, the frictional length scale is comparable to the tidal excursion, and both Re_f and K_c control the structure of the flow.

Material released in the vicinity of the headland is stretched and folded by the high strain and transient eddy formation associated with the strongly nonlinear tidal flow, resulting in much greater dispersion than that associated with tidal turbulence. The character and extent of particle dispersion depends strongly on the interior vorticity structure arising from the boundary layer separation, and cannot be accurately described by a uniform eddy diffusivity when separation occurs.

Supported by: National Science Foundation under grant Numbers OCE 87-11031 and OCE 87-16937, by the National Center for Atmospheric Research, and by the Woods Hole Oceanographic Institution's Ocean Ventures Fund and Coastal Research Center.

ACOUSTIC TOMOGRAPHY IN THE STRAITS OF FLORIDA

David B. Chester

Variability of the Florida Current has been monitored via acoustic tomography. A reciprocal tomography experiment was conducted in the eastern half of the Florida Straits during mid October and November, 1983. A triangular array of transceivers, with leg separations of approximately 45 kilometers, was deployed at 27°N. The presence of a surface mixed layer in the region allowed for the ducted propagation of acoustic energy in the surface layer. A deeper layer was sampled by an unresolved group of refracted, bottom reflected ray arrivals. Incorporating the complete set of arrivals, we are able to obtain depth dependent estimates of the temperature field, current velocity, and relative vorticity. The oceanography of the region has been shown to be dominated by the lateral shifting of the surface and subsurface core of the Florida Current. The influx of westward flowing water through the Northwest Providence Channel at 26°N also appears as a large scale signal in the eastern Florida Straits. Low frequency fluctuations of temperature, current velocity, and vorticity occur at periods ranging from several days to nearly two weeks, and are intimately related to meandering of the Florida Current system.

Supported by: ONR Contract N00014-86-K-0751.

COLLINEAR ANALYSIS OF ALTIMETER DATA IN THE BERING SEA

Deborah K. Barber

Eighteen months of sea height data from the GEOSAT altimeter along collinear subtracks were analyzed for information on the circulation pattern in the Bering Sea. Seventy subtracks from both ascending and descending orbits, with as many as 35 repeat cycles along each subtrack, were analyzed. Orbit errors were removed from the height data using a least-squares fit to a cubic polynomial, weighted by the inverse of the height variance. Addition of the weights decreased contamination of residual height profiles by the large geoid signal. Composite maps of variability along each track revealed patterns of increased variability in the regions of the documented Bering slope current (BSC) and the proposed western boundary current (WBC); however, no evidence was found of the expected bifurcation of the BSC near the Siberian coast. Past observations of tides in the Bering Sea were reviewed along with a local tide model to detect tidal contributions to the mesoscale sea surface height variability. The tidal analysis suggested that residual tides contributed primarily to the longer wavelengths which were removed in the collinear processing. Examination of the Schwiderski tidal correction proved it to be a sensible correction, reducing the height variance by approximately 60%. Finally, using a Gaussian model for the BSC velocity profile, synthetic residual heights were generated and fit to the actual data to produce estimates of absolute surface geostrophic velocity and transport. Comparisons of mean flow, height fluctuations and seasonal trends across the BSC, and WBC and Bering Strait support the hypothesis that the BSC turns north at Cape Navarin into the WBC which, in turn, is capable of supplying a major part of the transport through the Bering Strait.

THE STRUCTURE OF THE KUROSHIO WEST OF KYUCHU

Changsheng Chen

A triangular CTD/ADCP survey was made across the Kuroshio west of Kyushu aboard the R/V Thompson during January, 1986 in order to investigate the water properties and flow field in the Kuroshio. A similar CTD survey was made in July, 1986 aboard the R/V Washington to study the seasonal variability in the Kuroshio.

The Kuroshio in this region exhibited a marked seasonal change in its nearsurface stratification and water properties. In January, the Kuroshio water was separated from the vertically

well-mixed coastal water over the shelf by a strong front located near the shelf break. Horizontal mixing between the Kuroshio and coastal water was observed but was limited near the shelf break. In July, surface coastal water extended far past the shelf break over the Kuroshio region near the surface, and in turn, Kuroshio water intruded onto the shelf near the bottom. Mixing between the Kuroshio and coastal water was found over much of the mid and outer shelf and upper slope, spanning a cross-stream distance of 75 km. In addition, evidence of deep vertical mixing within the Kuroshio itself was found near 32.0°N and 128.2°E., most likely due to internal tidal mixing over the slope.

Since Loran C navigation coverage in the study region was poor during the R/V THOMPSON cruise, a simple averaging technique has been used to convert the ADCP data into an absolute velocity. An error analysis shows that the total error in the absolute ADCP velocity was about ± 5 cm/s. The absolute geostrophic velocity using the absolute Doppler velocity at 60 m as the reference velocity was then calculated for the sides of the triangle. The results show that the ADCP velocity shear was in good agreement with the geostrophic shear in the Kuroshio. The Kuroshio flowed through the western section as a coherent current, then split into two streams around a tall seamount as it left through the eastern section. Some recirculation also occurred between the core of the Kuroshio and the slope as well as near the seamount. The geostrophic velocity field calculated relative to the bottom missed some of the important features of the true flow field such as splitting of the Kuroshio and the recirculation in the slope region.

The volume, salt and heat transports of the Kuroshio during the January 1986 survey have been calculated using the absolute geostrophic velocity and CTD data. The volume transport of the Kuroshio west of Kyuchu in January 1986 was 31.7 ± 2.0 Sv, which is comparable to that of the Gulf Stream in the Florida Strait. The volume transport through the triangle was conserved within measurement uncertainty, so that a streamfunction field can be defined by the transport. The resulting streamlines clearly show the structure of the flow field in the Kuroshio west of Kyushu in January 1986 was $28.2 \pm 1.8 \times 10^{14}$ W. The salt transport in January 1986 was about $108.0 \pm 7.3 \times 10^{10}$ kg/s, and the net salt flux zero within measurement error.

Analysis of the potential vorticity based on the January 1986 absolute geostrophic velocity field shows that the total potential vorticity in the Kuroshio may be approximately given by the product of the vertical gradient of the potential density and the sum of the planetary and relative vorticities. The distribution of relative vorticity

plays a significant role in determining the structure of the potential vorticity in the Kuroshio. The path of the Kuroshio can be traced in the field of potential vorticity. Facing in the direction of the current, the axis of the maximum velocity is located to the right of the core of maximum potential vorticity. Finally, the Kuroshio was potentially unstable since the gradient of potential vorticity changed its sign on potential density surfaces across the Kuroshio.

A NUMERICAL MODEL OF MIXING AND CONVECTION DRIVEN BY SURFACE BUOYANCY FLUX

Xiaoming Wang

This thesis studies mixing and convection in a rectangular basin driven by a specified heat flux at the surface. A numerical model is constructed for this purpose. The main focus of the study is on the density and circulation structure resulting from the thermal forcing.

In chapter two, a simple vertical one-dimensional model is developed to examine the mixing processes under a given surface heat flux. In order to simulate strong vertical mixing in the region where stratification is unstable, turbulent processes are modeled by a convective overturning parameterization of eddy viscosity and diffusivity. The results show that the density structure is strongly affected by the convective overturning adjustment as surface cooling prevails, and the resulting density field is nearly depth independent.

In chapter three, a more complicated two-dimensional model is constructed to simulate mixing and circulation in a vertical rectangular basin with rigid boundaries. The aspect ratio of the basin ranges from 1 to 0.001 and Rayleigh number for 10^4 to 2×10^{12} . It is found that the circulation pattern is dominated by these two important numbers. The roles of density overturning and density-momentum overturning mixing are further investigated. The results show that the convective overturning not only homogenizes the density field in the unstably stratified region but also contributes to increase the circulation. A crude scale analysis of the system shows that the characteristics of the density and momentum fields from the analysis agree well with the numerical results.

Supported by: Massachusetts Institute of Technology.

DEEPLY-TOWED UNDERWATER VEHICLE SYSTEMS: A VERIFIED ANALYTICAL PROCEDURE FOR CREATING PARAMETERIZED DYNAMIC MODELS

Franz S. Hover

The dynamics of deeply-towed cable/vehicle systems are governed by nonlinear partial differential equations and as a result, trajectory control is generally difficult using the available techniques. This work examines the possibility of utilizing parametric dynamics models in differential equation form, to present a far more tractable controls problem. A learning-model method for generating accurate approximations of this type is used, and the identification process is unique in that an analytically-based model provides the primary data sets, allowing for *a priori* characterization of system responses without using any real data. The performances of the parametric forms are then *verified* through comparison of model output against actual sea data obtained during recent cruises in the Caribbean and Mediterranean Seas. The respective merits and limitations of several different model structures are discussed, with respect to both pure performance and identification efficiency.

Supported by: Office of Naval Research Fellowship.

A CONTROL SYSTEM DESIGN TECHNIQUE FOR NONLINEAR DISCRETE TIME SYSTEMS

David M. DeLonga

A new control methodology is proposed for use with a class of nonlinear, single-input discrete time systems. The technique is based on a discrete time approach that parallels existing continuous time sliding surface concepts. Modifications to the basic algorithm allow for system models with time-variant or uncertain parameters, time delays in the control input, and external disturbances. A major feature of the method is its straightforward extension to an adaptive control form which can be used to improve performance and maintain stability in the presence of large parametric uncertainty or time-variant behavior. Techniques are proposed for overcoming instabilities that frequently arise when using adaptive control schemes based on reduced order system models or in the presence of disturbances.

A framework is provided for the practical application of the methodology to continuous time systems. The discrete time nature of the development makes it especially well suited to

applications where sensor data is infrequently available or computational power is limited. An experimental study is performed using an underwater remotely operated vehicle to verify the validity of the approach. The ability of the method to use a nonlinear model and adapt to large parametric uncertainty is shown to result in improved performance over the use of a linear or time-invariant model.

Supported by: Office of Naval Research through contract Numbers N00014-36-C-0038 and N00014-87-J-1111.

ACOUSTIC DIFFRACTION FROM A SEMI-INFINITE ELASTIC PLATE UNDER ARBITRARY FLUID LOADING WITH APPLICATION TO SCATTERING FROM ARCTIC ICE LEADS

Peter H. Dahl

The problem of a low-frequency acoustic plane wave incident upon a free surface coupled to a semi-infinite elastic plate surface, is solved using an analytic approach based on the Wiener-Hopf method. By low-frequency it is meant that the elastic properties of the plate are adequately described by the thin plate equation ($kH \leq 1$). The diffraction problem relates to issues in long range sound propagation through partially ice-covered Arctic waters, where open leads to polynya on the surface represent features from which acoustic energy can be diffracted or scattered. This work focusses on ice as the material for the elastic plate surface, and, though the solution methods presented here have applicability to general edge diffraction problems, the results and conclusions are directed toward the ice lead diffraction process.

The work begins with the derivation of an exact solution to a canonical problem: a plane wave incident upon a free surface (Dirichlet boundary condition) coupled to a perfectly rigid surface (Neumann boundary condition). Important features of the general edge diffraction problem are included here, with the solution serving as a guideline to the more complicated solutions presented later involving material properties of the boundary. The ice material properties are first addressed using the locally reacting approximation for the input impedance of an ice plate, wherein the effects of elasticity are ignored. This is followed by use of the thin plate equation to describe the input impedance, which incorporates elements of elastic wave propagation.

An important issue in working with the thin plate equation is the fluid loading pertaining to sea ice and low-frequency acoustics, which cannot be characterized by simplifying heavy or light fluid loading limits. An approximation to the exact

kernel of the Wiener-Hopf functional equation is used here, which is valid in this mid-range fluid loading regime. Use of this approximate kernel allows one to proceed to a complete and readily interpretable solution for the far field diffracted pressure, which includes a subsonic flexural wave in the ice plate. By using Green's theorem, in conjunction with the behavior of the diffracted field along the two-part planar boundary, the functional dependence of Π_D (total diffracted power) in terms of k (wavenumber), H (ice thickness), α (grazing angle) and the combined elastic properties of the ice sheet and ambient medium, is determined.

A means to convert Π_D into an estimate of dB loss per bounce is developed using ray theoretical methods, in order to demonstrate a mechanism for acoustic propagation loss attributed directly to ice lead diffraction effects. Data from the 1984 MIZEX (Marginal Ice Zone Experiments) narrow-band acoustic transmission experiments are presented and discussed in this context.

Supported by: Office of Naval Research under contract Number N00014-87-K-0017.

EVOLUTION OF ICELANDIC CENTRAL VOLCANOES: EVIDENCE FROM THE AUSTURHORN PLUTONIC AND VESTMANNAEYJAR VOLCANIC COMPLEXES

Tanya H. Furman

There are several aspects of Icelandic magmatism which are not predicted from its geographic position along the mid-Atlantic Ridge. Specifically, local occurrences of primitive or evolved alkalic lavas and abundant silicic magmas are uncommon in a mid-ocean ridge setting. The focus of this study is to use field, petrologic and geochemical data to understand the petrogenesis of these diverse lava types. Two areas have been investigated: the volcanic Vestmannaeyjar archipelago and the hypabyssal Austurhorn intrusive complex. Vestmannaeyjar is located at the tip of a transgressive ridge segment (the eastern neovolcanic zone); the most recent eruption in this area was Eldfell in 1973. Austurhorn is an evolved central volcano in southeastern Iceland which was active approximately 6-7 Ma and has been exhumed by glaciation. In both areas, the relative contributions of fractional crystallization and crustal melting to geochemical trends among cogenetic magmas have been assessed.

The Vestmannaeyjar archipelago is composed of alkalic lavas erupted at the southern end of the active Eastern Volcanic Zone. Recent eruptions include the most primitive (Surtsey) and evolved (Eldfell) compositions found in this area.

Time-stratigraphic sample suites from both eruptions were studied to characterize the magmatic environment of Vestmannaeyjar. Compositional trends of lavas from the two eruptions are not consistent with fractionation in a near-surface environment, but rather with moderate pressure evolution of small magma batches. At Eldfell, mugearite lavas can be modeled by 30% closed system fractional crystallization of olivine + plagioclase + clinopyroxene + FeTi oxides from cogenetic parental hawaiite. The phase proportions are consistent with an experimentally determined moderate pressure (~8 kbar) cotectic in mildly alkaline systems (Mahood & Baker, 1986). The Surtsey lavas can be modeled by initial crystallization of orthopyroxene + clinopyroxene followed by removal of olivine + plagioclase + clinopyroxene + FeTi oxides. The presence of clinopyroxene with ~8 wt% Al_2O_3 in xenoliths from Surtsey lavas supports a moderate pressure fractionation scenario. Small variations in radiogenic isotopic ratios require limited source heterogeneity or some component of open system behavior. The alkaline nature of Vestmannaeyjar lavas is a primary feature of the parental basalt in this area, not the result of assimilation of lower crustal melts (cf. Oskarsson et al., 1985; Steinthorsson et al., 1985). Magmagenesis in the Vestmannaeyjar propagating rift tip involves small batches of mantle-derived melts which undergo fractionation in isolated pockets at various depths near the base of the lithosphere beneath southern Iceland.

The Austurhorn intrusion is a hypabyssal complex in southeastern Iceland which represents the exhumed remains of an evolved Tertiary central volcano. Field relations at Austurhorn provide convincing evidence for the existence of shallow Icelandic magma chambers, and allow documentation of the physical processes which accompany volcanic evolution. Initial magmatic activity at Austurhorn was basaltic, with a shallow chamber preserved today as a modally layered gabbro body. Felsic magmas were emplaced from below into the cooling gabbro and adjacent crust. Intrusion of felsic magmas into basalts with varying degrees of solidification produced an extensive net veined complex. Felsic replenishment was infrequent enough that a single large convecting felsic body did not develop. Individual felsic units identified in the field generally form small (<500 m extent) sills. Mafic liquids were available throughout the history of the Austurhorn system; the final phase of basalt intrusion forms a NE-trending dike swarm.

Investigation of mineralogic and geochemical trends among contemporaneous, compositionally diverse liquids from Austurhorn provides new insight into the genesis of evolved basalts and rhyolites at Icelandic central volcanoes. Mafic and

Felsic samples have comparable ranges in incompatible trace element ratios (Ba/La, La/Nb) and Sr-and Pb-isotopes (O'Nions & Pankhurst, 1973; B. Hanan, pers. commun., 1988) suggesting derivation from a common mantle source. The Austurhorn suite is strongly bimodal, with maximum MgO content 7.8 wtMgO. Austurhorn basalts are dominantly transitional tholeiitic, and the associated felsic rocks are metaluminous to mildly peralkaline. The distinctive basalt geochemistry and abundance of silicic rocks at Austurhorn are controlled by the crustal structure of an immature rift. A proposed Tertiary rift axis in central Iceland (along which Austurhorn developed) is parallel to the modern western and eastern zones in southern Iceland.

The principle finding of this study is that major and trace element systematics within Austurhorn basaltic and silicic sequences are consistent with progressive fractional crystallization of the observed minerals. Quartz normative basalts can be derived from mildly nepheline normative parental liquid (7.8 wt% MgO) by extensive low pressure crystallization. The inferred crystallizing assemblage of olivine, augite, plagioclase, magnetite and ilmenite is consistent with model mineralogy of the Hvalnesfjall gabbro. The cumulus mineralogy of leucocratic gabbros gives important evidence for fractionation processes in compositional interval not represented by dikes and sills (i.e., the "Daly gap"). Diversity among the mafic dikes reflects several additional factors: (1) crystallization under conditions of variable oxygen fugacity, (2) separate mantle melting events generating a range of Ce/Yb ratios, (3) contamination of a small number of dikes at depth, presumably by interaction with felsic magmas. Major and trace element trends among most felsic samples can be modeled by fractionation of the observed mineral phases: plagioclase, K-feldspar, clinopyroxene, magnetite, ilmenite, apatite. It is possible that crustal melting augments fractional crystallization in producing Icelandic rhyolites. However, most Austurhorn felsic samples are unlike liquids derived by progressive melting of hydrated basalts. Specifically, the Zr, Sr, La systematics of the felsic rocks are inconsistent with melting of a plagioclase- and amphibole-rich source. One felsic dike with petrographic evidence for in situ anatexis has anomalous trace element abundances and an unusually high proportion of ^{206}Pb is interpreted as a melt of an evolved substrate.

Supported by: Office of Naval Research through the Massachusetts Institute of Technology.

MODELLING BOTTOM STRESS IN DEPTH-AVERAGED FLOWS

Harry L. Jenter, II

The relationship between depth-averaged velocity and bottom stress for wind-driven flow in unstratified coastal waters is examined here. The adequacy of traditional linear and quadratic drag laws is addressed by comparison with a 21/2-D model. A 21/2-D model is one in which a simplified 1-D depth-resolving model (DRM) is used to provide an estimate of the relationship between the flow and bottom stress at each grid point of a depth-averaged model (DAM). Bottom stress information is passed from the DRM to the DAM in the form of drag tensor with two components: one which scales the flow and one which rotates it. This eliminates the problem of traditional drag laws requiring the flow and bottom stress to be collinear. In addition, the drag tensor field is updated periodically so that the relationship between the velocity and bottom stress can be time-dependent. However, simplifications in the 21/2-D model that render it computationally efficient also impose restrictions on the time-scale of resolvable processes. Basically, they must be much longer than the vertical diffusion time scale.

Four progressively more complicated scenarios are investigated. The important factors governing the importance of bottom friction in each are found to be 1) non-dimensional surface Ekman depth, u_{*s}/f where u_{*s} is the surface shear velocity, f is the Coriolis parameter and h is the water depth 2) the non-dimensional bottom roughness, z_o/h where z_o is the roughness length and 3) the angle between the wind stress and the shoreline. Each has significant influence on the drag law. The drag tensor magnitude, τ , and the drag tensor angle, θ are functions of all three, while a drag tensor which scales with the square of the depth-averaged velocity has a magnitude, C_d , that only depends on z_o/h .

The choice of drag law is found to significantly affect the response of a domain. Spin up times and phase relationships vary between models. In general, the 21/2-D model responds more quickly than either a constant τ or constant C_d model. Steady-state responses are also affected. The two most significant results are that failure to account for θ in the drag law sometimes leads to substantial errors in estimating the sea surface height and to extremely poor resolution of cross-shore bottom stress. The latter implies that cross-shore near-bottom transport is essentially neglected by traditional DAMs.

Supported by: Office of Naval Research and the National Science Foundation through the Massachusetts Institute of Technology.

AN APPLICATION OF OCEAN WAVE-CURRENT REFRACTION TO THE GULF STREAM USING SEASAT SAR DATA

Michael W. Byman

When ocean waves in deep water interact with a current, the direction of propagation and characteristics of the waves such as height and length are affected. Swell in the open ocean can undergo significant refraction as it passes through major current systems like the Gulf Stream or Atlantic Circumpolar Current. Remote sensing techniques such as synthetic aperture radars (SAR) have the potential to detect wave systems over a wide geographical area. Combining a model for wave refraction in the presence of currents with SAR measurements, the inverse problem of using the measured wave data can be solved to determine the direction and magnitude of the intervening currents. In this study the behavior of swell measured by SAR or a satellite pass over the Gulf Stream is examined. The refraction predicted by a numerical model under conditions of varying current profiles which results in the best correlation of wave refraction to the SAR data, the tomographic problem of measuring the Gulf Stream current is solved.

The best correlation between the model and SAR data is obtained when a current is modeled by a top hat velocity profile with a direction of 75° and a current speed of 2 m/s. The direction agrees with that visually observed from the SAR images, and the direction and speeds are close to the Coast Guard estimates for the Gulf Stream at the time of the SEASAT pass. The current profiles used did not take into account a possible widening of the Gulf Stream at the position of the satellite overpass. There is a great deal of scatter in the SAR data, both before and in the Gulf Stream, so it is difficult to correlate every point with specific current behavior, but the increase in wave length and change in wave angle in the center of the Gulf Stream seem to indicate that there may be a non-uniform feature such as the formation of an eddy or other lateral variability near the current's edge.

Supported by: United States Navy.

INCORPORATING THRUSTER DYNAMICS IN THE CONTROL OF AN UNDERWATER VEHICLE

John G. Cooke

The dynamics of an underwater vehicle are gently influenced by the dynamics of the thrusters.

Precise control, for example to perform repeatable survey or coordinated vehicle/manipulator control, should incorporate knowledge of thruster dynamics behavior. An energy-based lumped parameter model of the nonlinear thruster dynamic response is developed and experimentally verified using static and dynamic thruster relationships. Three controllers to compensate for the nonlinear dynamics are designed including analog lead compensation, model-based computed torque and adaptive sliding control techniques. The proposed controller designs are implemented and evaluated in a hybrid, one degree-of-freedom vehicle simulation using an actual thruster under digital control as the actuator. Controller evaluation and comparison is based on observed vehicle tracking performance.

The incorporation of thruster dynamics is shown to significantly improve vehicle tracking performance. Superior, robust tracking performance with significant model uncertainty is demonstrated in the application of the adaptive sliding control technique. The evaluated adaptive controller structure may permit on-line adaptation on complex hydrodynamic phenomena associated with complete vehicle/thruster configurations such as cross-flow and mutual interference.

Supported by: United States Navy.

SURFACE WAVE, INTERNAL WAVE, AND SOURCE MOTION EFFECTS ON MATCHED FIELD PROCESSING IN A SHALLOW WATER WAVEGUIDE

John R. Daugherty

Given well known environmental conditions, matched field processing has been shown to be a promising signal processing technique for the localization of acoustic sources. However, when environmental data are incomplete or inaccurate, a "mismatch" occurs between the measured field and model field which can lead to a severe degradation of the localization estimator. We investigate the possible mismatch effects of surface and internal waves on matched field processing in a shallow water waveguide. We utilize a modified ray theory, based on the work of Tindle, to calculate the acoustic pressure field. This allows us to simply incorporate range dependent environmental conditions as well as to generalize our work to deeper wave guides. In general, the conventional (Barlett) matched field beamformer does not provide sufficient resolution to unambiguously locate a source, even in a perfectly matched environment. The maximum likelihood method (MLM) matched field beamformer has much better resolution but is extremely susceptible to mismatch. The mismatch due to surface roughness

can result in a large reduction of the estimator peak. Part, but not all, of the peak can be regained by 1) using a model which includes incomplete reflection at the surface based on actual sea surface statistics and 2) short time averaging of the measured signal, with times on the order of the period of the surface waves. Mismatch due to internal waves can also result in a large degradation of the estimator. Averaging over the same time period as surface waves provides little improvement and leads one to surmise that internal waves may be a limiting constraint on matched field processing. Finally, we combine the surface and internal wave fields with a slowly moving source. This example highlights the necessity for the development of a beamformer which has a broader mainlobe while maintaining adequate sidelobe suppression, and we address this issue by looking at two such beamformers.

Supported by: United States Navy.

A CODE-DIVISION, MULTIPLE BEAM SONAR IMAGING SYSTEM

John M. Richardson

In this thesis, a new active sonar imaging concept is explored using the principle of code-division and the simultaneous transmission of multiple coded signals. The signals are sixteen symbol, four-bit, non-linear, block Frequency-Shift Keyed (FSK) codes, each of which is projected into a different direction. Upon reception of the reflected waveform, each signal is separately detected and the results are inverted to yield an estimation of the spatial location of an object in three dimensions. The code-division sonar is particularly effective operating in situations where the phase of the transmitted signal is perturbed by the propagation media and the target. Most imaging techniques presently used rely on preservation of the phase of the received signal over the dimension of the receiving array. In the code-division sonar, spatial resolution is obtained by using the combined effects of code-to-code rejection and the a-priori knowledge of which direction each code was transmitted. The coded signals are shown to be highly tolerable of phase distortion over the duration of the transmission. The result is a high-resolution, three-dimensional image, obtainable in a highly perturbative environment. Additionally, the code-division sonar is capable of a high frame rate due to the simplicity of the processing required. Two algorithms are presented which estimate the spatial coordinates of an object in the ensonified aperture of the system, and the performance of the two is compared for different signal to noise levels. Finally, the concept of code-division imaging is

employed in a series of experiments in which a code-division sonar was used to image objects under a variety of conditions. The results of the experiments are presented, showing the resolution capabilities of the system.

Supported by: United States Navy.

INFERENCE OF ECOLOGY FROM THE ONTOGENY OF MICROFOSSILS

Peter N. Schweitzer

Studies of microfossils typically regard ontogeny as a confusing influence. Properly understood, it can instead be an enlightening factor, because it shows more aspects of the lives of individuals than do the form and distribution of adults alone. This work comprises three studies in which information about ontogeny is crucial for making inferences about the conditions under which fossil organisms lived.

The first part of this thesis examines the theory that *heterochrony*, change in the relative timing of somatic and reproductive development, is the morphological results of life-history evolution. A large body of paleontological literature concerns the importance of ontogeny as a source of morphological variation for evolution; morphologies that appear during one stage of an organism's development are made available for use in another simply by modifying the developmental program. Paleontologists need to know why this occurs, both so they can study the mechanism of evolution of extinct animals and so they can speak of the fossil record in terms that are applicable to modern forms. If life-history evolution causes heterochrony then the fossil record provides evidence of the nature of selection (in particular the age-specific mortality) that extinct animals experienced.

Four species of the ostracode genus *Cyprideis* were studied to determine whether differences in age at maturity are correlated with heterochrony in the expected manner. For each species the changes in size and shape through geological time were judged in the statistical context of modern geographic and seasonal variation. Living populations were sampled regularly to detect differences in seasonality and to estimate the duration of development.

Evolution of ontogeny occurs at the level of species in this group, but it is not simply related to differences in life-history. In comparisons among species, we find evidence of heterochrony where there is no difference in development timing, and a difference in developmental timing where there is no heterochrony. Size shows a similar pattern. Three of the four species show the expected positive correlation between size and age at maturity. The other species show the expected

positive correlation between size and age at maturity. The other species is relatively large yet matures rapidly. *Cyprideis* does not support the generalization that life-history evolution causes heterochrony, and casts doubt on the inference of life-history evolution from heterochrony where the data are drawn exclusively from extinct forms.

The second part of the thesis concerns the use of ontogenetic information to determine the habitat of deep-living planktonic foraminifera. Through careful morphological analysis the populations of *Globorotalia menardii* and *G. tumida* were studied in detail at a single locality, the Ceara Rise. The foraminiferal test is dominated by two processes of growth, the accretion of chambers and the formation of an enveloping calcite crust. These can be recognized through measurements of shell size, shape, and density. The populations can be divided into groups according to their stage of chamber and crust development.

For both *Globorotalia menardii* and *G. tumida*, the measured isotopic composition of whole specimens indicates that the organisms live in the upper 50m of the water, and that the crust is emplaced at depths below 50m, assuming that the shell is precipitated in equilibrium with seawater $\delta^{18}\text{O}$. Measured values for *G. tumida* indicate crust formation at about 100m at the Ceara Rise in the western equatorial Atlantic, slightly shallower at the Sierra Leone Rise in the eastern equatorial Atlantic.

Assuming that smaller and noncrusted forms represent the early stages of larger and crusted forms, respectively, one can calculate the oxygen- and carbon-isotopic composition of calcite added by the two processes. Crust composition in *G. tumida* appears to be in equilibrium with seawater, while in *G. menardii* the crust is lighter in $\delta^{13}\text{C}$ than the equilibrium value.

Similar measures of isotopic composition from the Sierra Leone Rise and Bermuda Rise bear out these findings. At the Bermuda Rise, the isotopic data indicates growth in shallow water during the summer months, when a seasonal thermocline is well developed.

Apparently, both *G. menardii* and *G. tumida* require warm water or a shallow thermocline, with *G. menardii* occupying shallower water than *G. tumida*. These findings may be used to understand why these species disappear from the glacial Atlantic ocean, reappearing during interglacials, *G. tumida* preceding *G. menardii*.

The third part of the thesis shows a relatively simple relationship between characteristics of ontogeny such as proloculus size and rate of chamber expansion in 36 specimens of the planktonic foraminifer *Neogloboquadrina pachyderma* taken from sea ice in the Southern Ocean. The consequences for morphology of

variations in ontogeny can be understood and used (a) to explain latitudinal variations in morphology, (b) to show why carbon isotopic composition is so variable and (c) to suggest ways of selecting specimens that minimize ontogenetic variations in shell chemistry.

Some variations in morphology may be caused by variations in ontogeny. The latitudinal gradient in the number of chambers showing in the outer whorl of *Neogloboquadrina pachyderma* described by Kennett (1968) may be explained by latitudinal gradient in the size of the proloculus.

Previously published variation in carbon isotopic composition of *N. Pachyderma* with size is nearly as large as geographic gradients in the composition of specimens taken from a narrow size range. If the effect of ontogeny on $\delta^{13}\text{C}$ is more highly correlated with chamber accretion than with test size, then geographic variations in the patterns of growth (specifically the rate of chamber size increase) may explain most of the geographic variation in $\delta^{13}\text{C}$.

If the variation in growth patterns seen among these specimens is typical of most samples but the proportion of specimens having a given pattern of growth varies from place to place, specimens taken from a narrow size range having four chambers in the outer whorl may be expected to minimize ontogenetic variation consistently.

Supported by: Woods Hole Oceanographic Institution, National Science Foundation grants OCE82-14930, OCE84-10221, and OCE84-17040.

Index

Addison, Richard F.	B-18	Carlson, Cynthia	MP-4
Agardy, M. Tundi	MP-1,10	Caron, David A.	B-22,23,24,25,27,29
Altabet, Mark A.	C-2,3	Caruso, Michael J.	AOPE-4,PO-13,14,16
Anderson, D. M.	B-5,14,19,20,21,22,24	Caswell, Hal	B-30,31
Anderson, O. Roger	B-23	Catipovic, Josko A.	AOPE-3,6,7
Anderson, R. F.	B-4	Cayula, J. F.	PO-9
Armi, Larry	PO-9	Cembella, Allan D.	B-14,22
Arnold, M.	C-15	Cetta, Catherine M.	B-21
Aubry, Marie-Pierre	GG-1,14	Champ, M. A.	GG-12
Bacon, Michael P.	C-9	Chapman, David C.	PO-13
Baker, K. S.	PO-10	Chen, Changsheng	GS-10
Barber, Deborah K.	GS-10	Chester, David B.	GS-10
Bauer, David R.	C-6	Chiu, C.S.	AOPE-2
Bazylnski, Dennis A.	B-8,11,12	Choi, Joon W.	B-26
Beardsley, Robert C.	PO-12,17,18	Christensen, John P.	C-4
Beaufort, Luc	GG-14	Chu, D.	AOPE-8
Belastock, R. A.	C-15	Churchill, James H.	PO-11,12
Belkin, Shimshon	B-12	Clark, Christopher W.	B-6
Berggren, W. A.	GG-14	Clark, Dan W.	B-1
Bibigare, R. R.	PO-10	Clifford, C. Hovey	B-8
Bideau, Daniel	C-13	Coble, Paula Garfield	C-4
Biesiot, Patricia M.	B-13,14	Cochran, J. Kirk	C-10
Billings, J. D.	GG-13	Codispoti, L. A.	B-4,C-4
Binder, Brian J.	B-21	Cohen, Joel	B-30
Bird, James E.	B-6	Cole, Jonathan J.	B-25
Bishop, James K. B.	C-3,PO-1	Collins, John A.	GG-6,18,GS-1
Black, Dianne	B-7	Colodner, Debra	C-1
Black, Geoff	B-4	Commeau, Robert. F.	C-12
Blackwelder, P. L.	GG-13	Conway, Noellette	B-15
Blough, Neil V.	C-6,7	Cooke, John G.	GS-15
Bocconcelli, Alessandro	AOPE-5	Cordery, M. J.	GG-12
Bower, Amy S.	PO-4	Corliss, Bruce H.	GG-13
Boyer, Barbara C.	MP-9	Cornillon, Peter C.	PO-9,11,12
Boyer, Gregory L.	B-22	Cosper, Elizabeth	B-24
Brewer, Peter G.	C-10	Crescenti, Gennaro H.	PO-16,17,19
Bricelj, V. M.	B-14	Dahl, Peter H.	GS-12
Brichet, E.	C-15	Dailey, J. E.	GG-12
Brigham, Lawson W.	MP-1	Damuth, John E.	GG-16
Brink, K. H.	PO-11	Daugherty, John R.	AOPE-2,7,GS-15
Broadus, James M.	MP-2,3,4,12	Davidson, Lynn	MP-4
Brocher, T. M.	GG-6	Davis, Paul G.	B-29
Brown, Otis B.	C-12,PO-1	Dean, Jerome P.	PO-15,19
Brumley, B. H.	AOPE-3	Deffenbaugh, Max	AOPE-3
Bryden, Harry L.	PO-11	Degens, E. T.	GG-2,17
Brönnimann, Paul	B-1	DeLonga, David M.	GS-12
Buesseler, Ken O.	C-10	Dennett, Mark R.	B-9,24,26,C-5,16
Bullister, John L.	C-11	Desai, B. N.	GG-17
Burgess, James	AOPE-10	Detrick, R. S.	GG-12
Burns, Daniel R.	GG-5,6	Deuser, W. G.	C-12,15
Buskey, Edward J.	B-23	Dick, Henry J. B.	C-1,GG-1
Butler, Richard M.	MP-6	Dickey, Tommy D.	PO-10
Byman, Michael W.	AOPE-3,GS-15	Dickinson, W. H.	C-2
Caldwell, David K.	B-5	Distel, D.	B-13
Caldwell, Melba C.	B-5	Doherty, Kenneth W.	B-28
Cande, Steven C.	GG-10	Donahue, Douglas	C-5
Capotondi, A.	PO-12	Donelan, Mark A.	AOPE-1
Capuzzo, Judith McDowell	B-8,13,14,15,27	Dornblaser, Mark M.	C-10
Carangelo, Robert M.	C-2	Doucette, Gregory J.	B-22
Carey, D. A.	C-11	Dougherty, Martin E.	GS-9

Druffel, Ellen R. M.	C-4,5,6,15,16,17	Haake, B.	GG-17
Dunbar, R. B.	C-4	Hahn, Mark E.	B-7
Dunn, Chris	PO-16	Haidvogel, Dale B.	PO-6
Dyrssen, David	C-10	Hall, S.	B-20
Earles, J.	PO-9	Halley, Robert B.	GG-5
Early, Gregory A.	B-5	Hamelin, B.	C-13
Edwards, Margo H.	GG-2	Hamilton, Peter	PO-11
Eganhouse, Robert P.	C-17	Hampson, George R.	B-1
Eiswerth, Mark E.	MP-5	Haney, J. Christopher	MP-7
Elderfield, H.	C-12	Harvell, C. Drew	B-30
Elskus, Adria A.	B-7	Hay, Bernward	C-10,GG-2
Emerson, Steven R.	GG-13	Hekinian, Roger	C-13
Emery, K. O.	GG-1,3	Helfrich, Karl R.	PO-5
Engebretsen, Knut	AOPE-10	Hemleben, C.	C-15
Esaias, W. E.	C-12	Hermann, Diane	C-17
Evans, R. H.	C-12	Hernandez, Reyna Gil	MP-1
Faber, Walter W., Jr.	B-23	Hey, R. N.	GG-8
Falkner, Kelly K.	GS-2	Hibler, W. D. III	PO-8
Fang, C.	GG-12	Hirschberg, David	C-10
Farrington, John H.	B-8,C-5,7,11	Hoagland, Porter	MP-3
Farrow, Scott	MP-5	Hoffman, Daniela	MP-9
Feldman, G. C.	C-12	Hogg, Nelson G.	PO-5
Fleer, A. P.	C-15	Honjo, Susumu	B-4,C-10,GG-2,17,19
Flegal, A. Russell	B-4	Hoskins, Hartley	GG-11
Flierl, Glenn R.	PO-11	Hosom, David S.	PO-15,16
Fluck, Steven J.	B-7	Hover, Franz S.	GS-12
Fofonoff, N. P.	PO-14	Howes, Brian L.	B-8
Fornari, Daniel J.	GG-2	Hsu, Hsiao-ming	PO-6
Fossing, Henrik	B-11	Huang, Rui Xin	PO-6,7
Frankel, Richard B.	B-11,12	Huber, R.	B-5,10
Freitag, Lee E.	AOPE-3,6	Huh, Chih-An	C-9
Frew, Nelson M.	C-5	Humphris, S. E.	C-17
Friederich, Gernot E.	B-4,C-4	Hunt, John M.	C-6
Frisk, George V.	AOPE-2,9	Ittekkot, V. A.	GG-2,17
Fry, Brian	B-9	Iturriaga, R.	PO-10
Frye, Dan	AOPE-3	Izdar, E.	B-4,GG-2
Fukumori, Ichiro	GS-5	Jakobsson, Sveinn P.	C-12
Furman, Tanya H.	GS-13	Jannasch, Holger W.	B-4,5,8,9,10,11,12,C-8
Gagosian, Robert B.	C-4,8,13,14	Jansa, Lubomir F.	GG-1
Gaines, Arthur G.	MP-6	Jasper, John P.	C-13,14
Gallager, Scott M.	MP-12	Jenter, Harry L. III	GS-14
Gallo, David G.	GG-2	Jezeq, K. C.	AOPE-8
Geraci, Joseph A.	B-5	Jia, Xiaoping	B-8
Gerlock, John L.	C-6	Jickells, T. D.	C-15
Geyer, W. Rockwell	AOPE-1,6,9	Johnson, A. Sherwood	C-5
Giblin, Anne E.	MP-6	Johnson, David A.	GG-16
Gjerde, Kristina	MP-4	Johnson, H. Paul	GG-11
Glover, David M.	C-6	Johnson, Kevin T. M.	GG-1
Goldman, Joel C.	B-9,24,26,C-5	Jorgensen, Bo Barker	B-11,C-8
Gornitz, V.	MP-6	Joyce, Terrence M.	PO-1,13
Gow, A. J.	AOPE-8	Joyner, Christopher C.	MP-8,9
Goyet, Catherine	C-10	Jull, A. J. Timothy	C-5
Graber, Hans C.	AOPE-3,4,PO-12	Kanyo, Zoltan	C-18
Gradstein, Felix M.	GG-1	Kaoru, Yoshiaki	MP-10,11
Granata, Timothy C.	PO-10	Kaplan, Ilene M.	MP-9
Griffin, Sheila	C-5,6	Keigwin, Lloyd D.	GG-13
Groman, Robert C.	AOPE-9	Keller, William C.	AOPE-5
Grosenbaugh, Mark A.	AOPE-10	Kelly, Kathryn A.	PO-13,14
Grousset, F.	C-13	Kempe, S.	C-10,GG-2
Günther, Heinz	AOPE-3	Kenchington, Richard A.	MP-10

Kery, Sean M.	AOPE-5,7	McKee, Theresa K.	PO-19
Ketola, Matti	B-31	McKibbin-Vaughan, Thomas	C-10
Kieber, David J.	C-7	McLain, C. E.	GG-12
Kinder, Thomas H.	PO-11	Merzi, Nuri	AOPE-1
King, Stagg	B-9	Meyer, Peter S.	C-1
Kite-Powell, Hauke L.	MP-3	Michaels, Anthony F.	B-4,PO-10
Kleinrock, Martin C.	GG-7,8,9	Miles, Paul R.	B-6
Klinger, Barry	PO-11	Millard, R. C.	PO-3,14
Kloeppe-Sams, Pamela J.	GS-3	Miller, Kenneth G.	GG-14
Knapp, George P.	PO-14,17	Milliman, John D.	GG-5,17
Konuk, T.	C-10,GG-2	Minnis, S. A.	C-4
Krishfield, Richard	GG-9,19	Miosky, Donna	B-15
Kulis, David M.	B-19,20	Moffett, James W.	C-8,16
Kunze, Holly	B-24	Molyneaux, Stephen	B-9,11
Kurr, M.	B-10	Montani, Shigeru	B-22
Kurz, Mark D.	C-1	Montgomery, W. Linn	B-4
Lalou, C.	C-15,17	Moore, Michael J.	B-16,17
Lancaster, A.	B-15	Moore, Richard B.	C-1
Lancaster, Bruce A.	B-8,15	Moore, Robert M.	C-9
Lange, M. A.	AOPE-8	Moskowitz, Bruce M.	B-12
Leavitt, Dale F.	B-8,15	Mueller, Cornelia	B-3
Lech, John J.	B-17	Muller-Karger, F. E.	C-12
Lee, C.	B-20	Murray, J. W.	B-4
Lee, J. H.	B-14	Naiman, Robert J.	B-4
Lemke, Peter	PO-3,8	Nair, R. R.	GG-17
Lewitus, Alan J.	B-22	Nelson, Douglas C.	B-10,12
Li, F. K.	PO-14	Neumann, G.	PO-14
Lim, Ee Lin	B-23,24	Neuner, Annemarie	B-12
Limeburner, Richard	PO-17,18	Newhall, A. E.	AOPE-2
Lin, Jian	GG-3,9	Nicholls, Neville	MP-13
Lindsay, Sara M.	B-3	Nickolson, Jo Ann	B-9
Lindsey, Judith L.	B-23	O'Brien, Keran	C-1
Linick, Timothy W.	C-5	Ochi, Tadashi	B-22
Linn, L. J.	C-16	Okaichi, Tomotoshi	B-22
Lirdwitayaprasit, Thaithaworn	B-22	Olafsson, Jon	C-12
Little, Sarah A.	GG-3	Olmez, Ilhan	C-17
Liu, Zhengyu	PO-8	Owens, W. Brechner	PO-3,8,14,19
Livingston, Hugh D.	C-10	Pajor, Ana M.	B-16
Lobel, Phillip S.	B-3	Pak, H.	PO-10
Lohmann, G. P.	GG-15,16	Palenik, Brian P.	GS-1
Lovley, Derek R.	B-12	Parmentier, E. M.	GG-3
Lowry, Kem	MP-10	Payne, Richard E.	PO-15,16,17,19
Luyten, James R.	PO-1,2	Pedlosky, Joseph	PO-8,9
Lynch, James F.	AOPE-2,7	Peir, Jih-Kwon	PO-6
Madin, Laurence P.	B-25,31	Peltzer, E. T.	C-8
Madsen, John A.	GG-2	Pennington, Nancy J.	PO-15,16
Malme, Charles I.	B-6	Perfit, Michael R.	GG-2
Manganini, Steven J.	GG-17,19	Perovich, Donald K.	GG-9
Manheim, Frank T.	C-12	Pesch, Gerald G.	B-3
Mann, Stephen	B-11	Phipps-Morgan, Jason	GG-9
Marquette, Craig D.	PO-19	Plant, William J.	AOPE-5
Marra, J.	PO-10	Ponte, Rui M.	PO-2
Mayo, Charles A.	B-5	Porter, K. G.	B-25,27
McCaffrey, Mark A.	C-5,7,18	Prada, Kenneth E.	PO-16
McCarthy, J. J.	C-3	Pratt, Larry	PO-9
McCartney, M. S.	PO-2	Prescott, John H.	B-5
McClain, Charles R.	C-6	Pruell, Richard J.	B-7
McCorkle, Daniel C.	GG-13	Pu, S.	PO-3
McCormick, Stephen D.	B-4	Purdy, G. M.	GG-4,6,9
McDougall, Trevor J.	PO-1	Putt, Mary	B-26,27

Pyle, Robert W.	B-6	Stalcup, Marvel C.	PO-14,17
Rajan, Subramaniam D.	AOPE-2	Stanley, Robert J.	PO-14,17
Ramaswamy, V.	GG-17	Stanton, Timothy K.	AOPE-8
Rantamaki, Pirjo	B-8	Starczak, Victoria R.	B-2,3
Reeburgh, W. S.	B-4	Steele, John H.	MP-13
Reinisch, Carol L.	B-15	Stegeman, John J.	B-7,16,17,18
Renton, Kenneth W.	B-18	Stephen, Ralph A.	GG-6,10,11
Repeta, Daniel J.	C-7,8	Stern, Melvin E.	PO-11
Rhoads, Donald C.	B-1	Stetter, K. O.	B-10
Richardson, John M.	GS-16	Stewart, W. Kenneth	AOPE-1,6
Richardson, Philip L.	PO-2,19	Stoecker, Diane K.	B-23,26,27,28
Robertson, Ken	C-5	Stolzenbach, Keith D.	GG-3
Rona, P. A.	C-15,17	Stommel, Henry M.	PO-1,5,7
Rose, D.	B-5	Sulanowski, J.	C-5
Rosenthal, Wolfgang	AOPE-3	Sullivan, J. J.	B-20
Ross, David A.	GG-1,12	Susani, Lucia C.	B-7
Rudnick, Daniel L.	PO-15,16	Swanberg, Neil R.	B-25,28
Salmeen, Irving T.	C-6	Swift, Stephen A.	GG-11,18
Samelson, R. M.	PO-2,9	Takahashi, Kozo	GG-13,14
Sanders, Robert W.	B-25,27	Tang, Dajun	AOPE-9
Santala, Markku J.	AOPE-9	Tarafa, Martha	C-18
Santos, Kristen A.	MP-9	Taylor, Craig D.	B-28
Sayigh, Laela S.	B-6	Terray, Eugene A.	AOPE-1,3,9
Sayles, F. L.	C-2	Thomas, Peter	B-16
Scharold, Jill V.	GS-4	Thompson, Geoffrey	C-1,12,13,15,17
Scheltema, Amélie H.	B-2	Thompson-Rizer, Carolyn	C-9
Scheltema, Rudolf S.	B-1	Timperi, Ralph J.	B-5
Schmitt, Raymond W.	PO-10	Tivey, Maurice A.	GG-11
Schmitz, William J., Jr.	PO-2	Toole, J. M.	PO-3
Schouten, H.	GG-9	Toolin, Lawrence	C-5
Schubert, David M.	PO-13	Top, Z.	B-4
Schweitzer, Peter N.	GG-15,16,GS-16	Trask, Richard P.	PO-15,16,19
Scott, Michael D.	B-6	Triantafyllou, Michael S.	AOPE-10
Searle, Roger C.	GG-8	Trull, Thomas W.	C-1,GS-7
Sempere, J.-C.	GG-9	Tucholke, B. E.	GG-4
Shaw, Peter R.	GG-10	Tucker, Walter B. III	GG-9
Sherrell, Robert M.	GS-5	Twombly, Saran	B-31
Shimizu, Nobumichi	GG-1	Tyack, Peter L.	B-5,6,MP-13
Sholkovitz, Edward R.	C-12,13,17	Tyler, S.	B-28
Shor, Alexander N.	GG-2	Uchupi, Elazar	GG-3,18
Sieburth, John McN.	B-29	Upstill-Goddard, R.	C-12
Siegel, David A.	PO-10	Valdes, James R.	PO-16,19
Signell, Richard P.	AOPE-1,6,9,PO-12,GS-9	Valois, F. W.	B-13
Silver, M. W.	B-28	van Geen, Alexander F.M.J.	GS-8
Simpson, Daniel J.	C-6,8	Van Dover, Cindy Lee	B-1
Simpson, Paul	B-30	Vernhes, Jane Robertson	MP-4
Small, Lawrence F.	C-3	Villaret, Catherine	AOPE-1
Smith, D. K.	GG-10	Vogt, P. R.	GG-4
Smith, K. L., Jr.	C-17	von Alt, Christopher	AOPE-4
Smith, R. C.	PO-10	Von Herzen, R. P.	GG-12
Smith, V. Kerry	MP-10,11	Walls, Mari	B-31
Smolowitz, Roxanna	B-15,16,17,18	Wang, Xiaoming	GS-11
Solomon, Peter	C-2	Wang, Z.	PO-3
Solomon, S. C.	GG-4	Wargo, John	MP-4
Solow, Andrew R.	MP-6,11,12,13	Warren, Bruce A.	PO-4
Sparks, Nicholas H. C.	B-11	Waterbury, J. B.	B-13
Speer, Kevin S.	PO-4	Watson, S. W.	B-13
Spitzer, William S.	GS-6	Weinberg, James R.	B-1,2,3
Stössel, Achim	PO-3	Weller, Robert A.	PO-14,15,16,17,19
St. Aubin, David J.	B-5	Wellington, G. M.	C-4

Wells, Randall S.	B-6
Whelan, Jean K.	C-2,9,18
Whitehead, John A.	PO-4,5,11
Whittaker, John E.	B-1
Whorisky, Frederick G.	B-4
Wickremeratne, H. J. M.	MP-10
Wilber, R. Jude	GG-5
Wilcock, W. S. D.	GG-4
Wilkin, John L.	PO-13
Williams, A. J. III.	AOPE-3
Williams, Peter M.	C-5,17
Wirsen, Carl O.	B-8,9,10,11,12
Woodgate-Jones, M. E.	PO-2
Woodin, Bruce R.	B-7,16,18
Wooding, C. M.	PO-19
Wroblewski, J. S.	C-6
Xui, Xui	GG-13
Yoerger, Dana R.	AOPE-10
Zacmanidis, P. J.	C-6
Zafriou, Oliver C.	C-8,18
Zemanovic, M. E.	PO-19
Zervas, C.	GG-9
Zhang, Yu-Sheng	B-18
Zuosheng, Yang	GG-13

DOCUMENT LIBRARY

January 17, 1990

Distribution List for Technical Report Exchange

Attn: Stella Sanchez-Wade
Documents Section
Scripps Institution of Oceanography
Library, Mail Code C-075C
La Jolla, CA 92093

Hancock Library of Biology &
Oceanography
Alan Hancock Laboratory
University of Southern California
University Park
Los Angeles, CA 90089-0371

Gifts & Exchanges
Library
Bedford Institute of Oceanography
P.O. Box 1006
Dartmouth, NS, B2Y 4A2, CANADA

Office of the International
Ice Patrol
c/o Coast Guard R & D Center
Avery Point
Groton, CT 06340

NOAA/EDIS Miami Library Center
4301 Rickenbacker Causeway
Miami, FL 33149

Library
Skidaway Institute of Oceanography
P.O. Box 13687
Savannah, GA 31416

Institute of Geophysics
University of Hawaii
Library Room 252
2525 Correa Road
Honolulu, HI 96822

Marine Resources Information Center
Building E38-320
MIT
Cambridge, MA 02139

Library
Lamont-Doherty Geological
Observatory
Columbia University
Palisades, NY 10964

Library
Serials Department
Oregon State University
Corvallis, OR 97331

Pell Marine Science Library
University of Rhode Island
Narragansett Bay Campus
Narragansett, RI 02882

Working Collection
Texas A&M University
Dept. of Oceanography
College Station, TX 77843

Library
Virginia Institute of Marine Science
Gloucester Point, VA 23062

Fisheries-Oceanography Library
151 Oceanography Teaching Bldg.
University of Washington
Seattle, WA 98195

Library
R.S.M.A.S.
University of Miami
4600 Rickenbacker Causeway
Miami, FL 33149

Maury Oceanographic Library
Naval Oceanographic Office
Bay St. Louis
NSTL, MS 39522-5001

Marine Sciences Collection
Mayaguez Campus Library
University of Puerto Rico
Mayaguez, Puerto Rico 00708

Library
Institute of Oceanographic Sciences
Deacon Laboratory
Wormley, Godalming
Surrey GU8 5UB
UNITED KINGDOM

The Librarian
CSIRO Marine Laboratories
G.P.O. Box 1538
Hobart, Tasmania
AUSTRALIA 7001

Library
Proudman Oceanographic Laboratory
Bidston Observatory
Birkenhead
Merseyside L43 7 RA
UNITED KINGDOM

REPORT DOCUMENTATION PAGE	1. REPORT NO. WHOI-90-31	2.	3. Recipient's Accession No.
4. Title and Subtitle Abstracts of Manuscripts Submitted in 1989 for Publication		5. Report Date July, 1990	
7. Author(s) Editor: Alora Paul		8. Performing Organization Rept. No. WHOI 90-31	
9. Performing Organization Name and Address The Woods Hole Oceanographic Institution Woods Hole, Massachusetts 02543		10. Project/Task/Work Unit No.	
12. Sponsoring Organization Name and Address		11. Contract(C) or Grant(G) No. (C) (G)	
		13. Type of Report & Period Covered Technical Report	
15. Supplementary Notes This report should be cited as: Woods Hole Oceanog. Inst. Tech. Rept., WHOI-90-31.		14.	
16. Abstract (Limit: 200 words) This volume contains the abstracts of manuscripts submitted for publication during calendar year 1989 by the staff and students of the Woods Hole Oceanographic Institution. We identify the journal of those manuscripts which are in press or have been published. The volume is intended to be informative, but not a bibliography. The abstracts are listed by title in the Table of Contents and are grouped into one of our five departments, marine policy, or the student category. An author index is presented in the back to facilitate locating specific papers.			
17. Document Analysis a. Descriptors 1. abstracts 2. oceanography 3. ocean engineering b. Identifiers/Open-Ended Terms c. COSATI Field/Group			
18. Availability Statement Approved for publication; distribution unlimited.		19. Security Class (This Report) UNCLASSIFIED	21. No. of Pages 180
		20. Security Class (This Page)	22. Price